Editor's Choice

A New Method for Percutaneous Drug Delivery by Thermo-Mechanical Fractional Injury

Ronen Shavit, MSc[1]* and Christine Dierickx, MD[2]
[1]*R&D Department, Novoxel Ltd., 5 Weinshal st., Tel Aviv, Israel*
[2]*Skin and Laser Center, Beukenlaan 52, Boom, Belgium*

Background and Objectives: Percutaneous drug delivery (PDD) is a means of increasing the uptake of topically applied agents into the skin. Successful delivery of a photosensitizer into the skin is an important factor for effective photodynamic therapy. To evaluate the efficacy of pretreatment by thermomechanical fractional injury (TMFI) (Tixel®, Novoxel®, Israel) at low-energy settings in increasing the permeability of the skin to a known hydrophilic-photosensitizer medication, 5-amino-levulinic-acid hydrochloride (ALA) in compounded 20% ALA gel. To compare the effect of TMFI on ALA permeation into the skin in compounded gel to three commercial photosensitizing medications in different vehicles: ALA microemulsion gel, methyl-amino-levulinic-acid hydrochloride (MAL) cream, and ALA hydroalcoholic solution.

Study Design/Materials and Methods: Five healthy subjects were treated in two separate experiments and on a total of 136 test sites, with four topical photosensitizer preparations as follows: compounded 20% ALA gel prepared in a good manufacturing practice (GMP)-certified pharmacy (Super-Pharm Professional, Israel), 10% ALA microemulsion gel (Ameluz®, Biofrontera Bioscience GmbH, Leverkusen, Germany), 16.8% MAL cream (Metvix®, Galderma, Lausanne, Switzerland), and 20% ALA hydroalcoholic solution (Levulan Kerastick®, DUSA Pharmaceuticals, Inc., Wilmington, MA, USA). The dermal sites were pretreated by Tixel® (Novoxel® Ltd., Israel) prior to topical drug application. One site was untreated to serve as control. Protoporphyrin IX (PpIX) fluorescence intensity readouts were taken immediately and 1, 2, 3, 4, and 5 hours posttreatment.

Results: The highest average PpIX fluorescence intensity measurements were obtained for the compounded 20% ALA gel following pre-treatment by TMFI at 6 milliseconds pulse duration. After 2 and 3 hours, TMFI-treated sites exhibited an increased hourly rate in readouts of FluoDerm units, which were 156–176% higher than the control rates ($P \leq 0.004$). TMFI pre-treatment did not enhance the percutaneous permeation of either ALA or MAL following the microemulsion gel, hydroalcoholic solution, and cream applications.

Conclusions: Pretreatment with low-energy TMFI at a pulse duration of 6 milliseconds increased the percutaneous permeation of ALA linearly over the first 5 hours from application when the compounded 20% ALA gel was used. Formulation characteristics have substantial influence on the ability of TMFI pretreatment to significantly increase the percutaneous permeation of ALA and MAL. Lasers Surg. Med. © 2019 Wiley Periodicals, Inc.

Key words: percutaneous drug delivery; percutaneous permeation; diffusion; thermomechanical fractional injury; transepidermal drug delivery; tixel

INTRODUCTION

The therapeutic efficacy of topical drugs is correlated with both inherent potency and ability to penetrate the various skin layers. The principal barrier to drug permeation is the stratum corneum (SC), which has a structure of "brick" (corneocyte) and "mortar" (lamellar membranes). It consists of approximately 15 sublayers with a total thickness of 20 μm. The structure of the SC serves multiple barrier functions to protect internal cells and tissues while maintaining the internal environment and normal cellular functions [1]. The importance of the water content of the SC in determining its properties is well-documented. Warner et al. [2] reported a continuous increase in the water content of the SC, ranging from 15 to 25% at the skin surface to a constant level of approximately 70% in the viable stratum granulosum (SG) [3]. The mechanical properties of the SC are highly

Abbreviations: AFXL, ablative fractional laser; ALA, 5-aminolevulinic acid hydrochloride; CZ, coagulation zone; DSP, digital signal processing; FDU, FluoDerm Units; GMP, good manufacturing practice; HAZ, heat-affected zone; **IR**, infra-red; MAL, methyl-amino-levulinic acid hydrochloride; MAZ, micro-thermal ablation zone; PDD, percutaneous drug delivery; PDT, photodynamic therapy; PpIX, protoporphyrin IX; RH, Relative humidity; SC, stratum corneum; SG, stratum granulosum; TMFI, thermomechanical fractional injury; USP, United State Pharmacopeia.

Conflict of Interest Disclosures: All authors have completed and submitted the ICMJE Form for Disclosure of Potential Conflicts of Interest and have disclosed the following: RS is the Chief Technical Officer of Novoxel Ltd. and CD has no conflicts of interest.

*Correspondence to: Ronen Shavit, R&D Department, Novoxel Ltd., 5 Weinshal st, Tel Aviv 6941330, Israel.
E-mail: Ronen.shavit@windowslive.com

Accepted 28 May 2019
Published online in Wiley Online Library (wileyonlinelibrary.com).
DOI 10.1002/lsm.23125

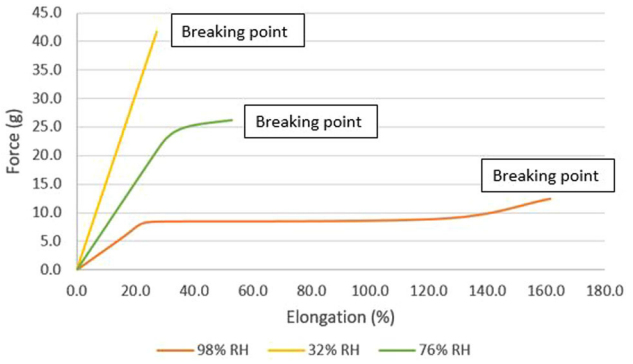

Fig. 1. Stratum corneum (SC) elongation to breakage versus relative humidity [4]. SC elongation to breakage is shown for three water content levels representing relative humidity. Extremely hydrated tissue (98% relative humidity [RH], orange curve) is very elastic, enabling large deflection of over 160% before breakage. Elongation to break is ~25% for the most dehydrated tissue (32% RH, yellow curve) [Color figure can be viewed at wileyonlinelibrary.com].

affected by the relative humidity (RH) within the layer. Wildnauer et al. [4] have shown that the breaking strength of the SC (defined as the force required to pull the SC until it breaks) increases from ~10 g at 80–100% RH to ~45 g at 0% RH, while the elongation to breakage (defined as the ratio between the increase in length after breakage to the initial length) decreases from 200% at 100% RH to less than 10% at 0% RH (Fig. 1).

Kinetics of Percutaneous Drug Delivery (PDD)

The efficiency of any PDD system is predominantly determined by the kinetics of skin permeation. Percutaneous absorption is determined by the penetration of substances into various layers of the skin and permeation across the skin into the systemic circulation. Fick's first law of diffusion relates the diffusion flux (J) of a chemical substance at steady state from a region of high concentration to a region of low concentration. The diffusion flux is proportional to the concentration gradient of the substance at a specified location in the material

$$J = -D\frac{dc}{dl} \tag{1}$$

where D is the diffusion coefficient, c is the concentration of the substance, and l is the location of the substance. The derivative dc/dl is the concentration gradient along the diffusion line [5]. Alkilani et al. [6] provided a simple model for expressing the relationship between the drug concentration and the rate of permeation in a conventional transdermal drug delivery system with an intact SC. The rate of permeation through the skin over time (dQ/dt) is given by:

$$\frac{dQ}{dt} = P(C_d - C_r) \tag{2}$$

where Q is the total amount of permeated substance, t is the duration of the process, P is the permeability coefficient, and C_d and C_r are the drug concentrations on the skin and inside the tissue, respectively. It is clear that C_d should be significantly greater than C_r in order to enable effective skin permeation through the SC. Specifically, the concentration of the material on the SC must be higher by an order of magnitude than its concentration within the target tissue.

Topical therapeutics, and especially hydrophilic ones, generally demonstrate poor total absorption and cutaneous bioavailability, with only 1–5% permeation into the skin [7]. Several techniques have been developed to modify or remove the SC barrier in order to increase the uptake of topically applied drugs. Commonly available techniques include electroporation, iontophoresis, fractional lasers, microdermabrasion, microneedles, pressure, radiofrequency, and sonophoresis. These techniques have demonstrated improved transdermal delivery of various materials, including drugs, into the skin. The greatest challenge for an effective transdermal drug delivery (TDD) is the creation of successful passage through the SC while minimizing damage to the viable epidermis and dermal tissue. Thermal or mechanical damage to the tissue might affect the drug's passage to the target cells, either as a result of thermal blockage (such as tissue coagulation) or an inflammatory healing process associated with mechanical damage. CO_2 laser-assisted drug delivery is a common technology used for TDD. The technology employs an ablative fractional laser (AFXL) to focally remove the SC and epidermis in order to allow access of topical drugs to the dermis [8]. The final outcome of the AFXL treatment is microthermal ablation zones (MAZs) that consist of ablated vertical channels surrounded by a coagulation zone (CZ). MAZs are characterized by the width of the ablative damage (ablative width [AW]), the depth of the ablative damage (ablative depth [AD]), and their surrounding CZ. The desired AW and AD of the MAZ can be achieved by adjusting treatment parameters: stacks (the number of delivered pulses per MAZ) and the fluence (the energy density). Typically, the AD varies between 95 and 630 μm, with an AW between 79 and 130 μm in CO_2 AFXL [9]. The ablated channel is surrounded by 1.5–41.3 μm of coagulated tissue. Segments of healthy skin between individual MAZs ensure rapid and scar-free wound healing. The deep holes created by the laser serve as a channel for transport of the topical drug into the epidermis by eliminating the SC barrier, while the CZ may serve as a reservoir for small hydrophilic drugs, allowing slow release into the dermis [10]. As reported by Choi et al. [11], typical settings are 10–20 mJ per micropore using a 10,600 nm CO_2 fractional laser (eCO2®; Lutronic Co., Ltd., Seoul, Korea).

Thermomechanical Fractional Injury (TMFI) Technology

Tixel® (Novoxel®, Israel) is a thermomechanical system developed for delivering fractional treatment. The system is designed for the treatment of soft tissue by direct conduction of heat, enabling rapid water evaporation with low thermal damage to the surrounding tissue. The

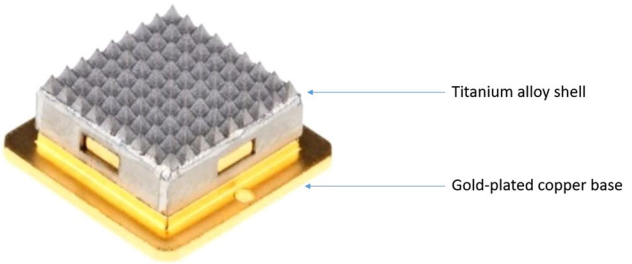

Fig. 2. The thermomechanical fractional injury (TMFI) tip (9×9 pyramids, $1\,cm^2$) [Color figure can be viewed at wileyonlinelibrary.com].

system consists of a handpiece connected to a console. The handpiece applies a therapeutic element, the "tip," which is affixed to the distal section. The tip is comprised of a gold-plated copper base and a thin-walled titanium alloy cover (Fig. 2).

The handpiece is equipped with a precise motion system, based on a low inertia linear motor, and a digital signal processing (DSP) motion controller. The system's design enables precise presetting of the duration of skin contact. The tip's surface of $1\,cm^2$ consists of an array of 81 (9×9) square-based pyramids. The pyramids are 1.25 mm tall and have a flat rectangular apex of approximately $0.01\,mm^2$. The blunt apex of the pyramid allows effective heat transfer and prevents mechanical puncturing of the skin. The backplane of the tip attaches to a ceramic heater maintained at a temperature of 400°C during the treatment. The heating process enables effective self-sterilization before and during treatment, thereby significantly reducing the risk of cross-contamination. The tip is safely retracted to its home position when the handpiece is not activated. When the handpiece is activated, the linear motor rapidly advances the tip, which comes into brief contact with the tissue and then pulls it back. Thermal energy is transferred to the skin, creating micropores by the evaporation of water without tissue carbonization. The tip recedes to its home position within a precisely controlled distance and time. The duration of the pulse, that is, time of contact between tip and skin, ranges from 5 to 18 milliseconds. An 18 milliseconds pulse delivers ~0.25 mJ/micropore, a 12 milliseconds pulse delivers ~0.20 mJ/micropore, and a 6 ms pulse delivers ~0.15 mJ/micropore.

A second parameter of the system is the travel or "protrusion" of the tip. Protrusion is defined as the distance that the tip travels from the distal edge of the handpiece (which also functions as a distance gauge) to the tissue (Fig. 3). Adjustment of the protrusion is measured in micrometers (μm), and it is designed to ensure good thermal coupling between the tip and the tissue, especially in relatively "flexible" regions, such as the cheeks. Thermal coupling or thermal resistance are influenced by two factors: the thermal conduction from the tip to the skin at the spots of contact and the thermal resistance due to entrapped air between the tip and the skin. Higher protrusion rates increase the

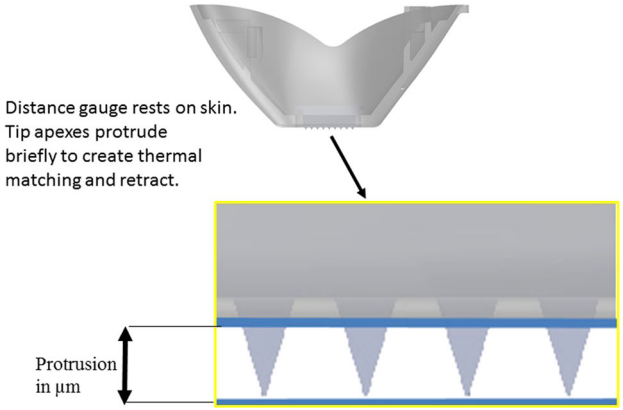

Fig. 3. The tixel tip protrusion [Color figure can be viewed at wileyonlinelibrary.com].

contact surface between the tip and the skin and reduces the air traps. Enhanced coupling results in lower thermal resistance between the tip and the tissue, yielding a more substantial dermal effect. A well-planned setting of the pulse duration and protrusion contribute to the desired thermal effect followed by a successful clinical outcome.

Thermal Model

Unlike radiant technologies, such as laser or radio-frequency, in which one form of energy (i.e., kinetic energy in laser) is converted to another form of energy, the TMFI delivers heat to the tissue by direct conduction. Conduction is the transfer of thermal energy from the more energetic particles of a substance to the adjacent less energetic ones as a result of interactions between the particles. The rate of heat conduction through a medium depends on geometry, that is, thickness, material properties, and the temperature gradient across the medium. The TMFI thermal transfer analysis is based on an analytical model that provides the solution of the transient (time-dependent) heat wave theory for semi-infinite bodies.

The heat wave theory enables the calculation of the penetration of the thermal wave versus time, using the following formula [12]:

$$\delta = 3.6\sqrt{\alpha t} = 3.6\sqrt{\frac{k}{\rho C_p}t} \tag{3}$$

where δ is the thermal wave penetration depth (m) α is the thermal diffusivity (m^2/s); t is the time (s); k is the conductivity (W/(m·K)); ρ is the density (kg/m^3); C_p is the heat capacity at constant pressure (J/(kg·K)).

The analytical model provides a simple equation for calculation of the heat-affected depth and width due to a heat pulse, similar to the one generated by the tip's pyramidal apex on the skin. The calculated temperatures at various tissue depths for given pulse durations are displayed in Figure 4.

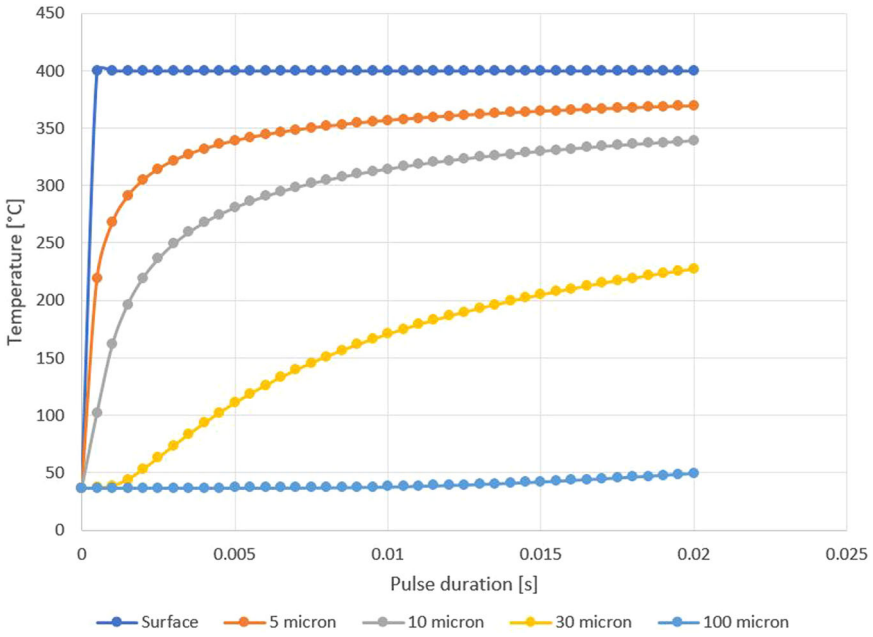

Fig. 4. Tissue temperature at varying depths according to pulse duration. The chart shows the tissue temperature at different distances from the skin's external surface. The blue line represents the surface temperature, and the orange line represents the tissue temperature 5 μm below the surface, etc. The *X* axis represents the pulse duration in milliseconds. The *Y* axis represents the tissue temperature in °C. The calculated surface temperature is 400°C at a pulse duration of 6 milliseconds (0.006 seconds), and the temperature is ~125°C at a distance of 30 μm from the surface [Color figure can be viewed at wileyonlinelibrary.com].

Fig. 5. Thermomechanical fractional injury (TMFI) treatment histopathology analysis. The coagulated effect on the tissue following TMFI treatment has a hemispherical shape. The two-dimensional histopathology analysis displays the thermal lesion's cross-section as a half-circle where the ratio between the base (flat part) and the radius is 2:1 (the base length is equal to the circle radius) [Color figure can be viewed at wileyonlinelibrary.com].

Analysis of the model's results revealed that the heat wave propagates in a hemispherical shape, with a maximum skin temperature of 400°C (the tip's temperature) on an isolated thin layer of approximately 5 μm depth. Tissue temperature drops to about 50°C at a depth of 100 μm.

Histopathology images at low settings (Fig. 5) reveal that the thermal effect does not vaporize the tissue (non-ablative) and is hemispherical (meaning that the ratio between the depth and width of the lesion is 1:2), as assumed in the analytical model.

Although the heat transfer model assumes that all of the heat is expended in tissue heating, it can be postulated that most of the heat is actually applied to evaporate the water in the upper skin layers since the effect is not ablative. Movement of the tip toward the skin during the pulse strains the dehydrated SC, resulting in tiny breakages of the layer, which becomes brittle at low water concentrations, as explained above. In addition, since most of the heat is expended by dehydrating the tissue, the water content in the viable epidermis and dermis changes gradually from low concentration in the hotter region to higher concentration in the cooler region.

The presented mechanism applies less than 0.2 mJ per micropore to fractionally and selectively remove the SC barrier. As a result, dry zones are formed in the viable epidermis and dermis, thereby establishing the required water concentration gradient for the initiation of material

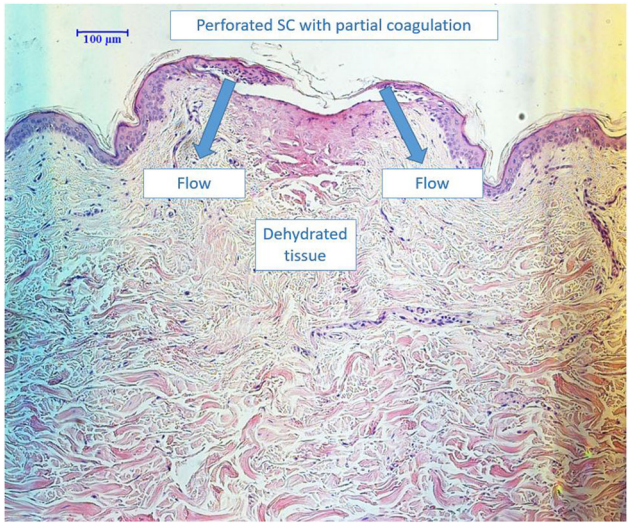

Fig. 6. Thermomechanical fractional injury (TMFI) combined thermal and motion effect on tissue. The TMFI transdermal effect perforates the stratum corneum (SC) by the combined drying and stretching of the tissue leading to the formation of small cracks in the tissue. The cracks perforate the tissue and break down the SC barrier. Since the temperature under the tip is high, some of the tissue located there coagulates, while other segments are dehydrated and establish the required water concentration gradient for the initiation of material flow inwards to the tissue in accordance with Fick's law [Color figure can be viewed at wileyonlinelibrary.com].

flow inwards to the tissue, in accordance with Fick's law. A general description of the transdermal thermal effect is given in Figure 6.

MATERIALS AND METHODS

The percutaneous permeation of 5-aminolevulinic acid hydrochloride (ALA) in TMFI's pretreated human skin was measured using compounded 20% w/v ALA gel and compared with three other selected known commercial medications. The specifications of those formulations are as follows:

1. Compounded 20% w/v ALA gel (200 mg/ml gel; Super-Pharm, Israel, a-GMP certified pharmacy, Petah - Tikwa). *List of excipients*: potassium sorbate 0.2%, oleic acid 10%, sepigel 305 10%, purified water ~59%, and hydrochloric acid 10% solution/potassium hydroxide 15% solution (for adjusting the pH to 4).
2. Commercial 10% w/w ALA microemulsion-gel (100 mg/g gel)—Ameluz® Biofrontera Bioscience GmbH. *List of excipients*: xanthan gum, soybean phosphatidylcholine, polysorbate 80, medium chain triglycerides, isopropyl alcohol, disodium phosphate dihydrate, sodium dihydrogen phosphate dihydrate, propylene glycol, sodium benzoate, and purified water.
3. Commercial 16.8% w/w methyl-amino-levulinic acid hydrochloride (MAL) cream (168 mg/g cream; Metvix®; Galderma, Lausanne, Switzerland). *List of excipients*: glyceryl monostearate, cetostearyl alcohol, polyoxyl stearate, cholesterol, oleyl alcohol glycerin, white petrolatum, isopropyl myristate, refined peanut oil, refined almond oil, edetate disodium, purified water, methylparaben, and propylparaben.
4. Commercial 20% w/w ALA hydroalcoholic solution (200 mg/1 g solution; Levulan Kerastick®; DUSA Pharmaceuticals, Inc.). *List of excipients*: Ethanol USP (48% v/v in purified water), laureth-4, isopropyl alcohol, and polyethylene glycol.

Treatment

Five healthy volunteers, aged between 35 and 65 years and with Fitzpatrick skin types II and III were recruited into the study. There was a total of 136 test sites which were located on the flexor side of the forearms. The test sites were pre-treated by Tixel® (Novoxel® Ltd., Netanya, Israel) prior to topical application of a specific ALA/MAL formulation in a thin layer. The control side was not pre-treated by TMFI. The forearms were treated at four different settings in the low energy range of the device (low energy settings create less coagulation) in order to determine optimal treatment settings.

Baseline fluorescence measurements were performed 5 minutes after degreasing the skin in all test sites prior to treatment and/or drug application. Protoporphyrin IX (PpIX) fluorescence intensity readouts were taken after 0, 1, 2, 3, 4, and 5 hours post-application. As is common practice, the control sites of Ameluz and Metvix were covered by a nylon wrap for occlusion, and shielded by aluminum foil to prevent initiation of a photochemical reaction. The sites of the Levulan and compounded 20% ALA gel were only shielded by aluminum.

Permeation was quantified indirectly by measuring PpIX fluorescence intensity with a FluoDerm fluorescence photometer (Dia Medico ApS, Gentofte, Denmark). The FluoDerm photometer illuminates a site with a diameter of 45 mm on the surface of the skin by means of a pulsating blue light (385–415 nm high brightness light-emitting diodes. The corresponding fluorescence from PpIX was detected at 600–805 nm by averaging the fluorescence intensity over that area. The measurements were performed in absolute values in linear arbitrary FluoDerm units (FDUs).

Statistical Method

An analysis of variance model followed by the Scheffe post hoc test was applied to evaluate the effect of time and settings of drug uptake expressed by FDU readouts. A paired T test was applied to compare the effect of Tixel over control samples for each formulation. The significance level was defined as $\alpha = 0.05$. All analyses were carried out with SPSS 25.0 (IBM, Armonk, New York).

RESULTS

Figure 7 depicts the results for TMFI pretreated sites followed by topical application of compounded 20% ALA gel at different TMFI energy settings and those of nontreated controls during a period of 5 hours. The chart

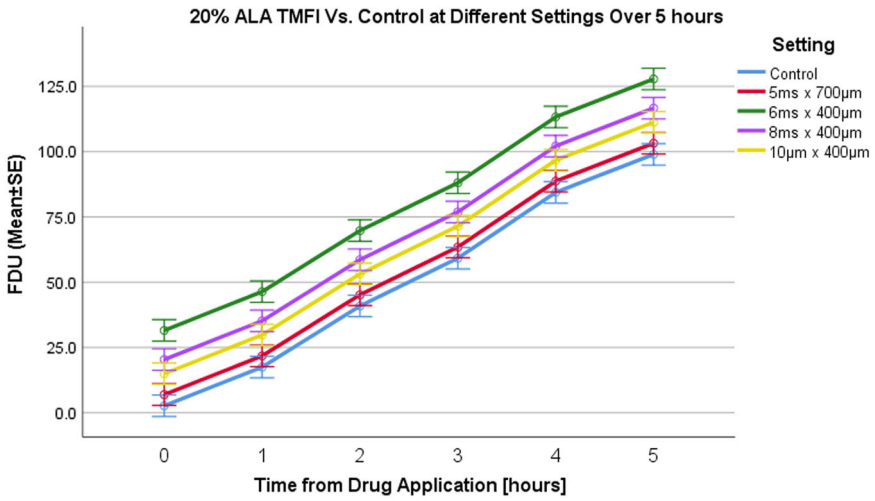

Fig. 7. 5-Amino-levulinic-acid hydrochloride (ALA) 20%—protoporphyrin IX (PpIX) fluorescence intensity (Y) for varying thermomechanical fractional injury (TMFI) operation settings over 5 hours (X). The chart displays the FluoDerm Unit (FDU) readouts taken at six time points following compounded 20% ALA gel application at baseline, and at 1, 2, 3, 4, and 5 hours after TMFI pretreatment at different settings. The optimum TMFI setting is 6 milliseconds × 400 µm, which is significantly higher than the control setting of 5 and 10 milliseconds ($P < 0.001$, $P < 0.001$, $P = 0.004$, respectively) [Color figure can be viewed at wileyonlinelibrary.com].

shows a linear pattern at all treatment and control settings. The FDU readings after TMFI treatments at 6 milliseconds × 400 µm were higher than at all other settings and of the control. The optimum TMFI setting was 6 millisesonds × 400 µm, which is significantly higher than the control and TMFI device setting at 5 and 10 milliseconds ($P < 0.001$, $P < 0.001$, $P = 0.004$, respectively).

Figure 8 presents FDU readouts of compounded 20% ALA gel at optimal TMFI settings (6 milliseconds × 400 µm) versus control settings over 1, 2, and 3 hours. This figure demonstrates the combined effect of time and optimal device setting ($P < 0.001$ for both). This implies that the TMFI-treated sites exhibited an hourly rate of increase in FDU readouts that was 156–176% higher than the control FDU readouts during the first 3 hours.

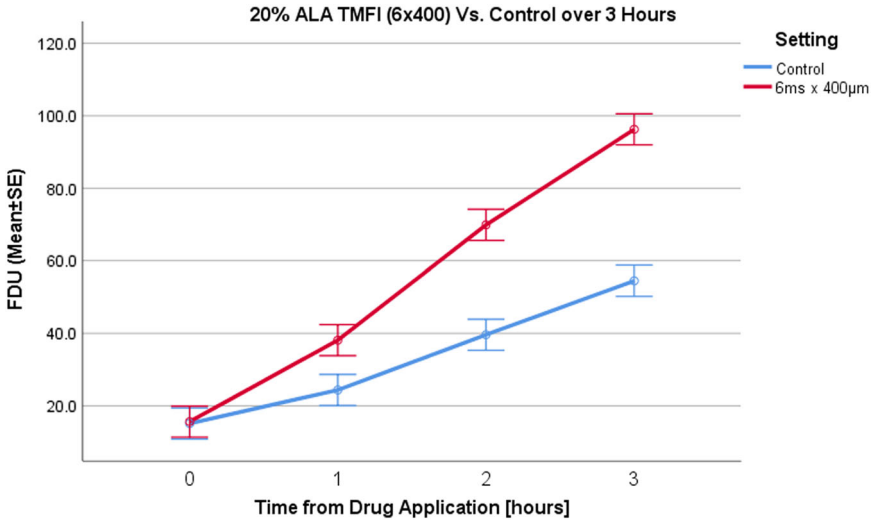

Fig. 8. The chart displays FluoDerm Unit (FDU) readouts of the compounded 20% 5-amino-levulinic-acid hydrochloride (ALA) gel at thermomechanical fractional injury (TMFI) (6/400) settings versus control settings over 1, 2, and 3 hours. The linear approximations are also shown. The TMFI-treated sites exhibited an hourly rate of increase in FDU readouts in the first 3 hours, which was twice that of the control sites. This figure demonstrates the combined effect of time and optimal device setting compared to that of the control ($P < 0.001$ for both) [Color figure can be viewed at wileyonlinelibrary.com].

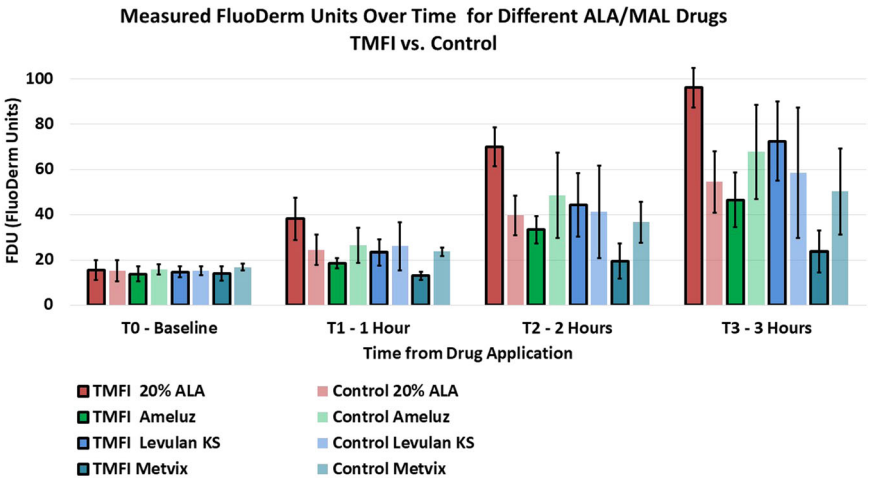

Fig. 9. Protoporphyrin IX (PpIX) fluorescence intensity (Y) for various drugs over time in hours (X). The chart displays the mean ± SD FluoDerm Unit (FDU) readouts taken at three periods of the thermomechanical fractional injury (TMFI) pretreated (6 milliseconds × 400 μm) 20% compounded 5-amino-levulinic-acid hydrochloride (ALA) drug, Levulan, Metvix, and Ameluz, and their controls. TMFI significantly enhanced uptake of the compounded 20% ALA gel compared with control after 1, 2, and 3 hours ($P = 0.058$, $P = 0.033$, $P = 0.016$, respectively). The increase after 1 hour was borderline [Color figure can be viewed at wileyonlinelibrary.com].

The results presented in Figure 9 compare standard topical application of all tested ALA/MAL drugs on untreated skin to that of TMFI at 6 milliseconds × 400 μm. All drugs were applied in accordance with the manufacturers' instructions. The PpIX fluorescence intensity was measured every hour from baseline up to 3 hours. TMFI significantly increased the uptake of compounded 20% ALA gel after 1, 2, and 3 hours ($P = 0.058$, $P = 0.033$, $P = 0.016$, respectively). The increase after one hour is borderline. TMFI did not enhance the uptake of any of the other vehicles.

DISCUSSION

This study demonstrates the success of TMFI pretreatment in enhancing the percutaneous permeation of ALA from the compounded 20% ALA gel as compared to control. TMFI pretreatment did not enhance percutaneous permeation of ALA when three selected commercial medications (Ameluz, Metvix, and Levulan Kerastick) were used. The prominent percutaneous permeation enhancement of ALA from the compounded gel formulation is due to a combination between the specific formulation and the TMFI's pretreatment technology.

TMFI thermal transfer to tissue is accomplished by the apexes of the tip's pyramids. They spread spatially, creating a hemispheric heat-affected zone (Fig. 5). Strains are formed inside the dehydrated layer when the tip moves forward onto the SC, generating cracks which allow drug permeation. The dimensions of the cracked layer are proportional to the dimensions of the pyramids' apexes.

A narrow-coagulated tissue layer is formed at short pulse durations (Fig. 5), and the tissue around the channel becomes dehydrated. The dry tissue creates a relatively high water concentration gradient between the liquid-based drug on the surface and the skin layers beneath it. Since the water content in the extracellular matrix is ~70%, it is expected that the dry tissue will be filled with water relatively quickly until the water concentration throughout the tissue will be equalized. Therefore, topical application of hydrophilic drugs must be performed immediately after the TMFI pretreatment. When the device is set to a short pulse of 6 milliseconds pulse duration and 400 μm protrusion the damaged stratum corneum (SC) area is wider than the coagulated tissue below. Hence the liquid can freely permeate into the skin in the gap between the two skin lesions. Results confirm that at 6/400 optimal flow conditions are created.

The four medical preparations used in this trial were designed to be applied on both intact skin as well as on skin lesions in order to permeate the SC. That challenge was best met by the Ameluz control formulation compared to the other three control preparations (Fig. 9). It was able to cross the 60 FDU line after 3 hours after application, and it did so with a 10% concentration of ALA, compared with the compounded medication (20% ALA), the Levulan Kerastick preparation (20% ALA), and the Metvix preparation (16.8% MAL). The Ameluz formulation represents a microemulsion gel, which combines oil-in-water dispersion of nano-sized (<50 nm diameter) vesicles composed of a lipid core surrounded by an emulsifying monolayer of phospholipids. This so-called nanoemulsion belongs to a class of microemulsions [13]. They are widely used in skin care and pharmaceutical formulations due to their biophysical properties that allow quick tissue penetration. This formulation contains four known chemical skin-penetrating enhancers: soybean phosphatidylcholine, polysorbate 80, isopropyl alcohol, and propyleneglycol [14,15].

Both the control arm of the compounded ALA gel and the Levulan Kerastick hydroalcoholic solution reached the 60 FDU line after 3 hours while Metvix reached the 50 DFU line during the same time. Thus, all four tested preparations succeeded in crossing the SC and in penetrating the percutaneous layer of the skin. The TMFI pretreatment technology removed the SC layer in a fractional manner and exposed the four preparations to the SG through the new micro-channels. It is reasonable to consider that preparations which adhere well to the skin's treated layer yielding longer contact time, will better penetrate the hydrophilic environment of the SG.

Viscosity is an important property of the preparation. Higher viscosity values can limit and attenuate the absorption of the hydrophilic molecules into the hydrophilic epidermal tissues. Also important are the physicochemical properties of the vehicle for solubilizing the penetrating molecule. As seen in Figure 9, only the compounded gel succeeded in taking advantage of the fractional perforation of the SC after 1, 2, and 3 hours after application. The average results of the TMFI 20% ALA column have a low standard deviation in comparison to other formulations. The compounded gel formulation is based on sepigel 305, which contains polyacrylamide, C13-14 isoparaffin, and laureth-7. It is a multifunctional vehicle with thickening, stabilizing, texturizing, and tissue-adhering properties in a wide pH range, including the acid environment needed to maintain ALA stability [16]. Oleic acid is a known enhancer of ALA penetration of the skin, with the best performance observed at a 10% concentration [17]. When dissolved and dispersed in water, sepigel 305 can emulsify oleic acid, which is a lipophilic agent [16]. The compounded formulation was shown to have a dual ability to overcome the SC barrier in the control arm, as well as to easily penetrate the epidermis and reach remarkable FDU levels after TMFI pretreatment compared with the control formulation and to the other formulations at 1, 2, and 3 hours after application (Table 1).

We hypothesize that the compounded preparation has good properties for adherence to the skin's treated layer, and adequate viscosity. The emulsion gel has appropriate physicochemical properties which enable ALA to have a high rate of percutaneous permeability. We assume that the Metvix formulation exhibited relatively poor performance due to the high viscosity of the lipophilic emulsion and the unsuitable physicochemical properties of the lipophilic cream. The Levulan Kerastick active arm with its hydroalcoholic solution demonstrated superiority over the control only 3 hours after drug application and with relatively high variability. Another hypothesis is that the main obstacle to penetration of the hydroalcoholic solution active arm into the viable epidermis is the rate of diffusion, since it took ~3 hours to accumulate in levels which are higher than the control. Another hypothesis is that the main penetration obstacle of the hydroalcoholic solution active arm into the viable epidermis is the rate of diffusion, as it took ~3 hours to surpass the control. We believe the results of this preparation demonstrate a constant flux of ALA into the skin but in a slow rate.

TABLE 1. TMFI Pretreatment Parameters

# Setting	Pulse duration (ms)	Protrusion (mm)	Energy (mJ/micropore)
1	5	700	0.13
2	6	400	0.15
3	8	400	0.17
4	10	400	0.19

The ability of TMFI pretreatment technology to prominently enhance ALA's percutaneous permeation using the compounded gel preparation resembles the performance of AFXL as reported by Choi et al. [11] at 10 and 20 mJ per micropore. Notably, TMFI applies 0.15 mJ per micropore at 6 milliseconds×400 μm. Due to this low level of energy, TMFI treatments are performed without analgesic creams, and there is no smoke, smell, bleeding, or oozing.

The transdermal effect created by the CO_2 laser is different compared with the effect of TMFI. The laser ablates the SC and creates a deep channel in the dermis surrounded by a thick coagulated tissue. Haedersdal et al. [18] showed that the differences between the PpIX fluorescence readout of MAL (98.6 AU) and ALA (112 AU) at 3 hours following CO_2 laser treatment are much smaller compared with those obtained in the current study. When drug is applied (hydrophilic or lipophilic) on the skin, it fills the vertical channels and diffuses through the coagulation layer. This process depends less on the drug carrier formulation. This study further substantiates the evidence introduced by earlier studies of low-energy TMFI pretreatments for PDD. Friedman et al. [19] reported treatment of rosacea with botulinum toxin following TMFI pretreatment, and Sintov et al. [20] described the permeation of several hydrophilic molecules after TMFI pretreatment in an ex vivo study.

Conclusions

TMFI treatment seems to provide an alternative, radiation-free, low-energy approach for effective delivery of compounded 20% ALA gel. The formulation's characteristics have a major and crucial influence on the ability of TMFI pretreatment to significantly increase percutaneous permeation of ALA and MAL. Further research should include a larger sample size, the evaluation of drug penetration depth profile over time, and the use of various vehicles and delivery modalities. Treatment factors, such as pain level and human variables, should be examined as well.

ACKNOWLEDGEMENTS

Eyal Zur, RPh, contributed the pharmaceutical contents of this paper. The study was funded by Novoxel Ltd.

REFERENCES

1. Uchida Y, Park K. Stratum corneum. In: Kabashima K, editor. Immunology of the Skin: Basic and Clinical Sciences in Skin Immune Responses. Tokyo, Japan: Springer; 2016. pp 15–30.
2. Warner RR, Myers MC, Taylor DA. Electron probe analysis of human skin: Determination of the water concentration profile. J Invest Dermatol 1988;90:218–224.
3. Stockdate M. Water diffusion coefficients versus water activity in stratum corneum: A correlation and its implications. J Soc Cosmetic Chemists 1978;29:625–639.
4. Wildnauer RH, Bothwell JW, Douglass AB. Stratum corneum biomechanical properties I. Influence of relative humidity on normal and extracted human stratum corneum. J Invest Dermatol 1971;56(1):72–78.
5. Cengel YA. Heat transfer, a practical approach. 2nd edition. New Jersey: McGraw-Hill; 2003.
6. Alkilani AZ, McCrudden MTC, Donnelly RF. Transdermal drug delivery: Innovative pharmaceutical developments based on disruption of the barrier properties of the stratum corneum. Pharmaceutics 2015;7:438–470. https://doi.org/10.3390/pharmaceutics7040438.
7. Erlensson AM, Wenande E, Haedersdal M. Transepidermal drug delivery: Overview, concept, and applications. Lasers Lights Other Technol 2017 https://doi.org/10.1007/978-3-319-20251-8_34-l.9.
8. Ibrahim O, Wenande E, Hogan S, Arndt KA, Haedersdal M, Dover JS. Challenges to laser-assisted drug delivery: Applying theory to clinical practice. Lasers Surg Med 2018;50(1):20–27.
9. Wenande E, Olesen UH, Nielsen MMB, Janfelt C, Hansen SH, Anderson RR, Haedersdal M. Fractional laser-assisted topical delivery leads to enhanced, accelerated and deeper cutaneous 5-fluorouracil uptake. Expert Opin Drug Deliv 2017;14(3):307–317.
10. Banzhaf CA, Wind BS, Mogensen M, Meesters AA, Paasch U, Wolkerstorfer A, Haedersdal M. Spatiotemporal closure of fractional laser-ablated channels imaged by optical coherence tomography and reflectance confocal microscopy. Lasers Surg Med 2016;48(2):157–165.
11. Choi JH, Shin EJ, Jeong KH, Shin MK. Comparative analysis of the effects of CO_2 fractional laser and sonophoresis on human skin penetration with 5-aminolevulinic acid. Lasers Med Sci 2017;32:1895–1900. https://doi.org/10.1007/s10103-017-2305-8.
12. Holman JP Heat Transfer. McGraw-Hill series in mechanical engineering. 10th edition. 2010. ISBN 978-0-07-352936-3–ISBN 0-07-352936-2.
13. Biofrontera company website: The Secret Behind Ameluz® (aminolevulinic acid hydrochloride) gel, 10% Ameluz. http://www.biofrontera.us.com/nanoemulsion/.
14. US Full Prescribing Information for Ameluz®, Updated September 20, 2018. https://dailymed.nlm.nih.gov/dailymed/drugInfo.cfm?setid=650daa9f-aeec-49ce-95b9-5fa20b988afd
15. Baroli B. Penetration of nanoparticles and nanomaterials in the skin: Fiction or reality? J Pharm Sci 2010;99:21–50.
16. Seppic company website: SEPIGEL 305™ The Pioneer of Liquid Multifunctional Polymers. https://www.seppic.com/sepigel-305.
17. Pierre Riemma MB, Ricci E, Jr, Tedesco CA, et al. Oleic acid as optimizer of the skin delivery of 5-aminolevulinic acid in photodynamic therapy. Pharm Res 2006;23(2):360–366.
18. Haedersdal M, Sakamoto FH, Farinelli WA, Doukas AG, Tam J, Anderson RR. Pretreatment with ablative fractional laser changes kinetics and biodistribution of topical 5-aminolevulinic scid (ALA) and methyl aminolevulinate (MAL). Lasers Surg Med 2014;46:462–469. https://doi.org/10.1002/lsm.22259.
19. Friedman O, Koren A, Niv R, Mehrabi JN, Artzi O. The toxic edge—A novel treatment for refractory erythema and flushing of rosacea. Lasers Surg Med. 2018 https://doi.org/10.1002/lsm.23023.
20. Sintov A, Hofmann MA. A novel thermo-mechanical system enhanced transdermal delivery of hydrophilic active agents by fractional ablation. Int J Pharm 2016;511(2):821–830.

Contact Lens and Anterior Eye xxx (xxxx) xxx

Contents lists available at ScienceDirect

Contact Lens and Anterior Eye

journal homepage: www.elsevier.com/locate/clae

The effect of non-ablative thermomechanical skin treatment (Tixel®) on dry eye disease: A prospective two centre open-label trial

Sunil Shah [a,b], Debarun Dutta [a], Ankur Barua [b], Ludger Hanneken [c], Shehzad A. Naroo [a,*]

[a] College of Health and Life Sciences, Aston University, Birmingham, UK
[b] Midland Eye, Solihull, UK
[c] Vallmedic Vision, Andorra

ARTICLE INFO

Keywords:
Tixel®
Ocular surface
Tear film
Dry eye disease
Tear osmolarity

ABSTRACT

Purpose: To determine the effects of a thermo-mechanical action-based peri-orbital fractional skin treatment (Tixel®) on dry eye disease.

Methods: This prospective, controlled, open labelled study was conducted at two study centres: Midland Eye, Solihull, UK, and Vallmedic Vision, Andorra. Participants were screened at the baseline visit (visit-1), received three Tixel® treatments at 2-weeks intervals including further assessment (visits 2, 3 and 4). Participants were followed up for three months post-treatment (visit 5). Vision, intraocular pressure (IOP), dry eye symptomatology were assessed, including the Ocular Surface Disease Index (OSDI) questionnaire, non-invasive tear break-up time (NIBUT) and tear osmolarity as well as detailed ophthalmic assessments.

Results: Seventy-four participants (41 in Birmingham and 33 in Andorra) with periorbital wrinkles and moderate to severe dry eye disease (DED) were enrolled. The mean age was 59.3 ± 13.3 years and 57 were females. No adverse events, no change in vision ($p = 0.310$) or IOP ($p = 0.419$) were observed. Tixel treatment was associated with clinically and statistically significant improvement in the DED symptoms, which was supported by a reduction of 21.40 ± 15.08 ($P < 0.001$) of the OSDI index. Non-invasive tear break-up time improved by 2.10 ± 0.91 s ($p < 0.001$) in the Birmingham cohort and 6.60 ± 2.13 s ($p < 0.001$) in the Andorra cohort. Tear osmolarity reduced from 299.8 ± 13.3 mOsm/L to 298.8 ± 15.6 mOsm/L following the Tixel treatment ($p = 0.271$).

Conclusions: Thermo-mechanical action-based *peri*-orbital fractional skin treatment Tixel® could be an attractive, safe and effective treatment for DED. This treatment is associated with high clinical and statistically significant improvement in DED signs and symptoms with no adverse events.

1. Introduction

Dry eye disease (DED) is a common and potentially debilitating disease that has been characterised by loss of tear homeostasis associated with numerous symptoms, such as itchy, sore, gritty and red eyes [1]. The loss of tear stability is a hallmark of DED where hyperosmolarity, ocular surface inflammation and damage, neurosensory abnormalities contribute aetiological roles [1]. The severity of DED can vary person to person, but the incidence is higher with age, prolonged computer user, contact lens wearers and people who have undergone recent ocular surgery [2]. Evaporative type DED is the commonest aetiological subtype which is frequently caused by underlying meibomian gland dysfunction (MGD). MGD is marked by an increased viscosity and melting point of the meibomian gland secretions leading to blockage and inflammation of the ductal system. Thus, MGD can trigger the vicious circle of tear film hyperosmolarity, evaporation, instability and inflammation. It is this vicious circle that needs to be broken to manage dry eye by intervening at any stage in the circle.

It is estimated that DED currently affects more than 344 million people worldwide including over 30 million in the United States [1]. Studies conducted in Asia (China, Japan, South Korea), and Europe (England, France) demonstrated the prevalence ranged from 4.1 % to 23.7 % [3].

DED is expensive for the economy and for an individual. It costs approximately US$ 3.84 billion from a taxpayer's perspective and as much as US$55.4 billion to society within the United States [4].

* Corresponding author.
E-mail address: s.a.naroo@aston.ac.uk (S.A. Naroo).

https://doi.org/10.1016/j.clae.2022.101811
Received 12 March 2022; Received in revised form 16 December 2022; Accepted 30 December 2022

Similarly, the mean annual direct cost per patient due to DED in the UK has been estimated at £525, including a significant indirect loss of work productivity [5].

Thermo-mechanical action (TMA®) is a relatively new technique used until now for aesthetic indications (Fig. 1). Heat is transferred directly onto the skin by a matrix of tiny pyramid-shaped pins made of biocompatible materials covering a treatment area of 1 cm^2 for the large therapeutic element (the tip) and 0.3 cm^2 for the small tip one which is used for the treatment of the eyelids. The pins are heated to a temperature of 400 °C, which rapidly transfers thermal energy (0.16 millijoules/pin) upon brief contact with the skin which only lasts for a few milliseconds (the contact duration and extent of thermal resistance of the tip with the skin can be set by the user). TMA® delivers thermal energy creating localised tissue coagulation. It is indicated for treatment of actinic keratosis and has been demonstrated in clinical studies also for the treatment of ageing skin [6,7], *peri* orbital wrinkles [8] facial rejuvenation [9], rosacea [10] acne vulgaris [11] and hypertrophic scars [12].

Many of the patients receiving TMA® based fractional skin treatment such as Tixel® for *peri*-orbital wrinkles are aged 50 years or older and suffer from DED. It was an observation by one of the co-authors (LH) that patients were experiencing a significant improvement of DED symptoms following aesthetic treatment sessions with Tixel®. This preliminary observation led to designing this prospective controlled open-label trial to characterise the effect of Tixel® treatment in alleviating DED and the associated signs and symptoms in those undergoing treatment for wrinkles.

2. Methods

2.1. Participants

A prospective, controlled open labelled study was conducted at two international sites: Midland Eye, UK, and Vallmedic Vision, Andorra. A total of 74 participants with DED were recruited. The study followed the declaration of Helsinki, received approval from the respective Institutional Human Ethics Committee and registered with ClinicalTrials.gov (NCT04730336). Written informed consent was received from all participants. Participants were provided with an emergency contact number for reporting any adverse event during the study, alternatively they were suggested to contact the clinical study centre for any emergency.

Strict inclusion criteria were employed prior to the recruitment of participants for this study. All participants were required to fulfil the following criteria: above 18 years of age; an Ocular Surface Dryness Index (OSDI) score of at least 23; a non-invasive tear break up point (NIBUT) <10 s; have *peri*-orbital wrinkles, no history of ocular surgery; no ocular medication and dry eye treatment other than artificial tears within the last 3 months; and able to attend for all five study visits. Presence of *peri*-orbital wrinkles was visually confirmed but was not measured in this study. The exclusion criteria for this study were: pregnant or lactating women; existing lesions or medication for the ocular or orbital area; acute ocular disease; significant blepharitis; outdoor or sunbed tanning with the last four weeks of participating the study; impaired immune system; history of bleeding coagulopathies; and use of anticoagulants. Blepharitis was graded followed Efron grading scale, anyone having blepharitis more than 3 was excluded.

2.2. Tixel treatment

Fractionated treatment of the eyelid skin was performed using Tixel® (Novoxel, Israel) equipped with the smaller Tixel tip consists of 24-pins (Fig. 1). The total surface of the tip which had 4 × 6 pyramids was 0.3 cm^2. Preorbital area including the upper and lower lid area as shown in the Fig. 1 were treated. The tip base temperature was maintained at 400 °C during treatment and superficial non-ablative tissue coagulation (250 μm deep, 300 μm diameter) induced by the quick protrusion and contact of the heated tip directly onto the periorbital skin surface. The contact duration in milliseconds and the extent of thermal matching (protrusion, in microns) is normally customised by the user. For the current study, the contact duration was standardised at all sites to 8 ms and protrusion was set to 400 μm as a single contact/shot (0.16 millijoules energy per point).

2.3. Study design

A total of 40 shots in the *peri*-orbital area during each treatment: 10 per eyelid, were placed directly on to the upper and lower eyelid skin. In one of the sites, Birmingham, the eye lids were anaesthetised with lignocaine 5 % cream for 15 min with a standard wrinkle treatment regime. In Andorra analgesic cream was not applied on any of the patients. Treatment required about 2 min for both eyes combined. Since the device does not emit radiation, eye shields were not required.

This study followed the tenets of good clinical practice. The activities and clinical assessment for each of the study visits are detailed in Table 1 and with a flow chat in Fig. 2. Three Tixel treatments were delivered at 2-weeks intervals. Participants were followed up over three months from last treatment with a total of five study visits, no additional maintenance therapy was adviced. Best corrected visual acuity was measured using a LogMAR visual acuity chart. Dry eye symptoms were assessed using the Ocular Surface Dry Index (OSDI) questionnaire, and participants were stratified for analysis by mild, moderate and severe dry eye symptoms based on criteria previously published.[13] The two sites performed

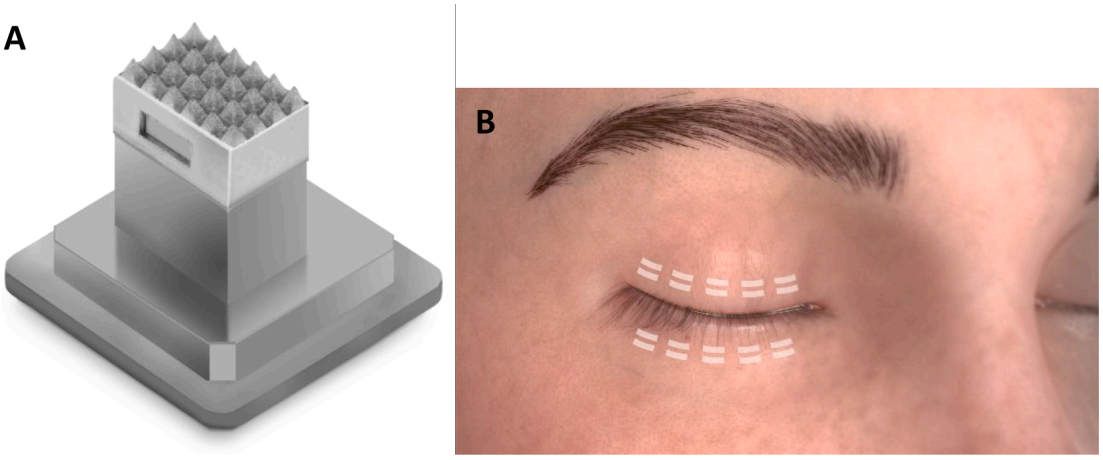

Fig. 1. (A) Titanium 24-pin Tip used for thermomechanical heat transfer to tissue. (B) Area of upper and lower lid for Tixel treatment shown in an animation.

Table 1
Details of the sequential clinical assessments and activities for each study visits.

Procedure	Visit 1 Treatment 1 T_0	Visit 2 Follow-up 1 followed by Treatment 2 $T_0 + 2w$ (±5days)	Visit 3 Follow-up 2 followed by Treatment 3 $T_0 + 4w$ (±5days)	Visit 4 Follow-up 3 $T_0 + 6w$ (±5days)	Visit 5 Follow-up 4 $T_0 + 18w$ (±5days)
Maximum duration for follow up	–	2 weeks± 5 days	4 weeks± 10 days	6w± 15 days	18w± 20 days
Participant screening, informed consent, detailed history, enrolment based on inclusion/ exclusion criteria, detailed ophthalmic examination	X				
For females - verbal Inquiry regarding pregnancy	X	X	X	X	X
OSDI questionnaire	X	X	X	X	X
Non-invasive tear break up time	X	X	X	X	X
Tear Osmolarity	X	X	X	X	X
Slit lamp examination, including lid margin profile	X	X	X	X	X
Intraocular pressure measurement	X	X	X	X	X
Concomitant therapy/medication (including ocular)	X	X	X	X	X
Periorbital general skin examination prior to treatment or follow up	X	X	X	X	X
Tixel® Treatment	X	X	X		
Post treatment care	X	X	X	X	X

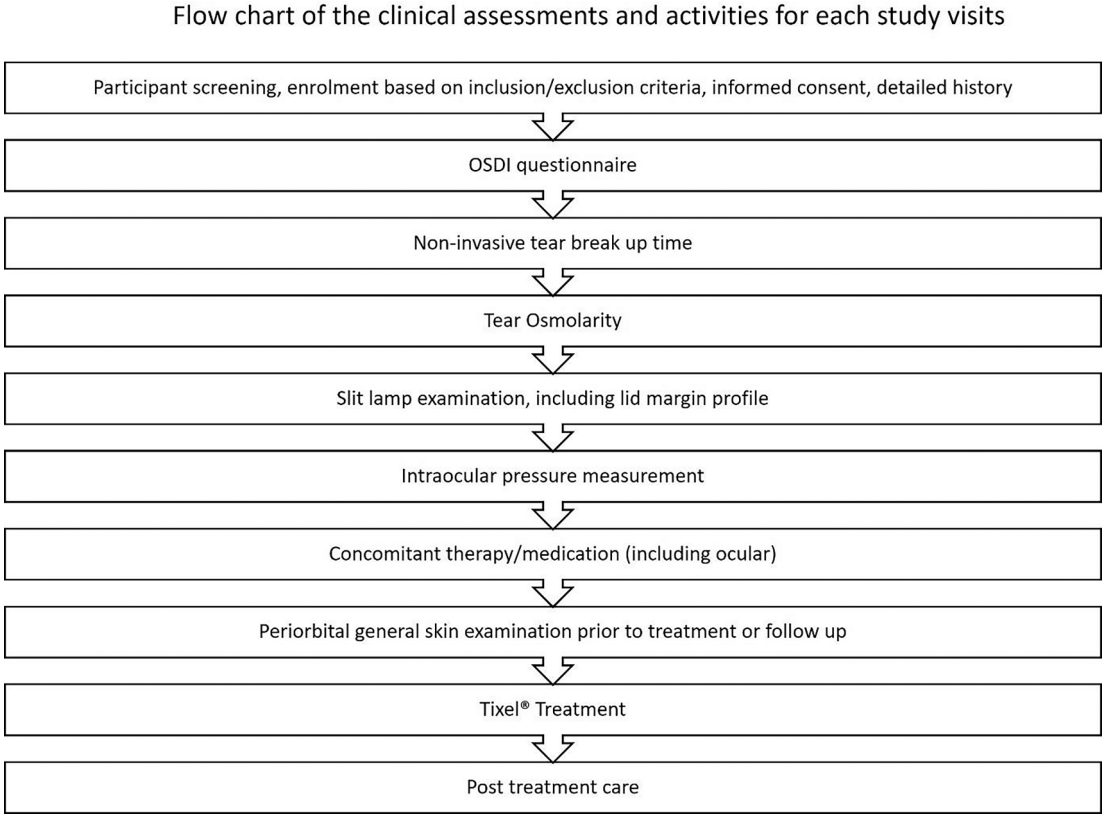

Fig. 2. Flow chart of the clinical assessments and activities for each study visits.

NITBUT and with the equipment available. Three measurements were taken, the average NIBUT was assessed using Oculus® Keratograph 5 M (Oculus®, Arlington, WA, USA) at the UK centre and automatic measurement by Sirius (CSO Costruzione Strumenti Oftalmici, Florence, Italy) at the Andorra centre. Tear osmolarity (TearLab, California, USA) was measured from the lower lateral canthal tear meniscus as per the Tearlab protocol. Detailed slit-lamp examination and measurement of intraocular pressure (IOP) by Goldmann applanation tonometry were also performed.

2.4. Statistical analysis

All data were analysed using Excel (Microsoft Office, Redmond, WA, USA), Graph Pad Prism version 8.01 (California, USA), or Statistical Package for Social Sciences (SPSS) for Windows software version 23.0 (IBM SPSS NY, USA). Sample size was calculated using G*Power version 3.1.9.4, which determined a total of 68 participants were required for the desired study power. The effect size dz was determined to be 0.446 based on a pilot study where NIBUT was the designated outcome to detect a clinically significant difference of 5.0 s following treatment at 80 % power ($\beta = 0.2$) and statistical significance level of 5 % ($\alpha = 0.05$),

with the standard deviation estimated to be approximately 5.5 s.

Results are presented as mean ± standard deviation (SD) including their descriptive statistics. Clinical data were collected from both the eyes, however, data that were randomly selected from one eye, right eye, in this case, were analysed in this study. A two-way mixed model analysis of variance (ANOVA) testing was conducted to determine the significance of treatment, followed by confirmation of normal distribution by Kolmogorov-Smirnov test. Categorical data were analysed with using chi-squared or Fisher's exact test based on the variable.

3. Results

Sixty-eight participants were required to determine clinically and statistically significant difference. A total of 74 participants (57 females and 17 males) were included in this study. 74, 74, 71, and 63 participants completed visit 2, 3, 4 and 5 respectively. Each study visit was about 45 min to one hour.

The mean age of all the participants was 59.3 ± 13.3 years (range 23 to 79 years). At Midland Eye, UK 41 participants were recruited: 41, 41, 38, and 34 participants completed visits 2, 3, 4 and 5 respectively. At the Andorra study centre, 33 participants were recruited, all the participants completed visit 2, 3, and 4, and 29 participants completed visit 5. Recruitment was within periods of COVID lockdown explaining some of the later dropouts.

There were no serious adverse events associated with the Tixel® treatment to the skin of the eyelids during this trial. No other safety-related event was observed.

Table 2 shows the results for the clinical measurements that were conducted during each visit. No major change with the visual acuity ($p = 0.310$) and IOP ($p = 0.419$) were observed during this study (Table 2).

3.1. Tear break-up time

Following three Tixel treatments, the NIBUT significantly improved for the groups of participants recruited at both sites ($p < 0.05$). For the UK cohort, NIBUT improved from 5.0 ± 2.6 s to 7.1 ± 1.3 s ($p < 0.001$, Fig. 3A), for the Andorra cohort it improved from 6.5 ± 3.1 to 13.2 ± 3.2 s ($p < 0.001$; Fig. 3B). It should be noted that the severity of initial NIBUT was different at the 2 sites.

3.2. Osmolarity

The combined tear osmolarity changed from 299.8 ± 13.3 mOsm/L at the start of this study to, 299.8 ± 12.8, 300.0 ± 11.7, 299.7 ± 10.1, and 298.8 ± 13.4 mOsm/L at visits 2, 3, 4 and 5 respectively. The overall improvement (reduction) of tear osmolarity was 1.0 ± 0.5 mOsm/L, which was not statistically significant ($p = 0.271$).

3.3. OSDI scores

A total of 80 % of participants had severe symptoms (33–100 OSDI index score), out of the rest 20 % had moderate (23–32 OSDI index score) symptoms at the baseline visit. By the end of the study, this proportion had changed to 36 %, 8 %, and 26 % having reported severe, moderate and mild dry eye symptoms respectively with 30 % reporting no dry eye symptoms. The OSDI index for the UK and Andorra cohort was 49.81 ± 16.44 and 45.49 ± 17.05 respectively, the difference was not statistically significant ($p = 0.318$).

The mean DED symptoms at visits 1, 2, 3, 4 and 5 were recorded as 47.47 ± 18.62, 35.76 ± 16.40, 32.02 ± 15.53, 28.00 ± 13.87 and 26.04 ± 13.69 respectively by the OSDI index score (Fig. 4). Overall, the results demonstrated a mean 21.43 ± 13.07 OSDI index score improvement during this study for all participants ($p < 0.001$). Results also showed clinically significant improvements with dry eye symptoms when a sub-analysis was performed as characterised by 18.0 ± 6.7 and 33.4 ± 9.2 OSDI index improvement for patients with moderate and severe dry eye symptoms at baseline respectively, indicating a larger improvement for more severe symptoms. Fig. 5 details the improvement of the OSDI index scores during the study stratified by the severity of DED.

4. Discussion

This prospective multicentre clinical trial reports the effect on DED symptoms of TMA® based fractional skin treatment around the *peri*-orbital area. It shows that Tixel can significantly improve DED signs and symptoms when followed for three months after treatment.

Tixel® is a radiation-free treatment, that has been deemed safe on the *peri*-orbital skin earlier [14]. There were no serious adverse events reported during the study.

The treatment did not affect the visual acuity and IOP. It was well accepted by patients and was very easy and quick to perform. Improvement in skin wrinkles was not an outcome measure for this study but the parameters used were the ones that are used for wrinkle treatments.

The study design for this proof-of-concept study was to perform 3 Tixel treatments at 2-week intervals (similar to a possible treatment protocol for DED patients undergoing treatment with intense pulsed light (IPL). The trend with DED signs and symptoms observed in this study confirms three Tixel treatment as an effective strategy for alleviating DED related signs and symptoms.

The improvements observed with DED symptoms were clinically significant. This was characterised by an improvement of 18.0 ± 6.7 (for moderate dry eye) and 33.4 ± 9.2 (for severe dry eye) OSDI index score for DED participants. The minimum clinically important difference (MCID) suggested by the Tear Film Ocular Surface Dry Eye Workshop (TFOS DEWS II) subcommittee for the same is up to 7.3 and 13.4 OSDI index scores respectively [2]. The mean improvement with symptoms recorded in this study was an OSDI index score of 21.4 which is higher than previously observed by Xue et al. [15] with IPL treatment and similar to reported by Tauber et al. [16] with iLux (Alcon, Fort Worth, TX, USA) treatment.

Significant improvement of NIBUT 2.1 and 6.6 s observed at the two trial centres [2]. This is higher than previously reported with IPL treatment [15], and iLux treatment [16]. This study could be improved by using the same instruments for measurement of NIBUT at each site, however, as a proof of concept study, this clearly shows improvements in both sites albeit with some variations. Andorra cohort had NIBUT baseline 1.5 s higher than the UK cohort, which could be due to higher relative humidity in Andorra compared to Birmingham (UK centre). Due to Covid restrictions, several participants towards the end of the study were recruited more than six months after the first-batch of participants. There are a number of other potential causes for the difference in the two sites – different instrumentation for measurements, different patient mix, different climate eg Andorra is at high altitude.

Osmolarity has been regarded to be the best single objective test for

Table 2
Clinical measurements conducted at baseline (visit-1), and during visit-2, visit-3, visit-4, and visit-5. P-value represents statistical significance. Asterisks* denotes statistically significant difference.

Measurement	Baseline (Visit-1)	Visit-2	Visit-3	Visit-4	Visit-5	Overall change	P-value (statistical significance)
Best corrected visual acuity (log MAR)	0.47 ± 0.21	0.03 ± 0.11	0.02 ± 0.10	0.04 ± 0.13	0.56 ± 0.19	0.00 ± 0.00	0.310
Intraocular pressure (mm of Hg)	14.6 ± 3.4	14.8 ± 3.5	14.1 ± 3.5	14.5 ± 3.1	14.0 ± 3.5	0.6 ± 0.1	0.419

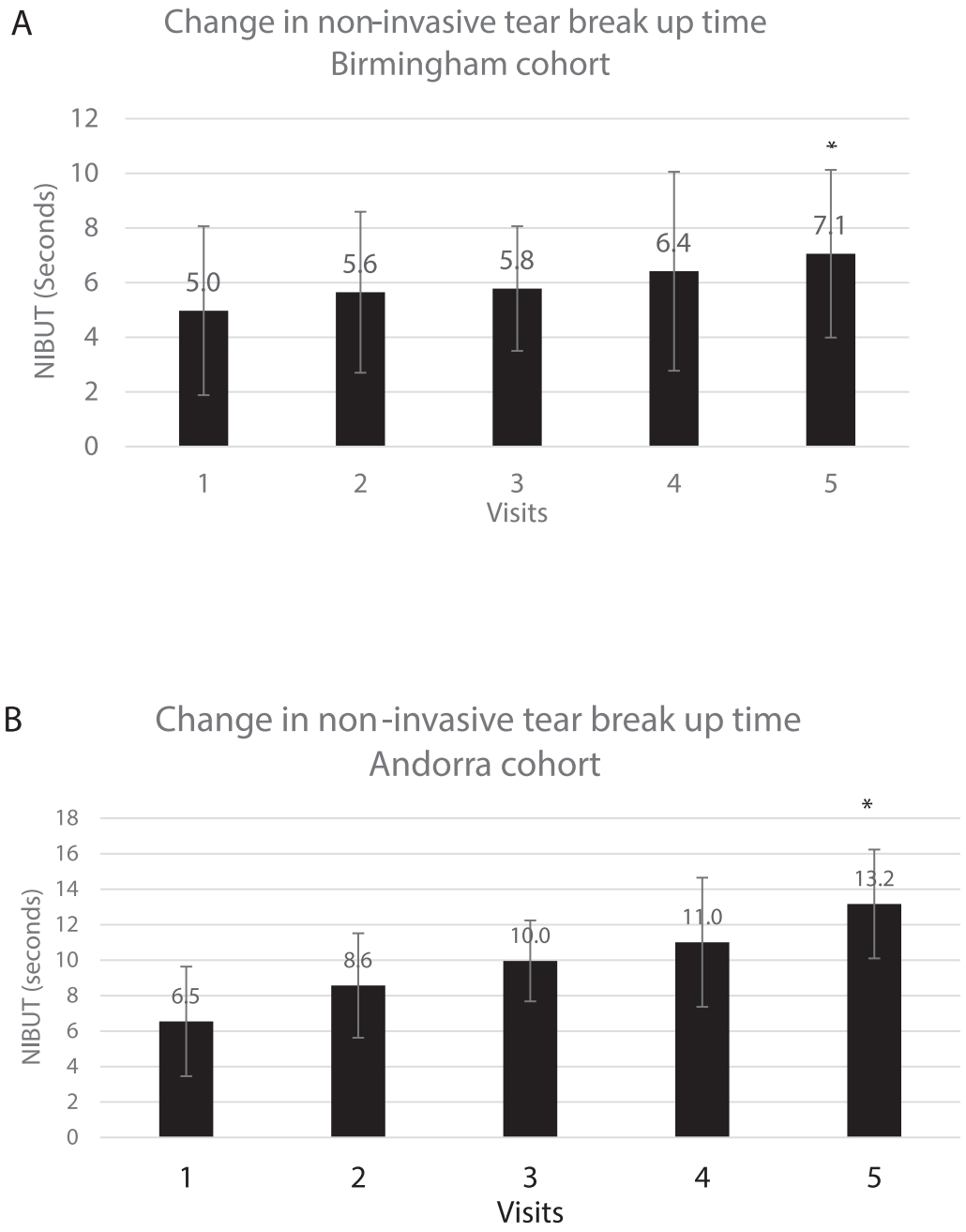

Fig. 3. Change of average non-invasive tear break up time during the study; (A) observation made in Birmingham cohort, the change was statistically significant compared to baseline visit-1 (*), (B) observation made in Andorra cohort; the change was statistically significant compared to baseline visit-1 (*).

the assessment of DED [17–19]. Following Tixel, mean tear osmolarity changed from 299.8 ± 13.3 mOsm/L before treatment to 298.8 ± 10.7 mOsm/L after treatment, indicating a minor reduction of tear osmolarity by 1.0 mOsm/L. This change was not statistically significant and fell short of the suggested MCID of 5.0 mOsm/L as suggested by TFOS DEWS II, it is a larger reduction than previously reported with IPL and LipiFlow [15,20,21].

The mechanisms of action of Tixel® treatment that underpin clinical improvements in DED patients are still under investigation. Several possible hypotheses can be tabled. Firstly, thermal energy transferred by Tixel® could help liquefy the inspissated meibum. This may open ductal obstruction and promote the release of liquid of meibum further improving quality of tear film lipid layer and shielding aqueous tear from undue evaporation. It is possible that Tixel reduces the microbial load of the periorbital and periocular area, thus can alter host immune and inflammatory responses. Other possible mechanisms may include reduction of epithelial turnover, fibroblast activation and modification of pro-inflammatory cascades leading to reduced ocular surface inflammation or that modification of growth factors from healing from the skin. It is likely more than one mechanism is involved following Tixel® in reducing DED signs and symptoms. Further research is ongoing to investigate these hypotheses.

There are limitations to this study. It started participant recruitment prior to the SARS-CoV-2 pandemic and faced challenges with following up research participants, particularly for the 3-months follow up (visit 5). Given the multinational nature of this study, the travel restrictions of different nations varied considerably which influenced the visit 5 attendance: in particular, this affected Andorra, where there were several cross-border patients. The NIBUT was measured in different study centres using different instruments, in Andorra without analgesia,

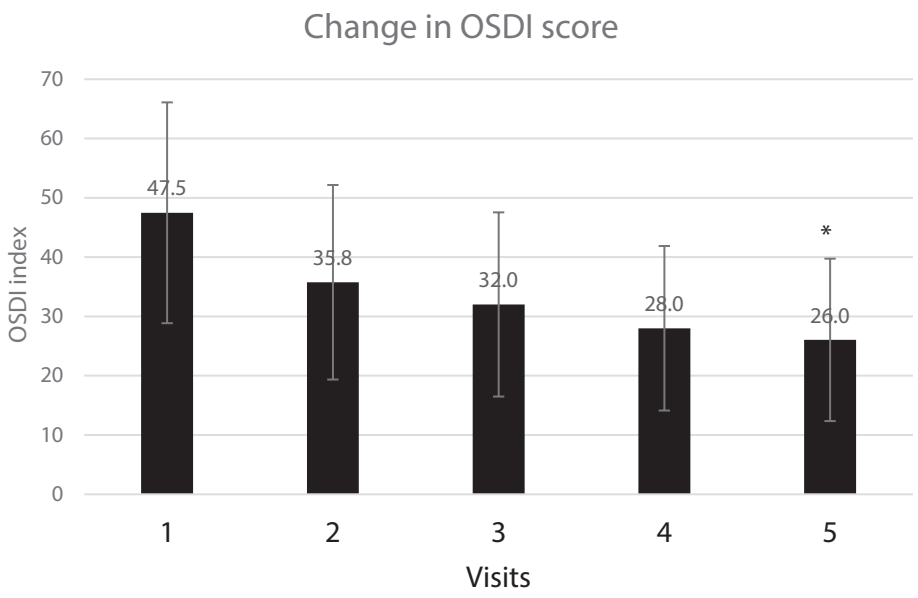

Fig. 4. Change of ocular symptoms measured by the ocular Surface Disease Index (OSDI) questionnaire during the study period; the change was statistically significant compared to baseline visit-1 (*).

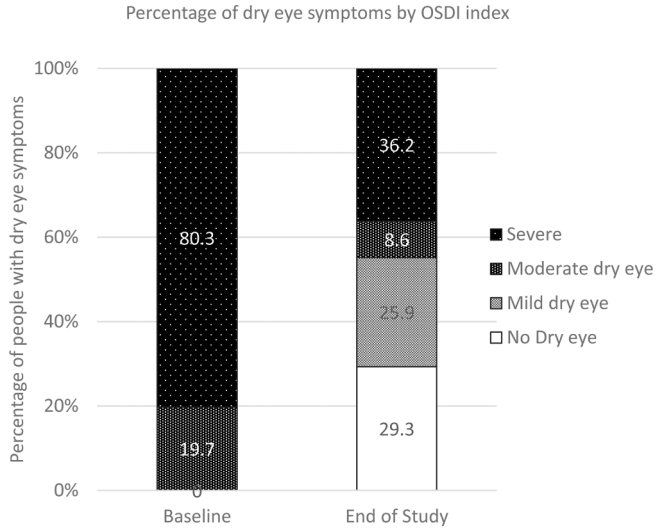

Fig. 5. Improvement of dryness stratified by the severity of ocular symptoms, measured by OSDI questionnaires during the study period.

in Birmingham lignocaine 5 % cream was applied. These factors may have had an influence on the results. Tixel treatment include heating sensation in the treatment area such as ocular adnexa and lid margin, which makes it is challenging to add a placebo group or employ double masking. However, participants recruited at all the study centres observed significant improvement with the measurement of tear break uptime. In addition, this study did not include assessments corneal staining and meibomian gland dysfunction such as meibomian gland scoring and assessment of meibum quality. It is expected that this treatment will improve the meibomian gland secretions and the authors are currently running further studies to characterise this.

The treatment protocol of 3 consecutive Tixel treatments was based on similar studies with IPL. It is not known whether more Tixel treatments would be beneficial and the period between treatments that would give the best results. The duration of benefit also needs to be investigated and whether a further treatment 6 or 12 months later as a 'top up' would be beneficial, given the chronic nature of MGD and DED.

In conclusion, Tixel treatment offered significant improvement in DED symptomatology, tear break up time, and most importantly improved tear homeostasis in this prospective two centre trial. The findings confirm that three Tixel treatments, each with a two-week interval provide encouraging clinical outcomes. These results appear to show at least comparable, and in many cases, superior results to other commercially available DED treatments and management regimes, making it a highly attractive treatment for DED.

5. Funding source

Novoxel partly funded the clinical trial in Andorra site. Both the authors Ludger Hanneken and Sunil Shah are the advisors of Novoxel.

6. Conflict of interest and disclosure

This work is original, has not been published and is not being considered for publication elsewhere. The authors received part funding from Novoxel to run this prospective study, However Novoxel was not involved in designing the study protocol, collecting or analysing the data, nor the writing of the paper.

Declaration of Competing Interest

The authors declare that they have no known competing financial interests or personal relationships that could have appeared to influence the work reported in this paper.

.

References

[1] Craig JP, Nichols KK, Akpek EK, Caffery B, Dua HS, Joo C-K, et al. TFOS DEWS II definition and classification report. Ocul Surf 2017;15(3):276–83.
[2] Wolffsohn JS, Arita R, Chalmers R, Djalilian A, Dogru M, Dumbleton K, et al. TFOS DEWS II diagnostic methodology report. Ocul Surf 2017;15(3):539–74.
[3] Stapleton F, Alves M, Bunya VY, Jalbert I, Lekhanont K, Malet F, et al. TFOS DEWS II epidemiology report. Ocul Surf 2017;15(3):334–65.
[4] Yu J, Asche CV, Fairchild CJ. The economic burden of dry eye disease in the United States: a decision tree analysis. Cornea 2011;30:379–87. https://doi.org/10.1097/ICO.0b013e3181f7f363.
[5] McDonald M, Patel DA, Keith MS, Snedecor SJ. Economic and humanistic burden of dry eye disease in Europe, North America, and Asia: a systematic literature review. Ocul Surf 2016;14:144–67. https://doi.org/10.1016/j.jtos.2015.11.002.

[6] Elman M, Fournier N, Barneon G, Bernstein EF, Lask G. Fractional treatment of aging skin with Tixel, a clinical and histological evaluation. J Cosmet Laser Ther 2016;18:31–7. https://doi.org/10.3109/14764172.2015.1052513.
[7] Oren-Shabtai M, Sloutsky N, Lapidoth M, Mimouni D, Chorny I, Snast I, et al. Efficacy and safety of a thermal fractional skin rejuvenation system (Tixel) for the treatment of facial and/or scalp actinic keratoses. Lasers Med Sci 2022;37(7): 2899–905.
[8] Salameh F, Daniely D, Kauvar A, Carasso RL, Mehrabi JN, Artzi O. Treatment of periorbital wrinkles using thermo-mechanical fractional injury therapy versus fractional non-ablative 1565 nm laser: a comparative prospective, randomized, double-arm, controlled study. Lasers Surg Med 2022;54:46–53. https://doi.org/10.1002/lsm.23494.
[9] Daniely D, Judodihardjo H, Rajpar SF, Mehrabi JN, Artzi O. Thermo-mechanical fractional injury therapy for facial skin rejuvenation in skin types II to V: a retrospective double-center chart review. Lasers Surg Med 2021;53:1152–7. https://doi.org/10.1002/lsm.23400.
[10] Friedman O, Koren A, Niv R, Mehrabi JN, Artzi O. The toxic edge-A novel treatment for refractory erythema and flushing of rosacea. Lasers Surg Med 2019; 51:325–31. https://doi.org/10.1002/lsm.23023.
[11] Hilerowicz Y, Friedman Or, Zur E, Ziv R, Koren A, Salameh F, et al. Thermomechanical ablation-assisted photodynamic therapy for the treatment of acne vulgaris. A retrospective chart review of 30 patients. Lasers Surg Med 2020;52 (10):966–70.
[12] Manuskiatti W, Yan C, Artzi O, Gervasio MKR, Wanitphakdeedecha R. Efficacy and safety of thermomechanical fractional injury-assisted corticosteroid delivery versus intralesional corticosteroid injection for the treatment of hypertrophic scars: a randomized split-scar trial. Lasers Surg Med 2022;54(4):483–9.
[13] Schiffman RM, Christianson MD, Jacobsen G, Hirsch JD, Reis BL. Reliability and validity of the ocular surface disease index. Arch Ophthalmol 2000;118:615–21. https://doi.org/10.1001/archopht.118.5.615.
[14] Kokolakis G, Grawert L, Ulrich M, Lademann J, Zuberbier T, Hofmann MA. Wound healing process after thermomechanical skin ablation. Lasers Surg Med 2020;52 (8):730–4.
[15] Xue AL, Wang MTM, Ormonde SE, Craig JP. Randomised double-masked placebo-controlled trial of the cumulative treatment efficacy profile of intense pulsed light therapy for meibomian gland dysfunction. Ocul Surf 2020;18:286–97. https://doi.org/10.1016/j.jtos.2020.01.003.
[16] Tauber J, Owen J, Bloomenstein M, Hovanesian J, Bullimore MA. Comparison of the iLUX and the LipiFlow for the treatment of meibomian gland dysfunction and symptoms: a randomized clinical trial. Clin Ophthalmol 2020;14:405–18. https://doi.org/10.2147/OPTH.S234008.
[17] Tomlinson A, Bron AJ, Korb DR, Amano S, Paugh JR, Pearce EI, et al. The international workshop on meibomian gland dysfunction: report of the diagnosis subcommittee. Invest Ophthalmol Vis Sci 2011;52:2006–49. https://doi.org/10.1167/iovs.10-6997f.
[18] Sullivan B. Challenges in using signs and symptoms to evaluate new biomarkers of dry eye disease. Ocul Surf 2014;12(1):2–9.
[19] Willcox MDP, Argüeso P, Georgiev GA, Holopainen JM, Laurie GW, Millar TJ, et al. TFOS DEWS II tear film report. Ocul Surf 2017;15(3):366–403.
[20] Finis D, Konig C, Hayajneh J, Borrelli M, Schrader S, Geerling G. Six-month effects of a thermodynamic treatment for MGD and implications of meibomian gland atrophy. Cornea 2014;33:1265–70. https://doi.org/10.1097/ICO.0000000000000273.
[21] Blackie CA, Carlson AN, Korb DR. Treatment for meibomian gland dysfunction and dry eye symptoms with a single-dose vectored thermal pulsation: a review. Curr Opin Ophthalmol 2015;26:306–13. https://doi.org/10.1097/ICU.0000000000000165.

Lasers in Surgery and Medicine 53:622–629 (2021)

Thermo-Mechanical Fractional Injury Enhances Skin Surface- and Epidermis- Protoporphyrin IX Fluorescence: Comparison of 5-Aminolevulinic Acid in Cream and Gel Vehicles

Camilla Foged,[1] Merete Haedersdal,[1] Liora Bik,[1,2] Christine Dierickx,[3] Peter A. Phillipsen,[1] and Katrine Togsverd-Bo[1]*

[1]*Department of Dermatology, Copenhagen University Hospital Bispebjerg and Frederiksberg, Nielsine Nielsens Vej 17, entrance 9, 2. floor, Copenhagen, Nordvest DK-2400, Denmark*

[2]*Department of Dermatology, Erasmus MC University Medical Center Rotterdam, Dr. Molewaterplein 40, Rotterdam, 3015, The Netherlands*

[3]*Skinperium, Private Dermatology Clinic, Rue Charles Martel 52, Luxembourg, 2134, Luxembourg*

Background and Objectives: Thermo-mechanical fractional injury (TMFI) impacts the skin barrier and may increase cutaneous drug uptake. This study investigated the potential of TMFI in combination with 5-aminolevulinic acid (ALA) cream and gel formulations to enhance Protoporphyrin IX (PpIX) fluorescence at the skin surface and in the skin.

Study Design/Materials and Methods: In healthy volunteers ($n = 12$) a total of 144 test areas were demarcated on the upper back. Test areas were randomized to (i) TMFI (6 milliseconds, 400 μm at a single pass) or no pretreatment and (ii) 20% ALA in cream or gel formulations. Skin surface PpIX fluorescence was quantified by PpIX fluorescence photography and photometry in 30-minute intervals until 3 hours. PpIX fluorescence microscopy quantified separate PpIX fluorescence in the epidermis, and in superficial-, mid-, and deep- dermis from punch biopsies sampled after 3 hours of ALA incubation. Local skin reactions (LSR) and pain intensities (numerical rating scale 0–10) were evaluated immediately, at 3 hours and 14 days after the intervention.

Results: TMFI exposure before photosensitizer application significantly increased *skin surface* PpIX fluorescence, both for ALA cream (TMFI-ALA-cream 7848 arbitrary units [AU] vs. ALA-cream 5441 AU, 3 hours, $P < 0.001$) and ALA gel (TMFI + ALA-gel 4591 AU vs. ALA-gel 3723 AU, 3 hours, $P < 0.001$). The TMFI-mediated increase in PpIX fluorescence was similar for ALA-cream and -gel formulations ($P = 0.470$) at the skin surface. In the *epidermis*, PpIX fluorescence intensities increased from combination treatment with TMFI and ALA-cream (TMFI + ALA-cream 421 AU vs. ALA-cream 293 AU, $P = 0.034$) but not from combination with TMFI and ALA-gel (TMI + ALA-gel 264 AU vs. ALA-gel 261 AU, $P = 0.791$). *Dermal* fluorescence intensities (superficial-, mid-, or deep dermis) were unaffected by TMFI pretreatment in both ALA-cream and ALA-gel exposed skin ($P = 0.339$). ALA-cream generally induced higher PpIX fluorescence intensities than ALA-gel (skin surface $P < 0.001$ and epidermis $P < 0.03$). TMFI induced low pain intensities (median 3) and mild LSR that were resolved at 14 days follow-up.

Conclusion: Given the present study design, TMFI, in combination with the standardized application of 20% ALA cream and gel formulations, significantly enhanced skin surface PpIX fluorescence compared to no pretreatment. Additionally, TMFI increased epidermal PpIX fluorescence combined with 20% ALA cream vehicle. Thus, TMFI pretreatment and formulation characteristics exert influence on PpIX fluorescence intensities in normal skin. Lasers Surg. Med. © 2020 Wiley Periodicals LLC

Key words: 5-aminolevulinic acid; actinic keratoses; fluorescence microscopy; Protoporphyrin IX; photodynamic therapy; stratum corneum; thermo-mechanical fractional injury; thermo-mechanical system; vehicle viscosity

INTRODUCTION

Topical photodynamic therapy (PDT) in dermatology is based on light activation of the endogenous photosensitizer

Conflict of Interest Disclosures: All authors have completed and submitted the ICMJE Form for Disclosure of Potential Conflicts of Interest and have disclosed the following: TMFI device was loaned by Novoxel (Novoxel LTD., Israel) for this particular study, accompanied by a research grant to Bispebjerg Hospital, represented by Merete Haedersdal, Novoxel Ltd. had no influence on data collection or interpretation of results. CD, CF, KTB, LB, and PAP have no conflicts of interest.

*Correspondence to: Katrine Togsverd-Bo, MD, Department of Dermatology, Copenhagen University Hospital, Bispebjerg and Frederiksberg, Nielsine Nielsens Vej 17, entrance 9, 2. Floor, DK-2400 Copenhagen Nordvest, Denmark. E-mail: katrine.togsverd-bo@regionh.dk

Accepted 13 September 2020
Published online 1 October 2020 in Wiley Online Library (wileyonlinelibrary.com).
DOI 10.1002/lsm.23326

Protoporphyrin IX (PpIX). PDT is an attractive treatment concept for keratinocyte dysplasia due to high efficacy, excellent cosmetic results, and the possibility to treat large skin areas in the same session [1,2]. Following topical application of PpIX precursors 5-aminolevulinic acid (ALA) or methyl aminolevulinate (MAL), the accumulated amount of PpIX can be quantified by fluorescence detection on the skin surface and in the skin [3–5].

The viable epidermis is an effective barrier for exogenous substances, including cutaneous drug delivery. The skins barrier function is due in large part to the stratum corneum (SC) that allows minimal skin penetration except for lipophilic ($\log P > 1$) and small molecules (molecular weight [MW] < 500 Da) [6,7]. Targeting SC, physical pretreatment techniques facilitate cutaneous uptake of ALA or MAL and is recommended in European PDT protocols for the treatment of actinic keratoses and basal cell carcinomas [1]. The most common method is curettage, but newer interventions, such as microneedling, microdermabrasion, ablative fractional laser (AFL), and non-AFL, are increasingly applied to enhance PpIX accumulation and PDT efficacy [8,9].

Thermo-mechanical fractional injury (TMFI) is a relatively new technique that by the protrusion of pyramid-shaped, titanium covered micro-tips, conducts heat to the skin, generating an array of fractional microscopic vertical columns of thermal injury [10,11]. TMFI has previously been explored for cutaneous uptake of hydrophilic drugs, such as verapamil, diclofenac sodium, 5-fluorouracil, and magnesium ascorbyl phosphate, after TMFI exposure [12–14]. In a recent study, TMFI pretreatment enhanced PpIX fluorescence at the skin surface following incubation with 20% ALA gel [14]. However, the formation of PpIX fluorescence in normal skin remains to be clarified, given different ALA formulations. Thus, in a randomized controlled trial applying standardized interventions, fluorescence photography, and fluorescence microscopy, we aimed to assess PpIX fluorescence intensities at the skin surface and in the skin after exposure to TMFI and ALA formulated in cream and gel vehicles.

MATERIALS AND METHODS

The study was conducted from April to July 2019 and approved by the Danish Medicines Agency (2018-004397-96), Ethics Committee of Capital Region (H-1900394), the Data Protection Agency (2019-3247), as well as registered with Clinical-Trials.gov (NCT04221126). The GCP Unit at the University of Copenhagen monitored the study according to Good Clinical Practice. Written informed consent was obtained from all volunteers prior to enrollment, and the study was performed in accordance with the Declaration of Helsinki.

Participants

The study was a randomized, controlled, intra-individual clinical trial. Healthy volunteers were assessed for eligibility and subsequent treatment at the Department of Dermatology, Bispebjerg Hospital, Copenhagen, Denmark. Inclusion criteria were age above 18 years, Fitzpatrick skin type I–III, and normal skin on the upper back. Exclusion criteria were lactating or pregnant women, allergy to ALA and lidocaine, conditions associated with risk of poor compliance, and PDT or laser treatment of the test areas within the past 6 months.

Interventions

Photosensitizing agents. 5-ALA powder (Gliolan, Medac, Roskilde, Denmark) was prepared at 20% weight/weight (w/w) concentrations in a cream vehicle (viscosity value 116,000 counts per second [cps]) and a gel vehicle (viscosity value 971 cps). Both vehicles were manufactured by the Capital Region Hospital Pharmacy (Herlev, Denmark) under good manufacturing practice (GMP) and the viscosity determined by an external laboratory (AminoLab, Ness Ziona, Israel). The excipients per 100 g vehicles included for the cream vehicle: 700 mg cetrimide, 5 g glycerol 85%, 8 g cestosterayl alcohol, 40 g paraffin liquid in purified water; and for the gel vehicle: 5.9 g glycerol, 0.6 g benzalkonium chloride, 0.3 g disodium edetate, and 1.8 g carmellose sodium in purified water.

Study procedures. In each participant, 12 test areas of each 3×3 cm were mapped on the upper back. Test areas were randomization to (i) TMFI or no pretreatment and (ii) 20% ALA gel or cream vehicle formulation, Table 1 illustrating an overview of test areas. Randomization was performed by a computer-generated random sequence (MatLab®; MathWorks, Natick, MA, USA) and treatment allocations selected from opaque, sequentially numbered, sealed envelopes. Treatment areas were documented at baseline and during all study procedures by clinical photography under standard lighting conditions (Canon EOS 60D, Tokyo, Japan). All study procedures were performed under dimmed light conditions after ALA application.

TMFI (Tixel; Novoxel Ltd., Hamelacha St 43, 420573 Netanya, Israel) exposure was delivered at 6 milliseconds pulse duration and 400 μm protrusion in a single pass to allocated test areas. The TMFI settings were based on previously published results, showing higher PpIX fluorescence at this setting compared to longer pulse durations with similar histologically evaluated tissue response as in the current study [14]. Immediately after pretreatment, 125 μg ALA-cream, ALA-gel, and vehicle controls were applied to relevant test areas and left without occlusion up to 3 hours (Table 1). The test areas were shielded from ambient light with non-occluding aluminum foil. Skin surface PpIX fluorescence was quantified every 30 minutes using a PpIX fluorescence photometer and PpIX fluorescence camera. After 3 hours, five punch biopsies (3 mm diameter) were sampled from each participant for PpIX fluorescence microscopy. The time point for biopsy sampling was determined in a pilot study ($n = 4$ participants) that documented higher PpIX fluorescence intensities at the skin surface and in the epidermis at 3 hours incubation with ALA gel formulation

TABLE 1. Study Setup and Standardization

Test area	Pretreatment	Vehicle	Incubation (min)[a]	PpIX fluorescence median (IQR), AU[b]	PpIX Photometry median (IQR) AU[b]
1	TMFI	ALA-cream	180	7848 (4285–12,836)	52 (41–63)
2	None	ALA-cream	180	5441 (2612–8235)	43.5 (28–52)
3	TMFI	ALA-gel	180	4591 (3821–7398)	36 (24–49)
4	None	ALA-gel	180	3723 (1722–5449)	20.5 (13–35)
5	TMFI	ALA-cream	120	6693 (3189–13,366)	47 (36–60)
6	None	ALA-cream	120	5992 (1414–6572)	35 (22–43)
7	TMFI	ALA-gel	120	5541 (3090–9807)	42.5 (28–56)
8	None	ALA-gel	120	3729 (20–7125)	18 (15–28)
9	TMFI	None	–	–	–
10	Untreated control	None	–	–	–
11	None	Cream vehicle	180	–	–
12	None	Gel vehicle	180	–	–

ALA, 5-aminolevulinic acid; AU, arbitrary units; PpIX, protoporphyrin IX; TMFI, thermo-mechanical fractional injury.
[a]Incubation: time when vehicle formulation was wiped off the skin.
[b]PpIX fluorescence intensities measured at 3 hours.

compared with 1 or 2 hours incubation. A total of 12 biopsies were assessed in the pilot study.

Outcome Assessment

Local skin response (LSR) and patient-evaluated pain. LSRs were evaluated as erythema, edema, scaling, pustules, and crusting. Each parameter was graded on a standardized 5-point severity scale representing none, mild, moderate, prominent, and severe [15]. LSR was supported by noninvasive reflectance measurement of skin redness and pigmentation percentages (UV Optimize Scientific Model, Chromo-light, Espergaerde, Denmark). LSR and reflectance measurements were conducted at baseline, immediately and 3 hours after interventions, and at 14 days follow-up. Finally, patient-assessed pain during TMFI was performed on a 0–10 numerical rating scale in which 0 is no pain and 10 worst imaginable pain.

Skin surface PpIX fluorescence. Skin surface PpIX fluorescence was quantified using two noninvasive techniques, a handheld fluorescence photometer, and PpIX fluorescence photographs. PpIX photometer (FluoDerm, Dia-Medico, Gentofte, Denmark) illuminates a circle at 4 cm diameter with blue light (400–420 nm) and detect emitted fluorescence between 610 and 700 nm [16]. The photometer was calibrated prior to the study start, and measurements adjusted for autofluorescence by subtracting the baseline value from corresponding PpIX fluorescence measurements.

PpIX fluorescence photographs were obtained by a fluorescence imaging system (Medeikonos AB, Gothenburg, Sweden) [4,17]. PpIX excitation was delivered with UVA2 and blue light at 365–405 nm for 2 seconds with the red fluorescent light captured by a CDD camera equipped with a long pass filter (610–715 nm). Subsequently, PpIX fluorescence intensities in each study area were calculated from the fluorescence photograph using an imaging analysis program (MatLab®, Natick, MA, USA), with each fluorescence photograph calibrated to a fluorescence standard (Bio-Science, Gilleleje, Denmark). ALA-induced PpIX fluorescence was defined as pixels with a value 500 higher than background fluorescence pixel values and adjusted for autofluorescence by subtracting baseline vehicle fluorescence values in each photograph. PpIX fluorescence values measured in arbitrary units (AU) can be relatively but not directly compared since different methods were used to quantify PpIX fluorescence.

PpIX fluorescence microscopy. Biopsies were immediately frozen (−20°C) and cut into 10 μm vertical sections for fluorescence microscopy [4]. Digital fluorescence microscopy was performed using a fluorescence microscope (Olympus IX70, Fluorescence Microscope, Olympus Germany, Düsseldorf, Germany) in a room with dim light to minimize photobleaching. PpIX was excited by a xenon lamp equipped with a 400–440 nm excitation filter (AT420/40x; Chroma, VT, USA) and fluorescence emission captured with a 510 nm long-pass filter (ET510lp; Chroma, VT, USA). Images were captured using a CCD camera (ORCA-R2 Digital CCD camera; Hamamatsu Photonics, Shizuoka, Japan) with associated software (HCImage Live; Hamamatsu Photonics). The stability of the excitation light was monitored prior to each microscopy session with a Grimson Blue fluorescent standard (Bio-Science, Gilleleje, Denmark) and varied less than 10%.

From each biopsy, three cryosections were selected for fluorescence microscopy. PpIX fluorescence quantification was obtained from four regions of interest (ROI), defined at epidermis (0–100 μm skin dept), superficial dermis (125–300 μm skin dept), mid dermis (800–1200 μm skin dept), and deep dermis (1600–2000 μm skin dept). From each section, three images were captured, representing epidermis, superficial dermis, mid dermis, and deep dermis, and median fluorescence intensities calculated from three measurement areas within each ROI. Image

analysis was performed by an investigator (CF), blinded to treatment intervention using an image analysis program (ImageJ, National Institutes of Health, Bethesda, Maryland, USA). Correction for autofluorescence was made by subtracting the untreated control value from the corresponding ROI-structure. A total of 540 images were reviewed for PpIX fluorescence intensity analysis. Subsequently, 90 sections were stained with hematoxylin and eosin (HE) and reviewed for histologic analysis of TMFI-tissue interactions.

Outcome Measures

The primary outcome measure was PpIX fluorescence intensities at the skin surface and in the skin, whereas ALA concentrations were not determined. Secondary outcome measures were histological assessment of TMFI impact on the skin, LSRs supported by reflectance measurements of skin redness and pigmentation, as well as participant-assessed pain.

Statistics

A study sample size of 10 patients was calculated, aiming at a 40% minimally relevant difference (MIREDIF) of PpIX skin surface fluorescence, a standard deviation of 20%, a 5% significance level, and power of 80%. To statistically allow for premature withdrawals, 12 participants were included in the study. Descriptive data were presented as medians, interquartile ranges (IQR), and minimum and maximum values. Nonparametric Friedman and Wilcoxon signed-rank tests were used to compare PpIX fluorescence intensities as data were non-normally distributed. $P < 0.05$ were considered significant. All statistical tests were performed using SPSS Statistics version 25 (IBM, Armonk, NY, USA) and visualized using Prism 6 (GraphPad Software, San Diego, CA, USA).

RESULTS

Twelve healthy participants with a median age of 22.5 years (range 18–25), male to female ratio of 1:1, and Fitzpatrick's skin types I ($n = 1$), II ($n = 5$), and III ($n = 6$) were enrolled in the study. All participants completed the study protocol and were included for outcome analysis.

Histology-Assessed TMFI-Tissue Interaction

HE sections of TMFI-exposed skin visualized a localized dermo-epidermal coagulation zone with a median maximum depth of 251 μm (range 154–498 μm) and a median maximum width of 463 μm (range 206–1054 μm) (Fig. 1G). Tissue interactions presented with intra-epidermal vacuolization, subepidermal clefting, and intense eosin staining corresponding to the photothermal treatment zone, as shown in Figure 1G.

Skin Surface PpIX Fluorescence

Skin surface PpIX fluorescence accumulated continuously from baseline to 3 hours, as visualized in Figure 2. By gross evaluation, TMFI induced homogenous and intensified PpIX fluorescence compared with less intense PpIX fluorescence in non-pretreated skin, illustrated in Figure 1C and 1D. Quantitatively, TMFI exposure significantly enhanced PpIX fluorescence

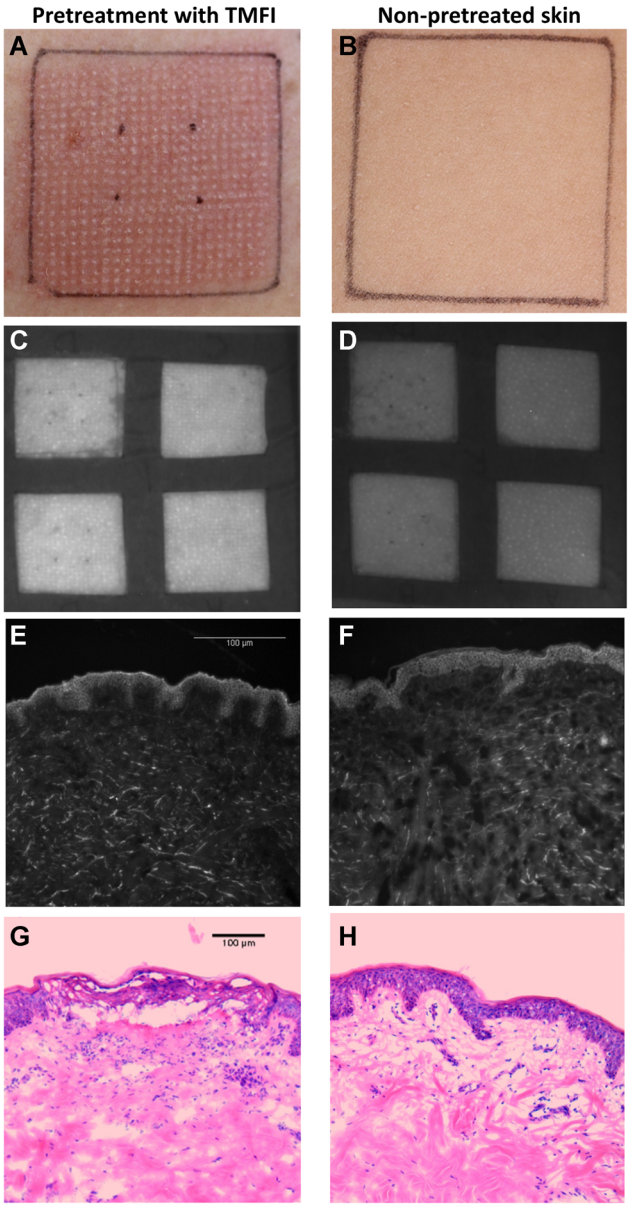

Fig. 1. Images illustrating impact of TMFI exposure on the skin and Protoporphyrin IX (PpIX) fluorescence. (**A**) The immediate erythema and edema following TMFI exposure and (**B**) non-pretreated skin. (**C**, **D**) Skin surface PpIX fluorescence photographs showing more intense fluorescence intensities at 3 hours in TMFI-pretreated skin (**C**) than un-pretreated skin (**D**) combined with ALA-cream (upper row) and ALA-gel (lower row) formulations. (**E**, **F**) Fluorescence microscopy illustrating enhanced epidermal PpIX fluorescence following TMFI pretreatment and ALA-cream (**E**) than ALA cream alone (**F**). (**G**, **H**) Hematoxylin-eosin (HE) stain showing subepidermal clefting and eosin coloring in the TMFI treatment zone (**G**) versus non-pretreated normal skin (**H**). ALA, 5-aminolevulinic acid; TMFI, thermo-mechanical fractional injury.

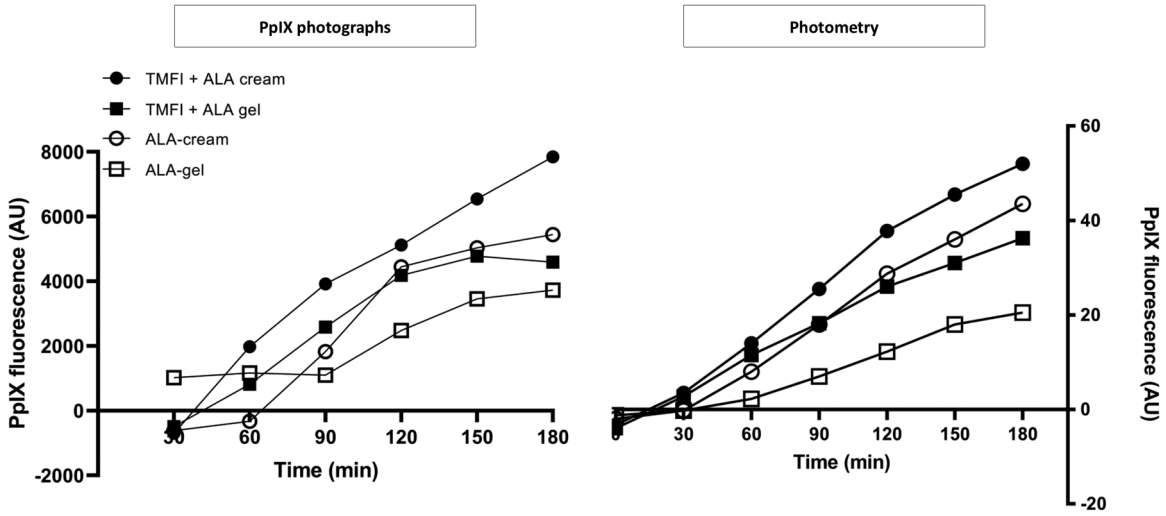

Fig. 2. Skin surface protoporphyrin IX (PpIX) intensities (median) accumulating over time in test areas exposed to TMFI, 5-ALA-gel, and cream vehicles incubated for 3 hours. Fluorescence units are expressed in arbitrary units (AU). ALA, 5-aminolevulinic acid; TMFI, thermo-mechanical fractional injury.

intensities compared with incubation with both ALA cream and ALA gel formulations without any pretreatment ($P < 0.01$) and were documented with PpIX fluorescence photography and PpIX fluorescence photometry, as listed in Table 1. Thus, at 3 hours of photosensitizer incubation, combination of TMFI-ALA-cream resulted in higher median PpIX fluorescence intensities than ALA cream alone (photometry 52 vs. 44 AU, $P < 0.001$; fluorescence photography 7848 vs. 5441 AU, $P < 0.01$). In ALA-gel-incubated skin, TMFI pretreatment increased PpIX fluorescence compared with no TMFI pretreatment (photometry 36 vs. 21 AU, $P < 0.001$; fluorescence photography 4591 vs. 3723 AU, $P < 0.043$).

The extent to which TMFI pretreatment increased PpIX fluorescence ranged from 48% to 136% after 3 hours of ALA-gel incubation compared with 20–44% after ALA-cream incubation ($P =$ ns). Overall, the ALA-cream vehicle achieved higher median PpIX fluorescence intensities than ALA-gel vehicle, both in combination with TMFI pretreatment ($P < 0.017$) and in non-pretreated skin ($P < 0.001$), Table 1. PpIX fluorescence intensities were slightly higher at 3 hours than 2 hours of ALA incubation when quantified with photometry ($P = 0.04$), whereas comparisons of fluorescence photographs showed no difference between incubation times ($P =$ ns).

PpIX Fluorescence Microscopy

Epidermal PpIX fluorescence reached overall higher intensities (range 261–421 AU) than dermal PpIX fluorescence (range, −41 to 92 AU), Figure 3. In the epidermis, the combination of TMFI and ALA-cream induced higher PpIX fluorescence than ALA-cream alone (medians, 421 vs. 293 AU; $P = 0.034$), whereas TMFI and ALA-gel did not enhance fluorescence intensities compared with ALA-gel alone (medians, 264 vs. 261 AU; $P = 0.791$). Furthermore, epidermal PpIX fluorescence reached higher intensities by TMFI-ALA-cream compared with TMFI-ALA-gel (medians, 421 vs. 264 AU; $P = 0.03$). In non-TMFI-pretreated skin, ALA-cream and ALA-gel induced similar median fluorescence values at 293 and 261 AU, respectively.

In the superficial, mid, and deep dermis, PpIX fluorescence intensities reached significantly lower values than in the epidermis (ALA-cream and ALA-gel range −41 to 92 AU). TMFI exposure did not increase fluorescence intensities in neither superficial, mid nor deep dermis.

Safety

TMFI was well-tolerated, resulting in mild LSRs and participant-assessed pain at low intensities (median, 3; range, 1–6) that cleared within minutes. Immediate skin responses included mild erythema (median, 2; range, 1–2) and edema (median, 1; range, 0–1), visualized in Figure 1A and 1B. Mild erythema and edema persisted at the 3 hours assessment but were cleared at day 14 follow-up. Supporting clinical evaluations, noninvasively quantified redness increased immediately and 3 hours after TMFI (median, 28–29%) compared with untreated skin (median, 23%; $P < 0.001$). At day 14 follow-up, two participants developed mild postinflammatory hyperpigmentation in all ALA-test areas that were unrelated to TMFI exposure. The TMFI device was easy to operate.

DISCUSSION

This study assessed the potential of TMFI pretreatment to enhance PpIX fluorescence at the skin surface and in the skin following standardized applications of 20% ALA in gel and cream vehicles. Quantified by two different fluorescence measurement techniques, skin surface PpIX fluorescence intensities significantly and consistently enhanced throughout the 3-hour incubation period when the

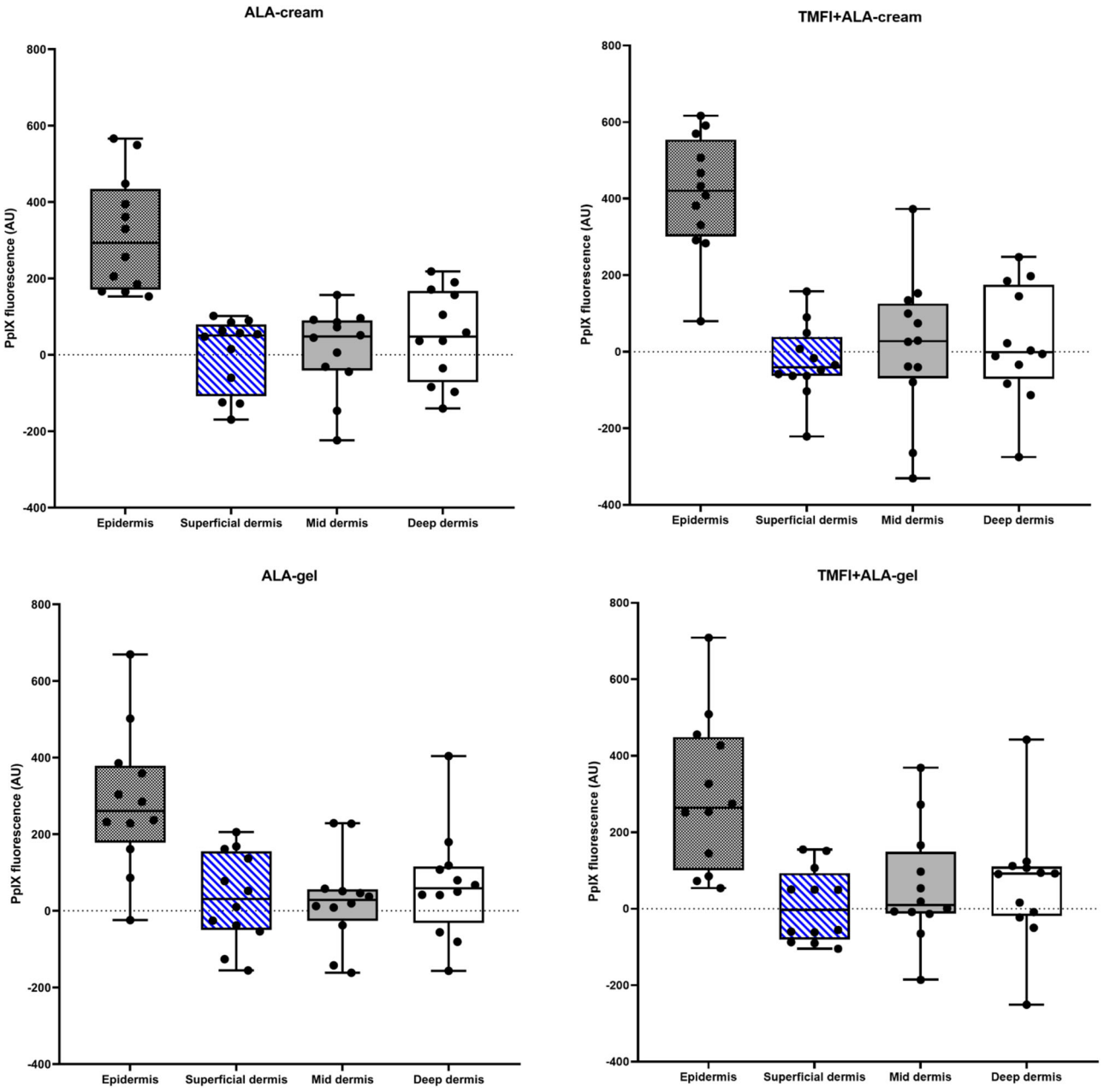

Fig. 3. Box-and-whisker plot of Protoporphyrin IX (PpIX) fluorescence intensities (arbitrary units, AU) after 3 hours ALA cream and ALA gel vehicle incubation, quantified in regions of interest (ROI): Epidermis, superficial dermis, mid dermis, and deep dermis. Epidermal PpIX fluorescence was more intense than dermalPpIX fluorescence. TMFI pretreatment enhanced epidermis PpIX fluorescence in the skin exposed to ALA cream. Dermal PpIX fluorescence intensities were not significantly different after correction for autofluorescence. Plot illustrates the median, interquartile range, and minimum and maximum fluorescence values.

skin was exposed to TMFI before application of photosensitizer. Furthermore, PpIX fluorescence microscopy demonstrated higher epidermal PpIX fluorescence intensities in the skin exposed to TMFI and 20% ALA-cream formulation compared to ALA-cream without TMFI pretreatment. These findings confirm TMFI as a novel and tolerable pretreatment technique that increases the accumulation of ALA-induced PpIX to superficial skin layers before PDT treatment.

TMFI-mediated thermal disruption of the skin barrier has been explored *in vitro* and *in vivo* for hydrophilic drugs that poorly penetrate the intact skin. Evaluated

drugs include verapamil hydrochloride, diclofenac sodium, botulinum toxin A, and ALA [10–13,18]. A recent study by Shavit and Dierickx determined skin surface PpIX fluorescence in normal skin after TMFI, combined with commercially available photosensitizers in different concentrations and vehicle formulations [13]. Photosensitizers included 7.8% ALA in microemulsion-gel (Ameluz®), 20% ALA in alcohol solution (Levulan Kerastick®), 16.8% MAL in a cream (Metvix®), and 20% ALA in a self-produced gel [13]. In accordance with our results, the authors found that TMFI enhanced PpIX fluorescence at 3 hours using 20% ALA in a gel formulation. In the present study, TMFI-20% ALA-cream achieved higher PpIX fluorescence intensities than TMFI-20% ALA-gel but was not compared to ALA in a low-viscosity vehicle formulation. The observed difference may rely on vehicle formulation characteristics as all factors associated with conventional drug diffusion are the same for ALA cream and gel vehicles, except for the partition coefficient. In general, hydrophilic molecules are less prone to partition from aqueous vehicles compared to lipophilic vehicle formulations [6]. Thus, being a hydrophilic molecule, ALA (logP −1.5) may easily partition from a lipophilic cream vehicle than from a gel vehicle resulting in faster diffusion from the vehicle and thereby generate higher PpIX fluorescence in the skin incubated with ALA cream than ALA gel. A lipophilic cream vehicle may potentially facilitate higher epidermal retention for increased probability of intracellular entry, although both ALA cream and gel were supplied in excess on the skin [19]. As a potential confounder, the applied cream vehicle contained cetrimide, not only an emulsifier but also a surfactant that may enhance ALA penetration of the cream vehicle compared to the gel vehicle.

By disruption of skin integrity, different physical pretreatments are available to facilitate cutaneous uptake of photosensitizers [3,6,8]. Hence, pretreatment modalities may focus on stratum corneum removals, such as curettage and microdermabrasion, or may target full epidermis by generating microscopic channels of ablated or coagulated tissue using fractional ablative or nonablative lasers [8,9], thus targeting the permeability barrier of the full epidermis [7]. Microneedling is a cost-effective technique that uses mechanical force to create transient micropores to enhance PpIX fluorescence accumulation [20]. In head-to-head comparisons and *in vitro* studies, the ablative fractional laser is the only pretreatment technique to provide deep and intense delivery of photosensitizers in deep dermal compartments, and is also associated with more pronounced LSR [3,9,21]. With the current settings, TMFI produced nonablative coagulation zones with low trauma to the skin barrier, resulting in enhanced PpIX accumulation in superficial skin layers, which is consistent with PDT's current Food and Drug Administration (FDA) indication for superficial AK. However, offering high tolerability and minimal downtime posttreatment [22], TMFI holds potential as a novel tool to enhance ALA-induced PpIX accumulation.

Assessed by PpIX fluorescence microscopy, TMFI in combination with 20% ALA in cream formulation augmented epidermal PpIX fluorescence intensities whereas dermal intensities remained low and were unaffected by TMFI pretreatment. The difference between epidermal and dermal PpIX fluorescence intensities results from a significantly low density of fibroblasts, responsible for the conversion of ALA to PpIX. Furthermore, delayed diffusion of ALA from the epidermis to dermis as well as elimination of ALA by dermal blood and lymphatic vessel structures affects the kinetics of ALA concentration and contributes to low dermal PpIX fluorescence [6].

A major study limitation is that interventions were performed on normal skin on the back as opposed to facial skin or diseased skin with localized hyperkeratoses that may influence TMFI coagulation zone dimensions and ALA-induced PpIX fluorescence. TMFI settings can, therefore, not be directly extrapolated to all skin regions but should be adjusted according to skin thickness and skin constitution in treatment areas. Likewise, longer TMFI pulse durations or deeper penetration depths as well as different ALA vehicle formulations may have produced different PpIX fluorescence kinetics or distribution in epidermal and dermal structures.

As an active photosensitizer for PDT, PpIX is a relevant, well-established surrogate marker for cutaneous and systemic ALA pharmacokinetics [1,19,23]. Hence, the scope of the study was not to determine ALA concentrations in epidermal or dermal structures but to investigate ALA-induced PpIX accumulation with and without TMFI pretreatment. The strengths of the study include standardized study interventions and assessment of endpoints, including three different techniques to quantify PpIX fluorescence. Although a limited number of participants were included in the study, the intra-individual design permitted a direct comparison of study interventions evaluated in 144 test areas.

In conclusion, using the given standardized settings and vehicle formulations, TMFI exposure combined with 20% ALA in cream and gel formulations effectively enhanced PpIX fluorescence intensities at the skin surface and in the epidermis combined with 20% ALA cream. Thus, TMFI present as a novel, tolerable pretreatment technique with the potential to enhance PpIX accumulation in conjunction with PDT procedure.

ACKNOWLEDGMENTS

The authors thank Catharina M. Lerche, MSc (Pharm), PhD for preparing photosensitizer formulations and medical laboratory technologist Diana Hoeeg for sectioning biopsies.

AUTHOR CONTRIBUTIONS

C.F., K.T.B., P.A.P., and M.H. had full access to all study data and take responsibility for data integrity and accuracy of data analysis. Study concept and design: C.D., K.T.B., and M.H.; acquisition, analysis, or interpretation of data: all authors; drafting of the manuscript: C.F., M.H.,

and K.T.B.; critical revision of the manuscript for important intellectual content: all authors; statistical analysis: C.F. and P.A.P.; obtained funding: M.H.; administrative, technical, or material support: all authors; study supervision: C.F., K.T.B., P.A.P., and M.H.

REFERENCES

1. Morton CA, Szeimies R-M, Basset-Seguin N, et al. European Dermatology Forum guidelines on topical photodynamic therapy 2019 Part 1: Treatment delivery and established indications—Actinic keratoses, Bowen's disease and basal cell carcinomas. J Eur Acad Dermatol Venereol 2019;33(12): 2225–2238.
2. Kennedy JC, Pottier RH. Endogenous protoporphyrin IX, a clinically useful photosensitizer for photodynamic therapy. J Photochem Photobiol B 1992;14(4):275–292.
3. Haedersdal M, Sakamoto FH, Farinelli WA, Doukas AG, Tam J, Anderson RR. Pretreatment with ablative fractional laser changes kinetics and biodistribution of topical 5-aminolevulinic acid (ALA) and methyl aminolevulinate (MAL). Lasers Surg Med 2014;46(6):462–469.
4. Togsverd-Bo K, Idorn LW, Philipsen PA, Wulf HC, Hædersdal M. Protoporphyrin IX formation and photobleaching in different layers of normal human skin: Methyl- and hexylaminolevulinate and different light sources. Exp Dermatol 2012;21(10):745–750.
5. Tierney E, Petersen J, Hanke CW. Photodynamic diagnosis of tumor margins using methyl aminolevulinate before Mohs micrographic surgery. J Am Acad Dermatol 2011;64(5):911–918.
6. Prausnitz MR, Elias PM, Franz TJ, Schmuth M, Tsai JC, et al. Skin barrier and transdermal drug delivery. In: Bolognia J, Jorizzo JL, Schaffer JV, editors. Medical Therapy. Philadelphia, Saunders: Elsevier; 2012. pp 2065–2073.
7. Andrews SN, Jeong E, Prausnitz MR. Transdermal delivery of molecules is limited by full epidermis, not just stratum corneum. Pharm Res 2013;30(4):1099–1109.
8. Champeau M, Vignoud S, Mortier L, Mordon S. Photodynamic therapy for skin cancer: How to enhance drug penetration? J Photochem Photobiolog B Biol 2019;197:111544.
9. Bay C, Lerche CM, Ferrick B, Philipsen PA, Togsverd-Bo K, Haedersdal M. Comparison of physical pretreatment regimens to enhance protoporphyrin IX uptake in photodynamic therapy: A randomized clinical trial. JAMA Dermatol 2017;153(4):270–278.
10. Elman M, Fournier N, Barnéon G, Bernstein EF, Lask G. Fractional treatment of aging skin with Tixel, a clinical and histological evaluation. J Cosmet Laser Ther 2016; 18(1):31–37.
11. Sintov AC, Hofmann MA. A novel thermo-mechanical system enhanced transdermal delivery of hydrophilic active agents by fractional ablation. Int J Pham 2016;511(2): 821–830.
12. Artzi O, Koren A, Niv R, Mehrabi JN, Mashiah J, Friedman O. A new approach in the treatment of pediatric hypertrophic burn scars: Tixel-associated topical triamcinolone acetonide and 5-fluorouracil delivery. J Cosmet Dermatol 2019;19:131–134.
13. Artzi O, Koren A, Niv R, Mehrabi JN, Friedman O. The scar bane, without the pain: A new approach in the treatment of elevated scars: Thermomechanical delivery of topical triamcinolone acetonide and 5-fluorouracil. Dermatol Ther 2019;9(2):321–326.
14. Shavit R, Dierickx C. A new method for percutaneous drug delivery by thermo-mechanical fractional injury. Lasers Surg Med 2019;52(1):61–69.
15. Rosen R, Marmur E, Anderson L, Welburn P, Katsamas J. A new, objective, quantitative scale for measuring local skin responses following topical actinic keratosis therapy with ingenol mebutate. Dermatol Ther 2014;4(2):207–219.
16. Nissen CV, Wiegell SR, Philipsen PA, Wulf HC. Short-term chemical pretreatment cannot replace curettage in photodynamic therapy. Photodermatol Photoimmunol Photomed 2016;32(3):146–152.
17. Wiegell SR, Wulf HC. Photodynamic therapy of acne vulgaris using 5-aminolevulinic acid versus methyl aminolevulinate. J Am Acad Dermatol 2006;54(4):647–651.
18. Bar-Ilan E, Koren A, Shehadeh W, Mashiah J, Sprecher E, Artzi O. An enhanced transcutaneous delivery of botulinum toxin for the treatment of Hailey-Hailey disease. Dermatol Ther 2020;33(1):e13184.
19. Rick K, Sroka R, Stepp H, et al. Pharmacokinetics of 5-aminolevulinic acid-induced protoporphyrin IX in skin and blood. J Photochem Photobiol B Biol 1997;40:313–319.
20. Mikolajewska P, Donnelly RF, Garland MJ, et al. Microneedle pre-treatment of human skin improves 5-aminolevulinic acid (ALA)- and 5-aminolevulinic acid methyl ester (MAL)-induced PpIX production for topical photodynamic therapy without increase in pain or erythema. Pharm Res 2010;27(10):2213–2220.
21. Haedersdal M, Katsnelson J, Sakamoto FH, et al. Enhanced uptake and photoactivation of topical methyl aminolevulinate after fractional CO_2 laser pretreatment. Lasers Surg Med 2011;43(8):804–813.
22. Kokolakis G, von Grawert L, Ulrich M, Lademann J, Zuberbier T, Hofmann MA. Wound healing process after thermomechanical skin ablation. Lasers Surg Med 2020; 52(8):730–734.
23. Szeimies RM, Landthaler M. Photodynamic therapy and fluorescence diagnosis of skin cancers. Recent Results Cancer Res 2002;160:240–245.

International Journal of Pharmaceutics 511 (2016) 821–830

Contents lists available at ScienceDirect

International Journal of Pharmaceutics

journal homepage: www.elsevier.com/locate/ijpharm

A novel thermo-mechanical system enhanced transdermal delivery of hydrophilic active agents by fractional ablation

Amnon C. Sintov[a,*], Maja A. Hofmann[b]

[a] Department of Biomedical Engineering, Faculty of Engineering Sciences, Laboratory for Biopharmaceutics, E.D. Bergmann Campus, Ben Gurion University of the Negev, Be'er Sheva 84105, Israel
[b] Department of Dermatology, Venerology and Allergy, Charité-Universitätsmedizin, Charitéplatz 1, 10115 Berlin, Germany

ARTICLE INFO

Article history:
Received 22 May 2016
Received in revised form 30 June 2016
Accepted 28 July 2016
Available online 29 July 2016

Keywords:
Transdermal drug delivery
Percutaneous permeation
Fractional skin ablation
Verapamil
Diclofenac
Magnesium ascorbyl phosphate

ABSTRACT

The Tixel is a novel device based on a thermo-mechanical ablation technology that combines a sophisticated motion and a temperature control. The fractional technology is used to transfer a very precise thermal energy to the skin thereby creating an array of microchannels, accompanying by no signs of pain or inconvenience. This study aimed to evaluate the effect of the Tixel on the skin permeability of three hydrophilic molecular models: verapamil hydrochloride, diclofenac sodium, and magnesium ascorbyl phosphate. Tixel's gold-platted stainless steel tip heated to a temperature of 400 °C was applied on skin for 8 ms or 9 ms at a protrusion of 400 μm (the distance in which the tip protrudes beyond the distance gauge). The experiments were carried out partly *in vivo* in humans using a fluorescent dye and a confocal microscopy and partly *in vitro* using porcine skin and a Franz diffusion cell system. The results obtained in this study have shown that (a) no significant collateral damage to the skin tissue and no necrosis or dermal coagulation have been noted, (b) the microchannels remained open and endured for at least 6 h, and (c) the skin permeability of hydrophilic molecules, which poorly penetrate the lipophilic stratum corneum barrier, was significantly enhanced by using Tixel's pretreatment.

1. Introduction

Transdermal drug delivery has been well-established as a potentially advantageous alternative for many therapeutically active compounds to the parenteral and oral routes. The adverse effects due to fluctuations in plasma drug levels, the high portion of hepatic first-pass metabolism (or other factors leading a low bioavailability), as well as a short biological half-life have been important reasons to intensively explore ways how to circumvent the skin barrier. The highly lipophilic nature of the skin provides the main barrier for influx of drugs and environmental chemicals into the body. The lipophilic properties are related to the outermost keratinizing layer, the stratum corneum (10–20 μm thickness), which is impermeable to most therapeutically active compounds, in particular high-molecular weight, hydrophilic or charged substances. Nonetheless, the advantages of transdermal drug delivery have motivated intensive research activity for the purpose of circumventing the skin barrier with optimal solutions (Barry, 2001; Davis et al., 2002). Various methods have been studied, such as those based on chemical enhancers (Walters, 1989; Smith and Maibach, 1995; Ben-Shabat et al., 2007), or those rely on physical techniques including microneedles (Henry et al., 1998; McAllister et al., 2000), iontophoresis (Singh et al., 1999; Marro et al., 2001; Guy et al., 2001 Sintov and Brandys-Sitton, 2006), electroporation (Prausnitz et al., 1993; Riviere et al., 1995; Vanbever et al., 1994, 1996; Prausnitz, 1999; Hu et al., 2000), ultrasound (Ogra et al., 2008), as well as a diversity of thermal ablation techniques (Sintov et al., 2003; Park et al., 2008; Bachhav et al., 2010, 2013; Lee et al., 2011). Thermal ablation for transdermal drug delivery has included lasers (Bachhav et al., 2010, 2013), radiofrequency (Sintov et al., 2003), or superheated steam (Lee et al., 2011) devices. A pioneering work by Park et al. (2008) has shown, by screening a broad range of temperatures (25°–315 °C) and durations (100 ms–5 s), that skin permeability strongly depends on the temperature and less on the duration of heating so even shorter durations (i.e., on a microsecond timescale) might be sufficient. Lee et al. (2011) later developed a microdevice that ejects superheated steam during only 100 μs at the skin surface, demonstrating a selective removal of stratum corneum of cadaver skin without significant collateral damage to the inner tissue. Recently, a thermo-mechanical ablation (TMAb) technology has been proposed (Lask et al., 2012; Elman et al., 2016), demonstrating

* Corresponding author.
E-mail address: asintov@bgu.ac.il (A.C. Sintov).

http://dx.doi.org/10.1016/j.ijpharm.2016.07.070
0378-5173/

fractional skin vaporization, which was similar to CO_2 laser but more cost effective than the laser (Lee et al., 2011). A resurfacing treatment device, given the name 'Tixel' (Novoxel® GmbH, Lanshut, Germany), has been consequently developed using the TMAb technology (Fig. 1). It includes an array of tiny metallic pins (1.25 mm pyramid-shaped, 3×10^{-4} cm^2 surface area at the apex) called 'the tip' which is attached to a handpiece, equipped with a linear motor. By activating the handpiece, the linear motor rapidly advances the preheated tip to the skin surface at a predetermined 'protrusion' for a brief duration (Fig. 1B), thus creating micro-craters by vaporization of the stratum corneum.

In the present study, we have demonstrated the effect of the Tixel on the skin permeability of three hydrophilic molecular models – verapamil hydrochloride, diclofenac sodium, and magnesium ascorbyl phosphate. Verapamil hydrochloride is very soluble in water and most polar organic solvents. Due to its hydrophilic properties, it is an ideal molecular model for evaluation of drug delivery system aimed to enhance percutaneous absorption. Although verapamil was used in this study as a model drug, it has also been proved to be beneficial as a topical drug (transdermal electromotive administration of 15% gel) for Peyronie's disease. This is due to its ability to inhibit fibroblasts and to increase collagenase activity, resulting in breaking down and remodeling the excess collagen (Anderson et al., 2000; Levine et al., 2002; Greenfield et al., 2007; Tuygun et al., 2009). Apart from the advantageous use of verapamil in Peyronie's disease, microneedle-mediated transdermal verapamil delivery was also proposed as a beneficial technology for patients with hypertension, as application of stainless steel microneedles has increased transdermal delivery of verapamil hydrochloride across porcine ear skin (Kaur et al., 2014). Diclofenac salt was used as a hydrophilic model drug which is highly soluble in aqueous solutions as ionized salts and its penetration into the skin is dependent upon partitioning of the unionized form into the lipophilic keratinic layer (Kriwet and Müller-Goymann, 1995). Diclofenac is a commonly-used, highly effective non-steroidal anti-inflammatory agent (NSAID) in the management of acute conditions of inflammation and pain, musculoskeletal disorders, arthritis, and dysmenorhea. It is a non-selective cyclooxygenase inhibitor but possesses a slightly preferential cyclooxygenase-2 inhibition activity (Giuliano and Warner, 1999). Thus, although diclofenac is a relatively safe and tolerable NSAID, serious gastrointestinal adverse effects occasionally appear after oral administration. Owing to its adverse effects, its high portion of hepatic first-pass metabolism (~50%) and its short biological half-life, the topical application of diclofenac provides, therefore, a preferred alternative to the oral dosage forms. The diethylammoniun salt of diclofenac in a topical medication, known as Voltaren® Emulgel®, is particularly suitable for musculoskeletal pain and localized forms of non-articular rheumatism and inflammations of well-defined areas near the body surface (Kriwet and Müller-Goymann, 1993). The third active compound, which we examined as a model compound in combination with Tixel's pretreatment, was the magnesium salt of ascorbic acid derivative. Apart from its antioxidant activity as a free radical scavenger, ascorbic acid and its chemically-stable derivatives (e.g., ascorbyl palmitate and magnesium ascorbyl phosphate), are well-established lightening (or whitening) agents, especially used in south-east Asia as a stylish approach that fair skin is associated with beauty. Ascorbic acid derivatives react with copper ions at the tyrosinase active site resulted in reduction of dopaquinone, the precursor of melanin (Farris, 2005).

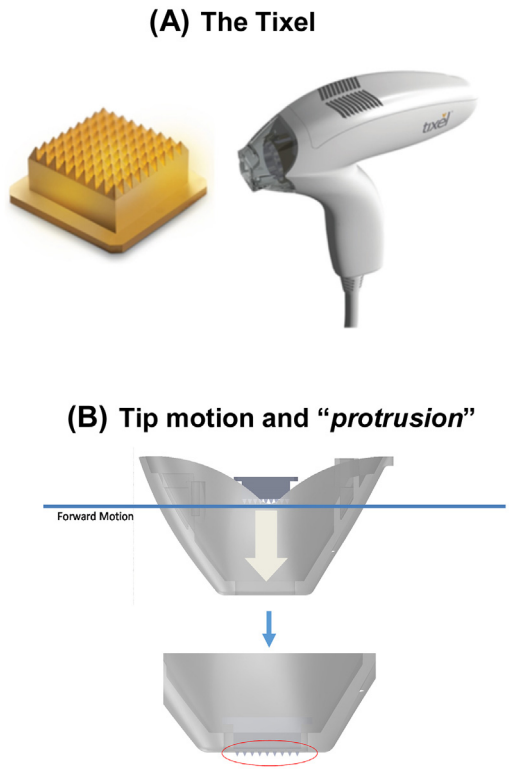

Fig. 1. The Tixel's handpiece and its metallic tip (A). Note that the term 'protrusion' refers to a distance of the pins beyond the gauge, being controlled to a desired length during tip motion operation (B).

The Tixel – TMAb technology – is presented and described in this paper. By using this device for drug delivery, we have demonstrated for the first time an increased permeability of hydrophilic active compounds. In this paper, we focus on low molecular-weight molecules as a model, which is apparently a first step in the widespread investigation of this technology. We have shown that a fractional ablation of the upper layer of the skin carried out by the Tixel's pretreatment procedure can result in an enhanced transdermal delivery of poorly permeable drugs. In addition, the microchannels or micropores formed by the Tixel-TMAb technique were microscopically observed after a histological procedure or after staining by diagnostic dyes.

2. Materials and methods

2.1. Materials

Diclofenac as a sodium salt was obtained from Sigma (Rehovot, Israel), verapamil hydrochloride was obtained from Euroasian Chemicals Pvt. Ltd. (Mumbai, India), and magnesium ascorbyl phosphate (Nikkol VC-PMG) was purchased from Nikko Chemicals (Tokyo, Japan). High-performance liquid chromatography (HPLC) grade water and organic solvents were obtained from J.T. Baker (Mallinckrodt Baker, Inc., Phillipsburg, NJ).

2.2. The Tixel

As shortly described in the Introduction section, the Tixel (Novoxel, Israel) is a thermo-mechanical system for fractional ablation, which applies a tip.

2.2.1. The Tixel's tip

The Tixel's tip is made of stainless steel (SS) plated by pure gold (Fig. 1A), being fixated at the distal section of the Tixel's handpiece. The tip's active surface consists of an array of 81 (9×9) pyramidal pins evenly spaced within a boundary area of 1×1 cm. The pin's height is 1.25 mm having a radius of about 100 μm at the apex, meaning that each miniature pyramid contacts the skin over

3×10^{-4} cm^2 surface area. The back plane of the tip is connected to a coin-size ceramic heater keeping the tip at a constant temperature of 400 °C during operation. The heater is pressed against the tip by a spring to ensure good thermal matching. When not in use, the tip is base-positioned at a distance of 2 cm from the skin's surface ('home position'). The tip is re-usable, while the system checks, validates, cleans, sterilizes and exchanges tips automatically.

2.2.2. Tip's sterility

the system is designed to sterilize the tip before the system is ready for operation. When the tip reaches the temperature of 350 °C, the system's operation is blocked until the tip is heated to temperatures varying from 350 °C to 400 °C for duration of 3 min. Tip sterility has been evaluated in accordance with the requirements of ISO 20857 (ISO 20857 Sterilization of health care products – Dry heat – Requirements for the development, validation and routine control of a sterilization process for medical devices). Sterility, which means an absence of all viable microorganisms including viruses, is measured as a probability of no more than one viable microorganism per one million sterilized items of the final product (the generally accepted pharmacopoeial sterilization procedures is called 'sterility assurance level' (or SAL) of 1×10^{-6}). Four validation tests were performed, three of these tests at a half time cycle (a sterilization cycle of 1.5 min long), and a forth test was performed at a full cycle (for 3 min). After each cycle, the tips were tested for sterility by immersing the tips inside soybean-casein digest agar medium (trypticase soy agar, TSA), resulting in a negative growth after 7-day incubation at 30 ± 1 °C. In all four tests, no growth was observed for all tested items. Following validation of the sterilization process, the theoretical ability of the Tixel system to maintain its antiseptic capability was also evaluated before and during operation, based on the different spores' lethal characteristics. The calculations were based on a statistical model from which the calculation of system sterility assurance level (SAL) had been derived (ISO 20857, 2010) (data not shown). Calculations were performed on two spore types: (a) *Bacillus atrophaeus*, and (b) *Staphylococcus aureus*, skin bacteria which commonly lead to a severe bacterial infection such as in cellulitis.

2.2.3. Tixel's operation

The handpiece weighs 270 g. When the user places the handpiece flat on the skin and activates it, the linear motor rapidly advances the tip which comes in a brief contact with the tissue. There is an opening in the distance gauge through which the tip can protrude at a desired length, perpendicular to the skin, usually 400 μm beyond the distance gauge (Fig. 1B). During tip motion the supply of electrical energy to the heater continues and all control operations are active. Controls operations include a precise monitoring of the speed, the protrusion distance and the temperature of the tip. The thermal energy is transferred to the skin, creating micropores (or micro-craters) by evaporation. The tip recedes within a precisely a controlled distance and time to its 'home position', away from the tissue. The duration of the pulse, i.e. the time of contact between the tip and the skin, can be adjusted between 6 ms to18 ms, however, we have operated the instrument at no higher than 9 ms since this time duration did not cause any coagulation or necrosis. A double pulsing mode is also enabled. The motor's displacement accuracy is in the range of 1–8 μm. Energy calculations have been previously made (Lask et al., 2012; Elman et al., 2016), showing that a 14 ms pulse duration creates a high energy of ~25 mJ/pore while a 10 ms pulse duration creates a medium energy of ~15 mJ/pore and a 6 ms pulse duration results in a low energy of ~10 mJ/pore. The utilization of the Tixel does not require any protective eyewear or a smoke evacuator.

2.3. *In-vitro* skin penetration study

Permeability of the active compounds through pig skin was determined *in vitro* with a Franz diffusion cell system (PermeGear, Inc., Hellertown, PA). The diffusion area was 1.767 cm^2 (15 mm diameter orifice), and the receptor compartment volumes was from 12 ml. The solutions in the water-jacketed cells were thermostated at 37 °C and stirred by externally driven, Teflon-coated magnetic bars. Each set of experiments was performed with at least four diffusion cells ($n \geq 4$). The use of animal skin was performed in accordance with protocols reviewed and approved by the Institutional & Use Committee, Ben Gurion University of the Negev, which complies with the Israeli Law of Human Care and Use of Laboratory Animals. Fresh pig ears were obtained from the Institute of Animal Research (Kibbutz Lahav, Israel). Full-thickness porcine skin was excised from the fresh ears of slaughtered white pigs (100 kg, aged 6 months, breeding of Landres and Large White). After subcutaneous fat was removed with a scalpel, the skin was used immediately (Sintov and Botner, 2006; Sintov and Greenberg, 2014). All skin sections were measured for transepidermal water loss (TEWL) before mounted in the diffusion cells or stored at lower temperatures until used. TEWL examinations were performed on skin pieces using Dermalab® Cortex Technology instrument, (Hadsund, Denmark) and only those pieces that the TEWL levels were less than 10 g/m^2/h were introduced for testing. The skin was placed on the receiver chambers with the stratum corneum facing upwards, and the donor chambers were then clamped in place. The excess skin was trimmed off, and the receiver chamber, defined as the side facing the dermis, was filled with phosphate buffered saline (PBS containing 10 mM PO_4^{-3}, 137 mM NaCl, and 2.7 mM KCl, pH 7.4). After 15 min of skin washing at 37 °C, the buffer was removed from the cells and the receiver chambers were refilled with fresh PBS solution. Aliquots (0.5 g each) of a solution of a test compound were applied on the skin at time = 0. Samples (2 ml) were withdrawn from the receiver solution at predetermined time intervals, and the cells were replenished up to their marked volumes with fresh buffer-ethanol solution each time. Addition of buffer solution to the receiver compartment was performed with great care to avoid trapping air beneath the dermis.

2.4. Intradermal delivery evaluation – skin extraction

In studies using magnesium ascorbyl phosphate as a model, the post-experimental skin tissue was wiped carefully with a moist cotton wool and tape-stripped (x10) to remove the residues of ascorbyl phosphate adsorbed over the stratum corneum. The tissue was then weighed and cut to small pieces and inserted into 2-ml vials. The skin pieces in each vial were extracted by 0.5 ml distilled water. The extraction was performed by incubation in a shaker (750 rpm) for 30 min. The receiver samples and the skin extracts were taken into 1.5-ml vials and kept at −20 °C until analyzed by HPLC within two days.

2.5. HPLC analysis of samples from receiver solutions and skin extracts

Aliquots of 20 μl from each vial containing verapamil, diclofenac, or ascorbyl phosphate were injected into HPLC system (Shimadzu VP series including diode-array detector for peak spectrum identification), equipped with a prepacked C_{18} column (Betasil C18, 5 μm, 250 × 4.6 mm, ThermoHypersil, UK) heated to a temperature of 30 °C.

2.5.1. Verapamil

The quantitation of verapamil was performed by integration of peaks detected at 200 nm. The samples were chromatographed using an isocratic mobile phase consisting of phosphate buffer

(0.02 M, pH 3.0)—acetonitrile (50:50) at a flow rate of 1.0 ml/min. A calibration curve (peak area versus drug concentration) was constructed by running working standard verapamil HCl solutions in PBS for every series of chromatographed samples. Calibration curves were linear over the range 0.1–100 μg/ml (0.1, 0.25, 0.5, 0.75, 1, 2.5, 5, 7.5, 10, 25, 50, 75, 100 μg/ml).

2.5.2. Diclofenac

The quantitation of diclofenac was performed by integration of peaks detected at 280 nm. The samples were chromatographed using an isocratic mobile phase consisting of acetate buffer (0.01 M, pH 6.3)—acetonitrile (60:40) at a flow rate of 1.0 ml/min. A calibration curve (peak area versus drug concentration) was constructed by running working standard sodium diclofenac solutions in PBS for every series of chromatographed samples. Calibration curves were linear over the range 0.5–75 μg/ml (0.5, 1.0, 3.0, 5.0, 7.0, 10, 20, 50, 75 μg/ml).

2.5.3. Ascorbyl phosphate

The quantitation of diclofenac was performed by integration of peaks detected at 255 nm. The samples were chromatographed using an isocratic mobile phase consisting of 75% acetate buffer (0.08 M, pH 5.0) containing 0.016% sodium edetate, 0.075% (v/v) *n*-octylamine, and 5% (v/v) methanol (Solution A) and 25% methanol (Solution B) at a flow rate of 0.9 ml/min. A calibration curve (peak area versus drug concentration) was constructed by running working standard solutions of magnesium ascorbyl phosphate (MAP) in PBS for every series of chromatographed samples. Calibration curves were linear over the range 0.1–20 μg/ml (0.1, 0.5, 1.0, 3.0, 5.0, 7.0, 10, 20 μg/ml).

2.6. Calculation of the in vitro data

A calibration curve (peak area versus drug concentration) was constructed by running standard solutions of the test compound in ethanol for each series of chromatographed samples. As a result of the sampling of large volumes from the receiver solution (and the replacement of these amounts with equal volumes of buffer), the receiver solution was constantly being diluted. Taking this process into account, the cumulative drug that permeated out into the receiver ($Q_{out}(t_n)$) at the end of the n^{th} sampling time ($n \geq 0$) was calculated according to the following equation:

$$Q_{out}(t_0) = C_{out}(t_0) = 0$$

$$Q_{out}(t) = VrC_{out}(t_n) + \sum_{i=0}^{n-1} VsC_{out}(t_n) n \geq 1$$

where $C_{out}(t_n)$ is the drug concentration in the receiver at sampling time t_n, expressed by a running number ($t = 1, 2, 3 \ldots t_n$). *Vr* and *Vs* are the constant volumes of the receiver and the sample solutions, respectively. Data was expressed as the cumulative drug permeation per unit of membrane surface area, $Q_{out}(t_n)/S$ ($S = 1.767\ cm^2$).

The steady-state fluxes (*Jss*) were calculated by linear regression interpolation of the experimental data at a steady state:

$$Jss = \Delta Q_{out}(t_n)/(\Delta t \cdot S)$$

Apparent permeability coefficients (*Kp*) were calculated according to the equation:

$$Kp = Jss/Cd$$

where *Cd* is the concentration of the test compound in the donor compartment (1.0 wt% or 1.0×10^4 μg/ml), and it assumed that under sink conditions the concentration of the test compound in the receiver compartment is negligible compared to that in the donor compartment.

2.7. Imaging of Tixel—treated skin by phenol red dyeing

Phenol red (phenolsulfonphthalein, $pK_a = 7.9$) was used to stain the channels once created. This dye is a common indicator used for monitoring pH changes. Its color gradually changes from yellow to red over the pH range 6.6–8.0. Phenol red's transition point from yellow to red occurs at pH = 7.5, which is approximately the physiological pH of body fluids. A few drops of the dye were placed on pig skin samples immediately after treated by the Tixel. After 2 h, the skin was wiped and examined under a magnifying glass.

2.8. In vivo imaging of tixel-treated skin in humans by fluorescence confocal microscopy

The experiments were carried out in 6 volunteers (healthy Caucasians aged between 33 and 61 years, female/male ratio = 1) on their lower arm skin. Institutional Helsinki Committee's approval had been granted by the local Ethics Committee (Berlin, Germany). The imaging was performed using a confocal laser scanning microscope (LSM), VivaScope 1500 multilaser (Lucid Inc, Rochester, NY, USA), which is commonly implemented for *in vivo*/*ex vivo* skin investigations. The VivaScope system allows using a laser beam in the near-infrared range (830 nm) to visualize horizontal (*en face*) sections of the human skin *in vivo* and non-invasively. Cellular details can be visualized at a high resolution and a good contrast without necessitating a biopsy and further histological processing or staining. Contrasts in the reflectance confocal microscopic (RCM) images are mainly due to variations in refractive indices of tissue structures. A near-infrared laser (785 nm, 26 mW on the skin surface) was used to analyze the skin samples in the fingerprint region (400–2000 cm^{-1}). The 785 nm excitation wavelength has been widely used for Raman measurements in the field of dermatology due to the reduced absorption and scattering by the skin and, as a result, the high penetration ability. The Raman fingerprint spectra were recorded from the skin surface down to a depth of 250 μm at increments of 10 μm. The immersion oil, the measurement window, and the skin, all possess the same refractive index of around 1.45; therefore, all the depths measured by RCM have been considered as real geometrical depth values. The acquisition time for one Raman spectrum was 5 s, and the detailed Raman profiles were acquired within the epidermis profile. A fluorescence imaging was examined in one volunteer in order to make the cellular structure visible. In this case, a fluorescent dye (0.2% fluorescein in water) was applied to the skin just before starting the LSM measurements. The stratum corneum is a penetration obstacle for sodium fluorescein, but the disruption of this horny layer by the Tixel (400 μm, 8 ms duration) enables the fluorescent probe to be used as a contrast agent for labelling the microchannels and their structures. To examine the relative sustainability of the microchannels (or microcraters), the fluorescein solution was applied 2 and 6 h after the treatment.

2.9. Histology

Skin samples were taken immediately after craters were created by the Tixel, and preserved in 4% buffered formaldehyde solution. The samples were embedded in paraffin wax, cut to a thickness of 4–5 μm, stained with hematoxylin and eosin (H&E) and examined microscopically.

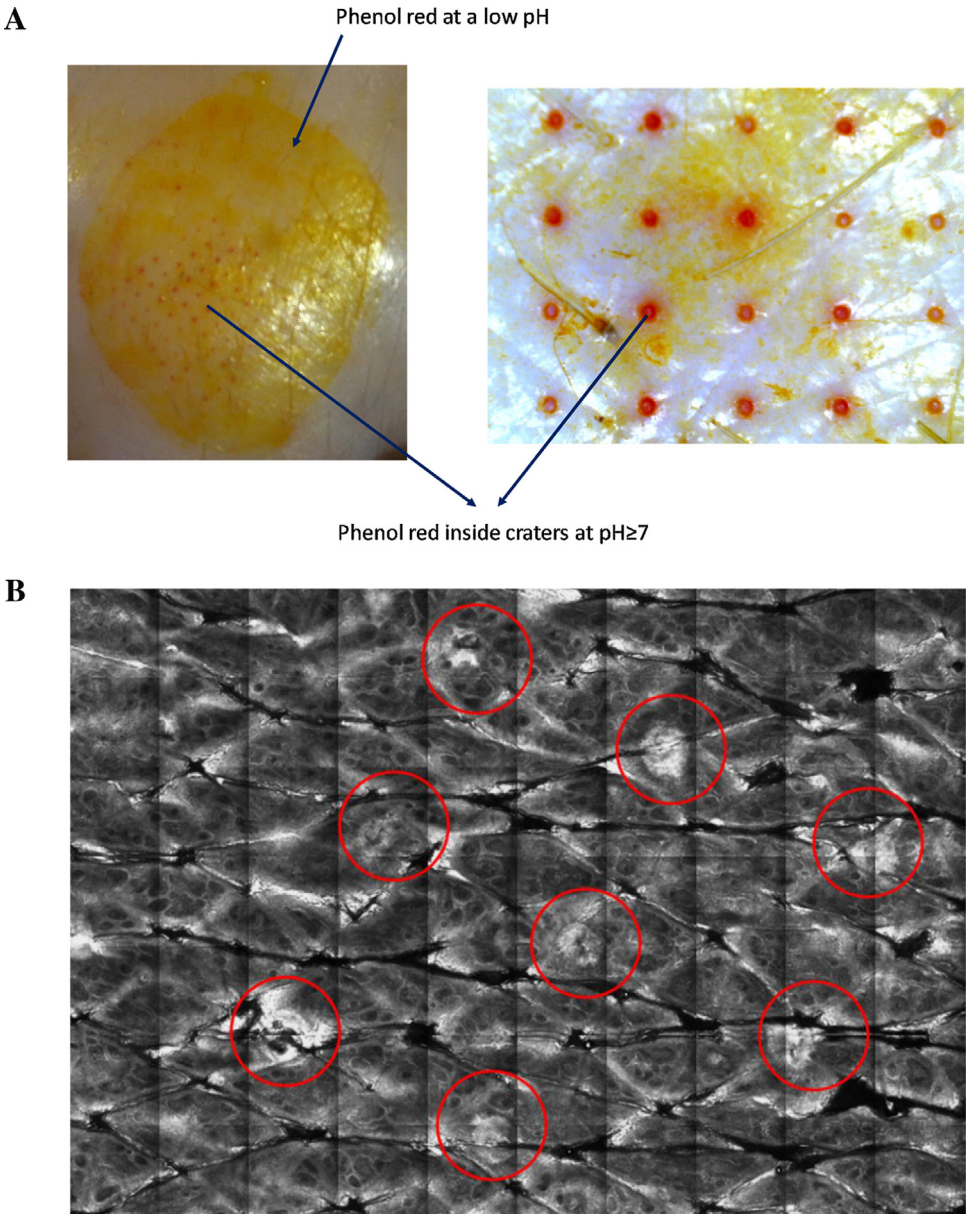

Fig. 2. A. Pig skin stained with Phenol red after Tixel treatment (400 μm protrusion, 8 ms pulse duration). Note the change from yellow to red when the dye penetrates inside the micropores, indicating an exposure to physiological pH. B. Micropores in the stratum corneum (red circles) as viewed by *in vivo* confocal microscopy on human skin (400 μm protrusion, 8 ms pulse duration). (For interpretation of the references to colour in this figure legend, the reader is referred to the web version of this article.)

3. Results and discussion

This study aimed to examine a novel thermo-mechanical technology for selective skin ablation, which does not damage the tissue or cause pain (Elman et al., 2016). The first goal was to establish by imaging and histological techniques the shape and morphology of the microchannels created through the stratum corneum by the new fractional ablative device. The penetrations of a hydrophilic fluorescent agent and a pH-sensitive dye were also imaged. The second goal was to evaluate the practical effectiveness of the method on skin permeability for the purpose of transdermal delivery of hydrophilic active agents.

3.1. Microscopic observation of Tixel-treated skin and imaging of micro-channels

After Tixel-treatment of fresh pig skin sections (8 ms, 400 μm protrusion) and dyeing with Phenol red (yellow color in the applied solution), red dots were observed (Fig. 2A) on the skin surface, most of them looked pretty much as open rings. This observation as shown in the photographs of Fig. 2A demonstrates uniform microchannels which were open enough to allow the interstitial fluid to fill them up. The fluid raised the pH to a physiological level,

Table 1
Depths (in μm) of Tixel-formed micropores as measured by confocal laser scanning microscopy.

Volunteer's code	Micropores' depth, μm		
	0 h after Tixel	2 h after Tixel	6 h after Tixel
C-L	178.19	169.30	168.17
P-S	164.57	165.78	163.56
M-L	187.45	189.01	186.73
R-S	164.59	153.54	151.20
F-K	169.17	161.75	159.73
M-H	173.74	172.41	170.56
Average (±SD)	172.95(±8.86)	168.63(±11.94)	166.65(±11.97)

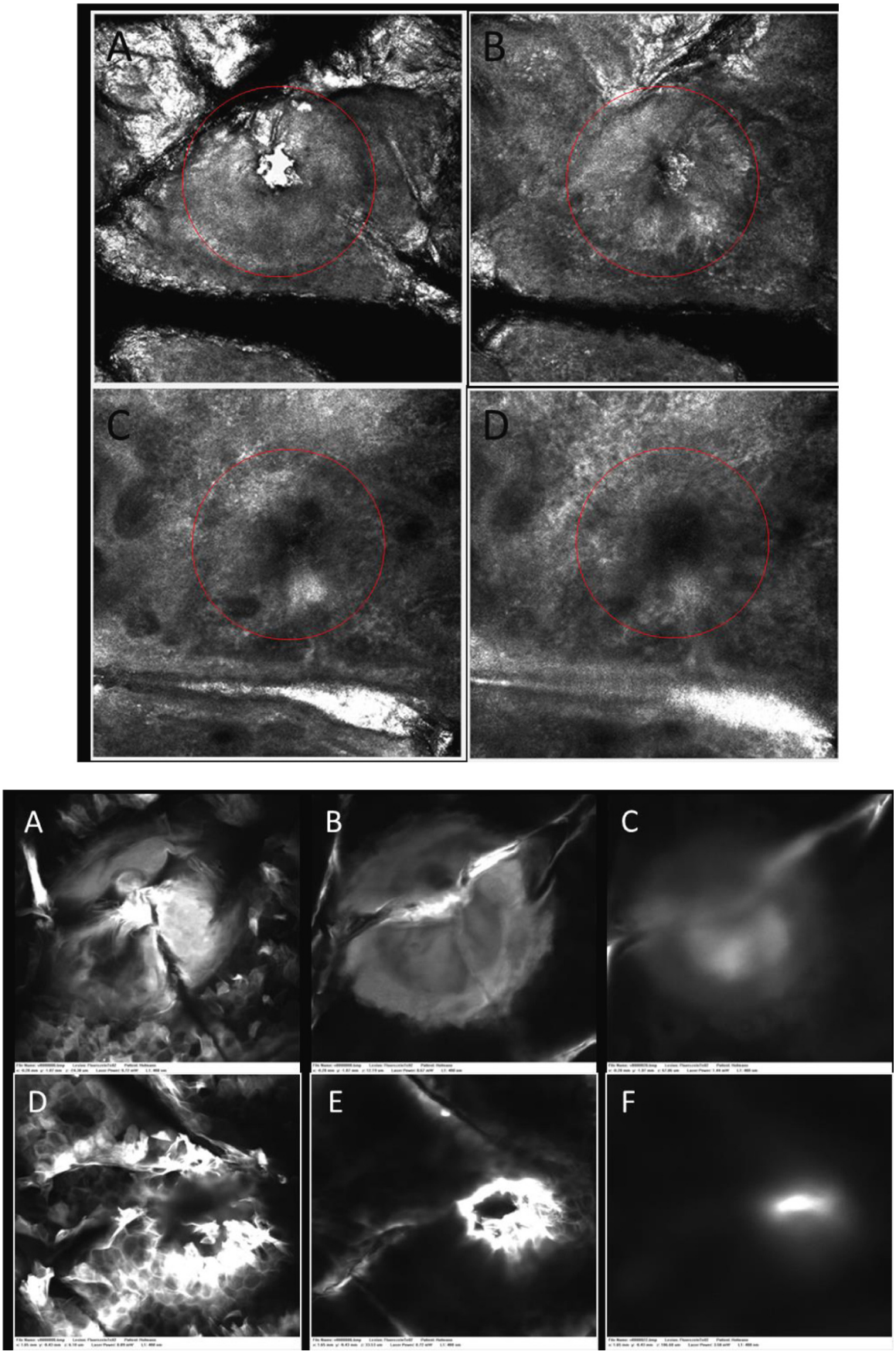

Fig. 3. Upper picture—Open microchannels generated by the Tixel as visualized *in vivo* by confocal microscope on human skin. The microchannels were stained by sodium fluorescein applied immediately after Tixel treatment. Red circle shows the microchannel (8 ms pulse): (A) skin surface, (B) epidermis layer, (C, D) papillary dermis layer. Lower

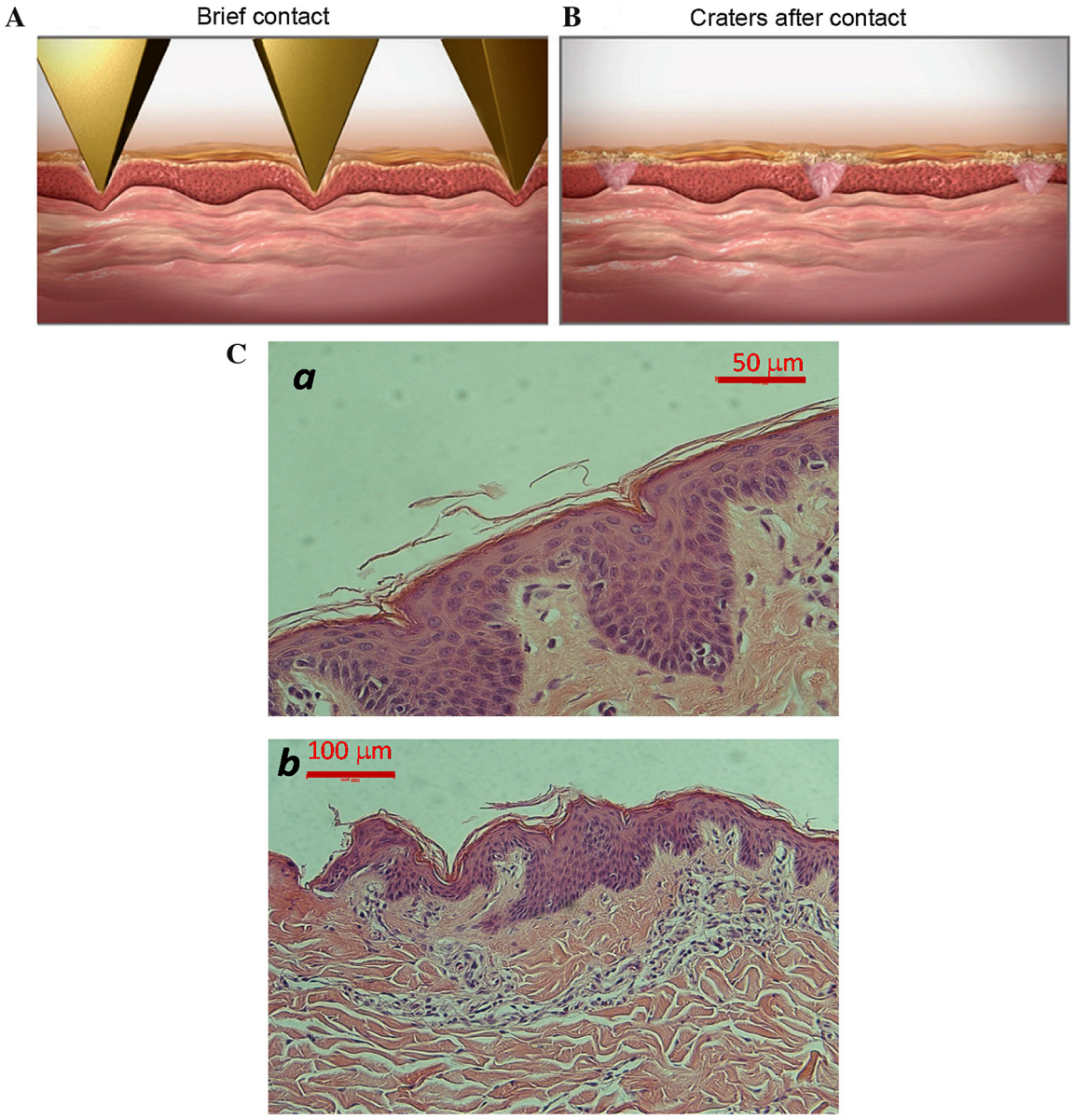

Fig. 4. Schematic presentation of the microchanneling process occurred during the high-temperature tip contact (A) and (B); Representative histological micrograph of cross-sectioned porcine skin after Tixel operation (C), 8 ms single-pulse (*a*) and 8 ms double-pulse (*b*) (400 μm protrusion).

and thereby, the dye changed its color. A fluorescent probe was also used to image penetration of hydrophilic compounds in a human volunteer after Tixel treatment. It should be noted that the *in vivo* treatment did not cause pain or inconvenience, however, very slight erythema sometimes occurred and disappeared within a few hours (Elman et al., 2016). Visualization of the microchannels by confocal microscopy showed clean holes (Fig. 2B), which remained open for at least 6 h, 172.9 ± 8.9 μm at $t = 0$, 168.6 ± 11.9 μm at $t = 2$ h, and 166.6 ± 12.0 μm at $t = 6$ h (Table 1). Fig. 3 shows that the fluorescent dye penetrated through the epidermis down to the papillary dermis *in vivo* (upper picture). Interestingly, the penetration of the fluorescent dye was enhanced when applied a few hours after Tixel treatment (Fig. 3, lower picture). The picture exemplifies the fluorescence emission in three skin layer within the epidermis, clearly demonstrating an increased intensity after 6 h compared with the intensity after 2 h post-treatment. It was evidenced therefore that (a) the microchannels endured for hours after their formation, and (b) the permeability of the hydrophilic dye even increased with time. Although the mechanism is unclear, it may imply that the ablated cells on the inside wall of the microchannel decomposed or cleared away as time has passed, enabling more permeant to undisturbedly diffuse. It is conceived that the abrupt ablation of the skin's superficial tissue is carried out by increments of thermal energy transfer during the perpendicular motion of the 400 °C-heated tip. By the first contact with the stratum corneum, water is evaporated resulting in partial cooling of the tip apex. In the next incremental movement, more surrounding cells are exposed to the advanced pin, particularly due to its pyramidal shape (Fig. 4), leading to a more water evaporation and cooling and so on until the pin retracts. Once the

picture—Diffusion of the fluorescent compound is visualized in the epidermis and the upper dermis. First row—Tixel was applied on the skin 2 h prior to the dyeing procedure, (A) 36 μm deep; (B) 54 μm deep; (C) 101 μm deep. Second row—Tixel was applied on the skin 6 h prior to imaging, (D) 30 μm deep; (E) 67 μm deep; (F) 113 μm deep. (For interpretation of the references to colour in this figure legend, the reader is referred to the web version of this article.)

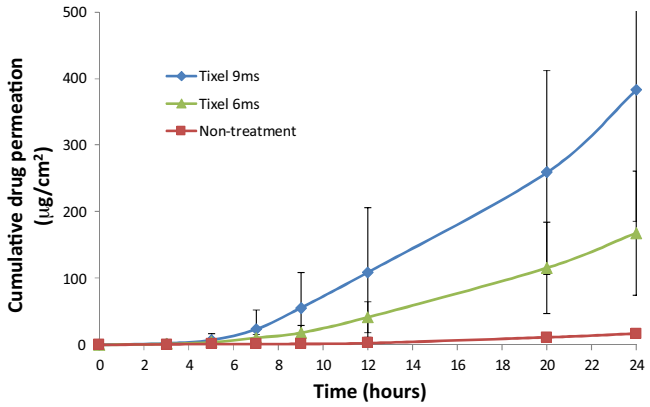

Fig. 5. Percutaneous permeation of verapamil hydrochloride (1% aqueous solution) through Tixel-pretreated pig skin at 6 ms (n = 5) and 9 ms (n = 9) pulse durations (400 μm protrusion) compared with untreated skin (n = 6). Drug permeation is expressed in μg per cm^2 of skin surface area vs. time in hours.

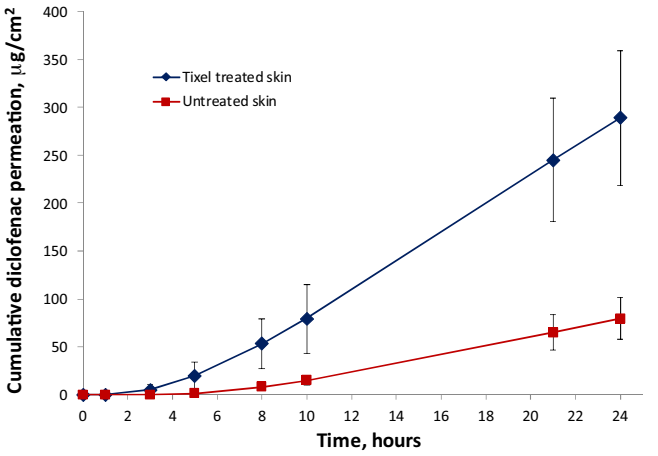

Fig. 6. Percutaneous permeation of sodium diclofenac (1% aqueous solution) through Tixel-pretreated pig skin at 8 ms pulse duration (and 400 μm protrusion) (n = 6) compared with untreated skin (n = 5). Drug permeation is expressed in μg per cm^2 of skin surface area vs. time in hours.

Tixel is activated, the very brief pulse combining with the low thermal conducting metal of the tip result in a minimal but sufficient energy for creation of water vapors. Thus, the generated water vapors carry most of the energy away sparing the viable epidermis and deeper skin tissues from a significant collateral thermal damage. Fig. 4C(*a*, *b*) shows cross-section histological micrographs of pig skin after treated by Tixel (SS tip, 400 μm protrusion; a. 8 ms single pulse, and b. 8 ms double-pulse). As observed in the micrographs, there was minimal damage to the epidermis with no necrosis or dermal coagulation.

3.2. Effect of the Tixel on skin permeability

The *in vivo* study has shown that (1) there was no real tissue damage when the Tixel had been operated in short durations (<9 ms) and a protrusion of 400 μm, (2) the diffusion of a hydrophilic dye such as fluorescein sodium confronted less impedance, due to an increase in skin permeability, and (3) the formed microchannels remained open or ajar for at least 6 h. Although application of a drug several hours after Tixel pretreatment is not clinically practical, it is an important finding suggesting that variations in the time interval from Tixel pretreatment to drug treatment would not be that critical for the therapeutic adequacy. Nonetheless, the latter *in vivo* finding is not relevant to the *in vitro* studies, in which the ablated luminal tissue of the microchannels in excised skin cannot be disintegrated and cleared to facilitate drug permeability. The *in vitro* permeation tests of drugs has been examined and determined after a single-pulse of the Tixel stainless steel tip. Although double-pulse might have resulted in a higher drug permeability (Fig. 4*b*), it was beyond the scope of this study aiming to only provide a proof of concept for the Tixel's function as an effective facilitating device for transdermal drug delivery.

3.2.1. Verapamil hydrochloride

Fig. 5 illustrates the transdermal permeation of verapamil. As shown, the penetration of verapamil hydrochloride increased about 10 and 20 times after skin had been pretreated with Tixel system for 6 ms and 9 ms, respectively ($Q_{24} = 168.2 \pm 93.0$ and 382.6 ± 196.8 μg/cm^2 compared to $Q_{24} = 17.0 \pm 6.1$ μg/cm^2 in untreated skin; $p < 0.05$, Student's *t*-test) (Table 2). In addition, lag time to get quantitative permeation across the skin decreased significantly from 9 to 10 h in untreated skin to 5 h in Tixel-treated skin. The permeability coefficient (*Kp*) of verapamil increased from 0.95×10^{-4} ($\pm 0.40 \times 10^{-4}$) cm/h in untreated skin to 9.32×10^{-4} ($\pm 5.40 \times 10^{-4}$) and 20.60×10^{-4} ($\pm 10.15 \times 10^{-4}$) cm/h in Tixel-pretreated skin at 6 ms and 9 ms pulse durations, respectively (Table 2 and Fig. 5).

3.2.2. Diclofenac sodium

Fig. 6 illustrates the transdermal permeation of the diclofenac. The penetration of sodium diclofenac increased about 3 times after skin had been pretreated with Tixel system for 8 ms ($Q_{24} = 289.1 \pm 70.5$ μg/cm^2 compared to $Q_{24} = 79.4 \pm 21.7$ μg/cm^2 in untreated skin; $p < 0.05$, Studetnt's *t*-test) (Table 2). In addition, lag time to get quantitative permeation across the skin decreased significantly from 5 h in untreated skin to 3 h in Tixel-treated skin. The permeability coefficient (*Kp*) of diclofenac increased from 4.26×10^{-4} ($\pm 1.18 \times 10^{-4}$) cm/h in untreated skin to 14.47×10^{-4} ($\pm 3.07 \times 10^{-4}$) cm/h in Tixel-pretreated skin (Table 2).

3.2.3. Magnesium ascorbyl phosphate

Fig. 7A illustrates the transdermal permeation of the ascorbyl phosphate. While no permeation was noted through untreated

Table 2
Apparent permeability coefficient (*Kp*) values of active compounds (in 1% aqueous solutions).

Active Substance	*Kp* (±SD) × 10^4 [cm/h]		Q_{end} (±SD) [μg/cm^2]	
	Non-Treatment	Tixel-treatment	Non-Treatment	Tixel-treatment
Verapamil	0.95 (±0.40)	6 ms: 9.32 (±5.40) 9 ms: 20.60 (±10.15)	17.0 (±6.1)	6 ms: 168.2 (±93.0) 9 ms: 382.6 (±196.8)
Diclofenac	4.26 (±1.18)	14.47 (±3.07) [a]	79.4 (±21.7)	289.1 (±70.5) [a]
Ascorbyl phosphate	0	2.02 (±0.49) [a]	0	10.5 (±1.8) [a]

[a] Skin was pretreated by the Tixel at a 8 ms pulse duration.

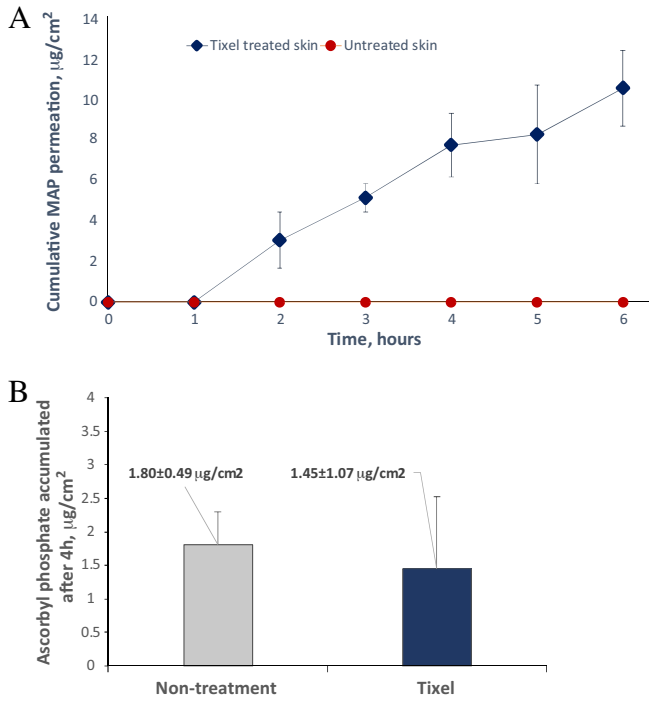

Fig. 7. Percutaneous permeation (A) and skin retention (B) of magnesium ascorbyl phosphate (1% aqueous solution) in Tixel-pretreated pig skin at 8 ms pulse duration (and 400 μm protrusion) (n = 5) compared with untreated skin (n = 5). Drug permeation is expressed in μg per cm^2 of skin surface area vs. time in hours. Drug retention is expressed in μg per cm^2 of skin surface area after 4 h.

skin, a quantitative transdermal penetration (6 h post-application) was detected after skin had been pretreated with Tixel system for 8 ms ($Q_6 = 10.5 \pm 1.8$ μg/cm^2; Table 2). The permeability coefficient (*Kp*) of the ascorbyl phosphate salt reached a value of 2.02×10^{-4} ($\pm 0.49 \times 10^{-4}$) cm/h in Tixel-pretreated skin (Table 2). Fig. 7B shows the retention of the vitamin derivative in the skin after 4 h post-application. Interestingly, no significant difference ($p > 0.05$, Student's *t*-test) has been found between the accumulative quantities within the skin although slight decrease can be denoted in the mean value determined in the Tixel-treated skin (1.45 μg/cm^2 vs. 1.80 μg/cm^2). This result has shown that the content of ascorbyl phosphate in Tixel-treated skin at steady-state was not significantly changed by the relatively high percutaneous flux created by Tixel pretreatment. However, the distribution of ascorbyl phosphate within the skin layers may be more homogeneous after Tixel pretreatment compared to untreated skin, where a high gradient of the active compound probably exists with a higher accumulation in the upper layers.

4. Conclusion

In conclusion, the results obtained in this study have shown that the skin permeability of hydrophilic molecules, which poorly penetrate the lipophilic stratum corneum barrier, was significantly enhanced by using the Tixel device. The Tixel, based on a TMAb technology, produced no skin damage in humans. The apparent safety of the fractional ablation technology is probably due to the short duration of the energy transfer, creating microchannels over a small portion of the total skin area exposed to the tip. Since the radius of each microchannel is approximately 100 μm and its surface area is 3×10^{-4} cm^2, the treated skin area is therefore occupied by only 2.4% of microchannels (the tip contains 81 pyramidal pins arrayed over a surface area of 1 cm^2). The sterility of the Tixel's tip is maintained before each operation as described in 'Materials and Methods'. After cleaning the skin by an alcohol swab, the application using a constant high temperature (400 °C) actually sterilizes the application area during the contact. After Tixel's operation, the skin might be further biosecured by utilizing aseptic or sterile topical preparations. Apart from the safety, an interesting phenomenon has been noted in the human study, which was the endurance of the microchannels hours after their formation. In addition, the permeability of the hydrophilic marker even increased with time. The mechanism of this phenomenon is not thoroughly clear and remains to be explored. The safety and the skin permeability of hydrophilic active compounds after Tixel's double-pulse (or multi-pulse) pretreatments of the skin should also be further experimented. In addition, high molecular weight compounds, such as proteins and polysaccharides, are remained to be studied widening the potential uses of the Tixel.

Acknowledgments

The authors are grateful for the professional assistance of Ms. Lillia Shapiro and Mr. Igor Greenberg at the Laboratory for Biopharmaceutics. We also gratefully acknowledge the help of the Institute of Pathology's laboratories at Soroka University Medical Center, Be'er Sheva, Israel.

References

Anderson, M.S., Shankey, T.V., Lubrano, T., Mulhall, J.P., 2000. Inhibition of Peyronie's plaque fibroblast proliferation by biologic agents. Int. J. Impot. Res. Suppl. 3, S25–31.
Bachhav, Y.G., Summer, S., Heinrich, A., Braganga, T., Bohler, C., Kalia, Y.N., 2010. Effect of controlled laser microporation on drug transport kinetics into and across the skin. J. Control. Release 146, 31–36.
Bachhav, Y.G., Heinrich, A., Kalia, Y.N., 2013. Controlled intra- and transdermal protein delivery using a minimally invasive Erbium:YAG fractional laser ablation technology. Eur. J. Pharm. Biopharm. 84, 355–364.
Barry, B.W., 2001. Novel mechanisms and devices to enable successful transdermal drug delivery. Europ. J. Pharm. Sci. 14, 101–114.
Ben-Shabat, S., Baruch, N., Sintov, A.C., 2007. Conjugates of unsaturated fatty acids with propylene glycol as potentially less-irritant skin penetration enhancers. Drug Dev. Ind. Pharm. 33, 1169–1175.
Davis, A.F., Gyurik, R.J., Hadgraft, J., Pellett, M.A., Walters, K.A., 2002. Formulation strategies for modulating skin penetration. In: Walters, K.A. (Ed.), Dermatological and Transdermal Formulations.. Marcel Dekker Inc, New York, pp. 271–317.
Elman, M., Fournier, N., Barneon, G., Hofmann, M., Bernstein, M.D., Lask, G., 2016. Fractional treatment of aging skin with tixel, a clinical and histological evaluation. J. Cosmet. Laser Ther. 20, 1–7.
Farris, P.K., 2005. Topical vitamin C: a useful agent for treating photoaging and other dermatologic conditions. Dermatol. Surg. 31, 814–817 (review).
Giuliano, F., Warner, T.D., 1999. Ex vivo assay to determine the cyclooxygenase selectivity of non-steroidal anti-inflammatory drugs. Br. J. Pharmacol. 126, 1824–1830.
Greenfield, J.M., Shah, S.J., Levine, L.A., 2007. Verapamil versus saline in electromotive drug administration for Peyronie's disease: a double-blind, placebo controlled trial. J. Urol. 177, 972–975.
Guy, R.H., Delgado-Charro, M.B., Kalia, Y.N., 2001. Iontophoretic transport across the skin. Skin Pharmacol. Appl. Skin Physiol. 14, 35–40.
Henry, S., McAllister, D.V., Allen, M.G., Prausnitz, M.R., 1998. Microfabricated microneedles: a novel approach to transdermal drug. J. Pharm. Sci. 87, 922–925.
Hu, Q., Liang, W., Bao, J., Ping, Q., 2000. Enhanced transdermal delivery of tetracaine by electroporation. Int. J. Pharm. 202, 121–124.
Kaur, M., Ita, K.B., Popova, I.E., Parikh, S.J., Bair, D.A., 2014. Microneedle-assisted delivery of verapamil hydrochloride and amlodipine besylate. Europ. J. Pharm. Biopharm. 86, 284–291.
Kriwet, K., Müller-Goymann, C.C., 1993. Binary diclofenac diethylamine-water systems, micelles, vesicles, and lyotropic liquid crystals. Eur. J. Pharm. Biopharm. 39, 234–238.
Kriwet, K., Müller-Goymann, C.C., 1995. Diclofenac release from phospholipid drug systems and permeation through excised human stratum corneum. Int. J. Pharm. 125, 231–242.
Lask, G., Elman, M., Fournier, N., Slatkine, M., 2012. Fractional vaporization of tissue with an oscillatory array of high temperature rods –Part I: ex vivo study. J. Cosmet. Laser Ther. 5, 218–223.
Lee, J.W., Gadiraju, P., Park, J.H., Allen, M.G., Praunitz, M.R., 2011. Microsecond thermal ablation of skin for transdermal drug delivery. J. Control. Release 54, 58–68.
Levine, L.A., Goldman, K.E., Greenfield, J.M., 2002. Experience with intraplaque injection of verapamil for Peyronie's Disease. J. Urol. 168, 621–626.

Marro, D., Guy, R.H., Delgado-Charro, M.B., 2001. Characterization of the iontophoretic permselectivity properties of human and pig skin. J. Control. Release 70, 213–217.
McAllister, D.V., Allen, M.G., Prausnitz, M.R., 2000. Microfabricated microneedles for gene and drug delivery. Ann. Rev. Biomed. Eng. 2, 298–313.
Ogra, M., Pahwal, S., Mitragotri, S., 2008. Low frequency sonophoresis: current status and future prospects. Adv. Drug Delivery Rev. 60, 1218–1223.
Park, J.H., Lee, J.W., Kim, Y.C., Prausnitz, M.R., 2008. The effect of heat on skin permeability. Int. J. Pharm. 359, 94–103.
Prausnitz, M.R., Bose, V.G., Langer, R., Weaver, J., 1993. 1993: Electroporation of mammalian skin: a mechanism to enhance transdermal drug delivery. Proc. Natl. Acad. Sci. U. S. A. 90, 10504–10508.
Prausnitz, M.R., 1999. A practical assessment of transdermal drug delivery by skin electroporation. Adv. Drug Delivery Rev. 35, 61–76.
Riviere, J.E., Monteiro-Riviere, N.A., Rogers, R.A., Bommannan, D., Tamada, J.A., Potts, R.O., 1995. Pulsatile transdermal delivery of LHRH using electroporation: drug delivery and skin toxicology. J. Control. Release 36, 229–233.
Singh, P., Liu, P., Dinh, S.M., 1999. Facilitated transdermal delivery by iontophoresis, In: Bronaugh, R.L., Maibach, H.I. (Eds.), Percutaneous Absorption, Drugs-Cosmetics-Mechanisms-Methodology.. 3rd ed. Marcel Dekker Inc, New York, pp. 633–657.
Sintov, A.C., Botner, S., 2006. Transdermal drug delivery using microemulsion and aqueous systems: influence of skin storage conditions on the in vitro permeability of diclofenac from aqueous vehicle systems. Int. J. Pharm. 311, 55–62.
Sintov, A.C., Brandys-Sitton, R., 2006. Facilitated skin penetration of lidocaine: combination of a short-term iontophoresis and microemulsion formulation. Int. J. Pharm. 316, 58–67.
Sintov, A.C., Greenberg, I., 2014. Comparative percutaneous permeation study using caffeine-loaded microemulsion showing low reliability of the frozen/thawed skin models. Int. J. Pharm. 471, 516–524.
Sintov, A.C., Krymberk, I., Daniel, D., Hannan, T., Sohn, Z., Levin, G., 2003. Radiofrequency–driven skin microchanneling as a new way for electrically assisted transdermal delivery of hydrophilic drugs. J. Control. Release 89, 311–320.
Smith, E.W., Maibach, H.I., 1995. Percutaneous Penetration Enhancers. CRC Press, Boca Raton, FL.
Tuygun, C., Ozok, U.H., Gucuk, A., Bozkurt, I.H., Imamoglu, M.A., 2009. The effectiveness of transdermal electromotive administration with verapamil and dexamethasone in the treatment of Peyronie's disease. Int. Urol. Nephrol. 41, 113–118.
Vanbever, R., Lecouturier, N., Preat, V., 1994. Transdermal delivery of metoprolol by electroporation. Pharm. Res. 11, 1657–1662.
Vanbever, R., Le Boulenge, E., Preat, V., 1996. Transdermal delivery of fentanyl by electroporation I. Influence of electrical factors. Pharm. Res. 13, 559–565.
Walters, K.A., 1989. Penetration enhancers and their use in transdermal therapeutic systems. In: Hadgraft, J., Guy, R.H. (Eds.), Transdermal Drug Delivery, Developmental Issues and Research Initiatives.. Marcel Dekker Inc, New York, pp. 197–246.

Thermomechanical Ablation-Assisted Photodynamic Therapy for the Treatment of Acne Vulgaris. A Retrospective Chart Review of 30 Patients

Yuval Hilerowicz,[1] Or Friedman,[2] Eyal Zur,[3] Roni Ziv,[4] Amir Koren,[1,4] Fares Salameh,[1] Joseph N. Mehrabi,[5] and Ofir Artzi[1,4]*

[1]*Department of Dermatology, Tel Aviv Sourasky Medical Center, Weizmann St 6, Tel Aviv, 6423906, Israel*
[2]*Department of Plastic Surgery, Tel Aviv Sourasky Medical Center, Sackler Faculty of Medicine, Tel Aviv University, Weizmann St 6, Tel Aviv, 6423906, Israel*
[3]*Compounding Solutions, 68 Masada street, Tel-Mond, 4062269, Israel*
[4]*Dr. Artzi and Associates—Treatment and Research Center, George weiss st 20, Tel Aviv, 6997712, Israel*
[5]*Sackler Faculty of Medicine, 35 klatzkin st, Tel Aviv, 6997801, Israel*

Background and Objectives: Acne vulgaris, a chronic inflammatory disease, affects more than 90% of teenagers. The first-line treatments for acne vulgaris are topical and oral medications, mainly antibiotics and retinoids. However, antibiotic resistance of *Propionibacterium acnes*, contraindications, partial response, significant adverse effects, or recurrence creates demand for novel treatment options in acne. Aminolevulinic acid (ALA) photodynamic therapy (PDT) is a well-established modality in the treatment of acne. Nevertheless, PDT has limitations: it may not be effective for every patient; several treatments are usually required to achieve sufficient outcome; incubation time is 1–3 hours; treatment pain and post-treatment downtime may be difficult for some patients to endure; and adverse effects may occur. This retrospective chart review was conducted to evaluate the efficacy and safety of PDT, assisted by a thermomechanical ablation (TMA) fractional injury device in the treatment of patients with moderate to severe acne.

Study Design/Materials and Methods: We conducted a retrospective chart review of 30 acne patients treated with TMA immediately before 5% ALA application with an incubation time of 1 hour and exposure to 60 J/cm^2 red light (630 nm). Patients received up to three monthly treatments and were followed for 16 weeks. Two independent investigators evaluated the subject outcomes according to high definition photographs taken at baseline, before each treatment and at follow-up visits. Three acne grading methods were used: Acne Grading Scoring System (AGSS), the Leeds revised acne grading system, and the general response to the treatment score. Patients also provided self-assessments of improvement using the patient global impression of change (PGIC).

Results: Compared with baseline, the AGSS has showed a statistically significant reduction of 26.7% and 23.7%, respectively, at weeks 8 and 16 after final treatment. The Leeds score showed 65.2% and 60.6% improvement at the respective visits. The overall response rate was graded 3.3 ± 0.5 out of 4. PGIC score given by the patients was 5.5 out of 7, reflecting high satisfaction.

Conclusion: TMA used immediately prior to ALA application may enhance the effectiveness of PDT in the treatment of acne with minimal side effects, reduced downtime, and fewer sessions. The exact mechanism of TMA-assisted PDT is still to be understood. Lasers Surg. Med. © 2020 Wiley Periodicals, Inc.

Key words: acne vulgaris; photodynamic treatment; ALA; tixel

INTRODUCTION

Acne vulgaris is a common condition among teenagers and adults, which might result in scarring [1]. Although highly effective, many patients refuse systemic treatment or pose relevant contraindications [1].

Photodynamic therapy (PDT) has been used as an alternative and effective evidence-based treatment for acne vulgaris since 2000 [2,3]. PDT is not effective for every patient. In most patients, several treatments are required to achieve an improvement. They are frequently associated with pain, downtime, and adverse effects. Preceding skin manipulation is aimed to enhance photosensitizer absorption and employed to improve PDT outcome, reduce pain and adverse effects, and ease downtime. Laser-assisted PDT has been advocated by many studies with impressive results when fractional

Conflict of Interest Disclosures: All authors have completed and submitted the ICMJE Form for Disclosure of Potential Conflicts of Interest and none were reported.
*Correspondence to: Ofir Artzi, MD, Department of Dermatology, Tel Aviv Sourasky Medical Center, Weizmann St 6, Tel Aviv 6423906, Israel. E-mail: ofira@tlvmc.gov.il
Accepted 30 March 2020
Published online in Wiley Online Library (wileyonlinelibrary.com).
DOI 10.1002/lsm.23246

TABLE 1. Acne Grading Scoring System (AGSS)

Acne Grading Scoring System (AGSS)	
1	Clear, indicating no inflammatory or non-inflammatory lesions.
2	Almost clear, rare non-inflammatory lesions with no more than one papule/pustule.
3	Mild, some non-inflammatory lesions, no more than a few papules/pustules but no nodules.
4	Moderate, up to many non-inflammatory lesions, may have some inflammatory lesions, but no more than one small nodule.
5	Severe, up to many non-inflammatory and inflammatory lesions, but no more than a few nodules.

ablative laser was used prior to PDT for the treatment of actinic keratosis [4].

The thermomechanical ablation (TMA) technology combines thermal energy with motion. At low energy settings, most of the thermal effect is concentrated in the stratum corneum (SC) leading to rapid heat transfer and dehydration of the layer. Heat from the thermal tip compromises the integrity of the SC, which consequently becomes brittle leading to layer breakage when the tip is progressed toward the treated tissue. Gentle elimination of the SC and desiccation of the upper epidermis establishes a concentration gradient by Fick's law. Thus, enhancement of drug delivery following TMA treatment is achieved. The aim of this study is to evaluate the efficacy and safety of TMA-assisted PDT for the treatment of patients with moderate to severe acne vulgaris.

MATERIALS AND METHODS

This is a retrospective chart review. All patients with acne vulgaris treated with TMA-assisted PDT in the Dr. Artzi & associates Treatment and Research Center between January 2018 and March 2019 were collected. Data collected included demographics, medical history, skin type, previous acne treatments, PDT treatment protocol, number of treatments, side effects, and patient photographs before treatment and at follow-up visits. The study included patients above the age of 16 years and excluded patients with concurrent acne treatment and pregnant and lactating women.

The TMA device (Tixel®, Novoxel®, Israel) combines thermal energy with motion. It consists of a titanium tip made up of an array of tiny pyramids heated to 400°C (752°F). The tip is advanced until contacted with the skin, dehydrates and breaks downs the SC, and, thus, facilitates the delivery and permeation of several drugs into the skin. This system is easy to operate and nearly painless.

Patients received up to three monthly treatments depending on the treating physician's recommendation, and their follow-up visits were done at week 8 and 16 after the final treatment. First, the face was washed with tap water and Cetaphil soap followed by the use of a dry towel. After the skin was pretreated with 2 cc 70% alcohol using a gauze, the TMA device was applied to the patient's face using contact intervals of 6 milliseconds with 400–600 protrusion. Immediately afterwards, aminolevulinic acid (ALA) gel in a concentration of 5% was applied under occlusion for 1 hour. Next, the face was illuminated with red light (630 nm) from a non-coherent light source (OMNILUX MEDICAL; PhotoTherapeutics a GlobalMed Technologies Co.Napa, California, USA) at a dose of 60 J/cm^2 for 12 minutes and 47 seconds while wearing protective eyewear. In the second and third treatments, the incubation time and light dose were elevated by 15 minutes and 5 J/cm^2, respectively, in each treatment. Immediate post-procedure care included topical cold wet dressings and thermal water (La Roche-Posay) applied continuously for 15 minutes. Patients were instructed to avoid sunlight for 48 hours and to use broad-spectrum sunscreen for 3 months after treatment. All patients were photographed using standardized high definition digital photography (VISIA; Canfield, Parsippany, NJ, USA) before and after each treatment session and in follow-up visits.

Two independent dermatologists, who were unaware of the treatment protocol, evaluated patient photographs and rated the improvement using the following scales: The acne grading scoring system (AGSS, a 1–5-point scale evaluating acne severity, Table 1), The Leeds revised acne grading system (a 12-point scale based on the comparison of the patient to a standardized, 12-color, pictorial grading series of facial acne, Table 2) and overall response rate (a 1–4 scale, Table 3). The patients' pain perceptions were evaluated using a visual analog scale ranging from 1 to 10. Downtime (days until returning to normal daily activity), reported adverse effects, and subjective patient global impression of changes (PGIC, a 1–7 scale, Table 4) were retrieved from the patients' charts.

The photosensitizer used in this trial was a compounded 5% w/v ALA gel (50 mg/ml gel). The source for the active pharmaceutical ingredient (API) ALA was Fagron (Netherlands). The compounded gel consisted of

TABLE 2. Leeds Revised Acne Grading System

Response to treatment	
1	Insignificant result-lesion numbers and erythema reduction between 0% and 25%.
2	Moderate result-lesion numbers and erythema reduction between 26% and 50%.
3	Good result-lesion numbers and erythema reduction between 51% and 75%.
4	Very good result-lesion numbers and erythema reduction between 76% and 100%.

TABLE 3. Overall Response Rate

Insignificant result (1)	Lesion numbers and erythema reduction between 0% and 25%.
Moderate result (2)	Lesion numbers and erythema reduction between 26% and 50%.
Good result (3)	Lesion numbers and erythema reduction between 51% and 75%.
Very good result (4)	Lesion numbers and erythema reduction between 76% and 100%.

the following excipients (% w/v): potassium sorbate 0.2% (preservative), oleic acid 10% (skin penetration enhancer), sepigel 305 10% (vehicle), purified water ~75% (solubilizer and part of the vehicle), and hydrochloric acid 10% solution/potassium hydroxide 15% solution (for adjusting the pH to 4). The decision to adjust the pH to 4 maintained the gel's stability [5]. The gel was prepared fresh before each participant's treatment. Sepigel 305, which creates the preparation's gel with the purified water, is a multifunctional vehicle with thickening, stabilizing, texturizing, and tissue-adhering properties in a wide pH range including the acid environment needed to maintain ALA stability [6,7]. Oleic acid is a known skin-penetrating enhancer of ALA with peak performance at 10% concentration [8].

RESULTS

A total of 30 patients (11 males and 19 females) received the TMA-assisted PDT treatment for acne vulgaris between January 2018 and March 2019. Their demographics are demonstrated in Table 5. None of the patients were excluded from the study. The average age of the participants was 29 ± 10.2 (range: 16–59). Fitzpatrick skin types II ($n = 19$) and III + IV ($n = 11$) were represented. Disease duration ranged from 1 to 22 years (mean 8.1 years, standard deviation [SD] $\pm$ 5.3). All patients failed at least one treatment modality (oral isotretinoin, oral antibiotics, and topical therapy) and rejected the possibility of oral isotretinoin cycle.

The mean number of treatments was 1.9 ± 0.86. Average pain level was 3.3 ± 0.8. There were no significant adverse events other than prolonged erythema (mean 12.4 days) encountered by 16 patients (53.3%). The average downtime was 6.4 ± 0.8 days. TMA-assisted PDT treatment showed significant responses in all measured scales (Figure 1). AGSS showed a mean improvement of 26.7%, 8 weeks after the final treatment, and this improvement persisted to be as high as 23.7% at 16 weeks after the final treatment follow-up. The Leeds score showed 65.2% and 60.6% improvement at 8 and 16 weeks after last treatment, respectively. Overall response rate was graded 3.3($\pm$0.5) out of 4, and the PGIC score given by the patients was 5.5 out of 7, reflecting high satisfaction.

TABLE 4. Patient Global Impression of Change (PGIC)

Patient Global Impression of Change (PGIC)	
1	No change (or condition has gotten worse).
2	Almost the same, hardly any change at all.
3	A little better, but no noticeable change.
4	Somewhat better, but the change has not made any real difference.
5	Moderately better, and a slight but noticeable change.
6	Better and a definite improvement that has made a real and worthwhile difference.
7	A great deal better and a considerable improvement that has made all the difference.

DISCUSSION

Acne vulgaris is a common multifactorial disorder of the pilosebaceous unit, affecting millions of teenagers and adults around the globe [1]. Moderate and severe acne are best treated with systemic drugs. These include oral antibiotics, isotretinoin, and contraceptives or antiandrogens. Oral antibiotics are usually prescribed for up to 6 months due to bacteria resistance, adverse effects, and lack of long-term efficacy. Isotretinoin is teratogenic, requires repeated blood and pregnancy tests, and incurs substantial side effects. Hormonal therapy is indicated only for female patients, and side effects include nausea, vomiting, abnormal menses, weight gain, breast tenderness, and increased risk for thromboembolism [1]. Nonmedical alternatives include intense pulsed light (IPL), Narrowband blue and red light, different diodes, lasers, and photodynamic therapy [2].

PDT has been used as an alternative and effective evidence-based treatment for acne vulgaris since 2000 [3]. The therapeutic effect of PDT is achieved by light activation of a photosensitizing agent, which, in the presence of oxygen, leads to the formation of reactive oxygen intermediates. These intermediates irreversibly oxidize essential cellular components, causing apoptosis and necrosis [9]. The efficacy of PDT treatment is limited by several factors, and one of them is the ability of the photosensitizer to reach the target zone—the sebaceous glands, which are located deep in the dermis.

Nevertheless, PDT has limitations. It is not effective for every patient; several treatments are usually required to achieve an outcome; intra-treatment pain and intolerable post-treatment adverse effects may occur. Most studies recommend 1–4 treatment sessions and show that more

TABLE 5. Demographics

Number of patients	30
Sex (% female)	63.3
Age (years)	29 ($\pm$10.2)
Disease duration (years)	8.1 ($\pm$5.3)

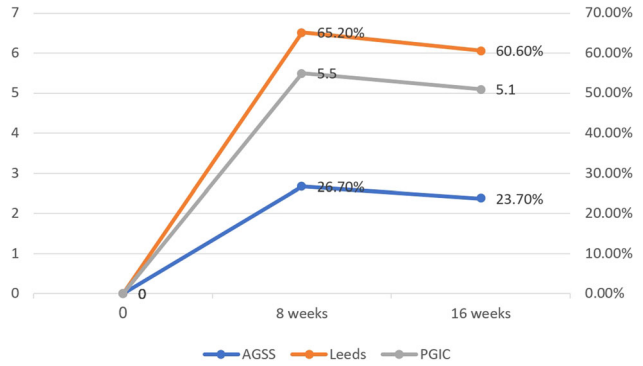

Fig. 1. The AGSS, Leeds, and PGIC scores before, at 8 and 16 weeks post-treatment. AGSS, Acne Grading Scoring System; PGIC, patient global impression of change.

PDT treatment sessions will result in a better acne clearance rate with 3–12 months remission post-treatment [5]. One study failed to demonstrate that three treatment sessions provide better results compared with a single treatment [10].

Over the years, six alterations have been suggested to improve PDT outcome and to decrease the difficult down-time and adverse effects. (i) The use of different photosensitizing agents such as *Propionibacterium acnes* intrinsic porphyrins, ALA hydrochloride, and methyl aminolevulinate. (ii) The use of lower concentrations of photosensitizing agents. ALA concentrations for acne vary between 5% and 20% [6]. Higher concentrations of ALA are considered to be more effective but with higher rate of adverse effects, pain level, and more difficult healing period [5]. Although, a few clinical trials supported the efficacy of 5% ALA for moderate to severe acne [11–13], using 10% ALA was shown to be more effective for severe acne than PDT using 5% ALA [14]. (iii) The use of different formulated photosensitizing agents aimed to optimize their skin permeation [13]. (iv) The use of different light sources —such as blue and red light [15], IPL, different lasers, and sunlight [5]. (v) The employment of different incubation and exposure times [5]. And lastly, (vi) preceding tissue manipulations aimed to enhance photosensitizer absorption. The latter showed impressive results when fractional ablative laser was used prior to PDT when treating actinic keratosis [4,16]. It is only reasonable to assume that pre-treatment with a laser will also enhance the efficacy when using PDT for acne allowing for lower ALA concentration and decreased incubation time.

Compared with lasers, mainly CO_2 lasers, the effect of TMA is more superficial [17,18]. However, pre-treatment with low-energy TMA was shown to increase the percutaneous permeation of compounded 20% ALA gel linearly over the first 5 hours from application, resulting in higher average PpIX fluorescence intensity measurements compared with only topical ALA application [17]. This was the rationale of our TMA-assisted PDT for our acne vulgaris patient. The same compounded formulation in 5% concentration was used. In our study the mean number of treatments was 1.9 (SD = 0.86) with a mean VAS score of 3.3. The clinical results observed at 8 and 16 weeks (Figure 2) post-treatment demonstrate relatively low side effect profile, minor erythema, and short downtime at lower cost (device and ALA costs).

Fig. 2. Representative patients before (**a**, **c**, **e**, **g**) and 16 weeks post last treatment (**b**, **d**, **f**, **h**).

Our study contains many limitations. This is a non-controlled retrospective chart review with no control arm, no comparison with higher ALA concentrations and with follow-ups, and limited to no longer than 16 weeks. In addition, the exact mechanism of TMA-assisted PDT is still to be understood. In general. PDT mechanism of action for acne is believed to be at least partially due to sebaceous gland damage. As compared with lasers, which create deep channels, allowing drugs to diffuse into dermis, TMA technology eliminate the SC barrier to allow substance into the epidermis. Other mechanisms that might explain the superior results of TMA-assisted PDT can be the effect of heat on the skin flora or other epidermal effect of ALA and subsequent epidermal–dermal intercellular influences. A controlled prospective randomized study comparing TMA-assisted PDT using appropriate ALA preparation and procedure, as discussed, to standard PDT or to fractional ablative laser-assisted PDT will better evaluate this procedure and establish its superiority or inferiority.

CONCLUSION

TMA used immediately prior to ALA application may enhance the effectiveness of PDT in the treatment of acne with minimal side effects, reduced downtime, and fewer sessions. The exact mechanism of TMA-assisted PDT is still to be understood.

REFERENCES

1. Lehmann HP, Robinson KA, Andrews JS, Holloway V, Goodman SN. Acne therapy: A methodologic review. J Am Acad Dermatol 2002;47(2):231–240.
2. Handler MZ, Bloom BS, Goldberg DJ. Energy-based devices in treatment of acne vulgaris. Dermatol Surg 2016;42(5): 573–585.
3. Sakamoto FH, Lopes JD, Anderson RR. Photodynamic therapy for acne vulgaris: A critical review from basics to clinical practice: Part I. Acne vulgaris: When and why consider photodynamic therapy? J Am Acad Dermatol 2010;63(2):183–193.
4. Steeb T, Schlager JG, Kohl C, Ruzicka T, Heppt MV, Berking C. Laser-assisted photodynamic therapy for actinic keratosis: A systematic review and meta-analysis. J Am Acad Dermatol 2019;80(4):947–956.
5. Boen M, Brownell J, Patel P, Tsoukas MM. The role of photodynamic therapy in acne: An evidence-based review. Am J Clin Dermatol 2017;18(3):311–321.
6. De Blois A, Grouls R, Ackerman E, Wijdeven W. Development of a stable solution of 5-aminolaevulinic acid for intracutaneous injection in photodynamic therapy. Lasers Med Sci 2002;17(3):208–215.
7. Risaliti L, Piazzini V, Di Marzo MG, et al. Topical formulations of delta-aminolevulinic acid for the treatment of actinic keratosis: Characterization and efficacy evaluation. Eur J Pharm Sci 2018;115:345–351.
8. Pierre MBR, Ricci E, Tedesco AC, Bentley MVLB. Oleic acid as optimizer of the skin delivery of 5-aminolevulinic acid in photodynamic therapy. Pharm Res 2006;23(2):360–366.
9. Serini SM, Cannizzaro MV, Dattola A, et al. The efficacy and tolerability of 5-aminolevulinic acid 5% thermosetting gel photodynamic therapy (PDT) in the treatment of mild-to-moderate acne vulgaris. A two-center, prospective assessor-blinded, proof-of-concept study. J Cosmet Dermatol 2019;18(1):156–162.
10. Kim BJ, Lee HG, Woo SM, Youn JI, Suh DH. Pilot study on photodynamic therapy for acne using indocyanine green and diode laser. J Dermatol 2009;36(1):17–21.
11. Lin M, Ding H, Xiang L. Photodynamic therapy with 5% 5-aminolevulinic acid in the treatment of acne: A randomized, controlled trial. Chin J Dermatol 2009;42(2):81–84.
12. Fan X, Liu L-H, Yue D-X, Yao M-H, Yang R-Y. Photodynamic therapy with 5% 5-aminolevulinic acid in the treatment of moderate to severe acne. Chin J Aesthet Med 2010;3.
13. Ma L, Xiang L-H, Yu B, et al. Low-dose topical 5-aminolevulinic acid photodynamic therapy in the treatment of different severity of acne vulgaris. Photodiagn Photodyn Ther 2013; 10(4):583–590.
14. Zhang J, Zhang X, He Y, et al. Photodynamic therapy for severe facial acne vulgaris with 5% 5-aminolevulinic acid vs 10% 5-aminolevulinic acid: A split-face randomized controlled study. J Cosmet Dermatol 2019;19:368–374.
15. Papageorgiou P, Katsambas A, Chu A. Phototherapy with blue (415 nm) and red (660 nm) light in the treatment of acne vulgaris. Br J Dermatol 2000;142(5):973–978.
16. Hædersdal M, Togsverd-Bo K, Wulf HC. Evidence-based review of lasers, light sources and photodynamic therapy in the treatment of acne vulgaris. J Eur Acad Dermatol Venereol 2008;22(3):267–278.
17. Shavit R, Dierickx C. A new method for percutaneous drug delivery by thermo-mechanical fractional injury. Lasers Surg Med 2019;52:61–69.
18. Kokolakis G, von Grawert L, Ulrich M, Lademann J, Zuberbier T, Hofmann MA. Wound healing process after thermomechanical skin ablation. Lasers Surg Med 2020;00:1–5.

Received: 8 March 2021 | Revised: 19 April 2021 | Accepted: 17 May 2021

DOI: 10.1111/jocd.14243

ORIGINAL CONTRIBUTIONS

JCD Journal of Cosmetic Dermatology WILEY

Retrospective study on the safety and tolerability of clinical treatments with a novel Thermomechanical Ablation device on 150 patients

Harryono Judodihardjo MB BCh BAO, MSc, PhD, DipGUM | Sajjad Rajpar MB ChB, FRCP

Belgravia Dermatology Limited, London, UK

Correspondence
Harryono Judodihardjo, Belgravia Dermatology Limited, 9A Wilbraham Place, London, SW1X 9AE, UK.
Email: harry@belgraviadermatology.co.uk

Abstract

Introduction: There are currently not many publications on the safety of thermomechanical ablation (TMA) devices, and those that are published only have small numbers of subjects. This treatment is gaining popularity in Europe and Asia, and thus there is a need to look at the safety of this treatment.

Objective: The purpose of this retrospective study was to evaluate the safety of the clinical use of the novel TMA system (Tixel, Novoxel, Israel) for facial rejuvenation and treatment of acne scars.

Methods: We did a retrospective review of our first 150 patients who were treated with the TMA device.

Results: One hundred and fifty consecutive patients aged 20 years to 82 years with Fitzpatrick skin types I to V treated with the TMA device were included in this study. The total number of treatment sessions was 327 (average 2.18 treatment per patient). The total number of pulses delivered to these patients was 1 48 856 (average 455 pulses per session). The indications for the treatment were photodamaged skin (n=145) and acne scarring (n=5). All patients were able to use makeup immediately after the treatment at lower settings, thus needing no real recovery time. Patients treated at higher settings were able to use makeup after 2 days. There were four reported complications: post-inflammatory hyperpigmentation (n=2), impetigo (n=1), and dermatitis (n=1).

Conclusions: Using the TMA device in the treatment of photodamage and acne scarring is safe in skin types I to V and has a low incidence of temporary side effects with no permanent side effects.

KEYWORDS
safety, tixel, thermo-mechanical ablation, TMA, photodamage, fractional skin ablation

1 | INTRODUCTION

Aging of the skin incorporates textural changes, wrinkles, and pigmentation. Treatment options for skin photoaging are plentiful and include chemical peels and energy-based devices such as ablative and non-ablative fractional laser devices and radiofrequency-based devices.[1-4] The fact that there are so many treatments suggest that none are perfect and there is a continuing development of new treatments that can improve the effectiveness and/ or safety of existing treatments.

Currently the most effective treatments for skin photoaging are the more invasive ones such as deep chemical peels and full-field ablative lasers.[5,6] While these treatments are highly effective, they are painful, have severe potential side effects such as scarring and permanent hypopigmentation, and require a long recovery time of about 10 to 14 days.[5-7] The post-treatment erythema that follows can take several months before going back to normal skin colour thus making these treatments unsuitable for men or women who are not used to wearing makeup.

The introduction of fractional laser technology has reduced the treatment discomfort, incidence of severe side effects, and recovery time of ablative lasers. However, the treatment is still uncomfortable, requiring nerve blocks and a recovery time of about 7 to 10 days.[8] Fractional lasers are also bulky and expensive and require expensive regular maintenance. Thus, a new device is needed to further improve on the fractional ablative lasers.

1.1 | The Thermomechanical Action (TMA) Device

The Tixel (Novoxel, Israel) is a non-laser, non-RF thermomechanical system which directly transfers thermal energy to the skin by conduction. The system is small and weighs about 6 kg (Figure 1).

The system combines thermal energy with motion to increase heat transfer efficacy. The system consists of a handpiece with a treatment tip assembled from a copper base with gold coating capped by a thin layer of implant-grade titanium shell that is heated to between 385℃ and 400℃ (Figure 2). When the trigger on the handpiece is squeezed, the tip moves towards the skin to achieve good thermal contact between the heated tip and the tissue to be treated. After the contact, the treatment tip then retracted quickly to its nested home position.

The amount of thermal energy delivered to the skin is determined by the treatment duration of the contact time between the tip and the skin, defined by the system as pulse duration. This ranges from 5 milliseconds (mS) to 18 mS. The second system parameter is the protrusion. This is defined as the distance in which the tip is moved beyond the transparent outer surface of handpiece distance gauge, that is, how much the tip 'presses' on the skin for pulse duration. A higher protrusion provides better contact between the tip and the tissue and ranges from 100 µm to 1000 µm. The treatment tip has a geometrical design which creates fractional damage on the skin that histologically appears very similar to ablative CO2 lasers but with no charring.[9] This is because at 400℃ the temperature is not hot enough to cause the skin to ignite as it would with carbon dioxide laser which operates at a temperature of over 700℃. The treatment tip is blunt causing no mechanical perforation therefore no bleeding occurs during the treatment. The Tixel machine offers two different handpieces, the standard handpiece with 1 cm^2 tip and the peri-orbital handpiece with 0.3 cm^2 tip, which enables accurate treatment of the periorbital tissues.

FIGURE 1 Photo of Tixel machine

This retrospective study aimed to assess the safety and tolerability of this novel non-laser, direct-conduction resurfacing system for the treatment of patients with photodamage and acne scars.

2 | METHODS

Data were extracted from the medical notes of 150 consecutive patients with photoaging and acne scars who were treated on the face and/or neck with the thermomechanical action device (Novoxel, Tixel, Israel) across two centres in the UK. Patients were treated by the authors only. Treatments took place between October 2016 and June 2018.

The pulse duration was set between 5 ms and 14 ms. The tip protrusion was set to between 400 µm to 1000 µm. All parameters were set according to the patient's skin type and treatment objectives.

Before treatment, makeup was removed, and the skin was sterilised with isopropyl alcohol 70% and wiped dry. With the lower treatment settings (under 8 mS contact time), no anaesthesia was needed. With higher settings (8 mS and above contact time), topical anaesthesia (Pliaglis by Galderma, Switzerland) was applied and left for 30 minutes before the treatment. During the treatment, the device treatment tip was applied carefully so that there is not too much overlap of the treated area. Patients were treated with a single pass. Areas with excessive skin laxity or with more severe acne scars were treated with two passes with a few minutes in between the passes to cool and prevent bulk heating of the skin.

Immediately after the treatment, nothing was applied to the skin to let it cool. Patients were advised to apply a moisturising lotion (Cetaphil by Galderma, Switzerland) in the evening of the day of treatment and then twice a day for the next 5 to 10 days. Patients were advised to avoid UV exposure for 3 months after the treatment, using a hat and sunscreen.

Patients were advised to have three to six treatments at 4 to 6 weeks interval, for optimal results. Review was not compulsory, but patients were asked to come back at 4 to 6 weeks after the last treatment for final assessment.

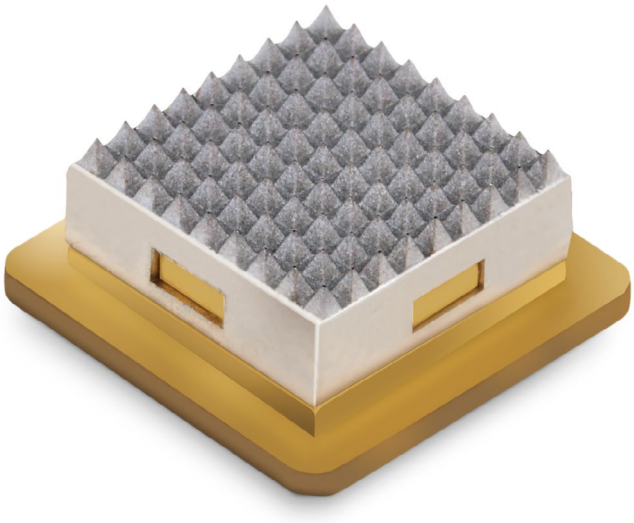

FIGURE 2 Tixel treatment tip

3 | RESULTS

The total number of treatments for the 150 patients (male=16 and female=134) in 21 months, when the data were collected, was 327 (Table 1). The areas treated were décolleté (n=1), peri-orbital (n=65), peri-orbital and neck (n=2), peri-orbital and peri-oral (n=2), entire face (n=178), face and neck (n=59), face, neck, and décolleté (n=2), neck (n=5), and peri-oral (n=13). The indications for the treatment were photodamage (n=145) and acne scars (n=5).

The age range of the 150 patients was 20 years to 82 years old with a mean age of 51.75 years, and the gender distribution was 16 male and 134 female patients. The Fitzpatrick skin types distribution are type 1 (n=8), type 2 (n=44), type 3 (n=51), type 4 (n=33), and type 5 (n=14).

The handpieces (HP) were used in the following manner: standard HP only (n=259), peri-orbital HP only (n=65), and combination of both HP (n=3). The pulse duration settings used were as follows: 5 mS (n=81), 6 mS (n=40), 8 mS (n=22), 10 mS (n=28), 12 mS (n=8), and 14 mS (n=148) (Table 2). The protrusion settings used are as follows: 400 mm (n=10), 500 mm (n=12), 600 mm (n=16), 700 mm (n=134) and 800 mm (n=13), and 1000 mm (n=142).

The number of pulses used ranged from seven pulses for treating a few acne scars to 1192 pulses for treating large areas of face, neck, and décolletage. The total number of pulses used in the 327 treatments was 1 48 856 pulses (mean 455 pulses per treatment).

Complications noted were post-inflammatory hyperpigmentation (n=2), dermatitis (n=1), and mild impetigo (n=1).

TABLE 1 Distribution of number of treatments completed by patients

Number of treatments	Number of patients
1	65
2	39
3	27
4	6
> 4	13

TABLE 2 Distribution of contact time in milliseconds (mS) according to patients' Fitzpatrick skin types

	Skin type 1	Skin type 2	Skin type 3	Skin type 4	Skin type 5
5 mS	1	25	17	24	14
6 mS	1	7	13	18	1
8 mS	2	3	9	3	5
10 mS	1	3	9	0	15
12 mS	2	2	4	0	0
14 mS	7	42	59	39	1

4 | DISCUSSION

Non-surgical aesthetic medical treatment has been gravitating towards less-invasive procedures with less discomfort and downtime with similar outcomes as more-invasive treatments. The demand for deep resurfacing treatment to the entire skin such as phenol peel and full-face CO^2 laser is in decline as more patients are electing for fractional skin resurfacing. Fractional CO^2 laser is debatably the current gold standard for fractional skin resurfacing, but it can be a painful treatment with about 7 days of downtime and potentially severe side effects such as scarring and damage to the eyes.[10]

The thermo-mechanical ablation (TMA) machine is a new treatment modality that promises results that can match that of fractional CO^2 and yet claimed to have less downtime and discomfort during treatment, and it is safe for the eyes.[11] TMA can achieve this because the heat it produces is capped at 400°C , which is below the temperature needed to ignite the skin. This means no charring after TMA treatment so that patient can cover the healing skin with makeup immediately after the treatment with the lower setting or after 48 hours in higher-setting treatments. The authors consider any pulse duration setting that is less than 8 mS as the low setting.

TMA is a device that uses conduction to transfer the energy or heat to the skin. Therefore, for the energy to be transferred most efficiently, the best possible contact between the treatment tip and the skin is needed. Initially, we were using a variable protrusion setting to adjust the amount of energy transferred, as was recommended by the manufacturer. However, after seeing the safety evidence of several hundreds of treatments, we then decided to keep the protrusion setting at the maximum so as to allow best conduction at all times and vary the intensity of the treatments by only adjusting the contact time. Based on our experience, we have now made the TMA treatments simpler by only having one variable, the contact time. The protrusion setting mentioned in this paper, less than 1000 μM, was the early parameter that we used when we were learning how to optimise the TMA treatment.

TABLE 3 Treatment details of the complications

Complication	Pulse Duration (mS)	Protrusion Setting (μM)	Total number of pulses used	Skin type	Treatment area
Post Inflammatory Hyperpigmentation	14	700	407	4	Face
Post Inflammatory Hyperpigmentation	14	1000	917	4	Face and neck
Impetigo	14	700	814	3	Face and neck
Contact Dermatitis	14	700	405	3	Face and neck

FIGURE 3 Erythema and oedema on the face due to contact allergy

This retrospective study specifically looked for the side effects due to the TMA treatment. Out of the 327 treatments in 150 patients, only 4 patients were found to have complications post treatment (Table 3). Two patients, both of whom were of Oriental origin with Fitzpatrick's skin type 4, developed post-inflammatory hyperpigmentation (PIH) about 3 weeks after the treatment. They had the higher pulse duration treatment setting of 14 mS, protrusion of 1000 μM for one patient and 700 μM for the other. The PIH cleared in about 3 months with no medical intervention other than the advice to avoid sun exposure and use sunblock daily. Since these two cases of PIH, the authors started to use pulse duration setting of no more than 10 mS for all patients with Fitzpatrick's skin type above 3, and no further cases of PIH were noted. One patient sent us pictures of herself four days after the treatment showing mild facial swelling and erythematous patches resembling dermatitis (Figure 3). She had treatment settings of 14 mS for pulse duration and 1000 μM protrusion. Upon specific questioning, she confessed that she had used several over the counter "anti-ageing" topicals instead of Cetaphil lotion that she had been advised. The authors suspected that she probably had contact dermatitis due to product ingredients penetrating into the treated skin that has a reduced barrier function. She was asked to immediately wash her face with copious amount of water to remove the topicals on her skin and not to apply anything else on the skin, not even the Cetaphil lotion. The mild facial swelling settled down in about 2 days, and the erythema cleared 7 days later. The last side effects of TMA noted in this study was mild impetigo, which was reported 2 days after the treatment. Her treatment setting was pulse duration of 14 mS and 700 μM protrusion. Yellow crust was noted on the right lower cheek area which cleared with the usage of Mupirocin twice daily as topical treatment for 5 days.

5 | CONCLUSION

This retrospective study showed that the novel TMA treatment is safe and has a very low incidence of side effects that can be mitigated further by reducing the pulse duration setting to 10 mS or less for Fitzpatrick skin types 4 and 5 and by advising the patient to protect the skin well against UV light post treatment. The main concern of energy-based treatment is permanent complications such as scarring or pigmentary changes, and none was seen in this study.

ETHICS STATEMENT

This study was a retrospective study by looking at the patients notes. No ethical approval was required for such study in the UK. We did not seek ethical approval for this study.

DISCLOSURE

Dr Harryono Judodihardjo is a member of the Medical Advisory Board of Novoxel (Israel) and is a Medical Director of AZTEC services UK which distributes Novoxel products in the UK and Ireland. Dr Sajjad Rajpar has no financial disclosure to make.

ORCID

Harryono Judodihardjo https://orcid.org/0000-0002-8213-9246

REFERENCES

1. Soleymani T, Lanoue J, Rahman Z. A practical approach to chemical peels: A review of fundamentals and step-by-step algorithmic protocol for treatment. *J Clin Aesthet Dermatol*. 2018;11(8):21-28.
2. Dadkhahfar S, Fadakar K, Robati RM. Efficacy and safety of long pulse ND:YAG laser versus fractional Erbium:YAG laser in the treatment of facial skin wrinkles. *Lasers in Medical Science*. 2018;34(3):457–464. https://doi.org/10.1007/s10103-018-2614-6
3. Hunzeker CM, Weiss ET, Geronemus RG. Fractionated CO2 laser resurfacing: our experience with more than 2000 treatments. *Aesthetic Surg J*. 2009;29:317-322.
4. Kim H-K, Choi J-H. Effects of radiofrequency, electroacupuncture, and low-level laser therapy on the wrinkles and moisture content of the forehead, eyes and cheek. *J Phys Ther Sci*. 2017;29:290-294.
5. Alt TH. Occluded Baker-Gordon chemical peel: Review and update. *J Dermatol Surg Oncol*. 1989;15:980-993.

6. Hamilton M, Campbell A, Holcomb JD. Contemporary laser and light-based rejuvenation techniques. *Facial Plast Surg Clin North Am*. 2018;26(2):113-121.
7. You H-J, Kim D-K, Yoon E-S, Park S-H. Comparison of four different lasers for acne scars: Resurfacing and fractional lasers. *J Plast Reconstr Surg*. 2016;69(4):e87-e95.
8. Tierney EP, Eisen RF, Hanke CW. Fractionated CO2 laser skin rejuvenation. *Dermatol Ther*. 2011;24(1):41-53.
9. Kokolakis G, Grawert L, Ulrich M, Lademann J, Zuberbier T, Hofmann MA. Wound healing process after thermomechanical skin ablation. *Lasers Surg Med*. 2020;52(8):730-734.
10. Chwalek J, Goldberg DJ. Ablative skin resurfacing. *Curr Probl Dermatol*. 2011;42:40-47.
11. Elman M, Fournier N, Barnéon G, Bernstein EF, Lask G. Fractional treatment of aging skin with Tixel, a clinical and histological evaluation. *J Cosmet Laser Ther*. 2016;18(1):31-37.

How to cite this article: Judodihardjo H, Rajpar S. Retrospective study on the safety and tolerability of clinical treatments with a novel Thermomechanical Ablation device on 150 patients. *J Cosmet Dermatol*. 2022;21:1477–1481. https://doi.org/10.1111/jocd.14243

The Toxic Edge—A Novel Treatment for Refractory Erythema and Flushing of Rosacea

Or Friedman, MD,[1,2*] **Amir Koren, MD**,[3,4] **Roni Niv, MD**,[4] **Joseph N. Mehrabi, BSc**,[2] **and Ofir Artzi, MD**[3,4]
[1]*The Plastic Reconstructive Surgery Department, Tel Aviv Sourasky Medical Center, Tel Aviv, Israel*
[2]*Sackler Faculty of Medicine, Tel Aviv University, Tel Aviv, Israel*
[3]*Department of Dermatology, Tel Aviv Sourasky Medical Center, Tel Aviv, Israel*
[4]*Dr. Artzi Treatment and Research Center, Tel Aviv, Israel*

Purpose: Rosacea is a common, chronic facial skin disease that affects the quality of life. Treatment of facial erythema with intradermal botulinum toxin injection has previously been reported. The primary objective of the study was the safety and efficacy of thermal decomposition of the stratum corneum using a novel non-laser thermomechanical system (Tixel, Novoxel, Israel) to increase skin permeability for Botulinum toxin in the treatment of facial flushing of rosacea.
Methods: A retrospective review of16 patients aged 23–45 years with Fitzpatrick Skin Types II to IV and facial erythematotelangiectatic rosacea treated by Tixel followed by topical application of 100 U of abobotulinumtoxin. A standardized high-definition digital camera photographed the patients at baseline and 1, 3, and 6 months after the last treatment. Objective and subjective assessments of the patients were done via Mexameter, the Clinicians Erythema Assessment (CEA), and Patients self-assessment (PSA) scores and the dermatology life quality index (DLQI) validated instrument.
Results: The average Maxameter, CEA, and PSA scores at 1, 3, and 6 months were significantly improved compared with baseline (all had a P-value <0.001). DLQI scores significantly improved with an average score of 18.6 at baseline at 6 months after treatment ($P < 0.001$). Self-rated patient satisfaction was high. There were no motor function side-effects or drooping.
Conclusion: Thermal breakage of the stratum corneum using the device to increase skin permeability for botulinum toxin type A in the treatment of facial flushing of rosacea seems both effective and safe. Lasers Surg. Med.

Key words: botulinum toxin; erythema; flushing; rosacea; drug delivery; percutaneous permeating; fractional skin ablation

INTRODUCTION

Rosacea is a chronic, relapsing inflammatory skin disease [1]. Symptoms include persistent facial erythema, papules, pustules, telangiectasia, and recurrent flushing [1]. The red, pimply facial rash can cause embarrassment, low self-esteem, anxiety, and have a considerable adverse effect on quality of life [2–4]. The prevalence of rosacea across populations is reported to range from less than 1% to 22% and is characterized by episodes of exacerbation and remission. [5–6]. Symptoms only partially respond to therapy and tend to recur. Frequently prescribed treatments include topical, oral, and light-based therapies [1]. Intradermal botulinum toxin has been investigated as a novel treatment of facial erythema and flushing [7–11]. Botulinum toxin (BTX) blocks the release of the neurotransmitter acetylcholine from peripheral nerves and thus might alter cutaneous vasodilatation [12–13]. Due to its characteristics and high molecular weight, BTX cannot penetrate the highly impermeable stratum corneum while applied to bare skin [14].

Disruption of the outer stratum corneum by mechanical, chemical, or physical approaches increases skin permeability [15–17]. Selective thermal ablation of stratum corneum dramatically increased skin permeability for transdermal drug delivery [18–19]. Above 360°C, transdermal flux increased by many orders of magnitude. [20].

This study aimed to assess the safety and efficacy of a novel non-laser thermal resurfacing system (Tixel, Novoxel, Israel) of increasing skin permeability for botulinum toxin type A in the treatment of patients with resistant facial flushing of rosacea. The system has already been demonstrated to significantly increase the permeability of several topically applied medications [21,22].

METHODS

A retrospective review of 16 patients ages 23–45 years (average 41 years) treated in a single center between January 2017 and March 2018. The standard treatment reviewed consisted of a novel thermomechano-ablative

Conflict of Interest Disclosures: All authors have completed and submitted the ICMJE Form for Disclosure of Potential Conflicts of Interest and none were reported.
*Correspondence to: Dr. Or Friedman, MD, Department of Plastic Reconstructive Surgery, Tel Aviv Sourasky Medical Center, 6 Weizman Street, Tel Aviv, 642906 Israel. E-mail: or.friedman@gmail.com
Accepted 8 September 2018
Published online in Wiley Online Library (wileyonlinelibrary.com).
DOI 10.1002/lsm.23023

device (Tixel, Novoxel, Israel) followed immediately by topical application of 100 U of abobotulinumtoxin A (Dysport®, Galderma, France) in 3 ml of bacteriostatic saline assisted by ultrasound impact system (Alma lasers GmbH, Germany). Tixel device settings included: 400°C, at contact intervals of 6-8 ms, 800–1000 protrusion. The Impact (Alma Lasers Ltd., Israel, Impact) setting was 50% energy intensity and 50 Hz acoustic pressure pulse rate for 2 minutes. Post-procedure care included topical Trolamine (Biafine; Genmedix Ltd, France) self-applied 3–4 times a day for 2 days and the use of broad-spectrum sunscreen with a sun protection factor of 50 for 3 months. All patients received two treatment sessions with 1-month interval and were followed up for 6 months after the last treatment to monitor results, recurrence, and adverse effects.

Skin cultures for Demodex folliculorum where taken before and at 1 month after treatment. The erythema index (EI) of the forehead, cheeks, nose, and chin was measured and averaged, before treatment and at 1, 3, and 6 months post-treatment, using a model MX18 Mexameter (CK Electronic GmbH, Cologne, Germany). The patients were photographed by a standardized high-definition digital camera (VISIA, Canfield) at baseline and 1, 3, and 6 months after last treatment.

Two independent non-treating investigators assessed the subjects' facial erythema using the Clinicians Erythema Assessment (CEA) score (0 = none, 1 = almost none, 2 = mild, 3 = moderate, and 4 = severe). The patients evaluated their own erythema using the Patients self-assessment (PSA) scores (0 = none, 1 = almost none, 2 = mild, 3 = moderate, and 4 = severe). The non-treating investigators and patients were blinded to the chronological sequence of the photos taken when evaluating them. Also, at 6 months post-treatment, the patients answered the dermatology life quality index (DLQI) questionnaire [23]. Pain perception, adverse effects, and recurrence of lesions were also documented at follow-up visits. The presence and severity of the following side effects were assessed in all subjects on clinical examination and written questionnaire: injection site pain, erythema, edema, muscle weakness, dysphagia, dry mouth, fatigue, headache, eye disorders, musculoskeletal pain, and dysphonia.

Statistical analysis was performed using SPSS software (version 21.0; IBM Corporation, Armonk, NY). The effect of treatment on erythema grade was evaluated using a one-way repeated-measures analysis of variance (ANOVA) and pairwise comparisons. A one-way repeated-measures ANOVA was used to determine whether the mean of subjects' rosacea score, at each time point, differed significantly. Student T-test was used to verify DLQI scores before and after treatment.

Stratum Corneum as a Barrier

In general, topical therapeutics demonstrate poor total absorption and cutaneous bioavailability with only 1–5% being absorbed into the skin. [24] Several physical techniques were developed to perforate the stratum corneum to increase the uptake of topically applied drugs. Among those techniques were electroporation, iontophoresis, lasers, microdermabrasion, microneedles, pressure, RF, and sonophoresis [15–17]. The most significant challenge in achieving an efficient transdermal drug delivery is to create a passage through the stratum corneum [25] while obtaining the lowest damage possible to the viable epidermis and dermis tissue. Mechanical or thermal damage to the tissue might affect the drug passage to the target cells either due to a mechanical blockage such as tissue coagulation or by an inflammatory healing process in case of mechanical damage [24]. The importance of the water content of the stratum corneum in determining its properties is well documented. Skin water content gradually increases, going from the upper layer of the stratum corneum to the viable epidermis, reaching an almost constant value [26,27]. The mechanical properties of the stratum corneum are profoundly affected by the relative humidity (RH%) within the layer. The breaking strength of the stratum corneum increases from about 10 g at 80–100% RH to 45 g at 0% RH, while the elongation to break decreases from 200% at 100% RH to less than 10% at 0% RH [28].

The Tixel Device

The Tixel (Novoxel, Israel) is a non-laser thermomechanical system which transfers thermal energy to the skin, dehydrates the stratum corneum and superficial epidermis and creates micropores, thus, enhancing drug delivery. The system combines thermal energy with motion. The system consists of a titanium tip heated to 400°C. The tip is moving towards the skin to achieve contact between the heated tip and the treated tissue. The amount of thermal energy delivered to the skin is determined by the pulse dwelling duration or pulse duration (range: 5 to 18 ms). A second system parameter is a protrusion, which is defined as the distance in which the heated tip is moving measured from the edge of the handpiece distance gauge. The protrusion is aimed to acquire better thermal matching between the tip and the tissue without skin perforation (including the stratum corneum), along with the process. In transdermal mode settings, the primary thermal effect is dehydration of stratum corneum with a very limited thermal effect on the viable epidermis and dermis. The stratum corneum becomes brittle consequentially to tip thermal effect

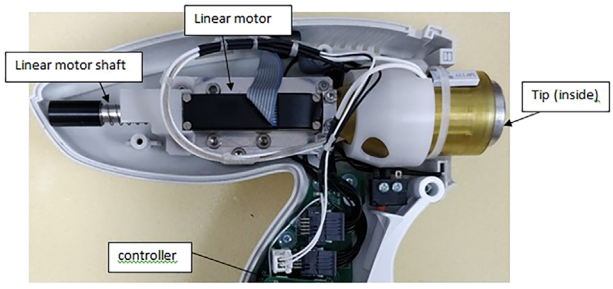

Fig. 1. Tixel handle motion assembly.

TABLE 1. Patient Demographics and clinical data

Patient	Sex	age	Fitzpatrick skin type	Disease duration (Y's)	Rosacea type: 1 = Erythematotelangiectatic type 2 = Papulopustular 3 = Phymatous 4 = Ocular	Previous treatments- 1-topical ABX, 2-oral ABX, 3-Isotretinoin, 4-laser, 5-Phototherapy, 6-Exsision
1	F	23	2	15	1+2	1,2,4
2	F	44	2	10	1+2	1,2,4
3	F	73	3	6	1+2	1,2,3,4
4	F	52	2	10	1+2	1,2,3,4
5	F	27	2	5	1	1,2,4
6	F	41	3	10	1	1,2,4
7	F	45	2	13	1	1,2
8	F	41	3	1	1+2	1,2,3,4
9	F	35	2	5	1	1,2
10	F	44	2	2	1	1,2
11	F	36	2	3	1	1,2,4
12	F	36	3	4	1	1,2
13	F	26	4	3	1	1,2,4
14	F	37	2	10	1+2	1,2,3,4
15	F	62	3	10	1	1,2,4
16	F	42	3	12	1	1,2,3,4

leading to layer breakage when the tip is progressed towards the treated tissue. The gentle elimination of the stratum corneum [20] and desiccation of the epidermis establishes a concentration gradient by Fick's law, enhancing drug delivery. The Tixel technology is mainly concentrated in the system handle. Figure 1 presents the general assembly of the handle. The tip motion is achieved by linear motor and motion controller. When the system is activated the linear motor (that act like pneumatic piston energized by electric power) shaft is moving forward and allows the tip to come in contact with the tissue for extremely short period of time. Since the motion controller is located extremely closed to the motor there are no time delays, that is, phase shift therefore the system maintains extremely tight control characteristics. It has been previously shown to enhance the delivery of several medications (e.g., verapamil, vitamin C, and sodium diclofenac) [29].

The Impact Device

Sonophoresis—the use of ultrasound to enhance the transport of a substance through a liquid medium—is particularly impressive given the emerging role of ultrasound in dermatology. A transdermal sonophoresis delivery system (Alma Lasers Ltd.) has been developed to enhance the delivery of topical cosmeceuticals. The device operates at low ultrasound frequency (~30 kHz) and emits acoustic wave air pressure from an ultrasonic horn applied on the skin surface. This horn device has a frequency up to 100 Hz (acoustic pulse vibration per second) and energy of peak of 0.4 W/cm^2. The hypothesis is that the device

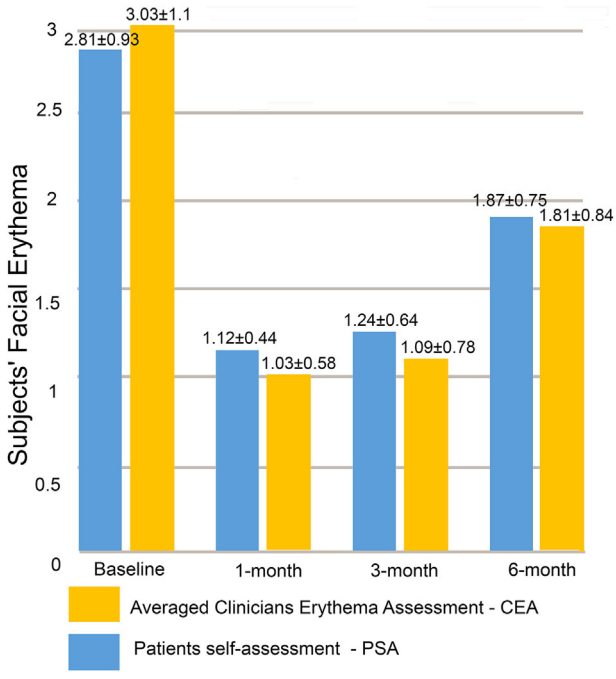

Fig. 2. Clinicians Erythema Assessment (CEA) score and Patient self-assessment (PSA) score – baseline, 0 = none, 1 = almost none, 2 = mild, 3 = moderate, and 4 = severe. The average CEA at 1, 3, and 6 months were significantly improved compared with baseline (all had P-value <0.001). Note that the greatest effect appeared 1 month after treatment with a slight gradual recurrence of the redness at 3 and 6 months, but none returned to the initial baseline values.

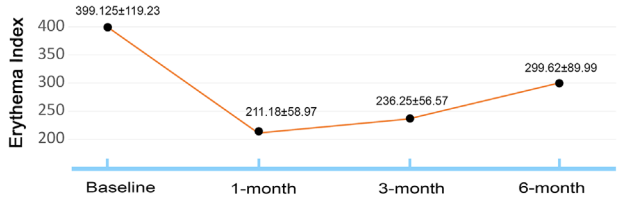

Fig. 3. Average Mexameter scores—baseline, 1, 3, and 6 months (P-value <0.001).

mechanical ultrasound wave/vibration pushes active components deeper into the skin and enhances topical absorption when paired with the thermomechanical stratum corneum destruction produced by the Tixel [30].

RESULTS

Age, Fitzpatrick skin type, previous treatments, and rosacea type are elaborated in Table 1. Positive Demodex folliculorum cultures were significantly reduced from nine patients before treatment to four patients after treatment. The CEA results from the two blinded dermatologists showed a strong correlation with a correlation coefficient of 0.9. The average CEA and PSA scores at 1, 3, and 6 months were significantly improved compared with baseline (all had a P-value <0.001, Fig. 2). The average Mexameter scores at baseline, 1, 3, and 6 months were 399.12, 211.18, 236.25, and 299.62 (P-value <0.001, Fig. 3), respectively. Note that the greatest effect appeared 1 month after treatment with a slight gradual recurrence of the redness at 3 and 6 months, but none returned to the initial baseline values (Fig. 4). DLQI Scores where significantly improved with an average score of 18.6 ± 1.9 at baseline and 9.6 ± 2.8 at 6 months after treatment ($P < 0.001$). Patient satisfaction was 2.3 ± 0.5 (on a scale of 0–4). Overall tolerance score was high (average: 3.2 ± 0.3, scale 1–4). Post-treatment side effects included transient erythema, edema, mild discomfort, and pinpointed micro crusts. All adverse effects were self-limited. Specifically, there were no subjects that developed motor function deficits or drooping.

DISCUSSION AND CONCLUSIONS

Rosacea is a chronic and recurrent inflammatory skin disease with a variety of cutaneous manifestations [1]. It consists of four subtypes: erythematotelangiectatic, papulopustular, phymatous, and ocular [8]. The disorder poses significant financial, physical, and psychological impacts [2–4]. There are some topical, oral, systemic, and energy-based device treatments available, but the treatment of rosacea remains difficult. The multifactorial nature of the disease combined with an incomplete understanding of the pathophysiology is challenging for providers and patients. Genetic factors, dysregulation of the innate and adaptive immune system, vascular and neuronal dysfunction, and microorganisms such as Demodex folliculorum appear to be involved [31–36].

Micro dermal injections of BTX have been shown to be effective in decreasing flushing, erythema, and inflammation within 1 week of treatment and persisting for up to 3 months [37–40]. BTX inhibits the exocytosis of preformed vesicles in cholinergic nerves (motor and autonomic) and results in the blockade of acetylcholine release [1]. One possible mechanism by which botulinum toxin might improve flushing is through the blockade of acetylcholine release from peripheral autonomic nerves of the cutaneous vasodilatory system. Other mechanisms might include the followings: BTX inhibits the release of other neurotransmitters (substance P, glutamate, and calcitonin gene-related peptide) or diminishes non-nociceptive stimuli, altering postganglionic cholinergic nerve fibers with blood vessels [41–45]. Due to its characteristics and high molecular weight, the botulinum toxin molecules cannot

Fig. 4. Representative rosacea status before (a,c,e) and 6 month after (b,d,f) treatment.

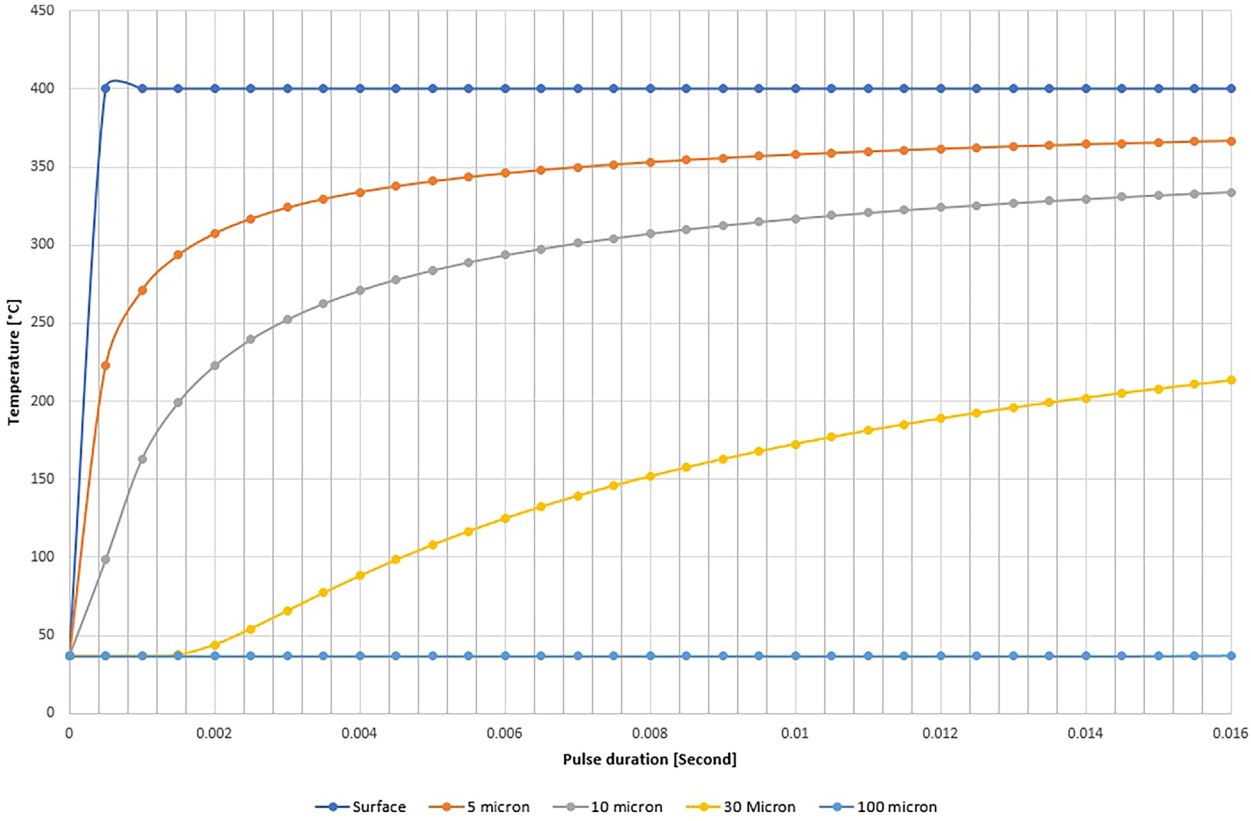

Fig. 5. Chart representing temperature as a function of depth. For example at 10 μm the maximal calculated temperature at pulse duration of 6 ms is 300°C and at 30 μn the maximal temperature is about 125°C.

penetrate the highly impermeable stratum corneum while applied to bare skin, unless disrupted [14].

Topical delivery of drugs is essential in dermatology. The efficacy of topical therapy is dependent on the ability of the therapeutic drug to reach its target. However, cutaneous biodistribution and bioavailability of most topically applied drugs are quite low. For a topical agent to be active, it must first traverse the rate-limiting barrier of the stratum corneum. In the last decades, drug delivery technology has advanced from unsophisticated and simple methods to more advanced chemical, mechanical and physical methods. The main skin permeation enhancement techniques include alteration of drug or vehicle interaction, the use of transepidermal carriers, the modification (e.g., hydration) or removal (microneedling, laser-assisted delivery [LAD]) of stratum corneum or the use of electrically assisted methods (sonophoresis or iontophoresis, transfollicular positive-pressure delivery). A good transepidermal delivery system is based on achieving a suitable balance between effective delivery, homogenous distribution, safety to the skin, and low pain and cost. As examples, tape stripping is a simple, efficient, and controllable method to remove stratum corneum, however it is associated with high incidence of irritation and difficulty in recovering. On the other side, laser-assisted delivery (LAD) can directly adjust the character of the channels in a predictable and controllable manner, however, these system are expensive to use, relatively painful and sometimes are not cost effective. The Tixel is a relatively inexpensive, very safe, efficient (no down time), non-painful system which allows effective delivery and homogenous distribution of topically applied medications. There are few different aspects of system operation that can provide explanation for the low pain level during Tixel treatment at low pulse duration. Due to the direct conduction in which the Tixel technology is based, the temperature below the stratum corneum (under 20 μm) is much lower than 400°C as shown in the Figure 5. For example, at 10 μm the maximal calculated temperature at pulse duration of 6 ms is 300°C and at 30 μm the maximal temperature is about 125°C. Nociceptors are located deeper at 50 μm [46]. In addition, nociceptors are extremely sensitive to temperature changes rate over time. CO_2 lasers, for example, generate heat at an extremely fast pathway (~200 ns), while Tixel heating effect is slower by at least one order of magnitude in the Tixel system [47].

This study demonstrates the successful and safe treatment of resistant rosacea-associated facial erythema using a dual modality treatment of thermal decomposition of the stratum corneum followed by the immediate application of botulinum toxin. No significant adverse

effects were reported with this approach. The authors do appreciate the considerable expense of the botulinum toxin needed for this treatment and the fact that in most countries the treatment would not be covered by insurance.

Limitations of this study include the small sample size, the short 6 month follow up period, and the lack of a control group. The use of botulinum toxin is a rational approach if one assumes that neuron-mediated vascular dysfunction plays essential pathogenic roles in rosacea [31,32]. The use of multiple modalities: thermomechanical device, botulinum toxin, ultrasound device, and Biafine limit our ability directly describe the mechanism of action leading to our observations. Each modality has been chosen based on its published literature and the end result seems greater than the expected additive effect.

However, this study raises many questions: What is the role of the Tixel device? Is it only a drug delivery enhancing system? Does the heat transfer affect the papillary dermal blood vessels or decrease the number of parasites (Demodex folliculorum)? What is the role of sonophoresis? Could the same effect be achieved without the concomitant use of the Impact device? Could the same results can be achieved with only topical application of BTX and sonophoresis? All of these questions more substantial, randomized, blinded, and placebo-controlled studies. Additionally, further investigation is needed to elucidate the mechanism of action by which botulinum toxin improves facial flushing of rosacea.

References

1. van Zuuren EJ, Fedorowicz Z, Carter B, van der Linden MM, Charland L. Interventions for rosacea. Cochrane Database Syst Rev 2015;4:CD003262.
2. Halioua B, Cribier B, Frey M, Tan J. Feelings of stigmatization in patients with rosacea. J Eur Acad Dermatol Venereol 2017;31:163–168.
3. Bewley A, Fowler J, Schöfer H, Kerrouche N, Rives V. Erythema of rosacea impairs quality of life: Results of a meta-analysis. Dermatol Ther (Heidelb) 2016;6:237–247.
4. Egeberg A, Hansen PR, Gislason GH, Thyssen JP. Patients with rosacea have increased risk of depression and anxiety disorders: A Danish nationwide cohort study. Dermatology 2016;232(2):208–213.
5. Elewski BE, Draelos Z, Dréno B, Jan-sen T, Layton A, Picardo M. Rosacea—Global diversity and optimized outcome: Proposed international *consensus* from the Rosacea International Expert Group. J Eur Acad Dermatol Venereol 2011;25:188–200.
6. Tan J, Berg M. Rosacea: Current state of epidemiology. J Am Acad Dermatol 2013;69(Suppl 1):S27–S35.
7. Alexandroff AB, Sinclair SA, Langtry JA. Successful use of botulinum toxin a for the treatment of neck and anterior chest wall flushing. Dermatol Surg 2006;32:1536.
8. Bansal C, Omlin KJ, Hayes CM, Rohrer TE. Novel cutaneous uses for botulinum toxin type A. J Cosmet Dermatol 2006; 5:268–272.
9. Sterodimas A, Nicolaou M, Paes TR. Successful use of Botulinum toxin-A for the treatment of neck and anterior chest wall flushing. Clin Exp Dermatol 2003;28:592–594.
10. Tugnoli V, Marchese Ragona R, Eleopra R, et al. The role of gustatory flushing in Frey's syndrome and its treatment with botulinum toxin type A. Clin Auton Res 2002;12:174–178.
11. Yuraitis M, Jacob CI. Botulinum toxin for the treatment of facial flushing. Dermatol Surg 2004;30:102–104.
12. Charkoudian N. Skin blood flow in adult human thermoregulation: How it works, when it does not, and why. Mayo Clin Proc 2003;78:603–612.
13. Kellogg DL Jr. *In vivo* mechanisms of cutaneous vasodilation and vasoconstriction in humans during thermoregulatory challenges. J Appl Phys 2006;100:1709–1718.
14. Egawa M, Hirao T, Takahashi M. In vivo estimation of stratum corneum thickness from water concentration profiles obtained with raman spectroscopy. Acta Derm Venereol 2007;87:4–8.
15. Gratieri T, Alberti I, Lapteva M, Kalia YN. Next generation intra- and transdermal therapeutic systems: Using non- and minimally-invasive technologies to increase drug delivery into and across the skin. Eur J Pharm Sci 2013;50(5):609–622.
16. Sklar LR, Burnett CT, Waibel JS, Moy RL, Ozog DM. Laser assisted drug delivery: A review of an evolving technology. Lasers Surg Med 2014(46):249–262.
17. Paudel KS, Milewski M, Swadley CL, Brogden NK, Ghosh P, Stinchcomb AL. Challenges and opportunities in dermal/transdermal delivery. Ther Deliv 2010;1(1):109–131.
18. Park JH, Lee JW, Kim YC, Prausnitz MR. The effect of heat on skin permeability. Int J Pharm 2008;359(1-2):94–103.
19. Lee JW, Gadiraju P, Park JH, Allen MG, Praunitz MR. Microsecond thermal ablation of skin for transdermal drug delivery. J Control Release 2011;54(1):58–68.
20. Lask G, Elman M, Fournier N, Slatkine M. Fractional vaporization of tissue with an oscillatory array of high temperature rods—Part I: Ex vivo study. J Cosmetic and Laser therapy 2012;5:218–223.
21. Elman M, Fournier N, Barneon G, Hofmann M, Bernstein MD, Lask G. Fractional treatment of aging skin with tixel, a clinical and histological evaluation. J Cosm Therap 2015;18(1):31–37.
22. Sintov AC, Brandys -, Sitton R. Facilitated skin penetration of lidocaine: Combination of a short-term iontophoresis and microemulsion formulation. Int J Pharma 2006;316:58–67.
23. Finlay AY, Khan G. Dermatology Life Quality Index (DLQI): A simple practical measure for routine clinical use. Clin Exp Dermatol 1994;19:210–216.
24. Erlendsson AM, Wenande E, Haedersdal M. Transepidermal drug delivery: Overview, Concept, and Applications. In: Issa M, Tamura B, editors. Lasers, lights and other technologies. Clinical Approaches and Procedures in Cosmetic Dermatology. Springer, Cham. 2018. pp 447–461.
25. Uchida Y, Park K. Stratum Corneum. In: Kabashima K, editor. Immunology of the skin. Tokyo: Springer; 2016. pp 15–30.
26. Warner RR, Myers MC, Taylor DA. Electron probe analysis of human skin: Determination of the water concentration profile. J Invest Dermatol 1988;90:218–224.
27. Stockdate M. Water diffusion coefficients versus water activity in Stratum Corneum: A correlation and its implications. J Soc Cosmetic Chemists 1978;29:625–639.
28. Wildnauer RH, Bothwell JW, Douglass AB. Stratum corneum biomechanical properties I. Influence of relative humidity on normal and extracted human stratum corneum. J Investig Dermatol 1971;56(1):72–78.
29. Sintov AC, Hofmann MA. A novel thermomechanical system enhanced transdermal delivery of hydrophilic active agents by fractional ablation. Int J Pharm 2016;511(2):821–830.
30. Waibel JS, Rudnick A, Nousari C, Bhanusali DG. Fractional ablative laser followed by transdermal acoustic pressure wave device to enhance the drug delivery of aminolevulinic acid: *In Vivo* fluorescence microscopy study. J Drugs Dermatol 2016;15(1):14–21.
31. Gomaa AH, Yaar M, Eyada MM, Bhawan J. Lymphangiogenesis and angiogenesis in non-phymatous rosacea. J Cutan Pathol 2007;34:748–753.
32. Guzman-Sanchez DA, Ishiuji Y, Patel T, et al. Enhanced skin blood flow and sensitivity to noxious heat stimuli in papulopustular rosacea. J Am Acad Dermatol 2007;57:800–805.
33. Schwab VD, Sulk M, Seeliger S, Nowak P, et al. Neurovascular and neuroimmune aspects in the pathophysiology of rosacea. J Investig Dermatol Symp Proc 2011;15: 53–62.
34. Sibenge S, Gawkrodger DJ. Rosacea: A study of clinical patterns, blood flow, and the role of *Demodex folliculorum*. J Am Acad Dermatol 1992;26:590–593.

35. Bernstein EF, Schomacker K, Paranjape A, Jones CJ. Pulsed dye laser treatment of rosacea using a novel 15 mm diameter treatment beam. Lasers Surg Med 2018;50(8):808–812.
36. Stephens DP, Saad AR, Bennett LA, et al. Neuropeptide Y antagonism reduces reflex cutaneous vasoconstriction in humans. Am J Physiol Heart Circ Physiol 2004;287: H1404–H1409.
37. Dayan SH, Pritzker RN, Arkins JP. A new treatment regimen for rosacea: OnabotulinumtoxinA. J Drugs Dermatol 2012;11-(12):e76–e79.
38. Park KY, Hyun MY, Jeong SY, Kim BJ, Kim MN, Hong CK. Botulinum toxin for the treatment of refractory erythema and flushing of rosacea. Dermatology 2015;230(4): 299–301.
39. Schlessinger J, Gilbert E, Cohen JL, Kaufman J. New uses of abobotulinumtoxinA in aesthetics. Aesthet Surg J 2017;37-(suppl_1):S45–S58.
40. Bloom BS, Payongayong L, Mourin A, Goldberg DJ. Impact of intradermal abobotulinumtoxinA on facial erythema of rosacea. Dermatol Surg 2015;41(Suppl 1):S9–16.
41. Guo BL, Zheng CX, Sui BD, Li YQ, Wang YY, Yang YL. A closer look to botulinum neurotoxin type A-induced analgesia. Toxicon 2013;71:134–139.
42. Pickett A. Re-engineering clostridial neurotoxins for the treatment of chronic pain: Current status and future prospects. BioDrugs 2010;24(3):173–182.
43. Patil S, Willett O, Thompkins T, et al. Botulinum toxin: Pharmacology and therapeutic roles in pain states. Curr Pain Headache Rep 2016;20(3):15.
44. Ney JP, Joseph KR. Neurologic uses of botulinum neuro-toxin type A. Neuropsychiatr Dis Treat 2007;3(6):785–798.
45. Purkiss J, Welch M, Doward S, Foster K. Capsaicin-stimulated release of substance P from cultured dorsal root ganglion neurons: Involvement of two distinct mechanisms. Biochem Pharmacol 2000;59(11):1403–1406.
46. Zhu YJ, Lu TJ. A multi-scale view of skin thermal pain: From nociception to pain sensation. Phil Trans R Soc A 2010; 368:521–559.
47. Harris M, Fried D, Reinisch L, et al. Eyelid resurfacing. Lasers Surg Med 1999;25:107–122.

Dermatol Ther (Heidelb)
https://doi.org/10.1007/s13555-019-0298-x

ORIGINAL RESEARCH

The Scar Bane, Without the Pain: A New Approach in the Treatment of Elevated Scars: Thermomechanical Delivery of Topical Triamcinolone Acetonide and 5-Fluorouracil

Ofir Artzi · Amir Koren · Roni Niv · Joseph N. Mehrabi · Or Friedman

Received: March 9, 2019

ABSTRACT

Introduction: Keloids are challenging to treat due to their inadequate response to treatment and high recurrence rate. Intralesional triamcinolone acetonide (TAC) injection with or without 5-fluorouracil (5FU) is considered the first-line treatment for keloids. Three significant disadvantages of intralesional injections are the pain associated with the procedure, the uneven topography, and epidermal atrophy. Fractionated ablative carbon dioxide (CO_2) laser-assisted drug delivery (LADD) of the topical solution can help facilitate transdermal drug delivery and shows promise in scar remodeling. This study examined the use of a thermomechanical device (Tixel, Novoxel) to facilitate the transdermal delivery of TAC and 5-FU in the treatment of keloid scars.

Methods: Seven patients each received eight topical thermal ablations, with one ablation performed every 2–3 weeks. TAC and 5FU were applied after each ablation. Outcomes were evaluated using the Vancouver Scar Scale (VSS), and pain was assessed using the Visual Analog Scale (VAS).

Results: Mean keloid VSS reduced from 8.6 ± 1.2 to 5 ± 2.7 after the eight treatments. Mean treatment pain VAS score was 2.4 ± 0.7. Patients rated their satisfaction level as moderate–high. No severe adverse reactions were noted.

Conclusion: Thermomechanical drug delivery of TAC and 5-FU is safe and effective. This is a promising option for the treatment of keloid scars, particularly in the pediatric population.

Enhanced Digital Features To view enhanced digital features for this article go to https://doi.org/10.6084/m9.figshare.7987415.

O. Artzi · A. Koren
Department of Dermatology, Tel Aviv Sourasky Medical Center, Tel Aviv, Israel

O. Artzi · A. Koren · R. Niv
Dr. Artzi Treatment and Research Center, Tel Aviv, Israel

J. N. Mehrabi · O. Friedman
Sackler Faculty of Medicine,
Tel Aviv University, Tel Aviv, Israel

O. Friedman (✉)
The Plastic Reconstructive Surgery Department,
Tel Aviv Sourasky Medical Center, Tel Aviv, Israel
e-mail: or.friedman@gmail.com

Keywords: Keloid; Fluorouracil; Fractional skin ablation; Percutaneous permeating; Resurfacing; Scar; Tixel; Transdermal drug delivery; Triamcinolone

INTRODUCTION

Keloid scars are an uncommon but severe result of impaired wound healing. Keloid scars may develop after acne vulgaris, trauma, surgical incisions, burn injuries, or without an obvious

Published online: 30 April 2019

trigger [1, 2]. Intralesional corticosteroid injection is considered the first-line treatment for keloid scars [3, 4]. Combination therapies with other adjuvant therapeutic modalities, such as pressure garments, silicone gel, radiation, or cryotherapy, seem to further increase treatment efficacy [5–7]. Complications associated with intralesional corticosteroid injection include tissue atrophy, hypopigmentation, hyperpigmentation, telangiectasia, and severe pain during the injection, perhaps due to random deposition within the scar if the corticosteroid follows the path of minimal resistance [8–10].

In recent years, laser-assisted drug delivery has been suggested as a means to overcome some of the complications associated with intralesional injections [11–14].

The aim of the present study was to explore the use of thermal decomposition of the stratum corneum to increase skin permeability for topical corticosteroid and 5FU application in the treatment of keloid scars.

METHODS

A retrospective review of 7 patients (4 males, 3 females) treated for keloid scars between January 2015 and December 2017 was performed. Patients were offered Tixel treatment following the failure of other modalities and their refusal of other options. Written consent was received after they had been informed of the nature of the procedure. Consent included the use of photos and data for teaching and in medical publications.

The patient's affected areas were treated with Tixel technology (Novoxel Ltd., Israel), which combines thermal energy with motion. The system consists of a titanium tip heated to 400 °C. The tip is advanced until it makes contact with the skin. The tip therefore exerts an ablative effect on the skin due to physical contact and the transduction of heat to the superficial layers of the skin, as opposed to laser energy, which targets chromophores within the skin and heats them.

The tip was heated to 400 °C and contact with the skin was made just once (i.e., a single "pulse") for a duration of 5–8 ms. A protrusion (the distance the heated tip is moved beyond the edge of the handpiece distance gauge) of 1000 μm was applied. Immediately after skin treatment, triamcinolone acetonide (40 mg/ml) and 5-fluorouracil (50 mg/ml) mixed in the ratio 1:9 were applied topically to the treatment area at a dose of 1 cc per cm^2 with no occlusion or bandaging. All scars received 8 treatments performed 2–3 weeks apart. Post-procedure care included topical trolamine (Biafine; Genmedix Ltd., France) applied by the patient 3–4 times a day for 3 days, as well as the use of a broad-spectrum sunscreen with a sun protection factor (SPF) of 50 for 3 months.

The scars were evaluated and photographed at baseline and 2–3 months after the last treatment. Scars were evaluated by two independent dermatologists using the Vancouver Scar Scale (VSS). Pain levels were assessed according to the Visual Analog Scale (VAS), while satisfaction was assessed using a four-point scale (0—not satisfied, 1—mildly satisfied, 2—moderately satisfied, 3—highly satisfied).

Statistical analysis was performed using SPSS software (version 21.0; IBM Corporation, Armonk, NY, USA).

RESULTS

Mean keloid VSS reduced from 8.6 ± 1.2 to 5 ± 2.7 ($p = 0.001$). Mean pain VAS score was 2.4 ± 0.7. Overall, patients rated their satisfaction level as moderate–high. No severe adverse reactions were noted. According to their VSS score, 1 patient did not respond to treatment (Table 1).

DISCUSSION

Keloid scars are an uncommon but troubling complication of dermal injury, with a predilection for younger patients and higher Fitzpatrick skin types, particularly patients of African, Asian, or Hispanic origin with an associated family history [1–3]. Intralesional corticosteroid injections are considered the first-line treatment for keloids [3, 4]. Corticosteroids can be used alone or in combination with other scar-

Table 1 Patient demographics and clinical data

Patient	Age (years)	Sex	Anatomical location	Disease duration (years)	Fitzpatrick skin type	Vascularity after	Vascularity before	Satisfaction	VAS	Average VSSa	Average VSSb
1	6	F	Thighs	3	3	2	2	0	2	10	9.5
2	4	F	Chest	3	2	3	2.5	3	2	5.5	8
3	55	M	Chest	20	3	3	2.5	2	3	6	8.5
4	23	M	Back arm	5	4	2	1.5	3	2	4	8.5
5	3	F	Abdomen	2	2	2	2	4	3	4.5	7.5
6	45	F	Chest	13	2	2	2.5	3	3	2	7
7	11	F	Chest	4	3	2.5	2	2	3	4	10
Average:						2.21	2.28	2.42	2.42	5.5	8.64
SD:						0.48	0.48	0.78	0.78	2.5	1.24

Fig. 1 Patient 3. Photographs of the keloid taken before treatment (left) and 3 months after the completion of eight treatment sessions (right)

modulating treatments such as intralesional 5-fluorouracil injection, cryotherapy, surgical excision, radiation therapy, compression therapy, and silicone-based dressings [5–7]. Potential adverse events associated with intralesional corticosteroid injection include dermal and subcutaneous atrophy, pigmentary alterations, and telangiectasia [8]. Also, the treatment is considered painful, which is a significant drawback, especially in pediatric patients [9, 10].

Fractionated ablative carbon dioxide (CO_2) laser-assisted drug delivery (LADD) of corticosteroids is considered less painful and distributes the drug more uniformly, and its use has resulted in encouraging clinical results [11, 12]. LADD facilitates corticosteroid delivery through the microscopic channels created by the ablative fractional laser [12–14]. That said, LADD is not pain-free and it cannot be tolerated by a significant number of patients.

The therapeutic efficacy of a topical drug relates to both its inherent potency and its ability to penetrate the different skin layers. The main barrier to drug permeation is its passage through the stratum corneum [15]. The importance of the water content of the stratum corneum in determining its properties is well documented. The water content of the skin gradually increases upon moving from the upper layer of the stratum corneum down to the viable epidermis, where the water content remains almost constant with depth [16, 17]. The mechanical properties of the stratum corneum are strongly affected by the relative humidity (RH%) within the layer. The breaking strength of the stratum corneum increases from about 10 g at 80–100% RH to 45 g at 0% RH, while the elongation at break decreases from 200% at 100% RH to less than 10% at 0% RH [18].

Tixel technology combines thermal energy with motion. The system consists of a titanium tip heated to 400 °C. The tip is advanced until it makes contact with the skin, and the duration of this contact (the pulse duration) determines the amount of thermal energy delivered to the skin. The system provides the user with predefined pulse duration parameters that range from 5 to 18 ms. A second system parameter is the protrusion, which is defined as the distance that the heated tip is moved as measured from the edge of the handpiece distance gauge. The protrusion is aimed to acquire better thermal matching between the tip and the tissue without skin perforation (including the Stratum Corneum), along with the process.

Most of the thermal effect is concentrated in the stratum corneum, leading to rapid heat transfer and dehydration of the layer. Gentle elimination of the stratum corneum and desiccation of the upper epidermis establishes a concentration gradient according to Fick's law [19], leading to enhanced drug delivery following Tixel treatment.

The patients in the study did not describe the procedure as painful (VAS score 2.4, SD 0.7). The overall satisfaction of the patients was moderate–high, and objective reduction (as assessed by two independent dermatologists) was significant, as can be seen in Fig. 1. Importantly, no notable adverse effects were reported with this approach. That said, one of the patients did not respond to treatment. The nonresponder had the highest VSS score (10.5) due to the significant height and rope-like bands of their scar. Thermal decomposition alone may not be enough to achieve the necessary drug delivery with in such cases, so alternative methods may be necessary.

Limitations of this study include the small sample size, the lack of a control group, and the short follow-up period. It is worth noting that these patients refused any other treatment modality due to the pain they had experienced previously with other treatments. We therefore assume that their subjective pain assessments took their experiences with previous treatments into account. This limitation of the study merits further evaluation in a properly controlled manner. Also, this study raises many questions, including: what is the role of heat progression? Is it only a drug delivery enhancement system? Does the heat transfer affect the dermal microvasculature as well? More substantial, randomized, blinded, placebo-controlled studies are needed.

CONCLUSIONS

Thermomechanical drug delivery of TAC and 5-FU is safe and effective. This is a promising option for the treatment of keloid scars, particularly in the pediatric population.

ACKNOWLEDGEMENTS

We thank the participants of the study.

Funding. No funding or sponsorship was received for this study or the publication of this article. The authors funded the article processing charges.

Authorship. All named authors meet the International Committee of Medical Journal Editors (ICMJE) criteria for authorship for this article, take responsibility for the integrity of the work as a whole, and have given their approval for this version to be published.

Disclosures. Ofir Artzi, Amir Koren, Roni Niv, Joseph N. Mehrabi, and Or Friedman have nothing to disclose.

Compliance with Ethics Guidelines. Written consent was received after they were informed of the nature of the procedure. Consent included the use of photos and data in teaching and medical publications.

Data Availability. This is a retrospective study. The datasets generated and analysed during study are not publicly available due to patient privacy but are available from the corresponding author on reasonable request.

REFERENCES

1. Ud-Din S, Bayat A. Strategic management of keloid disease in ethnic skin: a structured approach supported by the emerging literature. Br J Dermatol. 2013;169:71–81.

2. Chike-Obi CJ, Cole PD, Brissett AE. Keloids: pathogenesis, clinical features, and management. Semin Plast Surg. 2009;23(3):178–84.

3. Shah VV, Aldahan AS, Mlacker S, et al. 5-Fluorouracil in the treatment of keloids and hypertrophic scars: a comprehensive review of the literature. Dermatol Ther. 2016;6(2):169–83.

4. Juckett G, Hartman-Adams H. Management of keloids and hypertrophic scars. Am Fam Physician. 2009;80(3):253–60.

5. Al-Attar A, Mess S, Thomassen JM, Kauffman CL, Davison SP. Keloid pathogenesis and treatment. Plast Reconstr Surg. 2006;117:286–300.

6. Kim S, Choi TH, Liu W, Ogawa R, Suh JS, Mustoe TA. Update on scar management: guidelines for treating Asian patients. Plast Reconstr Surg. 2013;132:1580–9.

7. Gold MH, McGuire M, Mustoe TA, Pusic A, Sachdev M, Waibel J, Murcia C. International Advisory Panel on Scar Management. Updated international clinical recommendations on scar management: part

2—algorithms for scar prevention and treatment. Dermatol Surg. 2014;40:825–31.

8. Muneuchi G, Suzuki S, Onodera M, Ito O, Hata Y, Igawa HH. Long-term outcome of intralesional injection of triamcinolone acetonide for the treatment of keloid scars in Asian patients. Scand J Plast Reconstr Surg Hand Surg. 2006;40:111–6.

9. Mishra S. Safe and less painful injection of triamcinolone acetonide into a keloid—a technique. J Plast Reconstr Aesthet Surg. 2010;63:e205.

10. Chuang GS, Rogers GS, Zeltser R. Poiseuille's law and large-bore needles: insights into the delivery of corticosteroid injections in the treatment of keloids. J Am Acad Dermatol. 2008;59:167–8.

11. Waibel JS, Wulkan AJ, Shumaker PR. Treatment of hypertrophic scars using laser and laser-assisted corticosteroid delivery. Lasers Surg Med. 2013;45:135–40.

12. Cavalié M, Sillard L, Montaudié H, Bahadoran P, Lacour JP, Passeron T. Treatment of keloids with laser-assisted topical steroid delivery: a retrospective study of 23 cases. Dermatol Ther. 2015;28:74–8.

13. Issa MC, Kassuga LE, Chevrand NS, Pires MT. Topical delivery of triamcinolone via skin pretreated with ablative radiofrequency: a new method in hypertrophic scar treatment. Int J Dermatol. 2013;52:367–70.

14. Bloom BS, Brauer JA, Geronemus RG. Ablative fractional resurfacing in topical drug delivery: an update and outlook. Dermatol Surg. 2013;39:839–48.

15. Uchida Y, Park K. Stratum corneum. In: Kabashima K, editor. Immunology of the skin. Tokyo: Springer; 2016. p. 15–30. https://doi.org/10.1007/978-4-431-55855-2_2.

16. Warner RR, Myers MC, Taylor DA. Electron probe analysis of human skin: determination of the water concentration profile. J Invest Dermatol. 1988;90:218–24.

17. Stockdate M. Water diffusion coefficients versus water activity in stratum corneum: a correlation and its implications. J Soc Cosmetic Chemists. 1978;29:625–39.

18. Wildnauer RH, Bothwell JW, Douglass AB. Stratum corneum biomechanical properties. I. Influence of relative humidity on normal and extracted human stratum corneum. J Investig Dermatol. 1971;56(1):72–8.

19. Cengal YA. Heat transfer: a practical approach. 2nd ed. New York: McGraw–Hill; 2002.

Received: 28 March 2019 | Accepted: 25 September 2019

DOI: 10.1111/jocd.13192

ORIGINAL CONTRIBUTION

JCD Journal of Cosmetic Dermatology WILEY

A new approach in the treatment of pediatric hypertrophic burn scars: Tixel-associated topical triamcinolone acetonide and 5-fluorouracil delivery

Ofir Artzi MD[1,2] | Amir Koren MD[1,2] | Roni Niv MD[2] | Joseph N. Mehrabi[3] | Jacob Mashiah MD[1,3,4] | Or Friedman MD[3,5]

[1]Department of Dermatology, Tel Aviv Sourasky Medical Center, Tel Aviv, Israel

[2]Dr. Artzi Treatment and Research Center, Tel Aviv, Israel

[3]Sackler Faculty of Medicine, Tel Aviv University, Tel Aviv, Israel

[4]Pediatric Dermatology Clinic, Dana-Dwek Children's Hospital, Tel Aviv Sourasky medical center, Tel Aviv, Israel

[5]The Plastic Reconstructive Surgery Department, Tel Aviv Sourasky Medical Center, Tel Aviv, Israel

Correspondence
Or Friedman, Plastic Reconstructive Surgery Department, Tel Aviv Sourasky Medical Center, Affiliated with Sackler Faculty of Medicine, Tel Aviv University, Tel Aviv, Israel, 6 Weizman Street, Tel Aviv, 642906 Israel.
Email: orfriedman@tauex.tau.ac.il

Abstract

Background: Pediatric hypertrophic burn scars are challenging to treat due to their widespread nature and pain associated with the treatment. Intralesional triamcinolone acetonide (TAC) injection with or without 5-fluorouracil (5FU) is considered first-line treatment for severe hypertrophic scars. The pain associated with the procedure, the uneven topography, and epidermal atrophy, all limit the application of this treatment modality.

Aims: We sought to evaluate the clinical effectiveness and safety profile of a novel thermomechanical system (Tixel, Novoxel) for transdermal delivery of a topical solution containing TAC and 5-FU in the treatment of hypertrophic scars.

Patients/Methods: A retrospective study of pediatric hypertrophic burn scars treated between 2015 and 2017 was performed. Epidemiologic, treatment data, effectiveness score, and safety were reviewed.

Results: Four children (one male and three females, ages 3-10 years old) with hypertrophic burn scars treated with the Tixel device were evaluated. Mean scar VSS was reduced from 8.4 ± 0.8-5.2 ± 0.5 (*P*-value – .001) after eight treatments. The mean improvement of toughness, thickness, color, and general aesthetic impression was 3.1 ± 0.43 → 2.2 ± 0.31, 3.4 ± 0.5 → 1.9 ± 0.63, 2.7 ± 0.21 → 2.4 ± 0.25, and 3.23 ± 0.44 → 1.6 ± 0.64, respectively. Mean treatment pain VAS score was 1.74 ± 0.9. Patient's parents rated their satisfaction level as "moderate-high." No topical or systemic complications were observed.

Conclusion: Thermomechanical decomposition of the stratum corneum, in combination with topical application of TAC and 5-FU, is a safe, relatively painless, and efficient modality for the treatment of pediatric hypertrophic burn scars.

KEYWORDS

burn scars, fluorouracil, fractional skin ablation, hypertrophic, Percutaneous permeating, resurfacing, scar, Tixel, transdermal drug delivery, triamcinolone

1 | INTRODUCTION

Acute care of burn injuries has greatly improved in the last years; however, many patients develop hypertrophic scars that have permanent functional and social implications.[1,2] Hypertrophic scarring occurs when the normal healing process is disrupted by increased inflammation, and excess collagen accumulation, which can lead to an itchy, painful, erythematous, raised, and rigid scar.[2,3] The generally applied treatment for hypertrophic scars comprises of motion exercises, massage, pressure garments, steroid injections, silicone gel sheeting, laser and light-emitting diodes, cryotherapy, fluorouracil (5-FU), interferon, bleomycin, imiquimod 5% cream, and surgical interventions achieving only limited success, thus necessitating the development of newer, more effective treatment modalities.[4,6]

Burn scar treatment has important clinical and financial implications. For an example, in the United States alone, the cost of burn scar treatment has reached about $4 billion per year.[5]

Corticosteroid intralesional injections alone or combined with other modalities are the first-line treatment for hypertrophic scars and are considered the most efficacious.[7-11] Adverse events associated with corticosteroid intralesional injection include atrophy, hypo- or hyperpigmentation, telangiectasia, as well as severe pain during the injection, and laser-assisted corticosteroid drug delivery systems can ameliorate the depth and the amount of the drug which is been delivered.[12-18]

This study describes the safety and efficacy of thermal decomposition of the stratum corneum using a novel thermomechanical device to increase skin permeability for topical corticosteroid and 5FU application in the treatment of pediatric patients with hypertrophic scars.

2 | METHODS

This is a retrospective review of four patients (one male, three females) treated for hypertrophic burn scars between January 2015 and December 2017. Written consent was received from the legal guardians of the pediatric patients after they were informed of the nature of the procedure. Table 1 summarizes the patient demographics and clinical data.

The scars were treated by Tixel (NOVOXEL ltd). Device setting included 400°C at contact intervals of 5-8 ms, 1000 protrusion, and single pulse. Contact intervals were adjusted according to the patient's level of tolerance and comfort. Immediately after the Tixel treatment, triamcinolone acetonide (40 mg/mL) and 5-fluorouracil (50 mg/mL) mixed at a 1:9 ratio were topically applied to the treatment area at a dose of 1 cc per 1 cm^2. Sonophoresis was performed to enhance drug penetration using the impact device (Alma lasers GmbH, Germany, parameters: frequency 50 Hz, intensity 50%, 5 minutes) (Figure 1). Scars received eight treatments, 2-3 weeks apart.

Postprocedure care included topical trolamine (Biafine; Genmedix Ltd) self-applied 3-4 times per day for 3 days and the use of broad-spectrum sunscreen with a sun protection factor of 50 for 3 months.

The scars were evaluated using the Vancouver Scar Scale (VSS) by two independent dermatologists and photographed at baseline and 1-month postlast treatment. Pain level and satisfaction were assessed by the patient or his legal guardian by using the visual analog scale (VAS) and four-point scale (1-not satisfied, 2-mildly satisfied, 3-moderately satisfied, 4-highly satisfied), respectively. Scar toughness, thickness, color, and general aesthetic impression were rated on a four-point scale by the guardians as well (1-best, 4-worst).

Statistical analysis was performed using SPSS software (version 21.0; IBM Corporation).

3 | RESULTS

The study comprised of four patients: three girls 3, 4, and 4 years old, and 1 10-year old boy. All of which completed the study. There was a mean scar VSS reduction from 8.4 ± 0.8-5.2 ± 0.5 (*P*-value <.001) after eight treatments. Mean reduction of toughness, thickness, color, and general aesthetic impression were registered as follows: 3.1 ± 0.43 → 2.2 ± 0.31, 3.4 ± 0.5 → 1.9 ± 0.63, 2.7 ± 0.21 → 2.4 ± 0.25, and 3.23 ± 0.44 → 1.6 ± 0.64, respectively. Mean treatment pain VAS score was 1.74 ± 0.9. The patient's guardians rated their satisfaction level as "moderate-high." No severe adverse effects were noted.

4 | DISCUSSION

Hypertrophic scars are a common complication of wound healing process with a predilection to younger patients and higher Fitzpatrick

TABLE 1 Patient demographics and clinical data

Patient	Sex	Age	Fitzpatrick skin type	Disease Duration (Y's)	Anatomical location	VSSb-Average	VSSa-Average	VAS	Satisfaction	Vascularity before	Vascularity after
1	F	4	2	3	Chest	8	5.5	5.5	3	2.5	3
2	F	3	2	2	Abdomen	7.5	4.5	4.5	4	2	2
3	M	10	2	4	Shoulders	9.5	5.5	5.5	3	2.5	2.5
4	F	4	2	3	Abdomen	8.5	5.5	5.5	1	1.5	2
						8.375	5.25	5.25	2.75	2.125	2.375
						0.8	0.5	0.5	1.2	0.5	0.5

FIGURE 1 Patient # 1—Photograph immediately postfirst treatment

skin types, particularly patients of African, Asian, or Hispanic origin with an associated family history.[9] As topical steroid formulations demonstrate low poor cutaneous bioavailability, intralesional corticosteroid injections have been considered as first-line treatment mode for hypertrophic scars alone or in combination with other anti-scarring modalities such as intralesional injection of 5-fluorouracil, cryotherapy, surgical excision, radiation therapy, compression, and silicone-based dressings.[9,11] Potential adverse events associated with corticosteroid intralesional injection include dermal and fat atrophy, pigmentary alterations, and telangiectasia.[12] Severe pain during the multiple injection sessions is often a significant drawback, especially for children.[6,7]

Laser-assisted drug delivery of corticosteroid is considered a less painful treatment possibility and has demonstrated encouraging clinical results.[8,9] It provides efficient delivery of corticosteroids through the microscopic channels created by the ablative fractional laser.[9-11] Nevertheless, effective laser-assisted drug delivery is highly operator-dependent and painful enough. Lower energy might compromise penetration depth, whereas higher energy may cause coagulation, thus limiting drug delivery.[8-11]

The therapeutic efficacy of topical drugs relates both to their inherent potency and their ability to penetrate the different skin layers, with the primary permeation barrier being the stratum corneum. [19]

The Tixel system consists of a moving titanium tip heated to 400°C. The amount of thermal energy delivered to the skin is determined by the pulse duration and the protrusion. The pulse duration is the period of time that the tip is in contact with the skin, varying between 5 ms and 18 ms. The protrusion is defined as the distance in which the heated tip is moving measured from the edge of the handpiece distance gauge.

At low energy settings, the thermal effect on the viable epidermis and the dermis is limited. Most of the thermal effect is concentrated in the stratum corneum leading to rapid heat transfer and dehydration of the stratum corneum rather than coagulation. Desiccation leads to gentle elimination of the stratum corneum and establishes a concentration gradient by Fick's law; thus, enhancement of drug delivery following Tixel treatment is achieved.[20,21]

The impact device (Alma Lasers Ltd.) has been developed to enhance the delivery of topical cosmeceuticals. The device operates at low ultrasound frequency (~30 kHz-100 Hz) and energy of peak of 0.4 W/cm^2 effectively pushing topically applied liquids to enhance absorption when paired with the thermomechanical SC destruction produced by the Tixel.[22]

The primary outcome of the study was the significant reduction in the scars VSS score (*P*-value <.001). The secondary outcome was

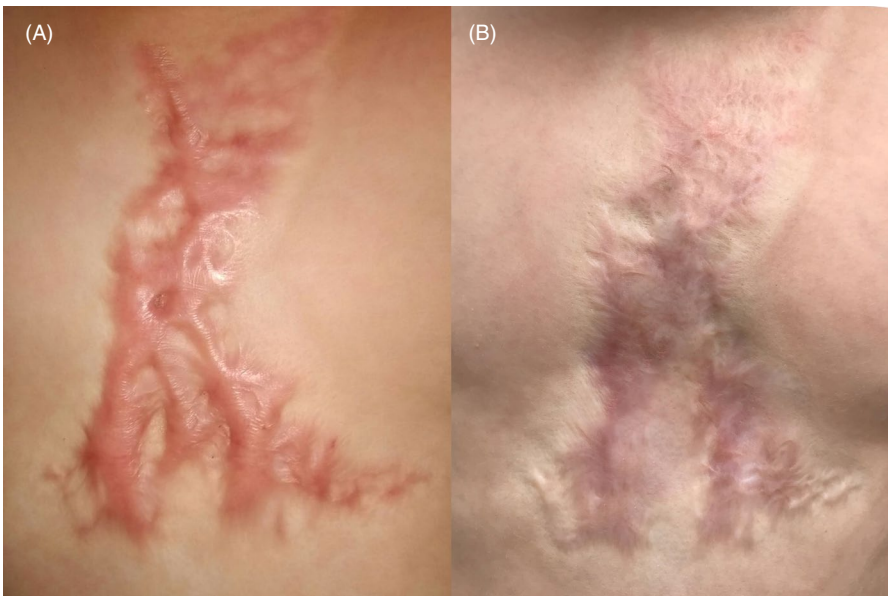

FIGURE 2 Patient # 1—Photographs of (A) baseline and (B) after completion of eight treatment protocol, 2 mo the last treatment

the consistently low pain reported during treatment with a mean VAS score of 1.74 (SD 0.9) (Figure 2).

This study demonstrates the successful and safe treatment of pediatric hypertrophic burn scars, thermal decomposition of the stratum corneum, followed by the immediate topical application of triamcinolone acetonide (TAC) with 5-fluorouracil (5FU). No significant adverse effects were reported with this approach. Moreover, the treatment was relatively painless and well tolerated in our patient group that refused alternative methods of treatment due to their previous painful experience. Even though our study was not explicitly aimed at achieving a uniform reduction of the scar, it is worthwhile noting that the scars seem to have been evenly reduced in height.

Additionally, the use of thermomechanical ablation as opposed to laser ablation eliminates the need for protective eyewear and could be performed by a nurse or medical assistant.

Limitations of this study include the small sample size and lack of a control group. Every new technology has a learning curve, and while results are significant and reproducible, further investigation is warranted to elucidate the best treatment protocol. The study raises several questions: What is the role of the Tixel in tissue remodeling? Is it only a drug delivery enhancing system? Does the heat transfer affect the dermal blood vessels? Might the thermal effect in itself lead to part of the improvement observed following treatment? Perhaps a combined treatment approach using both ablative and fractional laser therapy with Tixel may lead to superior results.

5 | CONCLUSION

Thermomechanical decomposition of the stratum corneum, in combination with topical application of TAC and 5-FU, is a safe relatively painless and efficient modality for the treatment of pediatric hypertrophic burn scars.

CONFLICT OF INTEREST

None.

ORCID

Amir Koren https://orcid.org/0000-0001-8667-9330
Or Friedman https://orcid.org/0000-0002-4362-7909

REFERENCES

1. Blome-Eberwein S, Gogal C, Weiss MJ, Boorse D, Pagella P. Prospective evaluation of fractional CO_2 laser treatment of mature burn scars. *J Burn Care Res*. 2016;37:379-387.
2. Alster TS, Tanzi EL. Hypertrophic scars and keloids: etiology and management. *Am J Clin Dermatol*. 2003;4:235-243.
3. Gauglitz GG, Korting HC, Pavicic T, Ruzicka T, Jeschke MG. Hypertrophic scarring and keloids: pathomechanisms and current and emerging treatment strategies. *Mol Med*. 2011;17:113-125.
4. Alster TS, Tanzi EL. Hypertrophic scars and keloids. *Am J Clin Dermatol*. 2003;4(4):235-243.
5. Aarabi S, Longaker MT, Gurtner GC. Hypertrophic scar formation following burns and trauma: new approaches to treatment. *PLoS Med*. 2007;4(9):e234.
6. Arno AI, Gauglitz GG, Barret JP, Jeschke MG. Up-to-date approach to manage keloids and hypertrophic scars: a useful guide. *Burns*. 2014;40(7):1255-1266. Published online 2014 Apr 24.
7. Al-Attar A, Mess S, Thomassen JM, Kauffman CL, Davison SP. Keloid pathogenesis and treatment. *Plast Reconstr Surg*. 2006;117:286-300.
8. Kim S, Choi TH, Liu W, Ogawa R, Suh JS, Mustoe TA. Update on scar management: guidelines for treating Asian patients. *Plast Reconstr Surg*. 2013;132:1580-1589.
9. Ud-Din S, Bayat A. Strategic management of keloid disease in ethnic skin: a structured approach supported by the emerging literature. *Br J Dermatol*. 2013;169:71-81.
10. Shah VV, Aldahan AS, Mlacker S, et al. 5-Fluorouracil in the treatment of keloids and hypertrophic scars: a comprehensive review of the literature. *Dermatol Ther*. 2016;6(2):169-183.
11. Gold MH, McGuire M, Mustoe TA, et al. International advisory panel on scar management. Updated international clinical recommendations on scar management: part 2—algorithms for scar prevention and treatment. *Dermatol Surg*. 2014;40:825-831.
12. Muneuchi G, Suzuki S, Onodera M, Ito O, Hata Y, Igawa HH. Long-term outcome of intralesional injection of triamcinolone acetonide for the treatment of keloid scars in Asian patients. *Scand J Plast Reconstr Surg Hand Surg*. 2006;40:111-116.
13. Mishra S. Safe and less painful injection of triamcinolone acetonide into a keloid—a technique. *J Plast Reconstr Aesthet Surg*. 2010;63:e205.
14. Chuang GS, Rogers GS, Zeltser R. Poiseuille's law and large-bore needles: insights into the delivery of corticosteroid injections in the treatment of keloids. *J Am Acad Dermatol*. 2008;59:167-168.
15. Waibel JS, Wulkan AJ, Shumaker PR. Treatment of hypertrophic scars using laser and laser assisted corticosteroid delivery. *Lasers Surg Med*. 2013;45:135-140.
16. Cavalié M, Sillard L, Montaudié H, Bahadoran P, Lacour JP, Passeron T. Treatment of keloids with laser-assisted topical steroid delivery: a retrospective study of 23 cases. *Dermatol Ther*. 2015;28:74-78.
17. Issa MC, Kassuga LE, Chevrand NS, Pires MT. Topical delivery of triamcinolone via skin pretreated with ablative radiofrequency: a new method in hypertrophic scar treatment. *Int J Dermatol*. 2013;52:367-370.
18. Bloom BS, Brauer JA, Geronemus RG. Ablative fractional resurfacing in topical drug delivery: an update and outlook. *Dermatol Surg*. 2013;39:839-848.
19. Kabashima K, Honda T, Ginhoux F, Egawa G. The immunological anatomy of the skin. *Nat Rev Immunol*. 2019;19(1):19-30. https://doi.org/10.1038/s41577-018-0084-5
20. Lask G, Elman M, Fournier N, Slatkine M. Fractional vaporization of tissue with an oscillatory array of high temperature rods – Part I: Ex vivo study. *J Cosmetic and Laser therapy*. 2012;5:218-223.
21. Cengel YA. *Heat Transfer: A Practical Approach*, 2nd (ed.). New York, NY: McGraw-Hill; 2002.
22. Waibel JS, Rudnick A, Nousari C, Bhanusali DG. Fractional ablative laser followed by transdermal acoustic pressure wave device to enhance the drug delivery of aminolevulinic acid. In Vivo fluorescence microscopy Study. *J Drugs Dermatol*. 2016;15(1):14-21.

How to cite this article: Artzi O, Koren A, Niv R, Mehrabi JN, Mashiah J, Friedman O. A new approach in the treatment of pediatric hypertrophic burn scars: Tixel-associated topical triamcinolone acetonide and 5-fluorouracil delivery. *J Cosmet Dermatol*. 2019;00:1–4. https://doi.org/10.1111/jocd.13192

Dermatology

Research Article

Dermatology
DOI: 10.1159/000507808

Received: January 14, 2020
Accepted: April 3, 2020
Published online: July 10, 2020

Enhanced Percutaneous Delivery of Beta-Blockers Using Thermal Resurfacing Drug Delivery System for Topical Treatment of Infantile Hemangiomas

Jacob Mashiah[a–c] Efrat Bar-Ilan[b] Amir Koren[b, e] Or Friedman[e] Eyal Zur[d] Ofir Artzi[b, c, e]

[a]Pediatric Dermatology Unit, Dana Children's Hospital, Tel Aviv Sourasky Medical Center, Tel Aviv, Israel; [b]Department of Dermatology and Venereology, Tel Aviv Sourasky Medical Center, Tel Aviv, Israel; [c]Sackler Faculty of Medicine, Tel Aviv University, Tel Aviv, Israel; [d]Compounding Solutions, Pharmaceutical Consultancy Company, Tel Mond, Israel; [e]Dr. Artzi and Associates – Treatment and Research Center Tel Aviv, Tel Aviv, Israel

Keywords
Beta-blockers · Enhanced percutaneous delivery · Infantile hemangioma · Pediatric dermatology · Tixel

Abstract
Background: Infantile hemangiomas (IHs) are the most common vascular tumors in children. In the past few years, topical beta-blockers (bBs) have been reported to be an effective treatment of superficial IHs. ***Objective:*** We sought to evaluate the clinical effectiveness and safety profile of enhanced percutaneous delivery of bBs for the treatment of IH. ***Methods:*** A retrospective study of all cases of IHs treated with enhanced percutaneous delivery of bBs between 2018 and 2019 was performed. Epidemiologic, clinical, and treatment data, including effectiveness score and safety, were reviewed. ***Results:*** The study included 11 patients with a total of 11 IHs. Of the total number of IHs, 7 (63.7%) showed a good response to treatment and 4 (36.3%) had a partial response; thus all patients (100%) had good or partial response to treatment. No systemic or local adverse effects were reported. ***Limitations:*** This is an uncontrolled retrospective study. ***Conclusion:*** Enhanced percutaneous delivery of bBs is a safe and efficient topical therapy for IH.

Introduction

Infantile hemangiomas (IHs) are the most common vascular tumors in children with an incidence of 4–10%, they are caused by proliferation of endothelial cells. Their natural history comprises of a rapid proliferation in the first months of life, followed by an involution phase that can take several years [1–3]. While most of the IHs does not require treatment, it is beneficiary and even obligatory in cases of IHs in high-risk distribution imposing dysfunction, disability, or disfiguration such as the eyes, nose, and throat. Treatment can also prevent post involution atrophy, telangiectasia, fibro-fatty tissue, and skin laxity which commonly occur in superficial hemangiomas [4–6].

Since the discovery of the effect of propranolol on IHs, oral propranolol is considered the first-line treatment for IHs [7]. In light of the possible adverse effects (AEs) profile of the systemic treatment, topical beta-blockers (bBs), namely propranolol hydrochloride and timolol maleate, are widely used for the treatment of superficial IHs [8–10], with an improvement in up to 90% of the cases, minor local AEs, and without any reported systemic AEs [11, 12]. The use of lasers, microneedles, as well as radio frequency waves, as topical drug delivery systems can en-

karger@karger.com
www.karger.com/drm

Jacob Mashiah
Pediatric Dermatology Unit, Dana Children's Hospital
Tel Aviv Sourasky Medical Center, 6 Weizmann Street
Tel Aviv 64239 (Israel)
ymashiah1@gmail.com

Table 1. Patient and treatment characteristics

Patient	Sex	Age at the beginning, months	Size, cm	Color	Type	Location	Total treatment duration, months	No. of treatments	Interval, weeks	Drug	Score (0–3)	Satisfaction (0–3)
1	M	11	1.5×2	Bright red	Substantial thickness	Extremities	4	6	2–3	P	2	3
2	F	1.5	6×4	Bright red	Moderate thickness	Extremities	3.5	4	2–3	T	3	3
3	M	13	2×2	Purple/ dusky red	Minor	Head	2	3	2	T	3	3
4	F	7	3×5	Bright red	Substantial thickness	Neck	3	4	2–3	P	3	2
5	F	16	2×3	Purple/ dusky red	Moderate thickness	Extremities	3	5	2–3	P	2	3
6	F	12	1.5×4	Purple/ dusky red	Minor	Extremities	4	4	2–3	T	3	3
7	M	5	6×4	Bright red	Substantial thickness	Extremities	4	5	2–4	2P 3T	1.6	2
8	F	5	20×6	Bright red	Minor	Extremities	8	9	2–4	5P 4T	3	3
9	M	6	10×5	Bright red	Minor	Extremities	7	9	2–4	4P 5T	2.6	3
10	F	10	2×3	Bright red	Substantial thickness	Head	3.5	5	2–4	T	1.3	3
11	M	9	5×3	Bright red	Moderate thickness	Extremities	6	7	2–4	4P 3T	3	3

T, timolol; P, propranolol.

hance bBs bioavailability, and by that augment the response to the treatment; yet, it might be inapplicable in pediatric population due to their low pain tolerance [13]. We report our experience of applying topical bBs following treatment with a non-painful, non-laser novel thermal drug delivery system (Tixel-Novoxel) [13] in 11 patients with IHs.

Materials and Methods

For further details, see the online supplementary material (see www.karger.com/doi/10.1159/000507808) [11–20] (Table 1).

Results

The study included 11 patients (6 girls and 5 boys) with an average age of 8.6 months (range: 1.5–16 months) and a total of 11 IHs. The initial size range of the examined IHs was from 3 to 120 cm^2 with an average of 24.5 cm^2. The color distribution at presentation was as follows: 8 (72.72%) were bright red, 3 (27.27%) were purple or dusky red. Four (36.3%) of the IHs had minor thickness, 3 (27.4%) had moderate thickness, and 4 (36.3%) had substantial thickness. Three (27.3%) hemangiomas were located on the head and neck area and 7 (63.7%) on the extremities. None of the IHs were ulcerated. The mean duration of treatment was 4.36 months (range: 2–8 months). Four (36.3) patients were treated with timolol with an average of 4 treatment (range: 3–5), three (27.3) patients were treated with propranolol with an average of 5 treatments (range: 4–6), and 4 (36.3) patients received propranolol at the beginning and were switched to timolol with an average of 7.5 treatments (range 5–9). Eight patients were treated only with the Tixel drug delivery system once every 2–4 weeks, followed by topical beta-blocker application immediately and once every hour for 3 h, while 3 patients received additionally topical propranolol 4% PLO gel over the IHs twice daily without occlusion for the first month of treatment; however, in light of the good response after each Tixel treatment, the daily treatment was ceased.

Of the 11 IHs, 7 (63.7%) showed good response to treatment, and 4 (36.3%) demonstrated a partial response. Altogether all patients had good or partial response to treatment (Fig. 1, 2). No recurrence was recorded in the 2-month posttreatment follow-up period. No systemic or topical AEs were reported. Although the Tixel treatment

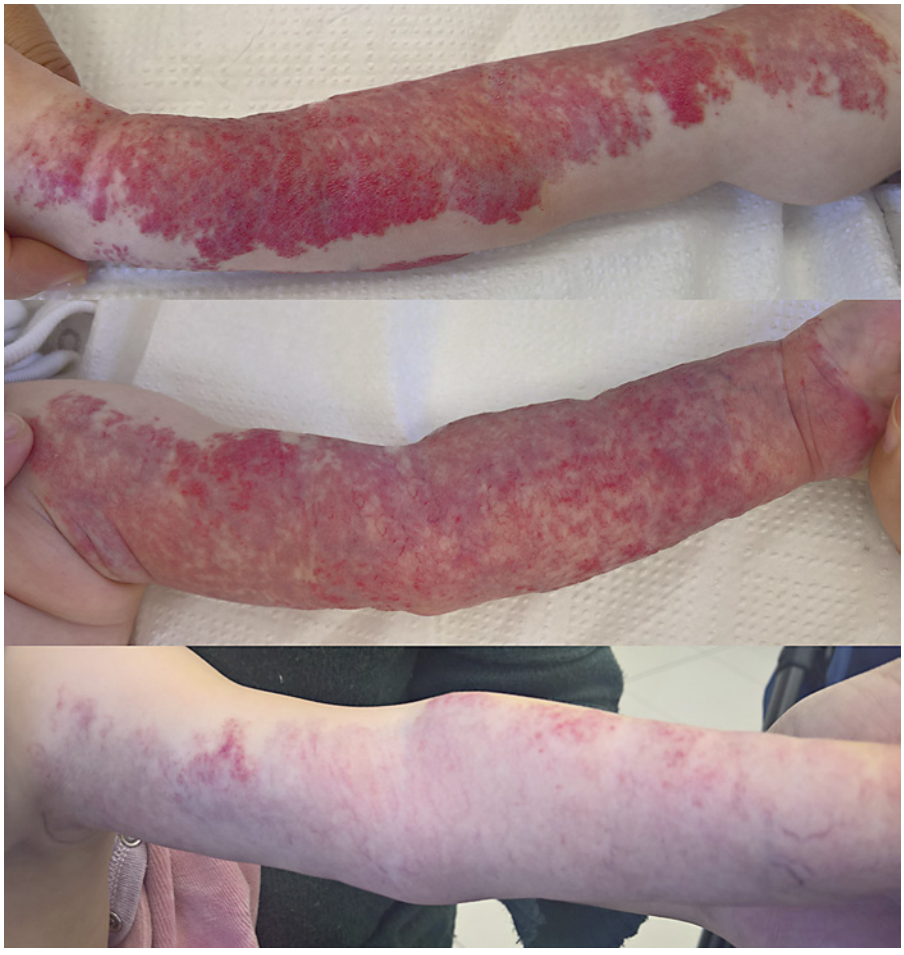

Fig. 1. Patient No. 8 is a 5-month-old girl with a large hemangioma on her left hand, measuring 6 × 20 cm before, during, and after the final treatment.

causes discomfort and even slight pain, the pain is bearable, remains only during the treatment time, and did not influence the decision of continuing or not the treatment.

Discussion

In the past decade, treatment of IHs has changed dramatically and oral propranolol has become the first-line treatment [7, 8]. The commonly reported AEs of oral propranolol are sleep disturbances and acrocyanosis. Rare but possible serious ones include bradycardia, hypotension, bronchospasm, and hypoglycemia [8, 9]. In light of the possible AEs profile of the systemic treatment, its length and the young age of the patients, a topical regimen of bBs, having a significant lower AEs rate, is used as an alternative treatment modality, mainly for superficial IHs [11, 12]. There is no commercial topical bBs medication registered, nor a consensus protocol for the treatment of superficial IHs with topical bBs [8] which is applied off-label, using various concentrations, vehicles, dosages, and application frequencies, of compounded propranolol or timolol eye drops solutions, with relatively good results [11, 12, 15]. Nevertheless, topical bBs treatment, usually requiring up to 16 months (average 5–7.5 months) in several studies) [11, 12] is not sufficiently efficacious for widespread or deep IHs. The major conflicting points regarding the topical treatment are as follows: (1) Which is the most suitable bB molecule for topical drug delivery? (2) What is the appropriate vehicle? (3) How can we enhance the percutaneous delivery? (4) What is the best treatment regimen – the easiest, least painful, shortest, and with best final cosmesis? The efficiency of topical treatment depends on the drug potency and its ability to penetrate the skin. Lasers, microneedles, radio frequency, and ultrasound have all been used to increase drug bioavailability in the skin [21]. Ma et al. [22] have reported the use of fractional carbon dioxide (CO_2) laser for assisted drug de-

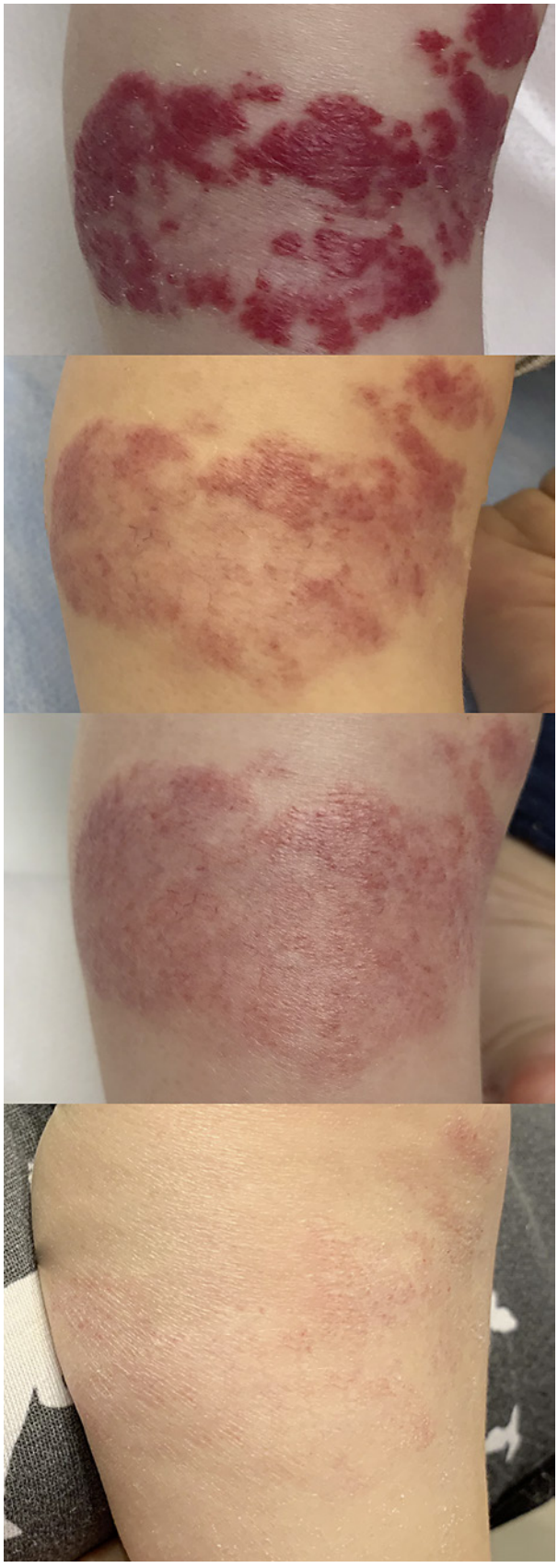

livery of topical timolol solution for the treatment of deep IHs. The fractional CO_2 laser was applied once weekly on the IHs of 9 patients followed by an application of a cotton pad saturated with 2–5 drops of topical ophthalmic solution of timolol 0.5% under occlusion for 30 min immediately after the laser treatment, as well as 4–5 times a day for the whole treatment period, with an average number of laser treatments of 11.6 and average treatment duration of 14.2 weeks. A total of 88% of patients demonstrated excellent and good regression. There were no systemic AEs or significant changes in vital signs and blood glucose level measured after the first timolol application. Pinpoint bleeding as well as erythema and edema which appeared after the laser treatment ceased 1–3 days later and the dot crusting resolved in 1 week [22]. The disadvantages of the CO_2 laser as enhanced drug delivery method of topical bBs in young children are the pain it causes, the need to protect the eyes during the treatment, and the high cost of the device. We used the Tixel drug delivery system once every 2–4 weeks with an average of 5.5 treatments and average treatment duration of 17 weeks. All patients, except 3 who additionally applied bBs twice daily for the first month, were treated solely with topical bBs, 4 times 1 h apart, after the Tixel drug delivery application without occlusion, and did not receive any treatment between the Tixel sessions, meaning that they were treated only 5.5 (range: 3–9) days during the whole treatment period. All patients showed good or partial response to treatment without systemic or local AEs. Another advantage of the drug delivery system used in our study over the CO_2 laser is the substantially lower pain during the treatment as well as lack of healing time, lasting few days after the treatment. Both enhanced drug delivery methods show better results, with shorter treatment period, than the reported results of the accepted regimen of topical bBs treatment for IHs, comprising of twice or three daily applications during the treatment period which varies between several weeks up to 16 months (average 5–7.5 months in several studies) [11, 12]. Propranolol and timolol have been used with similar efficacy and AEs profile for topical treatment of IHs [12]. We used a topical monotherapy of propranolol 4% gel or timolol 0.5% eye drops solution (in 3 and 4 patients each) and both agents (in 4 patients) with similar results but with a smaller number of treatments in the timolol group, probably due to its better ability to permeate the viable epidermis

Fig. 2. Patient No. 2 is a 1.5-month-old girl with a hemangioma on the anterior surface of her right shin, measuring 6 × 4 cm before, during, and after the final treatment.

and dermis as a hydrophilic molecule. Nevertheless, the small number of cases does not allow us to draw a solid conclusion. As in every topical treatment, treating bigger lesions, requires the use of substantially larger amounts of the drug, and enhances the risk of systemic AEs due to higher plasma concentration, thus requiring special considerations and precautions. The hydrophilic molecule of timolol gained a better penetration rate through the distorted and dehydrated SC, while the enhanced penetrating rate of propranolol can be attributed to the emulsion properties and appropriate viscosity of the PLO gel that does not block the micro-channels made by the Tixel. An explanation to the absence of systemic AEs, despite the penetration enhancement, can be that the bBs have enough retention time and its diffusion rate through the viable epidermis and dermis is appropriate and not too high.

The main limitation of our study is the small cohort. There is a need for a randomized double-blind, placebo-controlled study, with a much bigger cohort of patients treated for superficial, mixed, and deep IHs, with a longer follow-up period, in order to compare between topical treatment alone, or assisted drug delivery, and to establish the safety profile and the best treatment regimen.

Conclusion

We have demonstrated for the first time that Tixel-assisted percutaneous drug delivery of topical bBs shows promising results in the treatment of IHs. This approach seems effective as well as safe and should be further studied.

Key Message

Tixel assisted percutaneous drug delivery of topical beta-blockers shows promising results in the treatment of infantile hemangiomas.

Acknowledgment

We would like to thank the patients for the precipitant.

Statement of Ethics

The parents or guardians of all patients gave their written informed consent. The study protocol was approved by the institute's Helsinki committee on human research.

Disclosure Statement

The authors have no conflicts of interest to declare.

Funding Sources

No funding was received.

Author Contributions

All authors have contributed significantly, and are in agreement with the content of the manuscript.

References

1 Dickison P, Christou E, Wargon O. A prospective study of infantile hemangiomas with a focus on incidence and risk factors. Pediatr Dermatol. 2011 Nov-Dec;28(6):663–9.
2 Schwartz RA, Sidor MI, Musumeci ML, Lin RL, Micali G. Infantile haemangiomas: a challenge in paediatric dermatology. J Eur Acad Dermatol Venereol. 2010 Jun;24(6):631–8.
3 Holland KE, Drolet BA. Infantile hemangioma. Pediatr Clin North Am. 2010 Oct;57(5):1069–83.
4 LeauteLabreze C. Harper JI, Hoeger PH. Seminar Infantile haemangioma. Lancet. 2017;6736:1–10.
5 Léauté-Labrèze C, Prey S, Ezzedine K; Leaute-Labreze C. Infantile haemangioma: part II. Risks, complications and treatment. J Eur Acad Dermatol Venereol. 2011 Nov;25(11):1254–60.
6 Bauland CG, Lüning TH, Smit JM, Zeebregts CJ, Spauwen PH. Untreated hemangiomas: growth pattern and residual lesions. Plast Reconstr Surg. 2011 Apr;127(4):1643–8.
7 Leaute-Labreze C, Hoeger P, Mazereeuw-Hautier J, et al. A randomized, controlled trial of oral propranolol in infantile hemangioma. N Engl J Med 2015 Feb;372(8):735–46.
8 Hoeger PH, Harper JI, Baselga E, Bonnet D, Boon LM, Ciofi Degli Atti M, et al. Treatment of infantile haemangiomas: recommendations of a European expert group. Eur J Pediatr. 2015 Jul;174(7):855–65.
9 Marqueling AL, Oza V, Frieden IJ, Puttgen KB. Propranolol and infantile hemangiomas four years later: a systematic review. Pediatr Dermatol. 2013 Mar-Apr;30(2):182–91.
10 Novoa M, Baselga E, Beltran S, Giraldo L, Shahbaz A, Pardo-Hernandez H, et al. Interventions for infantile haemangiomas of the skin. Cochrane Database Syst Rev. 2018 Apr;4:CD006545.
11 Price A, Rai S, Mcleod RW, Birchall JC, Elhassan HA. Topical propranolol for infantile haemangiomas: a systematic review. J Eur Acad Dermatol Venereol. 2018 Dec;32(12):2083–9.
12 Zheng L, Li Y. Effect of topical timolol on response rate and adverse events in infantile hemangioma: a meta-analysis. Arch Dermatol Res. 2018 May;310(4):261–9.
13 Sintov AC, Hofmann MA. A novel thermomechanical system enhanced transdermal delivery of hydrophilic active agents by fractional ablation. Int J Pharm. 2016 Sep;511(2):821–30.

14 Zur E. Infantile hemangiomas, part 2: topical treatment with beta blockers. Int J Pharm Compd. 2011;15:458–63.
15 Mashiah J, Kutz A, Rabia SH, Ilan EB, Goldberg I, Sprecher E, et al. Assessment of the effectiveness of topical propranolol 4% gel for infantile hemangiomas. Int J Dermatol. 2017 Feb;56(2):148–53.
16 Mashiah J, Hadj-Rabia S, Slodownik D, Harel A, Sprecher E, Kutz A. Effectiveness of topical propranolol 4% gel in the treatment of pyogenic granuloma in children. J Dermatol. 2019 Mar;46(3):245–8.
17 Kumar R, Katare OP. Lecithin organogels as a potential phospholipid-structured system for topical drug delivery: a review. AAPS PharmSciTech. 2005 Oct;6(2):E298–310.
18 Guan Y, Zuo T, Chang M, Zhang F, Wei T, Shao W, et al. Propranolol hydrochloride-loaded liposomal gel for transdermal delivery: characterization and in vivo evaluation. Int J Pharm. 2015 Jun;487(1-2):135–41.
19 Waibel JS, Rudnick A, Nousari C, Bhanusali DG. Fractional Ablative Laser Followed by Transdermal Acoustic Pressure Wave Device to Enhance the Drug Delivery of Aminolevulinic Acid: In Vivo Fluorescence Microscopy Study. J Drugs Dermatol. 2016 Jan;15(1):14–21.
20 Chantasart D, Hao J, Li SK. Erratum to: Evaluation of Skin Permeation of β-Blockers for Topical Drug Delivery. Pharm Res. 2015 Feb;32(2):736.
21 Gómez C, Benito M, Teijón JM, Blanco MD. Novel methods and devices to enhance transdermal drug delivery: the importance of laser radiation in transdermal drug delivery. Ther Deliv. 2012 Mar;3(3):373–88.
22 Ma G, Wu P, Lin X, Chen H, Hu X, Jin Y, Qiu Y. Fractional carbon dioxide laser-assisted drug delivery of topical timolol solution for the treatment of deep infantile hemangioma: a pilot study. Pediatr Dermatol. 2014 May-Jun;31(3):286–91. https://doi.org/10.1111/pde.12299.

Received: 4 November 2019 | Accepted: 9 December 2019
DOI: 10.1111/dth.13184

ORIGINAL PAPER

DERMATOLOGIC THERAPY WILEY

An enhanced transcutaneous delivery of botulinum toxin for the treatment of Hailey–Hailey disease

Efrat Bar-Ilan[1] | Amir Koren[1] | Wasim Shehadeh[1] | Jacob Mashiah[1,2,3] | Eli Sprecher[1,2,3] | Ofir Artzi[1,2,4]

[1]Department of Dermatology and Venereology, Tel-Aviv Sourasky Medical Center, Tel-Aviv, Israel

[2]Pediatric Dermatology Unit, Dana Children's Hospital, Tel-Aviv Sourasky Medical Center, Tel-Aviv, Israel

[3]Sackler Faculty of Medicine, Tel-Aviv University, Tel-Aviv, Israel

[4]Dr. Artzi and Associates – Treatment and Research Center, Tel-Aviv, Israel

Correspondence
Ofir Artzi, Department of Dermatology, Tel Aviv Sourasky Medical Center, 6 Weizman Street, Tel Aviv 6423906, Israel.
Email: ofira@tlvmc.gov.il

Abstract

Successful treatment of Hailey–Hailey disease with intradermal botulinum toxin injections has been previously reported. The main disadvantages of this treatment are the excruciating pain and the risk of infections due to the numerous injections. We sought to evaluate the clinical effectiveness and safety profile of a novel approach using an energy-based device (Tixel, Novoxel, and Israel), followed by the topical application of botulinum toxin Type A for the treatment of Hailey–Hailey disease. A retrospective study of all cases of histologically diagnosed cases of Hailey-Hailey disease treated with Tixel device followed by topical application of botulinum toxin between 2018 and 2019 was performed. Epidemiologic, clinical, and treatment data, including effectiveness score and safety, were reviewed. The study included eight patients, of whom seven patients (87.5%) showed good or partial response. No systemic or local adverse effects were reported. There was no difference in effectivity between different body areas. Response to treatment ranged between patients with an average duration of 7.125 months after the second treatment. Tixel treatment followed by topical application of botulinum toxin can be considered in the treatment of Hailey–Hailey disease. This approach is less invasive, less painful, and yet effective as well as safe.

KEYWORDS

botulinum toxin, drug delivery, Hailey–Hailey disease

1 | INTRODUCTION

Hailey–Hailey disease or familial benign chronic pemphigus, first described in 1939 (Hailey & Hailey, 1939), is a rare chronic genetic blistering dermatosis, primarily involving the intertriginous areas, presenting with flaccid vesicles that can easily rapture, macerated fissured skin with chronic moist and vegetation (Burge, 1992), pain and malodor, significantly impairing patients' quality of life. The current treatment modalities comprise of corticosteroids, topical antimicrobials, oral antibiotics, laser ablation, photodynamic therapy, electron beam radiotherapy, dermabrasion, glycopyrrolate, afamelanotide, naltrexone, and botulinum toxin Type A (Campbell, McGrath, & Corry, 2018; Chiaravalloti & Payette, 2014; Farahnik et al., 2017; Kollman & Bass, 2018). Unfortunately, the disease is difficult to control and is recalcitrant to conventional therapies.

Treatment with botulinum toxin was first described in 2000 (Lapiere, Hirsh, Gordon, Cook, & Montalvo, 2000) with promising, several months lasting, results (Charlton, Stewart, & Rosen, 2018; Friedman, Koren, Niv, Mehrabi, & Artzi, 2019; Kothapalli & Caccetta, 2019). The main disadvantages of this treatment are the high cost of the toxin and the excruciating pain as well as the risk of infections due to the numerous needle punctures. Unfortunately, the skin barrier prevents the absorption of botulinum toxin while applied topically. Our case series study describes the clinical effectiveness and safety profile of a novel approach using an energy-based device (Tixel, Novoxel, and Israel) that thermally decomposes the stratum corneum,

followed by the topical application of botulinum toxin for the treatment for Hailey–Hailey disease.

2 | MATERIALS AND METHODS

This study was approved by an ethics committee and follows the tenets of the Declaration of Helsinki.

We performed a retrospective study of histologically diagnosed cases of Hailey–Hailey disease treated with Tixel device (parameters: exposure time 6–8 ms with 400–600 μm protrusion) followed by immediate topical application of botulinum toxin (125–250 units diluted with saline) and sonophoresis to enhance drug penetration using the Impact device (Alma lasers GmbH, Germany, parameters: Frequency 50 Hz, Intensity 50%, 5 min). This three steps treatment was preformed twice for each patient with 4–6 weeks intervals between the two treatments, bilaterally for the involved skin areas including axilla, groin, submammary and perianal areas. The patients were not treated with botulinum toxin 6 months prior to the treatment regimen. After each treatment, the patients applied topical cicalfate, and were instructed to avoid triggering factor including heat, sweating, and occlusive dressing. All patients signed a written consent form, after they were informed about the nature of the procedure and possible side effects. Epidemiological, clinical, treatment, and safety data were collected. Objective and subjective assessment was performed using the patient's global impression of change (PGIC) scale and the physician global assessment (PGA) scale. The treated area was photographed at baseline, before each treatment and 6–8 weeks after the two treatments. Two independent dermatologists retrospectively evaluated the patient's photographs. The PGA scale was graded on a scale of 0–7 with 0 being "no change or worsening" and 7 being "significant improvement." The PGIC was evaluated using a scale of 1–4, with 1 representing no remission, 2 representing partial remission, 3 representing nearly full, and 4 representing full remission. The last evaluating method used was the dermatology life quality index (DLQI). Histological changes of before (diagnostic biopsy) and 6–8 weeks following the two treatments were also evaluated in one patient.

3 | RESULTS

In total, eight patients (five males, three females; age range 32–57 years) with clinical presentation of Hailey–Hailey disease, confirmed histologically, were evaluated. The average disease duration was 16.875 years. The average weight and height were 70.5 and 170.2 respectively with the average body mass index (BMI) being 24.39. Patient's characteristics are shown in Table 1. Six patients received treatments for two body regions while the remaining two patients received the treatments for one involved area. The areas treated were axilla, groin, submammary, and perianal areas. Two (25%) patients achieved full remission, 4 (50%) showed a nearly full remission, one (12.5%) had a partial response and another one (12.5) did not response at all to the treatment. Thus seven patients (87.5%) had good or partial response to treatment. The baseline versus post-treatment representative clinical pictures of two patients and histology of one of the patients are shown in Figures 1 and 2, respectively. The average PGA scores 6–8 weeks after the final treatment were significantly improved compared with baseline. The average of the PGIC score was high with a mean of 5 in a scale of 0–7. The DLQI scores significantly improved with an average score of 22.75 before the treatments and an average score of 13.87, 6–8 weeks after the second treatment. Recurrence appeared up to 1 year with an average of 7.125 months after the second treatment. There was no difference in effectiveness between different body areas. Self-rated patients' satisfaction was high. No topical or systemic complications and

TABLE 1 Patients characteristics

#	Age	Sex	Weight	Height	FST	Family history	Disease duration	Areas involved	Past treatments
1	40	F	79	1,7	2	N	15	Axilla, groin, submamary, perianal	Topical: GBC
2	57	M	68	1,63	3	N	20	Groin, perianal	Topical: GBC, GPC, oral: Minocycline
3	59	M	69	1,8	2	Y	18	Axilla, groin, submamary, perianal	Topical: GBC, GPC, GBCC, oral: Minocycline
4	41	F	80	1,63	2	Y	25	Axilla, submamary	Topical: GBC
5	44	F	65	1,67	3	Y	12	Axilla, groin	Topical: Clobetasol propionate cream, betamethasone cream, tacrolimus ointment
6	32	M	66	1,78	3	N	15	Groin, perianal	Topical: GBC,GPC, GBCC, oral: Minocycline
7	45	M	78	1,69	3	Y	11	Axilla, groin, submamary	Topical: GBC, tacrolimus ointment, oral: Minocycline
8	37	M	59	1,72	2	Y	19	Axilla, submamary	Topical: GBC,GPC, oral: Minocycline
Average	44.375	–	70,5	170,2	2.5	–	16.875	–	–

Abbreviations: FST, fitzpatric skin type; GBC, gentamicin-betamethasone cream; GPC, gentamicin-prednisolone cream; GBCC, gentamicin-betamethasone-clotrimazole cream.

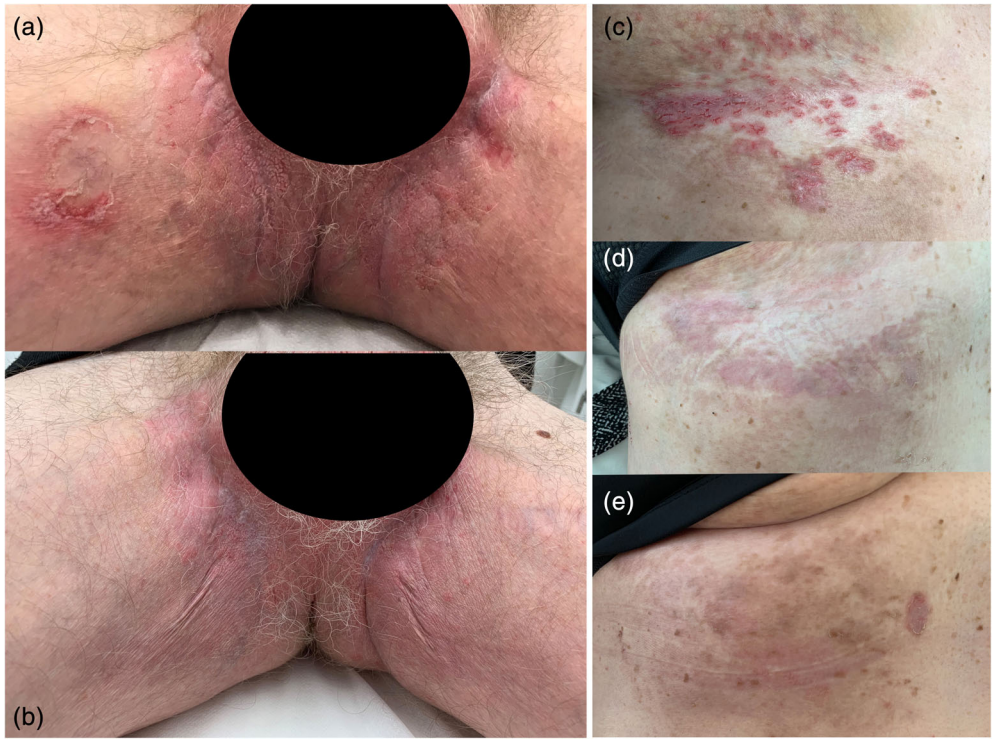

FIGURE 1 Representative before (a,c) and 1 month after (b,d) treatment photographs. Photograph "e" was taken 7 months post-last treatment

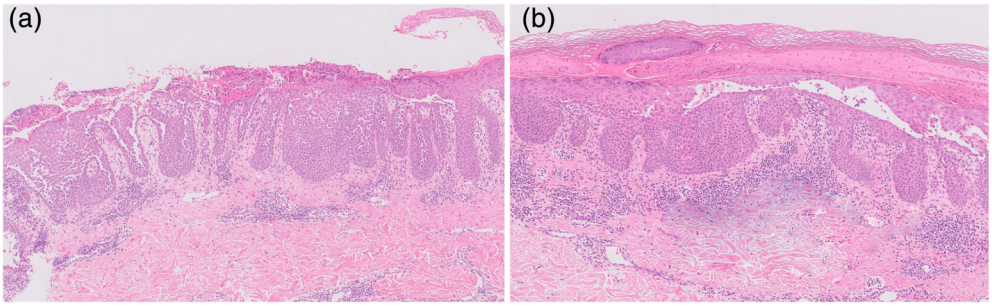

FIGURE 2 Histological comparison of before (a) and after (b) treatment. (a) Before: Skin showing intraepidermal acantholysis involving all the epidermal layers with surface erosion and a mild superficial perivascular lymphocytic infiltrate with scattered eosinophils. (b) After: Skin biopsy showing intraepidermal acantholysis in the mid stratum spinosum with regeneration of stratum spinosum, basal, and granular layers. Hyperkeratosis in basket wave pattern, subcorneal fibrin with scattered neutrophils, and parakeratotic cells. A denser (compared with baseline) superficial perivascular lymphocytic infiltrate present with numerous eosinophils

adverse effects were reported. Treatment characteristics and results are summarized in Tables 2 and 3, respectively.

4 | DISCUSSION

Hailey–Hailey disease is a chronic noncurable disease. Many treatment modalities were suggested in the past, however the disease is still recalcitrant to conventional therapy and significantly damage the quality of life of all patients. Since botulinum toxin decreases sweat production it is used for the treatment of hyperhidrosis (de Almeida & Montagner, 2014; Glaser & Galperin, 2014). This effect and the subsequent decrease of microorganism colonization might serve as one explanation for its efficacy in the treatment of Hailey–Hailey disease (Benohanian, 2005). Botulinum toxin cannot cross the stratum corneum, therefore, its injection is required for both the treatment of hyperhidrosis (de Almeida & Montagner, 2014; Glaser & Galperin, 2014) and for the treatment of Hailey–Hailey disease (Charlton et al., 2018; Friedman et al., 2019; Kothapalli & Caccetta, 2019; Lapiere et al., 2000). It is an effective treatment but a painful, expensive, and the duration effects is for several months only.

This led us to try a novel approach of enhanced transcutaneous delivery. Tixel is a novel nonlaser thermo-mechanical system (Tixel, Novoxel, and Israel), that is, a registered medical device in several countries worldwide. The mechanism of action is by evaporation and thermal decomposition of stratum corneum and the dehydration of epidermis (Elman, Fournier, Barneon, Bernstein, & Lask, 2015). These effects allow the penetration of topically applied Botulinum toxin into

TABLE 2 Treatments characteristics

#	No of treated areas	Treated area	Number of treatments	Tixel parameters	Dysport U/unit-1	Dysport U/unit-2	Dilution
1	2	Axilla, groin	2	6–8/400–500	250	125	500/6
2	2	Groin, perianal	2	6–8/400–501	250	250	500/6
3	2	Groin, submamary	2	6–8/400–502	250	250	500/6
4	2	Axilla, submamary	2	6–8/400–503	250	125	500/6
5	1	Axilla	2	6–8/400–504	250	250	500/6
6	1	Groin	2	6–8/400–505	250	250	500/6
7	2	Axilla, submamary	2	6–8/400–506	250	250	500/6
8	2	Axilla, submamary	2	6–8/400–507	250	125	500/6

TABLE 3 Results

#	PGICS	DLQI-base	DLQI-1.5 month	Delta-DLQI	PGA1	PGA2	PGA-Ave	VAS	Satisfaction	Remission (months)	Duration (months)
1	5	23	14	9	1	1	1	2	3	3	10
2	6	21	11	10	2	2	2	3	4	3	6
3	5	24	19	5	1	1	1	2	2	2	6
4	5	22	12	10	2	1	2	2	3	3	6
5	6	18	11	7	1	1	1	3	3	3	4
6	5	23	9	14	1	2	2	3	3	4	12
7	3	25	22	3	3	3	3	2	1	1	2
8	5	26	13	13	2	1	2	3	3	4	11
Average	5	2,275	13,875	8,875	1,625	1,5	1.75	2,5	2.75	2.875	7.125

Abbreviations: DLQI, dermatology life quality index; PGA, physician global assessment; PGA-Ave, physician global assessment average; PGICS, patient's global impression of change scale; VAS, visual analogue scale.

the skin through the stratum corneum. This system has already been demonstrated to significantly increase the permeability of a couple of topically applied medications including, lidocaine (Sintov & Brandys-Sitton, 2006) and as proved by Friedman et al. also Botulinium toxin (which was used in severe cases of rosacea; Friedman et al., 2019).

Our case series shows promising results with high satisfaction rate, high degree of symptoms resolution, lasting effect of up to 1 year (with an average duration of 7 months), and without any topical or systemic side effect. Out of the eight patients, one patient did not respond as well as the others. It was not clear what was the reason for the treatment failure. This 45 years old male patient received treatments for two body area: the axilla and the submammary area, as did other patients who responded well to the treatment. He had a BMI of 27.4 (a bit higher than the average), and disease duration was 11 years (less than the 16.7 years average).

The limitations of this case series are its nature—an uncontrolled retrospective study with a small study group and no control for comparison. Additional double blind, placebo controlled, comparative prospective studied with bigger cohorts, are required in order to strengthen our observation of the efficiency of enhanced transcutaneous botulinum toxin delivery for Hailey–Hailey disease.

In conclusion, Tixel treatment followed by the topical application of botulinum toxin showed good results in the treatment of Hailey–Hailey disease. This safe approach is an effective, long lasting, less invasive, and less painful additional tool in treating patients with Hailey–Hailey disease.

CONFLICT OF INTEREST

The authors declare no potential conflict of interest.

ORCID

Amir Koren https://orcid.org/0000-0001-8667-9330
Jacob Mashiah https://orcid.org/0000-0002-9417-2932
Ofir Artzi https://orcid.org/0000-0003-1391-5843

REFERENCES

Benohanian, A. (2005). The place of botulinum toxin type A in the treatment of focal hyperhidrosis. *The British Journal of Dermatology*, *153*, 460–461.
Burge, M. (1992). Hailey-Hailey disease: The clinical features, response to treatment and prognosis. *The British Journal of Dermatology*, *126*, 275–282.
Campbell, V., McGrath, C., & Corry, A. (2018). Low-dose naltrexone: A novel treatment for Hailey-Hailey disease. *The British Journal of Dermatology*, *178*(5), 1196–1198.

Charlton, O. A., Stewart, T. J., & Rosen, R. H. (2018). Treatment of Hailey-Hailey disease with botulinum toxin. *The Australasian Journal of Dermatology*, *59*(3), 229–231.

Chiaravalloti, A., & Payette, M. (2014). Hailey-Hailey disease and review of management. *Journal of Drugs in Dermatology*, *13*(10), 1254–1257.

de Almeida, A. R., & Montagner, S. (2014). Botulinum toxin for axillary hyperhidrosis. *Dermatologic Clinics*, *32*(4), 495–504.

Elman, M., Fournier, N., Barneon, G., Bernstein, E. F., & Lask, G. (2015). Fractional treatment of aging skin with tixel, am clinical and histological evaluation. *Journal of Cosmetic Therapy*, *18*(1), 31–37.

Farahnik, B., Blattner, C. M., Mortazie, M. B., Perry, B. M., Lear, W., & Elston, D. M. (2017). Interventional treatments for Hailey-Hailey disease. *J Am Acad Dermatol*, *76*(3), 551–558.e3.

Friedman, O., Koren, A., Niv, R., Mehrabi, J. N., & Artzi, O. (2019). The toxic edge: A novel treatment for refractory erythema and flushing of rosacea. *Lasers in Surgery and Medicine*, *51*(4), 325–331.

Glaser, D. A., & Galperin, T. A. (2014). Botulinum toxin for hyperhidrosis of areas other than the axillae and palms/soles. *Dermatologic Clinics*, *32*(4), 517–525.

Hailey, H., & Hailey, H. (1939). Familial benign chronic pemphigus. *Archives of Dermatology*, *39*, 679–685.

Kollman, N., & Bass, J. (2018). Generalized familial benign chronic pemphigus (Hailey-Hailey disease) treated successfully with low-dose naltrexone. *JAAD Case Rep*, *4*(7), 725–727.

Kothapalli, A., & Caccetta, T. (2019). Botulinum toxin type A for the first-line treatment of Hailey-Hailey disease. *The Australasian Journal of Dermatology*, *60*(1), 73–74.

Lapiere, J. C., Hirsh, A., Gordon, K. B., Cook, B., & Montalvo, A. (2000). Botulinum toxin type a for the treatment of axillary Hailey-Hailey disease. *Dermatologic Surgery*, *26*(4), 371–374.

Sintov, A. C., & Brandys-Sitton, R. (2006). Facilitated skin penetration of lidocaine: Combination of a short-term iontophoresis and microemulsion formulation. *International Journal of Pharmaceutics*, *316*, 58–67.

How to cite this article: Bar-Ilan E, Koren A, Shehadeh W, Mashiah J, Sprecher E, Artzi O. An enhanced transcutaneous delivery of botulinum toxin for the treatment of Hailey–Hailey disease. *Dermatologic Therapy*. 2020;33:e13184. https://doi.org/10.1111/dth.13184

Received: 23 March 2019 | Revised: 9 November 2019 | Accepted: 18 November 2019

DOI: 10.1111/dth.13172

DERMATOLOGIC THERAPY WILEY

ORIGINAL PAPER

Treatment of port wine stain with Tixel-induced rapamycin delivery following pulsed dye laser application

Ofir Artzi[1,2] | Joseph N. Mehrabi[3] | Lee Heyman[3] | Or Friedman[4] | Jacob Mashiah[2,3,5]

[1]Artzi Treatment and Research Center, Tel Aviv, Israel

[2]Department of Dermatology, Tel Aviv Sourasky Medical Center, Tel Aviv, Israel

[3]Sackler Faculty of Medicine, Tel Aviv University, Tel Aviv, Israel

[4]Plastic Reconstructive Surgery Department, Tel Aviv Sourasky Medical Center, Tel Aviv, Israel

[5]Pediatric Dermatology Clinic, Dana-Dwek Children's Hospital, Tel Aviv Sourasky Medical Center, Tel Aviv, Israel

Correspondence
Ofir Artzi, Department of Dermatology, Tel Aviv Medical Center, 6 Weizman Street, Tel Aviv 6423906, Israel.
Email: ofira@tlvmc.gov.il

Abstract

Although pulsed dye laser (PDL) is considered the gold standard treatment for port wine stains (PWS), post PDL revascularization is one of the main causes of incomplete regression and recurrence. Recently, topical sirolimus have been shown to improve treatment outcome probably through minimizing post-laser revascularization. We sought to evaluate the added value of the Tixel drug delivery system (DDS) to the PDL and topical rapamycin treatment for PWS. This case series includes three teenager patients with previously treated PWS with PDL. Upon enrollment, every stain was divided into A and B halves for treatment assignments to the following regimens: (A) PDL + DDS + rapamycin; (B) PDL + rapamycin. Subjects were instructed to apply rapamycin topically over the PWS twice daily for the entire treatment period. Assessment of the treatment and adverse reactions as well as photographs was performed at baseline and before every PDL treatment. There were clinically significant differences in blanching responses favoring PWS receiving PDL + DDS + rapamycin as compared to PDL + rapamycin alone. Transient hyperpigmentation was noted in one patient. Two patients developed mild transient irritation and dermatitis following the treatment on both halves. The use of drug delivery system combined with topical rapamycin has no remarkable adverse effects, improves the results of PDL treatment for port wine stains, and can reduce the total number of required PDL sessions.

KEYWORDS

drug delivery, port wine stain, pulsed dye laser, rapamycin, Tixel

1 | INTRODUCTION

Port wine stains (PWS) are congenital cutaneous vascular malformations, affecting approximately 0.3% of newborns, occurring as an isolated vascular malformation, or in association with capillary malformation syndromes (Kalick, Goldwyn, & Noe, 1981). They do not regress with age and in some cases may enlarge, darken, and develop thickening and hypertrophy of the surrounding soft tissue (Kalick et al., 1981; Lanigan, 1998; Nelson, Jia, Phung, & Mihm, 2011). Pulsed dye laser (PDL) remains the gold standard treatment of PWS (Griffin, Foshee, Finney, & Saedi, 2016). While it is very effective at producing initial lightening of PWS lesions, post PDL revascularization contributes to frequent recurrence and treatment failure. Resolution of PWS, as defined by persistent blanching of the lesion, is reported in less than 10–20% of cases. The revascularization is postulated to occur through post-laser angiogenesis via the induction of hypoxia inducible factor-1a (HIF-1a) and VEGF pathways (Anderson & Parrish, 1983; Chowdhury, Harris, & Lanigan, 2001; Frohm Nilsson, Passian, & Wiegleb Edstrom, 2010; Goldman, Fitzpatrick, & Ruiz-Esparza, 1993; Sajan et al., 2013; Scherer, Lorenz, Wimmershoff, Landthaler, & Hohenleutner, 2001; Tan et al., 1986; van der Horst, Koster, de Borgie, Bossuyt, & van Gemert, 1998). Sirolimus (rapamycin), a

specific inhibitor of mammalian target of rapamycin, can inhibit the neo-angiogenesis that is activated after the damage caused by PDL. Several studies reported an increased and persistent effectiveness of PDL in patients with PWS treated with oral rapamycin (Nelson et al., 2011; Tremaine et al., 2012). The application of topical 0.5–1% rapamycin preparations combined with PDL treatment has shown contradicting results probably in part due to low drug bioavailability while applied topically (Griffin et al., 2016). The Tixel technology is a painless, non-laser novel thermal resurfacing system which was demonstrated to significantly increase skin permeability thus enhancing drug delivery (Sintov & Hofmann, 2016).

We report our experience of applying rapamycin using this drug delivery system before and following PDL treatment in three patients with PWS.

2 | METHODS

This is a retrospective case series of three patients, who presented with one or more large flat port wine stains, which had gone previously through 8–12 PDL treatments, performed by different physicians, with the usually used parameters of spot size of 7 or 10 mm, pulse duration of 0.45 or 1.5 ms, and fluence of 8.5–10 J/cm^2 with insufficient improvement according to the patients and their parents, as well as the opinion of four dermatologists. Information regarding demographics and previous treatment is shown in Table 1.

Each stain was divided into two halves, A and B. The facial PWS was largely within the V3 dermatome, which is known to respond more favorably than V2, therefore no specific division of PWS was warranted (Renfro & Geronemus, 1993). The stains were cleansed with aqueous chlorhexidine solution and then treated with 595 nm PDL (Cynergy, Cynosure Inc., Westford, MA) without topical anesthesia every 4–6 weeks with the following parameters: spot size of 7 or 10 mm, pulse duration of 0.45 or 1.5 ms, and fluence of 8.5–10 J/cm^2. Tixel (Novoxel, Israel) treatment was performed, separately, once every 2 weeks, 2–14 days apart from the PDL treatment, as long as PDL treatment was performed, on half A of every stain with the following parameters: exposure time, which is the time the tip is in contact with the skin, of 6 ms, and protrusion, which is the distance the tip travels into the skin of 400 μm. Rapamycin 0.2% cream was applied on the entire stain twice daily and immediately following each DDS procedure. The patients were instructed to apply cool compresses during the first post PDL treatment day. During the study, the patients were advised to avoid sun exposure and use topical sun protection (SPF > 30). All three patients received a total of 2–3 PDL (halves A+B) and 7–9 DDS (only half A) treatments. Treatment characteristics are shown in Table 1.

TABLE 1 Subject demographics and clinical characteristics

Patient no	1	2	3
Sex	F	M	F
Age	12	16	10
PWS distribution	Left arm	Face	Face
Fitzpatrick skin type	3	2	2
No of previous PDL treatments	9	12	8
Age at the last previous treatment (year)	2	3	2
No of new PDL treatments	2	3	2
No of Tixel treatments	6	9	7

Clinical examination and photographic documentation were performed at baseline, before each PDL treatment, and 4 weeks after the last PDL treatment. Clinical photographs were taken with a digital camera under standardized lighting conditions and patient positioning (For non-facial stains: Canon EOD 70D, 100 mm Macro objective and flash-Canon Macro 100 mm, for facial stains – Visia, Canfield).

Four blinded dermatologists evaluated Half A (PDL-DDS-rapamycin regimen [PTR]) versus Half B (PDL-rapamycin regimen [PR]) by the pictures of each PWS taken 4 weeks after the last PDL treatment, using a 5-point scale based on clearance or lightening of each half compared to baseline photographs: excellent (>75%, score 5), good (51–75%, score 4), fair (25–50%, score 3), bad (<25%, score 2), or no clearance (score 1). The patients and their parents were asked to evaluate separately the improvement of both halves, 4 weeks after the last PDL treatment, using the same scale and to rate their satisfaction from regimen A versus B (0 = not satisfied, 1 = slightly satisfied, 2 = satisfied, 3 = very satisfied), and the scores were averaged. The patients' tolerance of regimen A versus B was evaluated on a scale of 1 to 4 (1 = poor and 4 = excellent). All side effects (blistering, erosions, purpura, dermatitis, crusting, hypopigmentation, hyperpigmentation, atrophy, hypertrophic or keloids scar, infection) in both halves were documented.

2.1 | The Tixel device

The Tixel (Novoxel, Israel) is a non-laser thermomechanical system which dehydrates the stratum corneum and enhances drug delivery. The system consists of a titanium tip heated to 400°C moving toward the skin to achieve short term contact with the treated tissue. In transdermal mode settings, the primary thermal effect is dehydration of the stratum corneum with a very limited thermal effect on the viable epidermis and dermis. The stratum corneum becomes brittle leading to layer breakage when the tip is progressed toward the treated tissue. Gentle elimination of the stratum corneum and desiccation of the epidermis establishes a concentration gradient by Fick's law, enhancing drug delivery (Lask, Elman, Fournier, & Slatkine, 2012). It has been previously shown to enhance the delivery of several medications (e.g., verapamil, vitamin C, and sodium diclofenac) (Sintov & Hofmann, 2016).

3 | RESULTS

The physicians' and patients' comparison of baseline versus pre third (patient 1 + 3) or fourth (patient 2) PDL treatment photos

demonstrated higher clearance of the PTR regimen halves compared to the PR regimen halves, which is demonstrated in Table 2. Figures 1 and 2 visually highlights the difference between the responses to treatment between half A (PTR) and half B (PR) based on the evaluating physicians and patients observations. The patients were more satisfied with the overall outcome of the PTR-treated side compared to the PR-treated side. The tolerance was nearly the same for both halves. Additional adverse effects in the DDS treated side were not observed, however, transient hyperpigmentation was noted in patient 1, in both sides. Two out of the three patients developed local reaction on both treated sides resulting in erythema, irritation, and crusting. These symptoms resolved completely within 2 weeks after topical rapamycin was withdrawn in addition to topical steroid application.

4 | DISCUSSION

Port wine stain (PWS) can have a substantial effect on the quality of life of the patients and their families (Kalick et al., 1981). Although PDL has become the treatment of choice for PWS birthmarks, only 10–20% of patients obtain full clearance of their PWS even after many PDL treatments (Anderson & Parrish, 1983; Goldman et al., 1993; Griffin et al., 2016; Lanigan, 1998; Sajan et al., 2013; Scherer et al., 2001; Tan et al., 1986; van der Horst et al., 1998). In the attempt to maximize treatment efficiency, the use of other technologies has been evaluated in many trials; 532 nm potassium titanyl phosphate laser (KTP) (Alster & Tanzi, 2009; Chen et al., 2012; Chowdhury et al., 2001; Frohm Nilsson et al., 2010; Pence, Aybey, & Ergenekon, 2005; Yang et al., 2005), long-pulsed 1064 nm neodymium:yttrium-aluminum-garnet (Nd:YAG) laser, alexandrite laser-755 nm (Carlsen et al., 2017; Izikson, Nelson, & Anderson, 2009) and the IPL (intense pulsed light) in a range of 500-1200 nm (Babilas et al., 2010; Faurschou, Togsverd-Bo, Zachariae, & Haedersdal, 2009; Savas, Ledon, Franca, Chacon, & Nouri, 2013). Other studies suggest the therapeutic effects of photodynamic therapy (PDT) or fractional ablative lasers alone or combined with PDL for synergistic effects (Chen et al., 2012; Frohm Nilsson et al., 2010; Kelly et al., 2004; Peters et al., 2012; Rajaratnam, Laughlin, & Dudley, 2011; Savas et al., 2013).

TABLE 2 Physician/patient evaluations

	Ph1		Ph2		Ph3		Ph4		Ph-Ave		Pa-Rat		Pa-Sat		Pa-Tol	
Half	A	B	A	B	A	B	A	B	A	B	A	B	A	B	A	B
Patient 1	4	3	4	2	4	3	4	2	4	2.5	4	2	3	1	2	2
Patient 2	5	3	5	3	4	2	4	2	4.5	2.5	4	2	3	1	2	3
Patient 3	4	2	4	2	3	2	4	1	3.75	1.75	3	2	2	1	2	2

Abbreviations: Pa-Rat, patient rating; Pa-Sat, patient satisfaction; Pa-Tol, patient tolerance; Ph#, physician number; Ph-Ave, average of physician ratings.

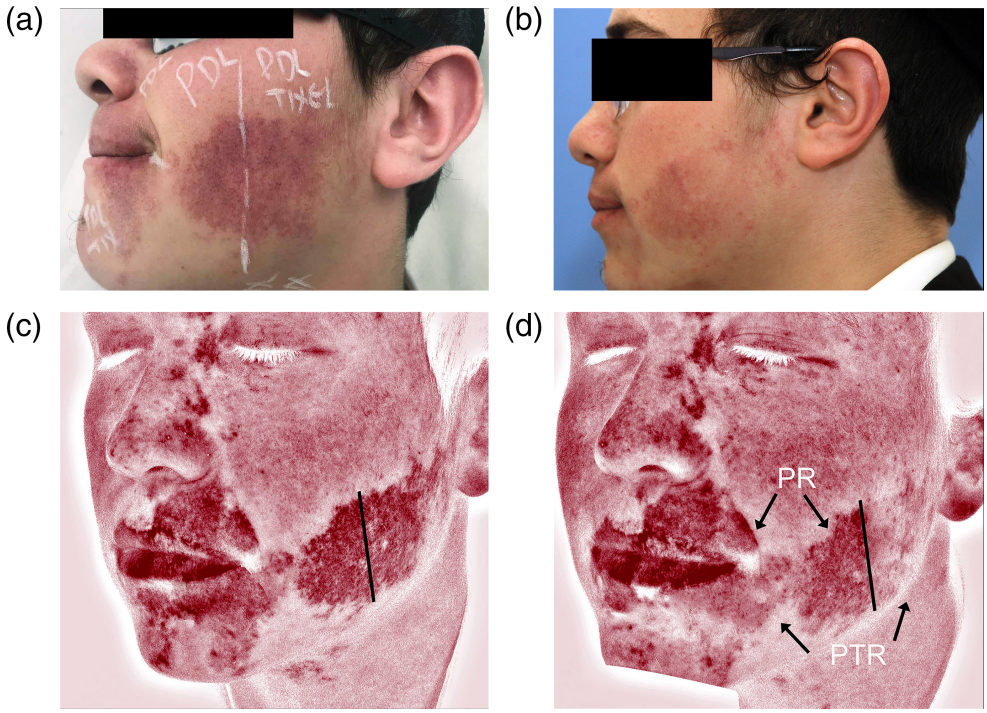

FIGURE 1 A 16-year-old male (patient 2) with Fitzpatrick skin type II who underwent treatment of a PWS on the left side of the face at baseline (a) and after treatment (b). Visualization with Visia (Canfield) at baseline (c) and after treatment (d) emphasizes the change in pigmentation in half A of the PWS

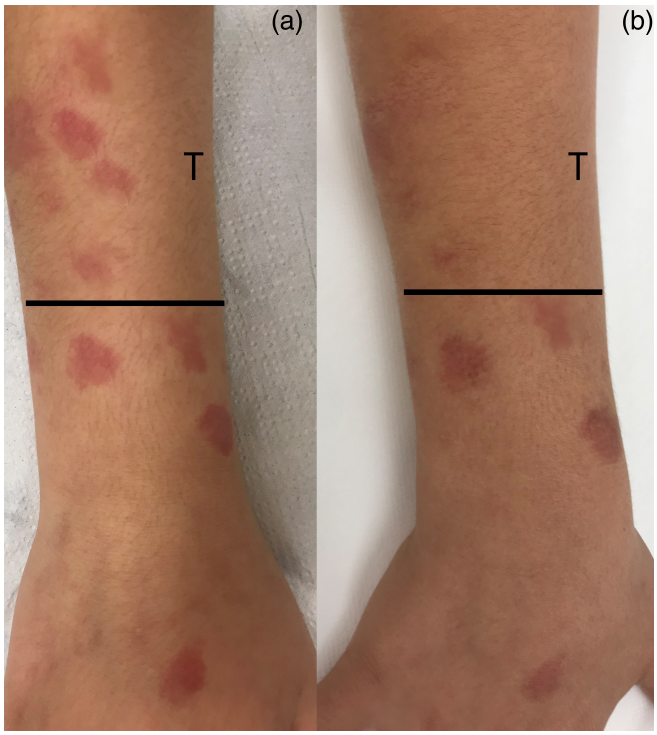

FIGURE 2 A 12-year-old male (patient 1) with Fitzpatrick skin type III who underwent treatment of a PWS on the left arm at baseline (a) and after treatment (b)

Additional approaches to increase efficacy is inhibition of post laser angiogenesis. Due to neo-angiogenesis evoked by the wound healing response to the laser therapy, blood flow is restored, and the treated lesions regain their pre-treatment morphology resulting in treatment failure. The use of anti-angiogenic drugs like imiquimod, axitinib, and rapamycin was advocated in several studies to overcome this neo-angiogenesis (Gao et al., 2014; Phung et al., 2008; Tremaine et al., 2012).

Rapamycin (RPM), a macrolide antibiotic used as an immunosuppressant medication, is a selective inhibitor of the mammalian target of rapamycin (mTOR). Through mTOR inhibition, RPM blocks hypoxia-induced angiogenesis. Histological evaluation and stem-cell proliferation markers quantification in skin treated with topical RPM after laser therapy exhibited considerably reduced vascular regeneration compared to PDL therapy alone (Gao et al., 2014; Kelly et al., 2004; Phung et al., 2008). The use of topical formulation should be considered for two primary reasons: to increase drug delivery to the site of presumed angiogenesis and to limit systemic absorption and subsequent side-effects from a well-known immunosuppressive medication. The limited effect of rapamycin can be related to its solubility properties and/or to low effective penetration (Gao et al., 2014, 2015).

Herein, we describe the combined use of PDL to induce PWS blood vessel injury, rapamycin to prevent PWS blood vessel reformation and recanalization after laser therapy, and Tixel as a drug delivery enhancing system. In all patients, the stain halves that underwent this combined approach demonstrated better clearance without any higher rate of adverse effects. The use of a different type of DDS did not yield similar effect as the Tixel in our report. Greveling et al. compared PDL-only treatment to PDL + rapamycin, PDL + Erbium YAG laser ablation without thermal of the stratum corneum + rapamycin, and rapamycin monotherapy, and reported that the highest percentage clearance was achieved with PDL-only treatment, but there were no statistically significant differences between treatments (Greveling, Prens, & van Doorn, 2017).

All three patients reported erythema and irritation at the site of application, on both sides. In previous published clinical trials topical rapamycin was generally well tolerated with a favorable adverse effect profile, beside minor reaction occurring at or near the application site, comprising mainly of mild discomfort or pain, pruritus, erythema, and irritation, rarely causing the cessation of the treatment (Greveling, Kunkeler, Prens, & van Doorn, 2016; Koenig et al., 2018; Wataya-Kaneda et al., 2017). Since topical application of rapamycin ointment was found to ameliorate induced atopic dermatitis in NC/Nga mice clinically and histologically through reduction in inflammatory cell infiltration in the dermis and alleviation of the increased serum IgE levels, the application site described side effects of topical rapamycin can be attributed mainly to the compound vehicle rather than to the rapamycin itself (Yang et al., 2014).

Limitations of our study include the small sample size as well as the comparatively advanced age-range of our sample population, the possible different response to treatment in various anatomical distribution and in flat versus hypertrophic PWS. The improved drug delivery could augment systemic absorption and thus merits consideration of rapamycin blood level. In a previous study topical application of up to 0.2%, sirolimus gel led to the detection of low blood levels of sirolimus (<0.25 ng/ml), with no abnormalities in the blood biochemical or urine tests, while in other reports there was no measurable systemic absorption although the applied rapamaycin concentrations reached 1%. In light of the superior short term effect of this new treatment modality longer follow up period is needed to confirm the long-term efficacy of the treatment. Further studies should be performed to explore the possibility of performing same-day procedure of first PDL treatment followed by Tixel then immediate application of rapamycin to evaluate potential synergistic effect of performing both PDL and DDS-rapamycin on the same day.

We have used the Tixel as drug delivery system because of its previously explained advantages, yet it is only now that is getting popularity. Therefore other drug delivery systems can be used as well.

In conclusion, our study suggests that the use of drug delivery system and topical rapamycin has no remarkable adverse effects, and the addition of Tixel allowed for improved response of PDL and topical rapamycin for port wine stains, that may be related to increased penetration of rapamycin.

CONFLICT OF INTEREST

There is no conflict of interest for all authors

ORCID

Jacob Mashiah https://orcid.org/0000-0002-9417-2932

REFERENCES

Alster, T. S., & Tanzi, E. L. (2009). Combined 595-nm and 1,064-nm laser irradiation of recalcitrant and hypertrophic port-wine stains in children and adults. *Dermatologic Surgery*, *35*, 914–918 discussion 8-9.

Anderson, R. R., & Parrish, J. A. (1983). Selective photothermolysis: Precise microsurgery by selective absorption of pulsed radiation. *Science (New York, N.Y.)*, *220*, 524–527.

Babilas, P., Schreml, S., Eames, T., Hohenleutner, U., Szeimies, R. M., & Landthaler, M. (2010). Split-face comparison of intense pulsed light with short- and long-pulsed dye lasers for the treatment of port-wine stains. *Lasers in Surgery and Medicine*, *42*, 720–727.

Carlsen, B. C., Wenande, E., Erlendsson, A. M., Faurschou, A., Dierickx, C., & Haedersdal, M. (2017). A randomized side-by-side study comparing alexandrite laser at different pulse durations for port wine stains. *Lasers in Surgery and Medicine*, *49*(1), 97–103.

Chen, J. K., Ghasri, P., Aguilar, G., van Drooge, A. M., Wolkerstorfer, A., Kelly, K. M., & Heger, M. (2012). An overview of clinical and experimental treatment modalities for port wine stains. *Journal of American Academy Dermatology*, *67*, 289–304.

Chowdhury, M. M., Harris, S., & Lanigan, S. W. (2001). Potassium titanyl phosphate laser treatment of resistant port-wine stains. *The British Journal of Dermatology*, *144*, 814–817.

Faurschou, A., Togsverd-Bo, K., Zachariae, C., & Haedersdal, M. (2009). Pulsed dye laser vs. intense pulsed light for port-wine stains: A randomized side-by-side trial with blinded response evaluation. *The British Journal of Dermatology*, *160*, 359–364.

Frohm Nilsson, M., Passian, S., & Wiegleb Edstrom, D. (2010). Comparison of two dye lasers in the treatment of port-wine stains. *Clincal and Experimental Dermatolgy*, *35*, 126–130.

Gao, L., Nadora, D. M., Phan, S., Chernova, M., Sun, V., Preciado, S. M., … Tan, W. (2015). Topical axitinib suppresses angiogenesis pathways induced by pulsed dye laser. *The British Journal of Dermatology*, *172*, 669–676.

Gao, L., Phan, S., Nadora, D. M., Chernova, M., Sun, V., Preciado, S. M., … Tan, W. (2014). Topical rapamycin systematically suppresses the early stages of pulsed dye laser-induced angiogenesis pathways. *Lasers in Surgery and Medicine*, *46*, 679–688.

Goldman, M. P., Fitzpatrick, R. E., & Ruiz-Esparza, J. (1993). Treatment of port-wine stains (capillary malformation) with the flashlamp-pumped pulsed dye laser. *The Journal of Pediatrics*, *122*, 71–77.

Greveling, K., Kunkeler, A. C., Prens, E. P., & van Doorn, M. B. (2016). Allergic contact dermatitis caused by topical sirolimus used as an adjuvant for laser treatment of port wine stains. *Contact Dermatitis*, *75*, 184–185.

Greveling, K., Prens, E. P., & van Doorn, M. B. (2017). Treatment of port wine stains using pulsed dye laser, erbium YAG laser, and topical rapamycin (sirolimus)-a randomized controlled trial. *Lasers in Surgery and Medicine*, *49*, 104–109.

Griffin, T. D., Jr., Foshee, J. P., Finney, R., & Saedi, N. (2016). Port wine stain treated with a combination of pulsed dye laser and topical rapamycin ointment. *Lasers in Surgery and Medicine*, *48*, 193–196.

Izikson, L., Nelson, J. S., & Anderson, R. R. (2009). Treatment of hypertrophic and resistant port wine stains with a 755 nm laser: A case series of 20 patients. *Lasers in Surgery and Medicine*, *41*, 427–432.

Kalick, S. M., Goldwyn, R. M., & Noe, J. M. (1981). Social issues and body image concerns of port wine stain patients undergoing laser therapy. *Lasers in Surgery and Medicine*, *1*, 205–213.

Kelly, K. M., Kimel, S., Smith, T., Stacy, A., Hammer-Wilson, M. J., Svaasand, L. O., & Nelson, J. S. (2004). Combined photodynamic and photothermal induced injury enhances damage to in vivo model blood vessels. *Lasers in Surgery and Medicine*, *34*, 407–413.

Koenig, M. K., Bell, C. S., Hebert, A. A., Roberson, J., Samuels, J. A., Slopis, J. M., … TREATMENT Trial Collaborators. (2018). Efficacy and safety of topical rapamycin in patients with facial angiofibromas secondary to tuberous sclerosis complex: The TREATMENT randomized clinical trial. *JAMA Dermatology*, *154*, 773–780.

Lanigan, S. W. (1998). Port-wine stains unresponsive to pulsed dye laser: Explanations and solutions. *The British Journal of Dermatology*, *139*, 173–177.

Lask, G., Elman, M., Fournier, N., & Slatkine, M. (2012). Fractional vaporization of tissue with an oscillatory array of high temperature rods – Part I: ex vivo study. *Journal of Cosmetic and Laser Therapy*, *14*, 218–223.

Nelson, J. S., Jia, W., Phung, T. L., & Mihm, M. C., Jr. (2011). Observations on enhanced port wine stain blanching induced by combined pulsed dye laser and rapamycin administration. *Lasers in Surgery and Medicine*, *4310*, 939–942.

Pence, B., Aybey, B., & Ergenekon, G. (2005). Outcomes of 532 nm frequency-doubled Nd:YAG laser use in the treatment of port-wine stains. *Dermatologic Surgery*, *31*, 509–517.

Peters, M. A., van Drooge, A. M., Wolkerstorfer, A., van Gemert, M. J., van der Veen, J. P., Bos, J. D., & Beek, J. F. (2012). Double pass 595 nm pulsed dye laser at a 6 minute interval for the treatment of port-wine stains is not more effective than single pass. *Lasers in Surgery and Medicine*, *44*, 199–204.

Phung, T. L., Oble, D. A., Jia, W., Benjamin, L. E., Mihm, M. C., Jr., & Nelson, J. S. (2008). Can the wound healing response of human skin be modulated after laser treatment and the effects of exposure extended? Implications on the combined use of the pulsed dye laser and a topical angiogenesis inhibitor for treatment of port wine stain birthmarks. *Lasers in Surgery and Medicine*, *40*, 1–5.

Rajaratnam, R., Laughlin, S. A., & Dudley, D. (2011). Pulsed dye laser double-pass treatment of patients with resistant capillary malformations. *Lasers in Surgery and Medicine*, *26*, 487–492.

Renfro, L., & Geronemus, R. G. (1993). Anatomical differences of port-wine stains in response to treatment with the pulsed dye laser. *Archives of Dermatology*, *129*, 182–188.

Sajan, J. A., Tibesar, R., Jabbour, N., Lander, T., Hilger, P., & Sidman, J. (2013). Assessment of pulsed-dye laser therapy for pediatric cutaneous vascular anomalies. *JAMA Facial Plastic Surgery*, *15*, 434–438.

Savas, J. A., Ledon, J. A., Franca, K., Chacon, A., & Nouri, K. (2013). Pulsed dye laser-resistant port-wine stains: Mechanisms of resistance and implications for treatment. *The British Journal of Dermatology*, *168*, 941–953.

Scherer, K., Lorenz, S., Wimmershoff, M., Landthaler, M., & Hohenleutner, U. (2001). Both the flashlamp-pumped dye laser and the long-pulsed tunable dye laser can improve results in port-wine stain therapy. *The British Journal of Dermatology*, *145*, 79–84.

Sintov, A. C., & Hofmann, M. A. (2016). A novel thermo-mechanical system enhanced transdermal delivery of hydrophilic active agents by fractional ablation. *International Journal of Pharmaceutics*, *511*, 821–830.

Tan, O. T., Carney, J. M., Margolis, R., Seki, Y., Boll, J., Anderson, R. R., & Parrish, J. A. (1986). Histologic responses of port-wine stains treated by argon, carbon dioxide, and tunable dye lasers. A preliminary report. *Archives of Dermatology*, *122*, 1016–1022.

Tremaine, A. M., Armstrong, J., Huang, Y. C., Elkeeb, L., Ortiz, A., Harris, R., … Kelly, K. M. (2012). Enhanced port-wine stain lightening achieved with combined treatment of selective photothermolysis and imiquimod. *Journal of American Academy Dermatology*, *66*, 634–641.

van der Horst, C. M., Koster, P. H., de Borgie, C. A., Bossuyt, P. M., & van Gemert, M. J. (1998). Effect of the timing of treatment of port-wine stains with the flash-lamp-pumped pulsed-dye laser. *The New England Journal of Medicine*, *338*, 1028–1033.

Wataya-Kaneda, M., Nakamura, A., Tanaka, M., Hayashi, M., Matsumoto, S., Yamamoto, K., & Katayama, I. (2017). Efficacy and safety of topical sirolimus therapy for facial angiofibromas in the tuberous sclerosis complex: A randomized clinical trial. *JAMA Dermatology*, *153*, 39–48.

Yang, F., Tanaka, M., Wataya-Kaneda, M., Yang, L., Nakamura, A., Matsumoto, S., … Katayama, I. (2014). Topical application of rapamycin ointment ameliorates Dermatophagoides farina body extract-induced atopic dermatitis in NC/Nga mice. *Experimental Dermatology*, *23*, 568–572.

Yang, M. U., Yaroslavsky, A. N., Farinelli, W. A., Flotte, T. J., Rius-Diaz, F., Tsao, S. S., & Anderson, R. R. (2005). Long-pulsed neodymium:yttrium-aluminum-garnet laser treatment for port-wine stains. *Journal of American Academy Dermatology*, *52*(3 Pt 1), 480–490.

How to cite this article: Artzi O, Mehrabi JN, Heyman L, Friedman O, Mashiah J. Treatment of port wine stain with Tixel-induced rapamycin delivery following pulsed dye laser application. *Dermatologic Therapy*. 2020;33:e13172. https://doi.org/10.1111/dth.13172

JOURNAL OF COSMETIC AND LASER THERAPY
http://dx.doi.org/10.3109/14764172.2015.1052513

Taylor & Francis
Taylor & Francis Group

CASE REPORT

Fractional treatment of aging skin with Tixel, a clinical and histological evaluation

Monica Elman[1], Nathalie Fournier[2], Gilbert Barnéon[3], Eric F. Bernstein[4], and Gary Lask[5]

[1]Elman Laser Clinic, Rishon Le-Zion, Israel; [2]CLDP, Clapiers, France; [3]Centre Pathology, Montpellier, France; [4]Main Line Center for Laser Surgery, Ardmore, PA, USA; [5]UCLA Medical School, Los Angeles, CA, USA

ABSTRACT

Objective: This study presents clinical results of Tixel, a new fractional skin resurfacing system based on thermo-mechanical ablation technology. Tixel employs a hot (400°C) metallic tip consisting of 81 pyramids. Treatment is performed by rapidly advancing the tip to the skin for a preset tip–skin contact duration. Thermal energy transfer to the skin creates micro-craters by evaporation. **Methods:** Treatment results with tip types, D and S, with high and low thermal conductivity, were evaluated. Twenty-six subjects received three facial treatments, with 4–5-week intervals between treatments, without analgesia or cooling. In addition, histopathologies of Tixel and CO_2 laser were performed. **Results:** Crater properties are related to contact duration and to thermal conductivity. The D tip created char-free ablative craters 100–320 µm wide with a thermal zone 100–170 µm deep. The S tip created non-ablative coagulation preserving the epidermis. Skin complexion improvement was achieved in all subjects; average treatment pain of 3.1/10, downtime of 0–1 days, and erythema clearance of 3.5 days. Subject's satisfaction was 75% and wrinkle attenuation was achieved in 75% of the cases. There was no incidence of bleeding, scarring, or post-inflammatory hyperpigmentation. **Conclusions:** Tixel may be used safely for ablative and non-ablative resurfacing with low pain, low downtime, and quick healing.

ARTICLE HISTORY
Received 9 December 2014
Accepted 12 April 2015

KEYWORDS
Ablation; fractional; resurfacing; skin rejuvenation; thermal model

Introduction

Fractional laser resurfacing technologies are widely used in dermatology. Short-pulse CO_2 lasers are generally considered to be among the best modalities for high-precision ablation of thin tissue layers without bleeding and with minimal collateral damage (1). They are widely utilized in skin fractional skin resurfacing (2,3) for improved skin texture and fine wrinkles. Treatment is painful, requiring pre-application of analgesic creams and protective eyewear. Downtime is about 5 days. With a penetration depth of only 30–50 µm by the 10.6-µm wavelength laser beam into tissue, it is possible to vaporize crater arrays of skin down to the papillary dermis or deeper, and achieve excellent skin resurfacing results. With an array of ~100–250 µm focused beam spots, fractional resurfacing of ~12–20% of the skin surface ensures fast healing. The energy responsible for vaporization of tissue with a CO_2 laser is purely thermal. In the vaporization process, the temperature produced by a single-pass laser beam attains ~350–400°C in the crater (4).

Since thermal energy causes tissue vaporization, one may expect that by bringing a metallic element having high thermal conductivity, heated to a temperature of ~350–400°C, in contact with the skin for a duration of a few milliseconds and a depth of ~50–150 µm, an ablative effect which is clinically identical to the CO_2 laser effect will occur.

The objective of the current article is to present a novel thermo-mechanical ablation (TMA) technology and to show clinical and histopathology data using the Tixel device. A comparison to fractional CO_2 laser histology is also provided.

Materials and methods

The Tixel

The Tixel (Novoxel, Germany) is a thermo-mechanical system for fractional ablation. It applies a tip, made of metallic, gold-plated biocompatible materials (Figure 1A). The tip is fixated at the distal section of the Tixel's handpiece which is equipped with a linear motor (Figure 1B). The tip's active surface consists of an array of 81 (9 × 9) pyramids evenly spaced within

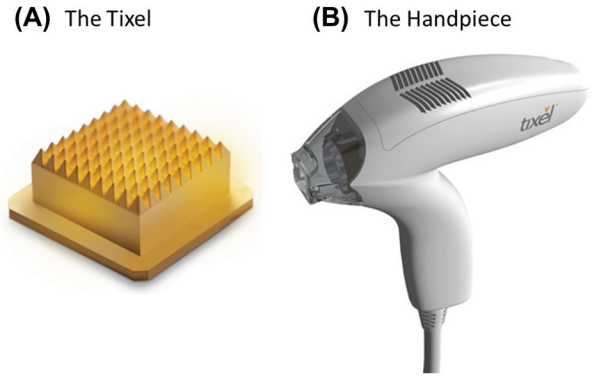

Figure 1. (A) D and S types of Tixel pyramidal tip array. (B) Tixel handpiece.

CONTACT Gary Lask ilrderm@gmail.com UCLA Medical School, Los Angeles, CA, USA.
Monica Elman and Nathalie Fournier are equal contributors to this paper.
Color versions of one or more of the figures in the article can be found online at http://www.tandfonline.com/ijcl

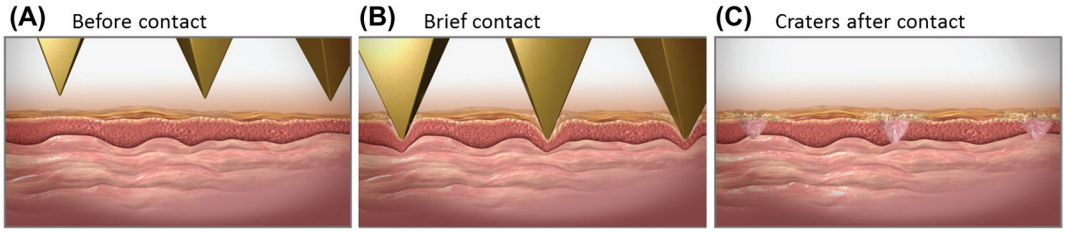

Figure 2. Schematic of the crater array vaporization process with high-temperature pyramidal tips. (A) Fast advance toward tissue; (B) Brief contact on skin surface and transfer of thermal energy to tissue; (C) Vaporized craters after tips retraction. Temperature of 400°C and short contact duration are identical to CO_2 laser parameters, and ensure a tissue interaction which is very similar to CO_2 (or erbium) lasers.

a boundary area of 1 × 1 cm. The pyramids are 1.25 mm tall having a radius of about 100 microns at peak vertex. The back plane of the tip is flat and is connected to a coin-sized heater which is kept at a constant temperature of 400°C during operation. When not in use, the tip is base-positioned at a distance of 20 mm from the skin's surface (home). The tip weighs 7 g and is re-usable. The system authenticates, inspects, monitors, sterilizes, and exchanges tips automatically. Tip cleaning after treatment is performed within 5 min at 540°C using an accessory heater. Self-sterilization is performed within 3 min at 350°C. Tip cleaning, sterilization, and biocompatibility have been validated. The handpiece weighs 270 g. Two tip types have been used: D with high thermal conductivity and S with low thermal conductivity. When the user activates the handpiece, the linear motor rapidly advances the tip which comes in brief contact with the tissue. Thermal energy is transferred to the skin, creating micro-craters in it by evaporation. The tip recedes within a precisely controlled distance and time to its home position, away from the tissue (Figure 2). The duration of the pulse, that is, time of contact between tip and skin, can range from 6 ms to 18 ms. A double pulsing mode is enabled. The motor's displacement accuracy is in the range of 1–8 µm and the pulse repetition rate is 1 Hz. A 14-ms pulse delivers a high-energy pulse of ~25 mJ/crater, while a 10-ms pulse delivers a medium-energy pulse of ~15 mJ/crater, and a 6-ms pulse delivers a low-energy pulse of ~10 mJ/crater. The theoretical and engineering foundations of the Tixel technology have previously been described in Lask et al. 2012 (5). The utilization of the Tixel does not require the use of protective eyewear or of a smoke evacuator.

The thermal model

The thermal effects of the Tixel tip on the skin were simulated (MATLAB, Version 8.5, Mathworks, USA) by a dynamic model which takes into account both the tip's motion profile and thermal properties of skin and the tip materials. The initial temperature of the tip is 400°C and it is assumed that during contact with the skin it evaporates the tissue's water content and cools down to 100°C. After reaching 100°C, it is assumed that only thermal damage occurs. At the first stage of simulation, the tissue evaporation is calculated. Each iteration of the model loop is built from 3 steps: calculation of the tissue volume that is vaporized by the thermal energy of the tip, propagation of the tip into the crater that is now vaporized, and calculation of the new temperature of the tip as well as collateral damage as described in reference 5.

Treatment procedure and assessments

Fractional resurfacing treatments by the Tixel device have been performed by two independent investigator-initiated groups.

Group 1 enrolled 10 female subjects for wrinkle reduction mainly on the periorbital and perioral regions. Eight completed the whole treatment procedure and 2 dropped for non-safety-related reasons. Subjects were between the ages of 42 and 65 years and with a Fitzpatrick Skin Type of II–IV. The treatment included 3 treatment sessions 35 days apart with 1–6 months follow-up after the third session. The full face ($n = 1$), periorbital area ($n = 6$), and/or perioral area ($n = 5$) were treated with the Tixel device using either the D tip (14-ms single pulse or 9-ms double pulse) or the S tip (9-ms single pulse). This prospective study was assessed by the investigator. Each treatment session and follow-up session included evaluation of the skin complexion, the Fitzpatrick's wrinkle scoring, pain level of the treatment, downtime, and time to clearance of erythema. Face photography at 0º, 90º right, and 90º left was performed with a Nikon D7100 camera before and after each session. Subjects' satisfaction was assessed after each session via questionnaire.

Group 2 enrolled 23 female subjects. 18 completed the whole treatment procedure and 5 dropped for non-safety-related reasons. Subjects were between the ages of 50 and 75 years and with a Fitzpatrick Skin Phototype of II–IV. Seventeen subjects presented mild-to-moderate photodamage. The treatment included 3 full-face treatment sessions 1–2 months apart with 2 follow-up visits at 1–2 months and 3–4 months after the third session. The full-face treatment ($n = 18$) was performed with

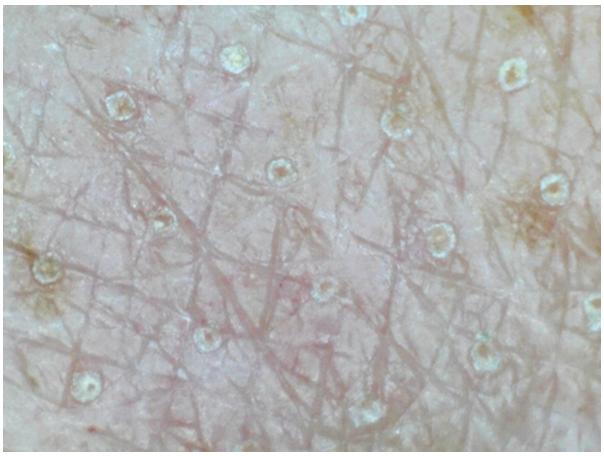

Figure 3. Microscope view of human skin immediately after treatment in which the array of coagulation points can be detected. Parameters: D tip, 9-ms double pulse.

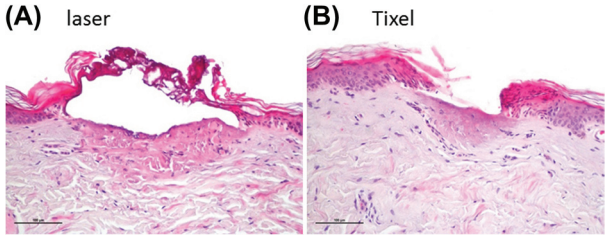

Figure 4. Histopathology of (A) laser and (B) Tixel immediately after treatment of human skin. Both craters present epidermal evaporation and dermal coagulation of the papillary dermis. Laser (Quanta, YouLaser, 24 W, 36 mJ/crater), Tixel (ablative mode, D tip, 9-ms double pulse).

the Tixel device applying either the D tip or the S tip at 9–16-ms single pulse. This study was a review of records retrospectively assessed by the investigator. Each session included an evaluation of the pain level during treatment, downtime and time to clearance of erythema. Face images at frontal, right oblique, and left oblique positions were acquired via a Canfield Reveal Imager before and after each session. Subject satisfaction was assessed at the follow-up session.

All patients applied Biafine or Cicalfate lotions following treatments, and were allowed to use sunscreen cream (SPF 50) and unperfumed makeup once microcrusting appeared.

In all cases, pain level has been graded on a scale of 1–10 by the subject where 1 is no pain and 10 is very painful. Tixel treatments were performed without applying any sort of analgesic substances or cooling.

The average ± standard deviation of downtime, clearance of redness, and pain level were reported, for all sessions combined.

Histopathology

Biopsies were taken from the forearms and upper arms of two male volunteers, immediately after treatment with Tixel at a range of parameters. In addition, CO_2 laser was applied for histopathology comparison (YouLaser, Quanta, 24 W, 750 µs, 2 stacks, density: 100 spots/cm^2, 36 mJ/point and Lumenis 1080 s, CW, 30 W, 50 ms/Pulse combined with Alma fractional Pixel CO_2 Omnifit handpiece, 9 × 9 array in 11 × 11 mm treatment zone). Histologies were evaluated in a blinded manner by the histopathologist.

In addition, a female domestic swine (7 weeks old, Kibbutz Lahav, Israel) was in vivo submitted to triplicates of Tixel treatments at the dorsal flank. Skin biopsies were extracted immediately after treatment and 7 days after treatment. Histologies were analyzed by a blinded histopathologist. The study was approved by the ethical committee of the Pre-clinical Research unit of Assaf Harofeh Medical Center.

Results

Crater characterization

Fractional TMA of skin utilizes pre-heated tips to generate a matrix of craters in the skin surrounded by healthy tissue (Figure 3). The clean craters shown in the figure have a coagulated diameter of about 320 µm on the skin surface corresponding with an active area of roughly 10%.

Tixel vs. laser

Figure 4 presents histopathology of laser versus Tixel craters at typical treatment parameters of both devices. An ablative Tixel crater using the D tip, 9-ms double pulse is compared with a CO_2 laser crater. Fractional thermal ablation with Tixel created a lesion 160 µm in diameter (vs. 320 µm with laser) and a thermal damage with dermal coagulation of the papillary dermis (depth of 170 µm, same as laser). Although Tixel and CO_2 laser craters have a general similarity, in contrast to the laser crater, the Tixel crates are clean of necrotic tissue or charring.

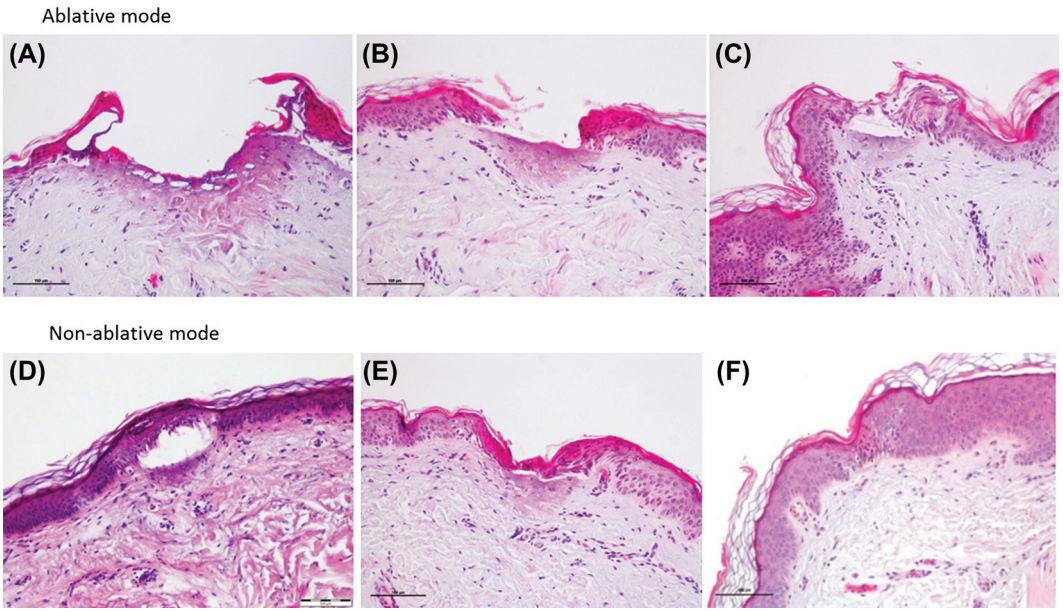

Figure 5. Histopathologies of Tixel treatments, at different settings, immediately after treatment of human skin. (A) D tip, 14-ms double pulse. (B) D tip, 9-ms double pulse. (C) D tip, 9-ms single pulse. (D) S tip, 14-ms single pulse. (E) S tip, 9-ms double pulse. (F) S tip, 9-ms single pulse.

Table 1. Summary of crater characteristics.

	Thermal damage		Thermal effect on				
Figure	Depth µm	Width µm	Dermis	Epidermis	Tixel pulse duration	Tip type	Device
4A	170	330	Coagulation of upper papillary dermis	Ablation Vaporized	–	–	Laser CO_2
5A	180	380	Coagulation of upper papillary dermis	Ablation Vaporized	14 ms double	D	Tixel
5B	170	160	Coagulation of upper papillary dermis	Ablation Vaporized	9 ms double	D	Tixel
5C	160	200	Coagulation of upper papillary dermis	Ablation Vaporized	9 ms single	D	Tixel
5D	165	210	Coagulation of upper papillary dermis	Non-Ablation Coagulated Vacuolation	14 ms single	S	Tixel
5E	170	160*	Coagulation of upper papillary dermis	Non-Ablation Coagulated Vacuolation	9 ms double	S	Tixel
5F	100	100	Normal	Non-Ablation Coagulated Vacuolation	9 ms single	S	Tixel

*Internal crater width measurement.

Tixel crater variety

Crater properties and extent of thermal damage with Tixel are closely related to the choice of the tip, the pulse duration, and the number of pulse repetitions. The D tip creates ablative craters (Figure 5A–C) while the S tip creates non-ablative thermal lesions (Figure 5D–F). Table 1 summarizes the main characteristics of craters at several Tixel pulse durations. Lesion dimensions are 100–380 µm wide and 100–180 µm deep. The histology shows no hemorrhage or edema.

The D tip generated clean epidermal evaporation and a dermal coagulation of maximum 180 µm in depth, which corresponds to the upper papillary dermis.

The S tip had a milder effect. The coagulated epidermis is preserved, forming an essentially dressed crater. The epidermis is compressed by the tip contact and the extracellular space between the cells is increased due to cell shrinkage. A process of vacuolation takes place and a cleft is formed between the damaged epidermis and dermis, as can be seen in Figure 5D and E, or a mild vacuolation in Figure 5F. In this later case, dermal coagulation at the upper papillary dermis is avoided due to the very brief pulse that has been applied.

The thermal model for ablation with Tixel shows the extent of the evaporation and thermal damage as a function of pulse duration, for both S tip and D tip (Figure 6). There is a profound difference between S and D tips in the extent of the ablative damage. The simulation predicts that the D tip ablates a considerable amount of tissue; while the S tip performs only minimal ablation. Simulation for a 9-ms single pulse is compatible with the histological results presented in Figure 5. The D tip that evaporated the whole epidermis (Figure 5C) presents a calculated 65-µm ablation (Figure 6 red triangle); the S tip that induced a non-ablative lesion (Figure 5F) presents a calculated 5-µm ablation (Figure 6 black triangle). This can be explained by the differences between their thermal diffusion coefficients. The D tip heat transfer rate to tissue is much faster than the S tip. For the 9-ms pulse duration, the model also predicts that ablation occurs in the first 0.25 ms for the D tip and in the first 0.01 ms for the S tip. Tissue ablation is thus a considerably rapid event when compared with the entire pulse length. Furthermore, the thermal damage that was calculated to be about 74 µm for both cases (Figure 6 circles) also matches the histologies. The coagulation damage, created during tip progression in the tissue, is determined by the thermal diffusivity of the tissue rather than the thermal diffusivity of the tip; and since both tips are in contact with tissue for a similar duration, a similar extent of tissue coagulation is expected.

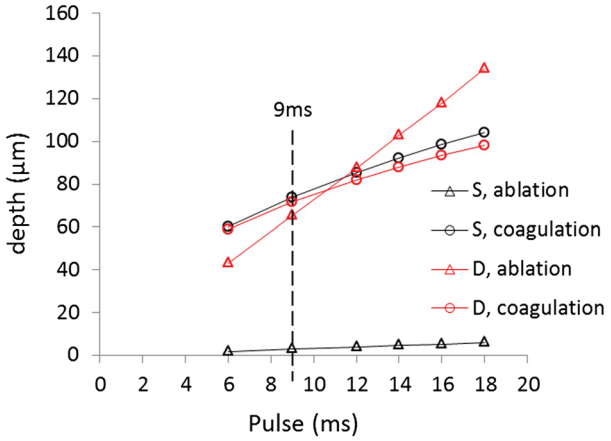

Figure 6. Theoretical thermal model of Tixel, with D tip and S tip, showing the extent of tissue ablation and tissue coagulation during various pulse durations.

The healing process

Histologies on the same day of Tixel treatment and after 7 days, on an in vivo porcine model, were examined (Figure 7). A Tixel crater 250 µm wide, 170 µm deep with focal necrosis of the epidermis and focal underlying dermal coagulation is presented (Figure 7A). Seven days after, epidermal regeneration is observed with a surface crust and a dermal epidermal cleft (150 × 50 µm) filled with new fibroblasts and macrophage cells (Figure 7D), indicating that healing occurs normally. This effect is associated with new collagen formation. A non-ablative pulse is also presented where the epidermis and stratum corneum are not ablated (Figure 7B). Rather they are compressed. A cleft is formed in the epidermal–dermal junction and minimal superficial necrosis is seen in the dermis. Seven days after (Figure 7E), there is complete epidermal regeneration with a focal crust on the stratum corneum and minimal dermoepidermal cleft with focal collagen degeneration and macrophage infiltration. A low-energy non- ablative crater is associated with minimal epidermal damage with vacuolation at the epidermal–dermal junction and no dermal coagulation (Figure 7C). After Seven days, complete regeneration of the epidermis with minimal crust and underlying minimal collagen degeneration is observed (Figure 7F).

Clinical results

All subjects (100%) agreed or strongly agreed in both studies that no analgesics or pain relievers are necessary during the treatment.

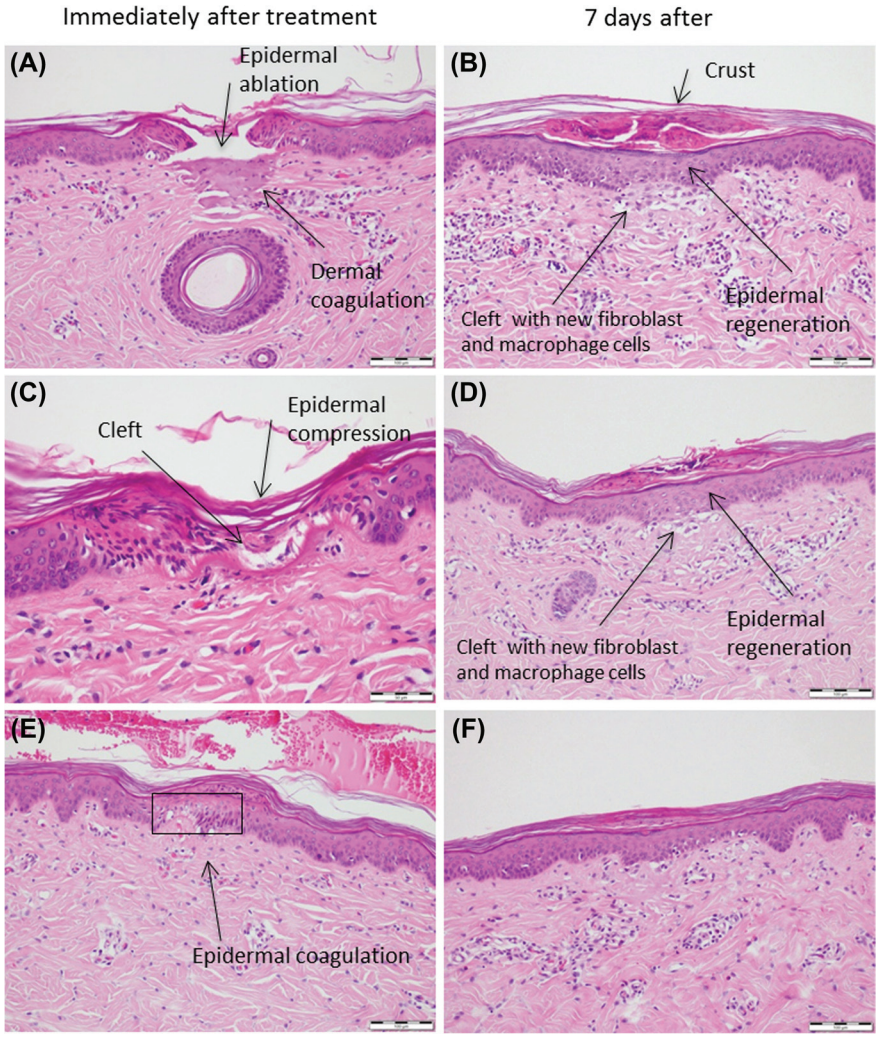

Figure 7. Tixel histologies with S tip on in vivo porcine skin immediately after and 7 days after treatment. (A,D) Ablative mode with high-energy pulse, (B,E) Non-ablative mode with medium-energy pulse, (C,F) Non-ablative mode with low-energy pulse.

Subjects' average treatment pain without analgesia was 3.3 ± 2 ($n = 13$) for group 1 and 3 ± 1.5 ($n = 56$) for group 2 (pain scale: 1 minimum to 10 maximum). Downtime was short in the two groups, ranging from zero to one day for group 1 and no downtime in group 2 (91% of treatment sessions, $n = 57$), independently of the tip type. The erythema resolved within 2–3 days for the 2 groups and in a few cases involved in more aggressive ablative treatment (i.e., D tip, 16 ms) within 4–6 days. In both groups of subjects, 75% were either satisfied or very satisfied at the follow-up visit, 1 month after third session.

All subjects have presented improvement in skin complexion or reduction of photo damage. In addition, in group 1 87% and in group 2 69% of subjects presented wrinkle attenuation with an average of 75% for both groups (Figures 8–10). Clinical results are summarized in Table 2. Improvement in skin complexion and in some cases in wrinkles was visible after the first treatment session with further improvement after the following sessions. In one subject who did not take prophylactic treatment, herpes was reactivated. There was no incidence of bleeding, scarring, or post-inflammatory hyperpigmentation. Figure 11 shows the erythema immediately after treatment and the apparent microcrusting after 5 days.

Discussion and conclusions

Tixel fractional treatment is a novel thermal resurfacing treatment which can generate ablative as well as non-ablative micro-craters in the skin. Superheating water molecules in the skin tissues with a high- conductivity metallic tip is effective in vaporizing the skin cells in a safe, precise, and predictable effect.

Tixel's D tip creates ablative craters with similar properties to fractional CO_2 lasers. At the settings applied, Tixel's S tip generates non-ablative "dressed" craters with underlying thermal damage extending down to the papillary dermis. The epidermal dressing of the crater enhances the healing providing rapid re-epithelialization and epidermal regeneration of the lesion. Moreover, the crater's cover may act as a natural physiologic dressing protecting from post-treatment infection during the healing process.

This technology is safe and offers good resurfacing results, with nearly no downtime. Craters with diameters narrower than those of laser crater are associated with rapid healing. As treatment downtime is very short, additional treatments can be performed as compared with fractional ablative and non-ablative lasers for optimal outcome.

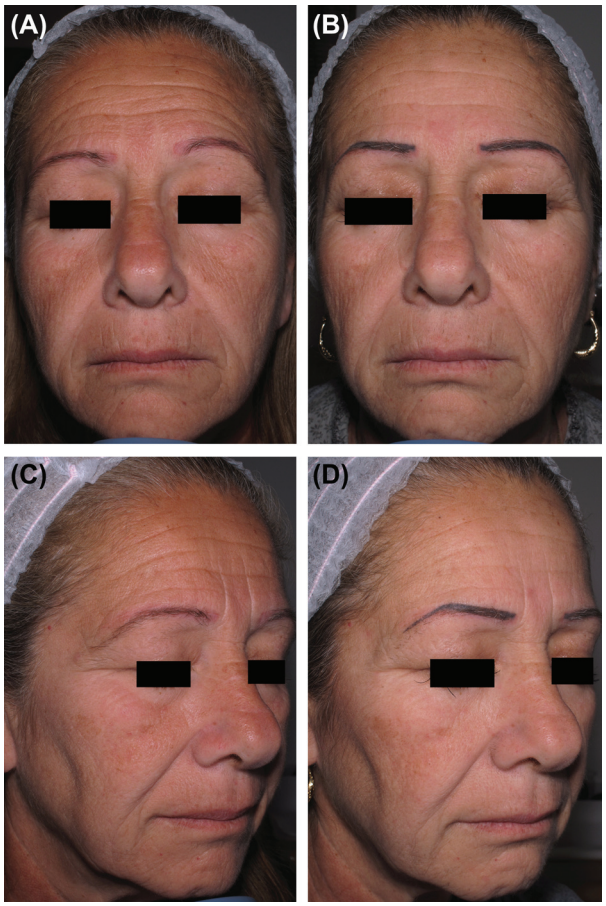

Figure 8. Full-face treatment. (A,C) Before and (B,D) after 4 months from the 3rd treatment session with D tip, 9–14-ms single-pulse one pass. Woman 58 years, phototype IV.

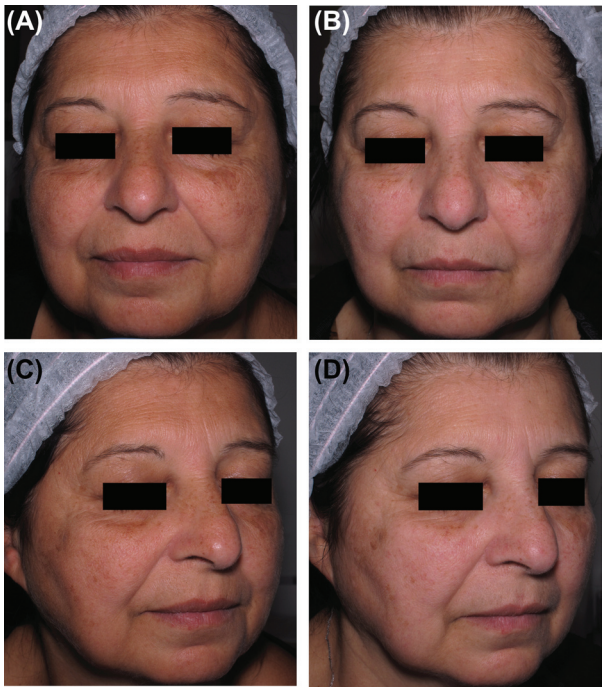

Figure 9. Full face treatment. (A,C) Before and (B,D) after 4 months from the 3rd treatment session with D tip, 9–14-ms single-pulse one pass. Woman 58 years, phototype IV.

Figure 10. Periorbital treatment. (A,C) Before and (B,D) after 1 month from the 2nd treatment session with D tip, 14-ms single-pulse one pass. Woman 59 years, phototype II.

Table 2. Clinical results, groups 1 & 2.

Number of subjects	26
Treatment pain level[a,b]	3.1
Downtime[b]	0.16 days
Clearance of erythema[b]	3.5 days
Subject's satisfaction	75%
Wrinkle attenuation[c]	75%

[a]In a scale of 1 minimal to 10 maximum, without analgesia or pain relief.
[b]Mean score.
[c]Percent of subjects that present wrinkle improvement.

Treatment presents low discomfort for the patient. The device is operator-friendly as there is no smoke, no protective eyewear is required, and there is no risk of accidental harm by invisible laser radiation on the patient, physician, or personnel. Treatment pain is low, not requiring the application of analgesic creams. Contrary to lasers, which require analgesia and cooling to limit the patient's pain, Tixel patients did not ask for any pain

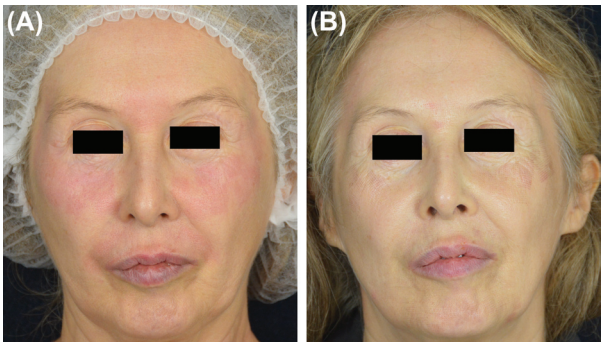

Figure 11. Periorbital treatment. (A) Immediately after treatment, (B) 5 days after treatment with D tip, 14-ms single pulse. Woman 59 years, phototype II.

relief during treatment or afterward. The low pain level experienced is probably the result of several factors: (a) smaller diameter craters in comparison to lasers; (b) while overall energy applied per crater is similar to laser, Tixel employs a fraction of the energy density; (c) The entire matrix of 81 Tixel craters is created in a single step lasting about 15 ms whereas a single laser beam having much higher energy density is applied within 0.5 ms repeatedly close to 100 times to generate 1-cm^2 treatment site. While further studies should be conducted to explore this new technology, this clinical evaluation was useful in providing both quantitative and qualitative understanding of Tixel's capabilities.

In conclusion, Tixel is a promising versatile fractional system for both ablative and non-ablative resurfacing.

Note

Some aspects of the TMA technology are patented and other aspects are patent pending.

Declaration of interest

All authors state lack of conflict of interest. The authors may be compensated in the future with company options.

References

1. Railan D, Kilmer S. Ablative treatment of photoaging. Dermatol Ther. 2005;18:227–241.
2. Bronz G. Clinical uses of CO_2 lasers in plastic surgery. Aesthetic Plast Surg. 2001;25:313–325.
3. Saluja R, Koury J, Detwiler S, Goldman M. Histologic and clinical response to varying density settings with fractionally scanned carbon dioxide laser. J Drugs Dermatol. 2009;8:17–20.
4. Choi B, Chan EK, Barton JK, Thomsen SL, Welch AJ. Thermographic and histological evaluation of laser skin resurfacing scans. IEEE Journal of selected topics in Quantum electronics. 1999;5: 1116–1126.
5. Lask G, Elman M, Fournier N, Slatkine M. Fractional vaporization of tissue with an oscillatory array of high temperature rods – Part I: Ex vivo study. J Cosmet Laser Ther. 2012;5:218–223.

Journal of Cosmetic and Laser Therapy, 2012; 14: 218–223

informa
healthcare

ORIGINAL RESEARCH REPORT

Fractional vaporization of tissue with an oscillatory array of high temperature rods – Part I: *Ex vivo* study

GARY LASK[1], MONICA ELMAN[2], NATHALIE FOURNIER[3] & MICHAEL SLATKINE[4]

[1]*UCLA Medical School, Los Angeles, CA, USA,* [2]*Beit Harofim, Holon, Israel,* [3]*CLDP, Clapier, France, and* [4]*Nova-B Ltd., Hadera, Israel*

Abstract

Background: Short pulse duration (~0.1–5 milliseconds) CO2 lasers are perceived as excellent tools for vaporization of craters arrays in fractional skin resurfacing. *Objectives:* To present a thermo-mechanical ablation technology, which affects tissue identically to fractional CO2 lasers, however at a fraction of the size and cost of a laser. *Material and methods:* The new technology is based on heating an oscillating array of thin metallic rods to a temperature of 400°C and advancing the rods into tissue down to a precise pre-selected depth for a duration of 0.1–5 milliseconds. As a result, an array of crater is vaporized with identical properties of those produced by CO2 lasers. An *ex vivo* test was performed with a thermo-metallic rod array prototype. *Results:* Arrays of 10×10 vaporized micro-craters of 350 micron diameter, 200 micron depth have been produced with lateral thermal damage of 80 micron while thermal damage below craters was 80–250 micron. *Conclusions:* A resonating thermo-mechanical array of high temperature (350–400°C) rods is capable of producing an array of craters identical to those produced with pulsed CO2 lasers.

Key Words: *skin resurfacing, CO2 lasers, fractional, wrinkles*

Introduction

Short pulse CO2 lasers are generally considered among the best tools for high precision ablation of thin layers of tissue without bleeding and with minimal collateral damage (1). They are widely utilized in skin resurfacing, including fractional skin resurfacing (2,3). By operating a 10.6 micron CO2 laser with energy density above a threshold of ~5 J/cm^2 and pulse duration below few milliseconds (0.1–5 milliseconds), vaporization rate is faster than thermal diffusion into tissue and collateral thermal necrosis is ~100–150 micron. With only 30–50 micron penetration of the 10.6 micron wavelength laser beam into tissue, it is possible to vaporize craters arrays of skin down to or deeper than the papillary dermis and achieve excellent skin resurfacing results. With an array of ~100–500 micron focused beam spots, fractional resurfacing of ~12–20% of the skin surface ensures fast healing. The energy responsible for the vaporization of tissue with a CO2 laser is purely thermal. The tissue parameters, which quantitatively dictate the threshold energy for vaporization with only 100–150 micron collateral damage, are the vaporization energy of tissue which is ~3000 J/cm^3 (4) and the beam penetration in tissue (30–50 micron). In the vaporization process, temperature craters produced by a single pass laser beam attain ~350° C (5).

Since thermal energy is responsible for tissue vaporization, we may expect that by bringing a metallic element of temperature ~350° C in contact with the skin for a duration of less than ~0.1–5 milliseconds and depth ~50–250 micron, a clinical ablative effect which is identical to the CO2 laser effect will occur. However, such extremely fast and accurate thermo-mechanical procedure with a 350° C array enclosed in a small size comfortable handpiece requires very specific geometrical, mechanical and thermal design, which has recently been developed in our laboratory. The objective of the current article is to describe the general design principles a the new 'ThermiXel' thermo-mechanical technology, which acts identically to a short pulse CO2 laser and can be used in a variety of surgical applications including fractional skin resurfacing. The advantage of the

Correspondence: Gary Lask, MD, UCLA Medical School, Dermatology, 200 UCLA Medical Plaza, Los Angeles, CA, United States. E-mail: micslatk@zahav.net.il

(Received 18 October 2011; accepted 5 May 2012)

ISSN 1476-4172 print/ISSN 1476-4180 online © 2012 Informa UK, Ltd.
DOI: 10.3109/14764172.2012.698284

technology is its very low cost as compared to a laser as well as its small size. In the following, we shall present an *ex vivo* confirmation of the expected results of crater vaporization in tissue with an oscillating thermo-mechanical element.

The 'ThermiXel' technology[1]

The new tissue ablation technology is based on the supply of vaporization heat from an extremely hot (~350–400°C) array of miniature rods down to a preselected depth (50–250 microns) in tissue within ~0.1–5 milliseconds, thus mimicking the pulsed CO2 laser action. As is shown below, this can be practically realized in a small device due to exploitation of a fortunate coincidence of thermal characteristics of some metals and tissue.

Operating principles

The operating principles of the 'ThermiXel' technology are schematically presented in Figures 1A–C. A high thermal conductive copper block with an integrated array of copper rods is located inside a hand held treatment handpiece and is heated by a high power (~100 W) miniature electric heater cartridge to a temperature of 350–400°C. The high temperature block is held in a loaded position by a compressed spring. A thermally isolated protective plate (which may be chilled to a temperature of ~10°C) with a corresponding array of holes serves as the distal end of the treatment handpiece and is placed on the skin to be treated. Once the handpiece is placed on the treatment site and a treatment command is given by the operator, the high temperature block/rods unit is released and allowed to move forward and perform a single harmonic oscillation (with the aid of the attached spring) of ~30 milliseconds duration, with an amplitude which is set to allow all rods penetrate a preselected distance (of 50 – 250 micron) into the skin (Figure 1B). A thermally insulating spacer provides additional assurance of penetration depth accuracy. Since the rods penetration into the skin occurs when the spring is fully stretched and copper block velocity is decelerated to zero, there is no mechanical impact on patient. Once the vaporizing rods have 'flicked' a thermal impact into the skin, the stretched spring returns the oscillating element back to its original retained position where it is reheated and gets ready for the next treatment command. We note here that the rods do not affect tissue at all if not heated, as opposed to mechanical needles. An analysis of the copper block movement reveals that the dwelling time of the rods in their distal 50–250 micron section of their oscillatory journey depends on the initial compression loading force (spring constant × loading amplitude) and can be practically set to ~0.1–5 milliseconds. This implies that the vaporizing rods stay in the skin for that time duration. As a result, an array of vaporized craters (Figure 1C) is formed in the skin within ~0.1–5 milliseconds, which is similar to craters formed by a many pulsed 'Fraxel' CO2 laser of same pulse duration (6).

Theoretical analysis – selection of operational parameters

The following conditions are prerequisites for the high temperature rods to practically mimic high quality CO2 (as well as Erbium) lasers operation as describes above:

(a) The thermal energy, which is stored in the distal end of each rod, should be equal to (or higher than) the latent heat of vaporization of tissue for a volume equal to the vaporized crater volume.
(b) The thermal energy should be delivered within ~0.1–5 milliseconds (depending on depth), namely: the thermal relaxation time of the thermal energy storage section of the rod should be shorter than ~0.1–5 milliseconds.
(c) Rods (as well as copper block) should attain a temperature of ~350–400°C in order to mimic pulsed CO2 laser action (5) as well as avoid sticking of tissue to the metallic rods and, as shown below, provide the necessary vaporizing energy.
(d) Treatment repetition rate should be high enough – at least 1 Hz as achievable by most pulsed CO2 lasers with treatment spot size $\sim 10 \times 10$ mm^2, for an unlimited number of treatment spots. This implies temperature rise of rods distal tip within < 1 second following each treatment 'flick' and movement to the next treatment spot, without gradual decrease of distal end temperature.
(e) Initial heating up of the fixed metallic block to a temperature of 400°C prior to a treatment session should practically take only a few minutes. On the other hand, the preheated block should be large enough since it serves as a passive energy reservoir for the vaporizing rods. Yet, it should be small enough to be integrated in of a small hand held treatment handpiece.
(f) The treatment device should be hand held and only few centimetres in size.

i) Adjustment of dwelling time duration in tissue

In the process of vaporizing tissue craters of depth H, the copper block and rods array (of total mass M)

[1]*Note:* The 'ThermiXel' technology is patent pending.

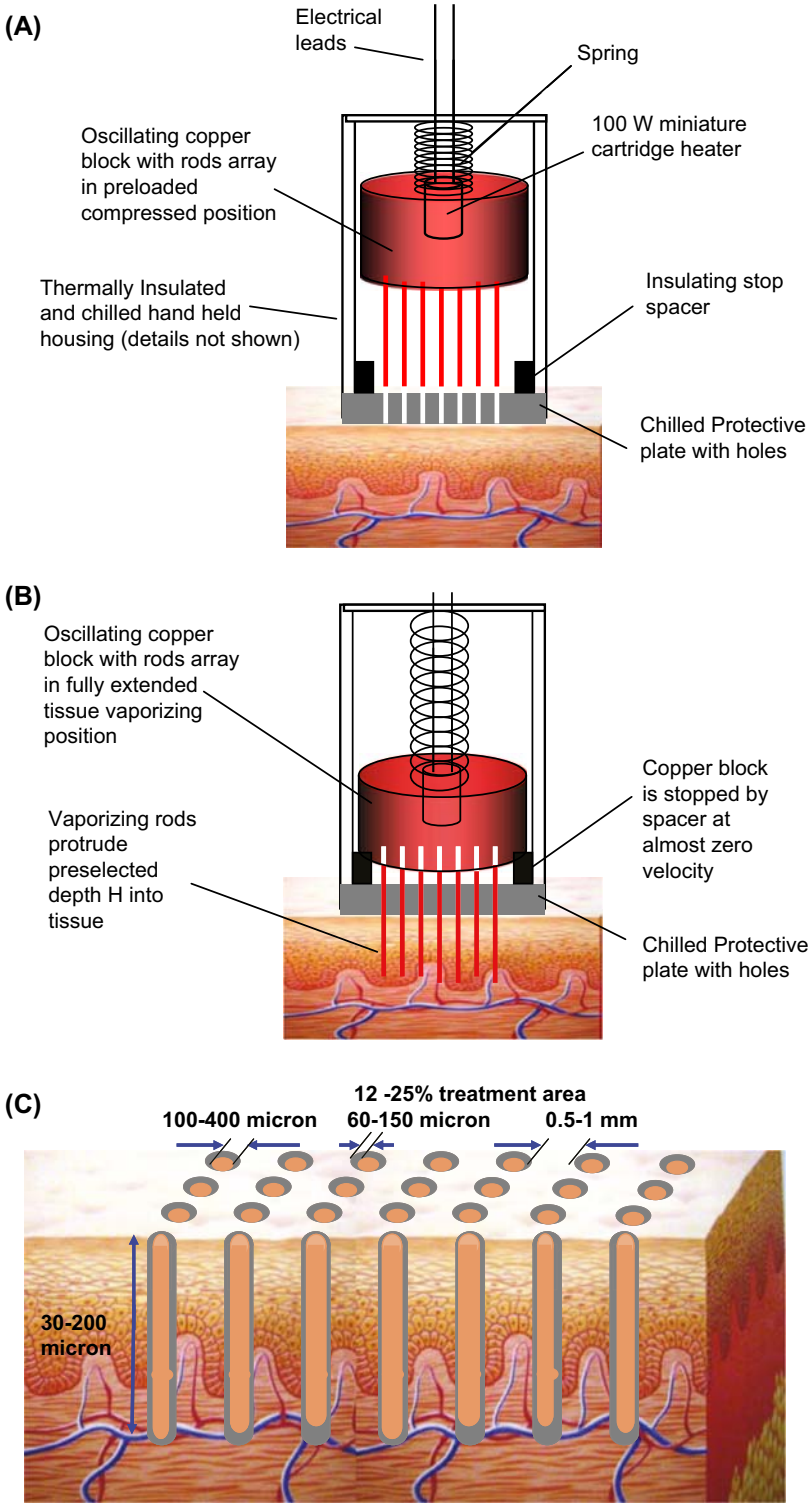

Figure 1. (A) The operating principle of 'ThermiXel' technology. High temperature array of treatment rods in upper spring loaded position. (B) The operating principle of 'ThermiXel' technology. High temperature array of treatment rods in lower spring stretched position while vaporizing craters. (C) Schematic presentation of craters array produced 'ThermiXel' technology.

are located at the distal end of their oscillatory track, with zero velocity. As schematically shown in Figure 2, the restoring force F induced by the stretched spring accelerates the mass M away from tissue back to its original loaded position. The acceleration a of the mass M is $a = F/M$, and the time duration t needed for the rods to leave tissue (or travel a distance H) fulfils the equation:

$$H = at^2/2 = Ft^2/2M. \quad (1)$$

As a result, $t = \sqrt{(2MH/F)}$. The dwelling time in tissue is twice as long, since the rods array is

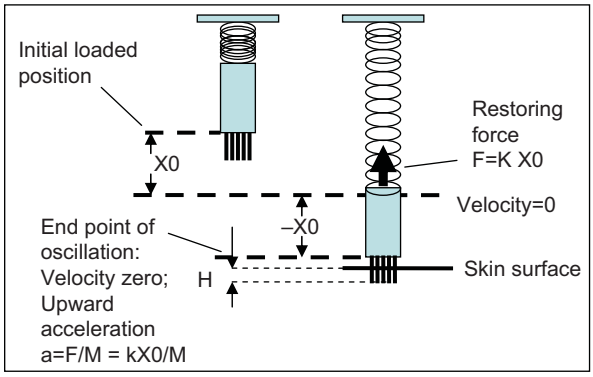

Figure 2. Model for analysing the dwelling time of vaporizing rods in tissue.

decelerated prior to the backward acceleration, implying:

$$t \text{ dwelling} = 2\sqrt{(2MH/F)}. \quad (2)$$

As explained in the section 'Experimental results', our design parameters were: $M = 150$ g; $H = 100$ micron; $F = KX$, $K =$ spring constant $= 8$ kg/cm; $X =$ loading distance (spring compression) $= 10$ mm. According to Equation (2), this implied dwelling time ~1 milliseconds. Dwelling time duration is proportional to $\sqrt{\boldsymbol{H}}$ and can be adjusted by varying the initial compression F (by varying the distance X).

ii) Thermal parameters

We hereby calculate the thermal parameters of the metallic rods, which can fulfil the stated above prerequisites.

The energy E needed to vaporize a crater with, for example, a square shape of width d and a depth H is:

$$E_{vaporiz} = H_{vaporiz} d^2 H, \quad (3)$$

where $H_{vaporiz}$ is the latent vaporization energy of 1 cm^3 of tissue (approximately 3000 J/cm^3) (6).

The thermal energy E, which is stored in a distal length L of the vaporizing metallic rod and may be available for vaporizing tissue, is given by:

$$E = CLd^2T, \quad (4)$$

where $C =$ heat capacity, $\rho =$ vaporizing rod material density, $T =$ rod temperature (~400°C).

Based on the first pre-requisite, namely $E > \sim E_{vaporiz}$ and equations (3) and (4):

$$L > \sim H_{vaporiz} H/(C\rho T). \quad (5)$$

In the case of a copper rod, $C \sim 0.4$ J/g °C; density: $\rho \sim 9$ g/cm^3, implying that for a vaporization depth $H = 100$ micron.

$$L > \sim 650 \text{ micron}.$$

Namely, the vaporizing energy flows into the skin from a distance of 650 micron in the rod.

The rate of heat flow W from a rod of length L, width d, thermal conductivity K and a temperature T above the temperature of the tissue is approximately:

$$W = KTd^2/L = E/t, \quad (6)$$

where t denoting the rods 'flicking' duration or vaporization time duration, as well as the duration of delivery of thermal energy from the rod to tissue. This implies:

$$t \sim H_{vaporiz} HL/KT. \quad (7)$$

For $L \sim 650$ micron, $T \sim 400$°C, K (copper, 400°C) $= 2$ W/cm °C and $H = 100$ micron we obtain,

$$t \sim 2 \text{ milliseconds}.$$

These results lead to the following observations:

The distal end of length 650 micron of a copper rod, which is elevated to a temperature of 400°C, can provide the necessary energy to vaporize a 100 micron deep crater in tissue within ~2 milliseconds. Shorter time durations are achievable with higher compression or smaller size copper blocks (smaller mass M).

iii) Treatment repetition rate

The treatment repetition rate has been analysed by solving the one dimensional heat Equation (7)

$$\partial^2 T/\partial^2 X = 1/a^2 \partial T/\partial t \ (a^2 = K/c\rho), \quad (8)$$

for the flow of heat in the treatment rods (of 10 mm length) with boundary conditions: T = 400°C on the proximal end of the treatment rod and $T = 37$°C on the 650 micron distal section each time rod is in contact with tissue for a duration of 1 millisecond. We assume that during that period of time, rod distal end is emptied from its thermal energy (heat has flown to tissue and vaporized a crater), and we use Equation (8) to find out how fast the rod distal end is recharged with heat for the next treatment.

Figure 3 presents the solution to Equation (8) and shows that a repetition rate as high as 1 Hz is attainable with the 'ThermiXel' technology for an unlimited number of treatments.

iv) Residual heat

In similarity to CO2 laser treatments, the heat accumulated in the ~50–150 micron width coagulated zone (initially at 100°C) which surrounds the vaporized craters, diffuses to surrounding tissue and elevates its temperature. By chilling the skin to a temperature of 10°C for a short time duration of ~0.5 seconds (depth of ~0.5–1 mm) with the protective plate before each treatment pulse, we increase the number of epidermal cells between the craters

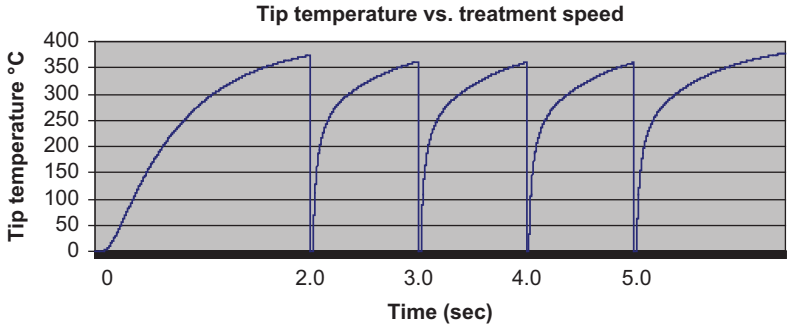

Figure 3. Speed of temperature recovery of rods array for 1 Hz treatment speed.

which do not sense any increase of temperature and allow faster healing.

Experimental results

Experimental vaporizing unit

A 18 mm diameter and 40 mm length copper blocks with an integrated array of 10 × 10 rods (500 micron × 500 micron × 10 mm size rods, 1 mm spacing) has been produced (Figure 4). A miniature 100 W, high temperature heater was activated with a small 100 W, 24 V DC power supply. The copper block/rods array assembly attained a temperature of 400°C within ~3 minutes as measured with a type K thermocouple.

The protrusion of the rods array beyond the skin contact plate (= skin vaporization depth) was preset to 50–250 micron. The oscillatory assembly was integrated into a handpiece, which was air cooled and comfortably hand held.

The rods protrusion time duration was electronically measured by monitoring the short circuit created between the copper rods and an aluminium foil, which was placed in electrical isolation under the handpiece and simulated the conductive skin surface.

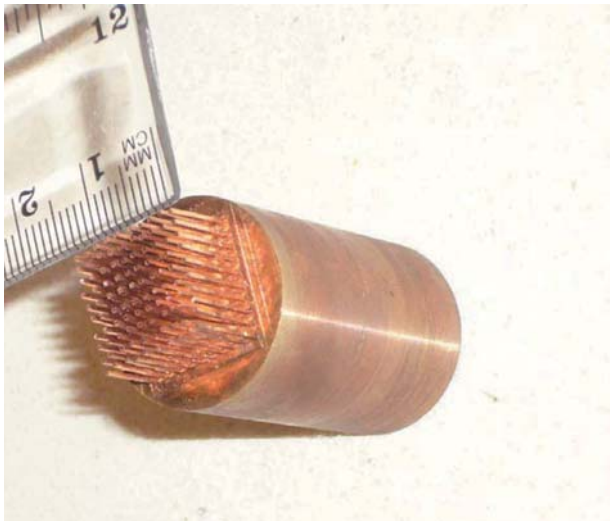

Figure 4. Treatment array (10 × 10) of high temperature (350–400°C) copper rods. Rods width 100–500 micron. Separation: 1000 micron.

The measured short circuit duration was 2.5 milliseconds.

Ex vivo test

The 'ThermiXel' prototype has been tested on the shaved skin of the abdomen of domestic white pig cadaver (the fresh abdomen was purchased from a slaughter house). The skin surface was chilled to a temperature of 14°C with ice for a duration of 5 seconds prior to firing the treatment pulse. Ice

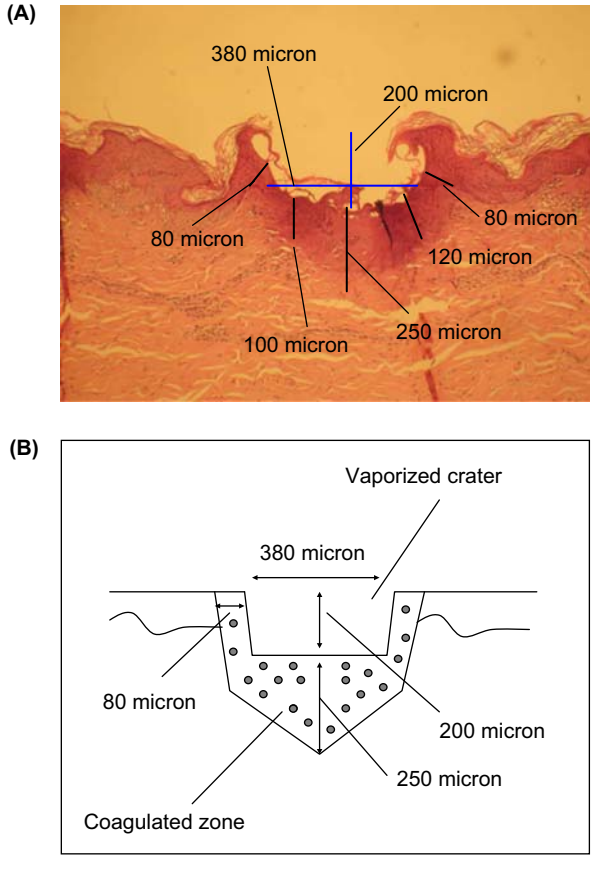

Figure 5. (A) Cross section of a conical crater produced by 'ThermiXel' technology. Vaporized crater width: 380 micron; vaporization depth: 200 micron; collateral thermal damage: 80 micron on the sides and 250 micron at the centre. (B) Schematic presentation of the conical vaporized crater. Lateral coagulation zone is 80 micron wide. Vaporized craters as well as coagulation zone can be set to either conical or flat shape.

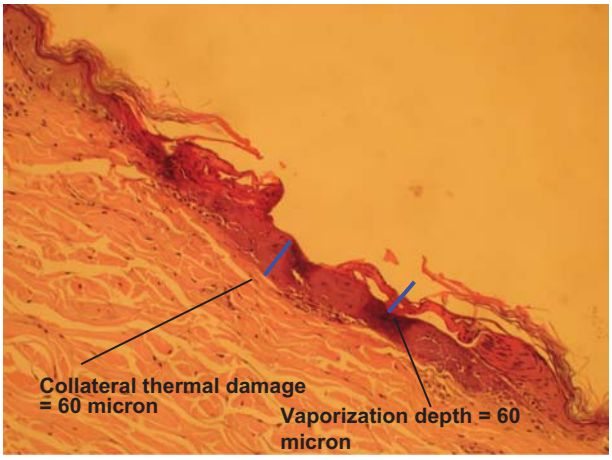

Figure 6. Cross section of a flat shallow crater produced by 'ThermiXel' technology. Vaporization depth 60 micron; collateral thermal damage 60 micron.

substituted the thermoelectric chilling of the protective plate which has not been incorporated in the prototype. Figure 5A presents a histology section of a vaporized crater produced on the skin. The crater width is 380 micron, and the vaporization depth is 200 micron. Thermal collateral damage is 80 micron on the sides and 250 micron in a 100 micron wide cone in the centre. Figure 5B provides a schematic view of the crater. Figure 6 shows a very shallow flat crater which was obtained while setting the preselected rods protrusion distance from the skin plate to a lower value. Vaporization depth is 60 micron and collateral thermal damage is 60 micron as well.

Discussion and conclusions

We believe that we have demonstrated the capability to utilize arrays of high temperature metallic rods to vaporize deep as well as very shallow craters with minimal collateral thermal damage without char, while leaving the skin between the treatment spots intact. That operation generally mimics the operation of most scanning fractional pulsed CO2 (and Erbium) lasers. This is made possible with the selection of metals with high thermal conductivity at high temperature ($T = 350–400°C$) and the use of a single 'flicking' harmonic oscillation with short (0.1–5 milliseconds) dwelling time in tissue. With well-designed thermal isolation the treatment unit can be integrated in a small comfortably hand held handpiece and be utilized in fractional skin resurfacing. A multicentre clinical study for fractional skin resurfacing is currently being initiated.

Declaration of interest: Michael Slatkine is cofounder of NovaB and its chief scientist. All other authors will be compensated in the future (in the form of payments/stock options) for running the multicentre clinical trial and for serving in the medical advisory board of NovaB.

References

1. Railan D, Kilmer S. Ablative treatment of photoaging. Dermatol Ther. 2005;18:227–241.
2. Bronz G. Clinical uses of CO2 lasers in plastic surgery. Aesth Plast Surg. 2001;25:313–325.
3. Saluja R, Koury J, Detwiler S, Goldman M. Histologic and clinical response to varying density settings with fractionally scanned carbon Dioxide laser. J Drugs Dermatol. 2009;8(1).
4. Carruth JAS, McKenzie AL. Medical lasers – science and clinical practice. Bristol and Boston: Adam Hilger Ltd; 1986: p. 60, Ch. 3.
5. Choi B, Chan EK, Barton JK, Thomsen SL , Welsh AJ. Thermographic and histological evaluation of laser skin resurfacing scans. IEEE J Select Top Quant Electron. 1999;5: 1116–1126.
6. Le Pillouer-Prost A, Zerbinati N. Fractional laser skin resurfacing with SmartXide DOT. Initial Results. J Cosmet Laser Ther. 2008;10:78–84.
7. Hildebrand FB. Advanced calculus for applications. Englewood Cliffs, New Jersey: Prentice/Hall; 1962: p. 429, Ch. 9.

A Prospective Study of the Safety and Efficacy of a Thermo-Mechanical Fractional Ablative Device for Periorbital Rejuvenation in Asians

Kwankamol Woottisheattapaiboon, M.D., Woraphong Manuskiatti, M.D., Nudpanuda Tevechodperathum, M.D.

Department of Dermatology, Faculty of Medicine Siriraj Hospital, Mahidol University, Bangkok, Thailand

Background: Demand for noninvasive procedure to correct the unattractive feature of peri-orbital area is increasing because of the popularity of aesthetic medicine. However, data on the safety and efficacy of noninvasive procedures for treatment of periorbital photo-damaged skin in Asians are limited.

Objective: This prospective, self-controlled study was conducted to evaluate the safety and efficacy of a thermo-mechanical fractional ablative device for the treatment of photo-damaged peri-orbital skin in Asians.

Materials and Methods: Twenty females (mean age of 48.7 years old) with skin type IV with peri-orbital line and laxity were enrolled. All subjects were treated with a fractional thermo-mechanical device (a tip protrusion of 400 μm and a pulse duration of 10 milliseconds), every 4 weeks for a total of 5 treatments. Objective (measurement of skin color and roughness using 3D photography and skin elasticity analysis using cutometer) and subjective [evaluated using the Physician Global Aesthetic Improvement Scale (GAIS) by two blinded dermatologists] assessments were obtained at baseline and at 1 and 3 months after the final treatment.

Results: GAIS assessments at 3 months after the last treatment indicated that 55.6%, 22.2% and 11.1% of the subject showing improvement, much improvement and very much improvement of their peri-orbital wrinkles and laxity, respectively. Improvement progressed significantly from 1- to 3-month follow-up. There was statistically significant brown lift ($P<.001$), comparing between baseline and 3 months after the final treatment. Reductions in periorbital indentation and wrinkles corresponded to clinical evaluation. Mild-moderate post-inflammatory hyperpigmentation (PIH) was observed in 22% of the subjects. All PIH was temporary and resolved on an average of 4 weeks.

Conclusions: The thermo-mechanical fractional ablative device is safe and effective for the treatment of peri-orbital lines and laxity in Asian.

SAFETY AND EFFICACY OF THERMOMECHANICAL FRACTIONAL INJURY FOR PERIORBITAL REJUVENATION

Jordan V Wang, MD, MBE, MBA; Shirin Bajaj, MD; David Orbuch, MD, MBA; Roy G Geronemus, MD

Background:

Periorbital rejuvenation is a common cosmetic concern by patients. A fractional thermomechanical skin rejuvenation system was recently developed to offer clinical improvements through neocollagenesis from direct heat transfer by pyramidal tips, which causes large volumes of dermal coagulation. The technology has been shown to be well tolerated and safe in various treatment areas. This study evaluates the safety and efficacy of the device for periorbital rejuvenation.

Study Design:

Subjects with moderate to severe periorbital rhytides were enrolled and underwent 4 monthly treatments with a novel device using thermomechanical fractional injury (Tixel 2, Novoxel, Netanya, Israel). Safety data was recorded during the study. Photographs were taken at all visits.

Results:

36 subjects were enrolled. 29 subjects completed the 4 monthly treatments and returned for 1-month follow-up evaluation. The mean age at time of treatment was 57.6 years (R: 38-69), and 89.7% of subjects were female. For Fitzpatrick skin type, 24.1% were type I, 31.0% were type II, 34.5% were type III, and 10.3% were type IV. For Fitzpatrick Wrinkle Classification System (FWCS), the mean score was 5.8 (R: 4-7).

All (100%) treatments were completed at 800um protrusion, with the majority (93.8%) at 12 msec pulse duration. The majority (92.5%) were treated using a double-pass method. There was a mean number of 92.9 (R: 38-132) pulses using the standard tip (1cm2) and 105.3 (R: 43-149) pulses using the small tip (0.3cm2). The mean pain score was 2.4 out of 10 during the treatment using only forced air cooling.

At 1-month follow-up, all (100%) of subjects had clinical improvement. For FWCS score, 10.3% had a 3-grade improvement, 65.5% had a 2-grade improvement, and 24.1% had a 1-grade improvement. There were no unexpected or severe adverse events observed throughout the study. Subjects experienced minimal post-procedural downtime with each treatment.

Conclusion:

A novel device using thermomechanical fractional injury has been demonstrated to be safe and efficacious in the treatment of periorbital rhytides.

Accepted: 5 November 2021

DOI: 10.1002/lsm.23494

CLINICAL REPORTS

Treatment of periorbital wrinkles using thermo-mechanical fractional injury therapy versus fractional non-ablative 1565 nm laser: A comparative prospective, randomized, double-arm, controlled study

Fares Salameh MD[1,2] | Danny Daniely MD[1,2] | Arielle Kauvar MD[3,4] | Rafael L. Carasso MD[5] | Joseph N. Mehrabi MD[2] | Ofir Artzi MD[1,2,6]

[1]Department of Dermatology, Tel Aviv Sourasky Medical Center, Tel Aviv, Israel

[2]Sackler Faculty of Medicine, Tel Aviv University, Tel Aviv, Israel

[3]New York Laser & Skin Care, New York, New York, USA

[4]Department of Dermatology, NYU Grossman School of Medicine, New York, New York, USA

[5]Department of Neurology and Pain Clinic, Hillel Yaffe Medical Center, Hadera, Israel

[6]Dr. Artzi and Associates Treatment and Research Center, Tel Aviv, Israel

Correspondence

Ofir Artzi, Sackler Faculty of Medicine, Aviv University, Aviv, Israel, 6 Weizman St, Aviv, 642906 Israel.
Email: benofir@gmail.com

Abstract

Background: Non-ablative fractional laser is an effective modality for the treatment of periorbital wrinkling, one of the earliest signs of skin aging. Thermo-mechanical fractional injury (TMFI) therapy (Tixel®, Novoxel®, Israel) is an innovative technology that is now being used for facial skin rejuvenation. Our study compares the clinical results, side effects, and downtime profile between TMFI treatment and non-ablative fractional 1565 nm laser (ResurFX®, Luminis, Israel).

METHODS: This was a prospective study of 68 patients (64 women, 4 men) with skin types I–VI in two medical centers (34 from Israel, 34 from the USA) that were randomized to receive either TMFI or NAFL treatment for periorbital wrinkling. Patients received 3–5 treatments, 3–5 weeks apart. Six months after the last treatment, the change in Fitzpatrick Wrinkling Classification System (FWCS) was calculated by three non-involved physicians and compared to pretreatment results. Side effects and downtime profiles were assessed in each group (including VAS pain assessment, time required to refrain from work and social activity, and time required for the resolution of redness, edema, and crusts.)

RESULTS: A moderate improvement in periorbital wrinkling was demonstrated in both groups, with an average improvement of 1.6 ± 0.6 in FWCS in the TMFI group and an average improvement of 1.7 ± 0.8 in the NAFL group ($p < 0.001$). Postprocedural VAS score was 5.86 ± 2.3 in the NAFL group and 4.01 ± 2.6 in the Tixel® group. Approximately 80% of subjects returned to both work and social activities two days postprocedure. Crusts were reported by 52% of patients in the TMFI group, compared to 16% of patients in the NAFL group more than 48 hours postprocedure ($p < 0.05$). There were no statistically significant differences in the other parameters between the two groups.

CONCLUSION: TMFI is an effective and safe modality for the treatment of periorbital wrinkling, with comparable results to the 1565 nm NAFL.

KEYWORDS

non-ablative fractional laser, periorbital rejuvenation, periorbital rhytides, periorbital wrinkling, thermomechanical fractional injury

INTRODUCTION

The periorbital area is one of the most challenging aesthetic regions to treat,[1] as most patients present with multiple changes, including edema, fine and coarse wrinkles, hyperpigmentation, dryness, and uneven texture.[2] Several modalities improve periorbital wrinkling. Aggressive invasive procedures are more likely to yield improved cosmesis but can result in longer downtime and a higher rate of adverse effects.[3–8] Non-ablative fractional 1565 nm Er:glass fiber laser (NAFL), was recently demonstrated to offer a mild-moderate improvement in periorbital wrinkling,[9] and was cleared for marketing this indication by the US Food and Drug Administration (FDA).

The Tixel is a non-laser, non-radiofrequency, thermomechanical fractional skin treatment device intended for cutaneous procedures requiring coagulation of soft tissue; it transfers heat to the skin directly without emitted radiation. Thermal energy is delivered to the tissue via a tip consisting of a grid of miniscule titanium pyramids. The tip is heated within the handpiece, and it is rapidly projected forward to contact the skin surface and coagulate tissue, creating microcraters of minor damage by evaporation and desiccation. The amount of thermal energy delivered to the skin is determined by the pulse duration (PD; range: 5–18 milliseconds) and protrusion distance or depth (100–1000 μm). The protrusion is defined as the distance the tip projects from the edge of the handpiece. A greater protrusion distance leads to a greater degree of skin contact between the titanium pyramids, thus fewer air gaps and greater thermal transfer are achieved. Importantly, thermal transfer in thermomechanical fractional injury (TMFI) spares the epidermis from full penetration. Representative histology of the skin damage from the Tixel in prior studies[10] are enclosed demonstrated in Figure 1.

Safety goggles are not required. Such technology offers an user-friendly method for performing fractional skin treatment, including the periorbital region and was recently demonstrated to moderately improve periorbital wrinkling as well.[11]

The purpose of this clinical trial is to compare the efficacy and adverse event (AE) profile of TMFI with 1565 nm Er:glass fiber laser in the treatment of periorbital wrinkling.

METHODS

This was a prospective, double-arm, randomized study of 68 patients with mild to moderate periorbital wrinkles, in two centers (Tel Aviv, Israel, and New York, NY, USA)

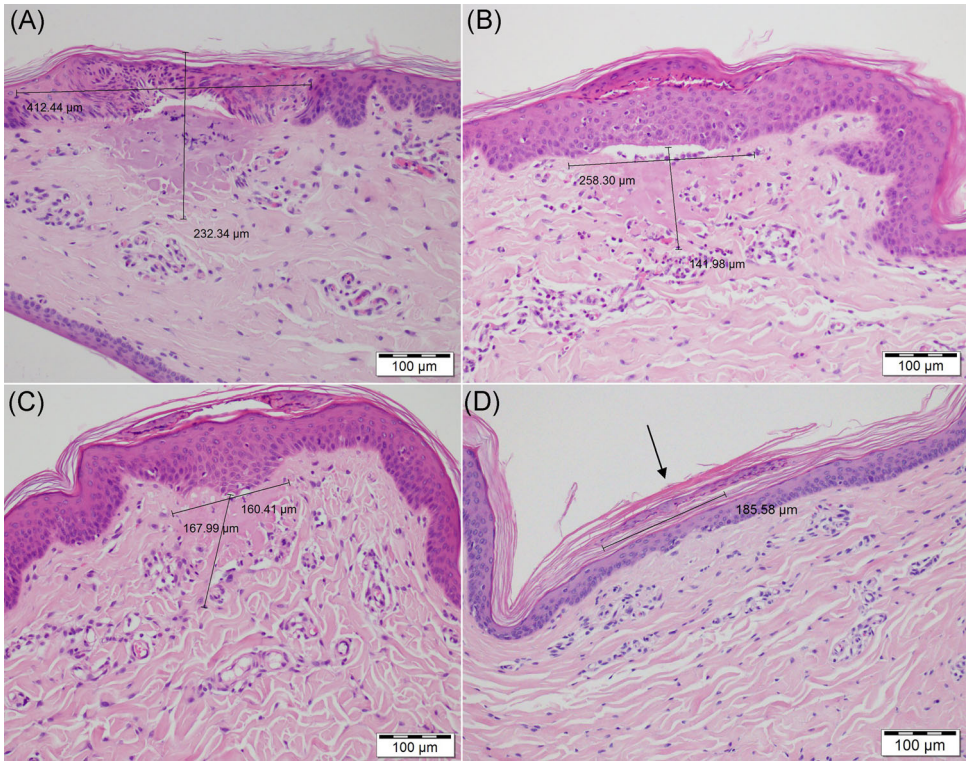

FIGURE 1 Representative skin biopsies in pigs demonstrate the following: (A) Immediately post Tixel treatment, a wedge-shaped dermal area of collagen coagulation (acute thermal necrosis), with no immediate (acute) inflammation, edema, or hemorrhage is found with capillary dilation. (B) At 24 hours posttreatment, thermal necrosis remains in both the dermis and epidermis. There may be separation of the dermoepidermal junction with minimal numbers of leukocytes and a serocellular crust with viable epidermis. (C) After 3 days, the epidermis is regenerated and remnants of degenerated dermal collagen are observed with separation of the dermoepidermal junction as well as scant number of leukocytes are observed. (D) At 14 days, there is a complete regeneration of lesions with minimal crust and minimal superficial fibroblast proliferation

using TMFI (34 patients) or NAFL (34 patients) that was conducted between March 2018 to November 2019. Three to five monthly treatments were performed, and patients were assessed during follow-up visits at 1, 3, and 6 months after the final treatment. The study was approved by an ethics committee/institutional review board and was performed consistent with the ethical standards of the Declaration of Helsinki. The participation in the study was voluntary, and participants were allowed to withdraw from the study at any time. Informed consent was obtained from each subject.

Participants

Inclusion criteria were as follows: healthy males or females, Fitzpatrick skin types I–VI, aged 40–70 years with clinically evident periorbital wrinkling who were willing and able to provide informed consent. Exclusion criteria were as follows: women who are pregnant or lactating; severe sun damage, keloid scarring or open wounds in the treatment areas; a prior cosmetic procedure to improve facial rhytids (i.e., rhytidectomy, periorbital or eyelid/eyebrow surgery, brow lift, CO_2/Erbium/similar laser/fractional resurfacing, or radiofrequency treatment) within 12 months; prior facial treatments with laser, surgical, chemical or light-based facial treatments within the previous 6 months (e.g., botulinum toxin injections, retinoid or glycolic acid treatment, or microdermabrasion); injectable filler in the treatment area within 9 months of the study, permanent facial implant, and inability to understand the treatment protocol or to give informed consent.

Device

The Tixel® (Novoxel®, Israel) is a non-laser, fractional, non-ablative, thermomechanical skin rejuvenation system which combines thermal energy with motion. The thermal energy is delivered to the tissue via a tip. The system consists of two types of tips, (1) a standard tip consisting of 81 (9 × 9) tiny titanium pyramids, and (2) a small tip (also known as the periorbital tip) consisting of 24 (6 × 4) tiny pyramids. The tip base is heated to 400°C within a handpiece, which quickly moves towards the skin surface to achieve contact and coagulate tissue, creating microcraters by evaporation and desiccation. The amount of thermal energy delivered to the skin is determined by the pulse duration (PD; range: 5–18 milliseconds) and distance by which the tip apexes extend beyond the distance gauge surface (protrusion) (100–1000 μm). A greater protrusion leads to a greater degree of skin contact between the titanium pyramids, fewer air gaps, and greater thermal transfer. Importantly, thermal transfer in TMFI technology does not involve any mechanical penetration of the epidermis. The fractional thermal effect typically consists of superficial epidermal ablation and vaporization and coagulation of the papillary dermis.

Treatment with both modalities was performed following the application of a topical anesthetic cream. Patients in the TMFI group were treated with both tip types. During each session, subjects received treatment with a constant PD of 10 milliseconds and a constant protrusion depth of 500 μm in one pass. Patients in the NAFL group were treated with the ResurFX™ (Lumenis) using the following settings: treatment density range between 150 and 300/cm^2, scan size: 8–17 mm, (mean 12 mm), and the energy range was 13–25 mJ (mean: 21 mJ).

AEs (redness, edema, and crusting) and downtime (number of days before returning to work and social activities) were recorded after each treatment. Standardized photographs were obtained under the same lighting conditions before each treatment and at the 6 months follow-up visit. The Visia skin analysis system (Canfield) was used in Israel and the Intellistudio system (Canfield) was used in the NY site.

Blinded grading of photographs

The degree of improvement observed following TMFI and NAFL treatments was assessed by presenting pre-treatment and 6-month follow photographs in a randomized order to three independent physicians who were not involved in the study. Scores were assessed using the Fitzpatrick Wrinkle Classification System (FWCS), a scoring system on a scale of 0 (no wrinkles) to 9 (deep and numerous wrinkles). The mean improvement was calculated and compared between the two groups.

Patient questionnaires

Patients evaluated their treatment pain, AEs, and recovery time at each follow-up visit. This consisted of rating the tolerability of the treatment using the Visual Analog Scale (VAS) for pain assessment (1–10), reporting the presence of redness, edema, and crusts (less or more than 2 days post-procedure), and calculating the time to return to work and social activity (less or more than 2 days postprocedure). The results were compared between the two treatment groups.

Analyses were mainly descriptive in nature, summarized by count and percentage for categorical variables and mean, median, minimum, and maximum percentiles with standard error for continuous variables. Baseline and posttreatment outcomes were analyzed using Fisher's test for categorical variables. All statistical analyses were performed by SPSS version 25.0 (IBM Corporation).

RESULTS

Sixty-eight patients (34 from Israel, 34 from the United States; 64 women, 4 men) were included in this study. The age of the participants ranged from 40 to 70 years

TABLE 1 Demographics and treatment characteristics

Demographics	Tixel		ResurFX	
	N	%	*N*	%
Gender				
Male	0	0	4	11.8
Female	34	100	30	80.2
Ethnicity				
Asian	2	5.9	2	5.9
Black or African American	0	0	3	8.8
White	30	88.2	24	70.6
Other	2	5.9	5	14.7
Fitzpatrick Skin Type				
I	1	2.9	0	0
II	15	44.1	15	44.1
III	12	35.3	10	29.4
IV	5	14.7	5	14.7
V	1	2.9	2	5.9
VI	0	0	2	5.9
No. of Tx				
3	11	44	9	41
5	13	56	13	59

(average 52 years). Patient's demographics are elaborated in Table 1. Forty-four percent (11 patients) and 41% (9 patients) completed three treatments, while 56% (14 patients) and 59% (13 patients) completed five treatments with TMFI and NAFL, respectively.

Blinded photographic analysis using the FWCS demonstrated a moderate improvement with both devices six months after treatment; there was an average improvement of 1.6 ± 0.6 in the TMFI group (Figures 2 and 3) and an average improvement of 1.7 ± 0.8 in the NAFL group. There was no difference between the two treatment groups with regard to FWCS score improvement ($p > 0.05$), and improvement from baseline was statistically significant for both treatment modalities ($p < 0.001$).

There was a statistically significant ($p < 0.05$) difference in the average pain score using the VAS between the two treatment groups, with a VAS score of 5.86 ± 2.3 in the NAFL group versus $4.01 + 2.6$ in the TMFI group. There was no difference between the two groups in the time required for resolution of erythema and edema. Figure 4 demonstrates the 5-day healing process for a representative patient treated with the Tixel. However, in the TMFI group, crusts lasted for more than 2 days postprocedure and were present in 52% of patients compared to 16% of the NAFL group. There was no statistically significant difference in downtime between the two groups, and 83%/81% of patients returned to work and 79%/77% returned to social activities two days postprocedure for TMFI/NAFL respectively (Figure 5). For most patients, the pinpoint scabbing and crusting that results immediately after treatment can be masked by makeup and lasts from a few hours to 1 day postprocedure. Patients described a mild burning and stinging sensation for 1–2 hours postprocedure.

Three separate subjects (4.4%) reported four total AEs. Two subjects (5.9%) in the TMFI arm reported dry and/or watery eyes, and one subject (2.9%) in the NAFL arm developed uveitis, which was determined to be unrelated to the treatment. All AEs resolved except for the uveitis, the outcome of which was unknown because the patient was lost to follow-up.

DISCUSSION

Periorbital wrinkles are an early manifestation of photoaging. The cause of periorbital wrinkling is multifactorial and includes intrinsic aging, extrinsic aging (largely ultraviolet light exposure), repetitive use of facial muscles with expressions, skin type, hormonal status, genetic inclination, ethnicity, nutrition, and other medical disorders.[12] Periorbital wrinkles may occur as early as the third decade of life and often distressing to patients, causing them to seek rejuvenation procedures.

There are a variety of treatment options to mitigate the signs of periorbital skin aging, including topical retinoids,[13] radiofrequency,[14,15] broadband infrared,[16] intense pulsed light,[17] chemical peels,[18] botulinum toxin,[19] and platelet-rich plasma (PRP),[5] and non-ablative and ablative laser resurfacing procedures.[15,20] Full surface and fractional ablative resurfacing procedures are effective in improving periorbital wrinkles and laxity, but, because the epidermis is ablated, the recovery may take 1–2 weeks, and posttreatment erythema and hyperpigmentation commonly emerge, especially in darker skin types. Fractional ablative resurfacing has safely improved rhytid and periorbital line clearance, but because of the removal of the epidermis, patients treated with CO_2 resurfacing can have many side effects.[21] Over the course of the last decade, NAFL treatments have gained increasing popularity because of the limited recovery time and incidence of AEs, by delivering energy into the dermis without destroying the overlying epidermis.[22] Several studies have corroborated their efficacy in improving skin elasticity and enhanced tightening with minimal AEs and downtime.[9,23,24]

The present study compares the safety and efficacy of two non-ablative fractional technologies in the treatment of periorbital wrinkles: TMFI technology and NAFL with a 1565 nm laser. Blinded evaluation of pretreatment and posttreatment photographs using the FWCS demonstrated similar wrinkle improvement with both

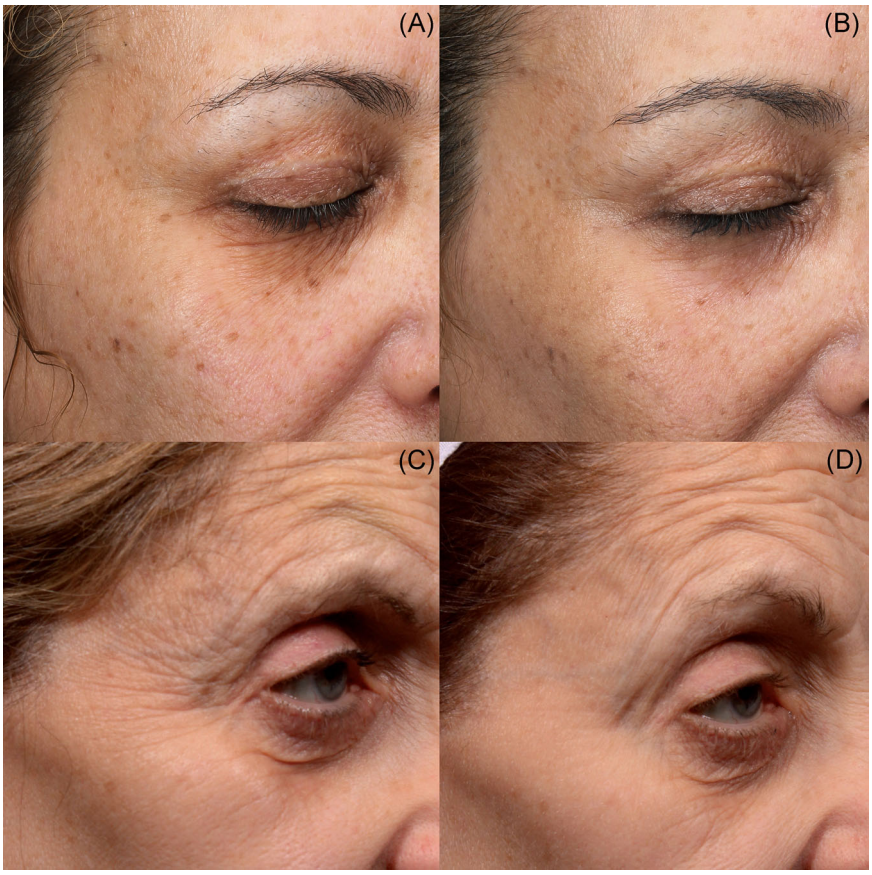

FIGURE 2 Representative patients before (A, C) and after (B, D) 4 (upper) and 3 (lower) Tixel® treatments. Please note the change in periorbital wrinkles

FIGURE 3 Representative patients before (A, C) and after (B, D) 4 (upper) and 3 (lower) Tixel® treatments. Please note the change in periorbital wrinkles

devices. Mean improvement of the FWCS was 1.6 ± 0.6 for TMFI and 1.7 ± 0.8 for the laser. The observed AEs of both devices were mild and transient.

The settings chosen with the NAFL in this study are frequently used and recommended for treatment of periorbital regions. The developers of the Tixel provided recommended settings for periorbital rejuvenation for their device, which was a pulse duration of 12 milliseconds and 600 μm protrusion. In this study, we chose a more conservative approach with a pulse duration of 10 milliseconds and 500 μm protrusion. It has been previously shown that pulse durations around 6 milliseconds are used for drug delivery and those greater than 10 milliseconds are used for rejuvenation; common settings for rejuvenation are 12–14 milliseconds.[11,25,26] As the periorbital region is a sensitive area, coordinating treatment at two centers in different countries with diverse populations warranted more conservative treatment parameters. The depth was chosen based

FIGURE 4 Images of a representative patient's periorbital treatment with the Tixel and recovery at baseline (A, B), Day 1 (C, D), Day 2 (E, F), Day 3 (G, H), and Day 5 (I, J) after treatment

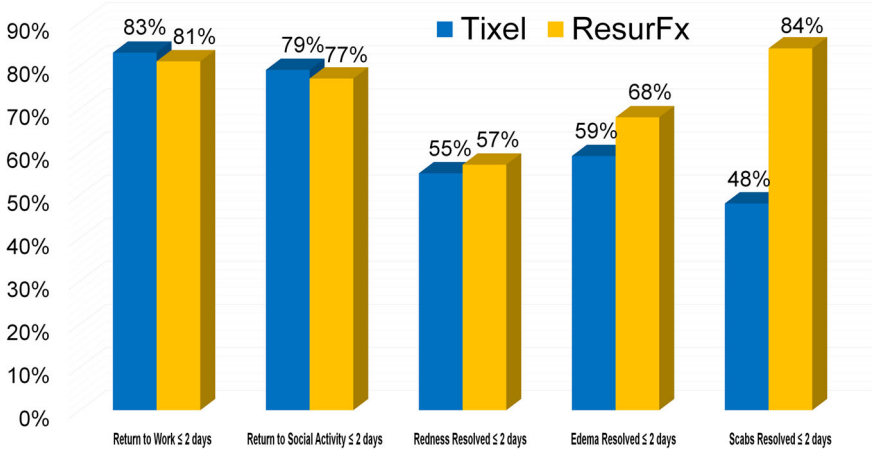

FIGURE 5 A comparison of downtime parameters between the two treatment groups

on the depth of the periorbital skin to the reach the papillary dermis ~300 μm (Figure 1).

The drop-out rate in this study was relatively high, potentially due to poor patient selection and the relatively high number of visits required. However, a lower rate of study withdrawal was observed in the TMFI arm (Tixel: 9/34 [26.5%] vs. laser: 12/34 [35.3%]). This may indicate better patient satisfaction and or lower treatment discomfort and posttreatment pain following TMFI treatment compared with the laser device. The VAS score for pain with the Tixel was significantly lower than with the laser. No statistically significant differences were found between the devices with regard to downtime, with the exception of longer duration of crusts after TMFI treatment. This is an anticipated finding, due to focal epidermal ablation induced by the pyramid tips.

This study has many limitations. Frequently, patients presented with periorbital comorbidities including hypertrophy of the orbicularis oculi muscle, fat herniation, dyspigmentation, and edema, which were not exclusion criteria. Furthermore, this study is limited due to its inability to address the underlying issue of limiting the movement of the orbicularis oculi muscle to mitigate periorbital rhytid formation. It is possible that more pronounced improvement would have been observed if patients with no comorbidities and pure periorbital skin laxity were selected. In this study, a single TMFI pass was applied, yielding 7%–8% active area. To potentially enhance improvement with this therapy in the future, multiple passes should be performed to increase coverage and yield better results.

The patient cohort was limited in size, especially since patients were lost to follow-up, and comparison was performed between treatment arms rather than a split-face design, making it more difficult to control for different posttreatment responses among different patients. As this study was conducted at two separate treatment centers, consistent photography was difficult to maintain. To accommodate our patients, treatment schedules were flexible, allowing for 3–5 treatments, adding an element of inconsistency.

In this study, we demonstrate that the TMFI device is effective in improving periorbital wrinkles with minimal AEs, and recovery time. TMFI technology is an excellent modality for drug delivery owing to its formation of micron-sized wells in the epidermis lined by a thin rim of coagulation.[11,27–29] As wrinkling in the periorbital region is exacerbated by constant contraction of the orbicularis oculi muscles with facial expression, the use of TMFI technology to deliver botulinum toxin may achieve a more profound improvement, by both diminishing muscle contraction and stimulating collagen production and remodeling in a region where the skin is thinnest.

CONFLICT OF INTERESTS

The authors declare that there are no conflict of interests.

ORCID

Danny Daniely http://orcid.org/0000-0002-8852-9384
Arielle Kauvar http://orcid.org/0000-0001-7594-1399
Ofir Artzi http://orcid.org/0000-0003-1391-5843

REFERENCES

1. Yaar M, Gilchrest BA. Photoageing: mechanism, prevention and therapy. Br J Dermatol. 2007;157(5):874–87. https://doi.org/10.1111/j.1365-2133.2007.08108.x
2. Glaser DA, Patel U. Enhancing the eyes: use of minimally invasive techniques for periorbital rejuvenation. J Drugs Dermatol. 2010;9(8 suppl ODAC Conf Pt 2):s118–28.
3. Woodward J. Review of periorbital and upper face: pertinent anatomy, aging, injection techniques, prevention, and management of complications of facial fillers. J Drugs Dermatol. 2016;15:1524–31.
4. Manaloto RMP, Alster TS. Periorbital rejuvenation: a review of dermatologic treatments. Dermatol Surg. 1999;25(1):1–9. https://doi.org/10.1046/j.1524-4725.1999.08049.x
5. Evans AG, Ivanic MG, Botros MA, Pope RW, Halle BR, Glassman GE, et al. Rejuvenating the periorbital area using platelet-rich plasma: a systematic review and meta-analysis. Arch Dermatol Res. 2021;313:711–27. https://doi.org/10.1007/s00403-020-02173-z
6. Glaser DA, Kurta A. Periorbital rejuvenation: overview of non-surgical treatment options. Facial Plast Surg Clin North Am. 2016;24(2):145–52. https://doi.org/10.1016/j.fsc.2016.01.003
7. Alster TS, Garg S. Treatment of facial rhytides with a high-energy pulsed carbon dioxide laser. Plast Reconstr Surg. 1996;98(5):791–794. https://doi.org/10.1097/00006534-199610000-00005

8. Shook BA, Hruza GJ. Periorbital ablative and nonablative resurfacing. Facial Plast Surg Clin North Am. 2005;13(4):571–82. https://doi.org/10.1016/j.fsc.2005.06.007
9. Horovitz T, Clementoni MT, Artzi O. Nonablative laser skin resurfacing for periorbital wrinkling—a case series of 16 patients. J Cosmet Dermatol. 2021;20(1):99–104. https://doi.org/10.1111/jocd.13851
10. Elman M, Fournier N, Barneon G, Bernstein EF, Lask G. Fractional treatment of aging skin with Tixel, a clinical and histological evaluation. J Cosmet Laser Ther. 2016;18(1):31–7. https://doi.org/10.3109/14764172.2015.1052513
11. Daniely D, Judodihardjo H, Rajpar SF, Mehrabi JN, Artzi O. Thermo-mechanical fractional injury therapy for facial skin rejuvenation in skin types II to V: a retrospective double-center chart review. Lasers Surg Med. 2021;53:1152–57. https://doi.org/10.1002/lsm.23400
12. Roh NK, Yoon YM, Lee YW, Choe YB, Ahn KJ. Treatment of periorbital wrinkles using multipolar fractional radiofrequency in Korean patients. Lasers Med Sci. 2016;32(1):61–6. https://doi.org/10.1007/s10103-016-2084-7
13. Bagatin E, Gonçalves HS, Sato M, Almeida LMC, Miot HA. Comparable efficacy of adapalene 0.3% gel and tretinoin 0.05% cream as treatment for cutaneous photoaging. Eur J Dermatol. 2018;28(3):343–50. https://doi.org/10.1684/ejd.2018.3320
14. Kwon SH, Choi JY, Ahn GY, Jang WS, Shin JW, Na JI, et al. The efficacy and safety of microneedle monopolar radiofrequency for the treatment of periorbital wrinkles. J Dermatolog Treat. 2019;32:1–5. https://doi.org/10.1080/09546634.2019.1662880
15. Milante RR, Doria-Ruiz MJ, Beloso MB, Espinoza-Thaebtharm A. Split-face comparison of grid fractional radiofrequency vs 1064-nm Nd-YAG laser treatment of periorbital rhytides among Filipino patients. Dermatol Ther. 2020;33(6):e14031. https://doi.org/10.1111/dth.14031
16. Monica E. Periorbital skin tightening with a broadband infrared device: preliminary study results. J Cosmet Laser Ther. 2010;12(1):38–41. https://doi.org/10.3109/14764170903449760
17. Barikbin B, Akbari Z, Vafaee R, Razzaghi Z. The efficacy of IPL in periorbital skin rejuvenation: an open-label study. J Lasers Med Sci. 2019;10(suppl 1):S64–s67. https://doi.org/10.15171/jlms.2019.S12
18. Lee KC, Sterling JB, Wambier CG, Soon SL, Landau M, Rullan P, et al. Segmental phenol-Croton oil chemical peels for treatment of periorbital or perioral rhytides. J Am Acad Dermatol. 2019;81(6):e165–6. https://doi.org/10.1016/j.jaad.2018.11.044
19. Eftekhari MH, Aghaei H, Kangari H, Bahrami M, Eftekhari S, Tabatabaee SM, et al. Abobotulinum toxin A for periorbital facial rejuvenation: impact on ocular refractive parameters. Clin Exp Optom. 2021;104(1):115–8. https://doi.org/10.1111/cxo.13117
20. Augustyniak A, Rotsztejn H. Fractional non-ablative laser treatment at 1410 nm wavelength for periorbital wrinkles - reviscometrical and clinical evaluation. J Cosmet Laser Ther. 2016;18(5):275–9. https://doi.org/10.3109/14764172.2016.1157370
21. Bonan P, Campolmi P, Cannarozzo G, Bruscino N, Bassi A, Betti S, et al. Eyelid skin tightening: a novel 'Niche'for fractional CO2 rejuvenation. J Eur Acad Dermatol Venereol. 2012;26(2):186–93.
22. Alexiades-Armenakas MR, Dover JS, Arndt KA. The spectrum of laser skin resurfacing: nonablative, fractional, and ablative laser resurfacing. J Am Acad Dermatol. 2008;58(5):719–37. https://doi.org/10.1016/j.jaad.2008.01.003
23. Jung JY, Cho SB, Chung HJ, Shin JU, Lee KH, Chung KY. Treatment of periorbital wrinkles with 1550- and 1565-nm Er:-glass fractional photothermolysis lasers: a simultaneous split-face trial. J Eur Acad Dermatol Venereol. 2011;25(7):811–8. https://doi.org/10.1111/j.1468-3083.2010.03870.x
24. Sukal SA, Chapas AM, Bernstein LJ, Hale EK, Kim KH, Geronemus RG. Eyelid tightening and improved eyelid aperture through nonablative fractional resurfacing. Dermatol Surg. 2008;34(11):1454–8. https://doi.org/10.1111/j.1524-4725.2008.34308.x
25. Artzi O, Mehrabi JN, Heyman L, Friedman O, Mashiah J. Treatment of port wine stain with Tixel-induced rapamycin delivery following pulsed dye laser application. Dermatol Ther. 2020;33(1):e13172. https://doi.org/10.1111/dth.13172
26. Hilerowicz Y, Friedman O, Zur E, Ziv R, Koren A, Salameh F, et al. Thermomechanical ablation-assisted photodynamic therapy for the treatment of acne vulgaris. A retrospective chart review of 30 patients. Lasers Surg Med. 2020;52(10):966–70. https://doi.org/10.1002/lsm.23246
27. Shavit R, Dierickx C. A new method for percutaneous drug delivery by thermo-mechanical fractional injury. Lasers Surg Med. 2020;52(1):61–9. https://doi.org/10.1002/lsm.23125
28. Foged C, Haedersdal M, Bik L, Dierickx C, Phillipsen PA, Togsverd-Bo K. Thermo-mechanical fractional injury enhances skin surface-and epidermis-protoporphyrin IX fluorescence: comparison of 5-aminolevulinic acid in cream and gel vehicles. Lasers Surg Med. 2020;53(5):622–9.
29. Sintov AC, Hofmann MA. A novel thermo-mechanical system enhanced transdermal delivery of hydrophilic active agents by fractional ablation. Int J Pharm. 2016;511(2):821–30. https://doi.org/10.1016/j.ijpharm.2016.07.070

How to cite this article: Salameh F, Daniely D, Kauvar A, Carasso RL, Mehrabi JN, Artzi O. Treatment of periorbital wrinkles using thermo-mechanical fractional injury therapy versus fractional non-ablative 1565 nm laser: a comparative prospective, randomized, double arm, controlled study. Lasers Surg Med. 2021;1–8. https://doi.org/10.1002/lsm.23494

Accepted: 4 December 2021

DOI: 10.1002/lsm.23511

CLINICAL REPORT

Efficacy and safety of thermomechanical fractional injury-assisted corticosteroid delivery versus intralesional corticosteroid injection for the treatment of hypertrophic scars: A randomized split-scar trial

Woraphong Manuskiatti MD[1] | **Chadakan Yan MD**[1] | **Ofir Artzi MD**[2] | **Mia Katrina R. Gervasio MD**[1] | **Rungsima Wanitphakdeedecha MD**[1]

[1]Department of Dermatology, Faculty of Medicine Siriraj Hospital, Mahidol University, Bangkok, Thailand

[2]Department of Dermatology, Tel Aviv Sourasky Medical Center, Tel Aviv, Israel

Correspondence

Woraphong Manuskiatti, MD, Department of Dermatology, Faculty of Medicine Siriraj Hospital, Mahidol University, 2 Wanglang Rd, Bangkok 10700, Thailand.
Email: woraphong.man@mahidol.edu

Abstract

Background: Disruption of the natural skin barrier in a controlled manner may be used to deliver drugs that enhance scar resolution.

Objective: To compare the efficacy and safety of thermomechanical fractional injury (TMFI)-assisted topical corticosteroid delivery with corticosteroid injection in the treatment of hypertrophic scar (HTS).

Materials and Methods: This was a randomized, split-scar, double-blinded study. Twenty-one subjects with HTS on the abdomen received five split-scar treatments of TMFI + Steroid and steroid injection alone. Changes in scar thickness, scar volume, and Vancouver Scar Scale (VSS) were analyzed. Patient self-assessment, VAS scores, and adverse effects were also evaluated.

Results: Scar thickness, volume, and VSS scores of both segments improved significantly compared to baseline. On every follow-up visit, there were no significant differences in mean scar thickness reduction between the two treatment groups except at the 6-month follow-up where the mean scar thickness reduction of the steroid injection segment was significantly lower than that of the TMFI + Steroid segment (95% confidence interval [CI], 0.09–0.35; $p = 0.002$). Scar volume, VSS scores, and patient self-assessment also showed no significant differences between both segments on all visits. The steroid injection segment was significantly more painful than the TMFI + Steroid segment (95% CI, −2.16 to −1.29; $p < 0.001$). Adverse effects of skin atrophy, telangiectasia, and post-inflammatory hyperpigmentation were noted in the steroid injection segment, while no adverse effects were observed at the TMFI + Steroid segment.

Conclusions: TMFI-assisted topical corticosteroid delivery is an effective treatment for HTS with a lower risk of adverse effects compared with corticosteroid injection.

KEYWORDS

corticosteroids, drug delivery, hypertrophic scar, intralesional injection, keloid, thermomechanical fractional injury

INTRODUCTION

Hypertrophic scar (HTS) is a dermal fibroproliferative disorder that presents at sites of prior injury and wound repair. It is characterized by excessive deposition of collagen with altered morphology following local skin trauma or inflammatory skin disorders.[1,2] HTS may present with symptoms of pain, pruritus, and hyperesthesia.[3] These cause cosmetic disfigurement, and when present over mobile areas of the skin, may even cause contractions and limitations in joint mobility.[1]

Intralesional corticosteroid injection remains to be one of the most widely used first-line monotherapies for HTS.[3,4] Corticosteroids exert their effects on HTS via several mechanisms: (1) inflammatory response suppression, (2) vasoconstriction, (3) antimitotic inhibition of keratinocytes and fibroblasts causing slowed re-epithelialization and new collagen formation, and (4) downregulation of α-1-antitrypsin and α-2-macroglobulin inhibitors resulting in collagen degradation via increased collagenase activity.[5,6] The major drawback of corticosteroid injections is pain during administration, especially for pediatric patients and for those with large or multiple areas of involvement.[7] Other local side effects include bleeding at the injection site, infection of the injected skin areas, thinning and atrophy of the skin and subcutaneous tissue, development of steroid acne, telangiectasias, and hypopigmentation.[5,7]

Thermomechanical fractional injury (TMFI) facilitates the transcutaneous absorption of topical medications via the creation of micropores through the stratum corneum.[8–11] This relatively novel technique uses a heated (400°C) titanium medical grade tip comprising of 81 (9 × 9) pyramid-shaped micro-pins covering an area of 1 cm^2. The handpiece is placed vertically on the skin and when activated the tip travels at a preset speed and recedes in an automated fashion. The tip's apex comes into brief contact with the skin (6–18 milliseconds) to conduct heat, directly applying about 0.2 mJ/pyramid. At low settings, it creates an array of 81 fractional microscopic porous hemisphere-shaped thermal injury sites (200-μ deep and 300-μ wide) in which the stratum corneum layer is partially ablated. These sites exhibit enhanced permeability to hydrophilic topically applied substances. Permeability is facilitated by the humidity gradient that is formed between the skin surface and its underlying layers. The tip evaporates water during contact with the surface, with skin temperature decreasing relative to the distance between the tip (apex) and the affected tissue. Hence, water concentration within the tissue varies from very low concentration near the tip (low relative humidity) to that of normal skin water concentration at the base (high relative humidity), thereby providing an alternative pathway for drug flow into the skin.[10]

TMFI-assisted drug delivery has been shown by recent studies to overcome the local complications of intralesional injections while maintaining therapeutic concentrations of the drug at the target area.[12–15] The aim of this study is to compare the efficacy and safety of TMFI-assisted corticosteroid delivery with intralesional corticosteroid injection for the treatment of HTS.

METHODS

This was a prospective, randomized, split-scar, double-blinded comparative clinical study conducted between April 2020 and January 2021. The study was approved by the Siriraj Institutional Review Board, Faculty of Medicine, Siriraj Hospital, Mahidol University, Thailand (Si 719/2018) and was registered at ClinicalTrials.gov online registry (NCT04597060). Written informed consent was obtained from all subjects before treatment.

A total of 27 subjects with Fitzpatrick skin types (FST) III–IV with abdominal HTS resulting from surgery of at least 6 months' duration were enrolled. Subjects received a total of five treatment sessions given at 1-month intervals. Each scar was divided equally into two segments along its long axis to receive either "TMFI + Steroid" or "Steroid injection" only. Treatment assignment for each scar segment was generated using a block randomization plan from an online random block generator (www.randomization.com). Half of each scar assigned to the "TMFI + Steroid" treatment arm received TMFI (Tixel®; Novoxel® Ltd.) followed by immediate topical corticosteroid application using triamcinolone acetonide (TAC) suspension (40 mg/ml; 0.1 ml per 1 cm scar length) gently rubbed onto the scar for 2–3 minutes. A TMFI device (exposure time of 10 milliseconds; protrusion depth of 400 μm) was used to treat the designated scar section and a commercially available air-cooling machine (Cryo 6; Zimmer Aesthetics) was used to minimize pain and discomfort during the treatment. The "Steroid injection" segment was treated with intralesional TAC suspension (10 mg/ml) injection with a sufficient amount achieving complete blanching of the lesion. Only the treating physician (W.M.) was aware of the scar treatment assignment, while physician-observers involved in the preliminary and posttreatment assessment of the scars were blinded to the split-scar distribution.

Postoperatively, the scars were occluded under a transparent film dressing (Tegaderm™; 3M Health Care) left in place for at least 3 hours. No other post-procedural wound care instructions were given to the subjects.

CLINICAL ASSESSMENT

Objective and subjective evaluations regarding clinical improvement of the scars and adverse effects were obtained at baseline, then at 4-week intervals for a total of five sessions during the treatment phase, and during post-procedure follow-ups at 1-, 3-, and 6-month after the final (5th) treatment. All clinical photographs were taken with identical camera settings, lighting, and positioning. The objective evaluation included the measurement of HTS thickness using a dial caliper (Mitutoyo; Kanagawa, Japan), and scar volume using a skin imaging device (Antera® 3D CS; Miravex Limited). The means of three measurements of HTS thickness and scar volume for each subject were recorded. Systematic evaluation using the Vancouver Scar Scale (VSS)[16] was conducted by two treatment-blinded dermatologists.

This numerical scale ranging from 0 to 13 assesses four scar characteristics including vascularization, pliability, pigmentation, and height/thickness—the larger the number the worse the scar.

Patients were also asked to evaluate pain levels following the treatment for each segment using a visual analog scale (VAS), with the scale ranging from 0 (no pain) to 10 (severe pain). Recovery time and adverse effects and were also recorded at each treatment session and follow-up visit. During the final follow-up (6 months after the 5th treatment), patient self-assessment of overall scar improvement was done. The patients graded the improvement compared to a standardized photograph taken at baseline. Grading was done using percentages at 25% increments ranging from 0% (no improvement) to 100% (complete improvement).

Statistical analyses

Descriptive analysis was used for demographic data. Data were analyzed using a two-sided paired *t-test* with a confidence interval of 95% to assess the difference between the two treatment arms. Repeated measure analysis of variance (ANOVA) was used to compare differences between individual split-scars. Statistical analysis was performed using statistical software (IBM SPSS version 24.0; IBM) with $p < 0.05$ considered to be significant.

RESULTS

Patient demographic information is shown in Table 1. Twenty-one (18 females and 3 males) of the 27 subjects (77.8%) successfully completed the study protocol and were included in the final analysis. Six subjects withdrew from the study due to scheduling conflicts or were lost to follow-up. The mean age of the participants was 35.5 years (range, 22–54 years) and the majority had FST III (71.4%). The median scar duration was 3 years (range, 0.8–20 years).

HTS thickness

At baseline, there were no significant differences in the mean scar thickness between the two treatment groups (95% CI, −0.02 to 0.43; $p = 0.072$). In both TMFI + Steroid and steroid injection groups, mean scar thickness showed significant improvement when compared to baseline at all time points ($p < 0.001$) (Figure 1). On every follow-up visit, there were no significant differences in mean scar thickness reduction between the two treatment groups except at the 6-month follow-up where the mean scar thickness reduction of the steroid injection segment was significantly lower than that of the TMFI + Steroid segment (95% CI, 0.09–0.35; $p = 0.002$). Compared to baseline, the mean percentages of scar thickness reduction of the TMFI + Steroid segment were 56.7%, 60.5%, and 64.3% at 1-, 3-, and 6-months posttreatment, respectively, whereas the mean percentages of scar thickness reduction of the steroid injection segment were 46.9%, 65.0% and 74.2% at 1-, 3-, and 6-months posttreatment, respectively. Figure 2 shows the appearance of HTS in a representative patient at baseline and at 6 months after the final treatment.

Scar volume

At baseline, there were no significant differences in the mean scar volume between the two treatment segments

TABLE 1 Patient demographics

Characteristics	Value	*p* Value
Age, mean ± SD (min–max)	35.5 ± 7.96 years (22–54)	
Sex, *n* (%)		
Male	3 (14.3)	
Female	18 (85.7)	
Fitzpatrick skin type, *n* (%)		
III	15 (71.4)	
IV	6 (28.6)	
Duration of Scar, median (min–max)	3.0 years (0.8–20)	
Scar thickness by caliper, mean ± SD (min–max)	1.63 ± 0.83 mm (0.40–3.80)	0.072
TMFI + Steroid		
Steroid injection alone	1.43 ± 0.93 mm (0.10–4.10)	

Abbreviations: max, maximum; min, minimum.

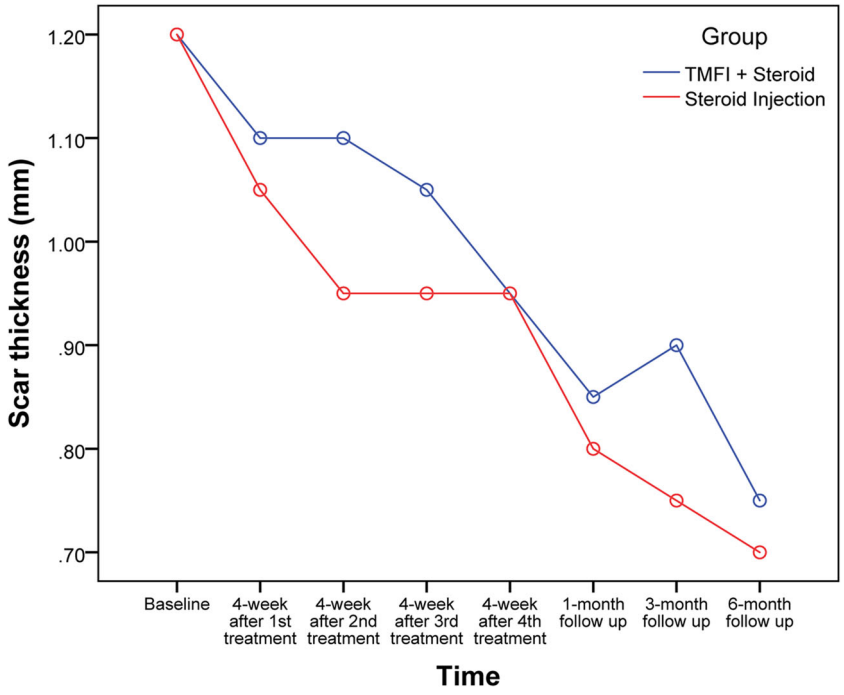

FIGURE 1 Mean scar thickness from baseline up to the 6-month follow-up visit

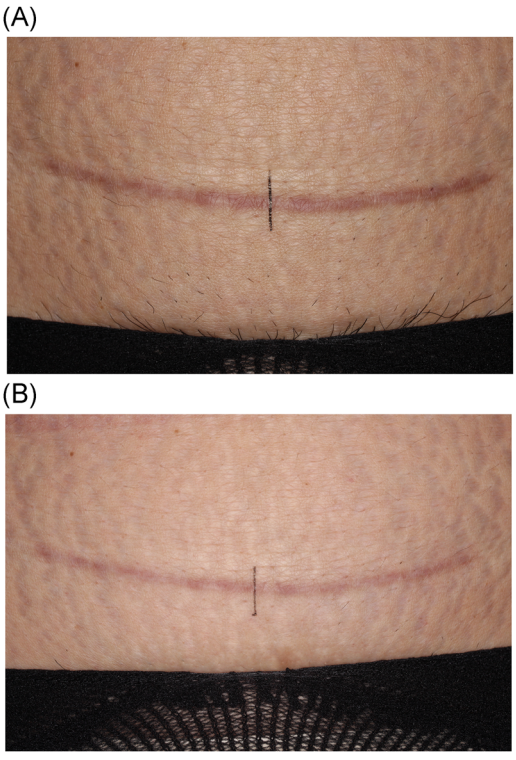

FIGURE 2 A 1-year duration hypertrophic scar in a 30-year-old patient with FST IV. The left half of the scar was treated with thermomechanical fractional Injury (TMFI) + steroid and the right half was treated with steroid injection. (A) Before treatment, (B) 6 months after five treatments

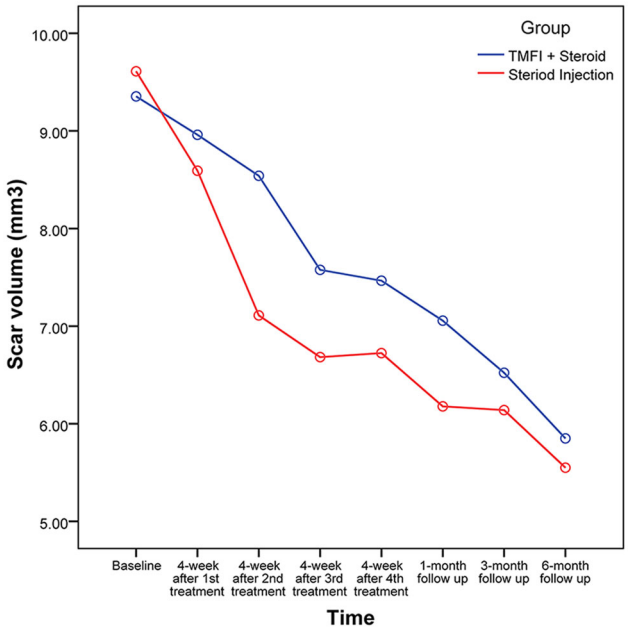

FIGURE 3 Mean scar volume from baseline up to the 6-month follow-up visit

(95% CI, −1.88 to 1.37; $p = 0.745$). In both TMFI + Steroid ($p = 0.014$) and steroid injection ($p = 0.001$) arms, the mean scar volume significantly decreased when compared to baseline at all time points (Figure 3). However, there were no significant differences in mean volume reduction from baseline when comparing the two interventional segments on every follow-up visit. The mean scar volume of the TMFI + Steroid segment decreased by 24.6%, 30.3%, and 37.5% from baseline, at 1-, 3-, and 6-month follow-ups, respectively, whereas the mean scar volume of the steroid injection segment decreased by 35.7%, 36.1%, and 42.3% from baseline, at 1, 3, and 6 months after the final treatment, respectively.

VSS

Before treatment, the VSS scores showed no significant differences between the two treatment segments (95% CI, −0.35 to 0.44; $p = 0.803$). The mean VSS scores of both the TMFI + Steroid and steroid injection branches showed significant improvement when compared to baseline at all time points ($p < 0.001$). At 6 months after the final treatment, the mean VSS of the TMFI + Steroid reduced from 6.61 ± 1.82 at baseline to 2.28 ± 1.70 (95% CI, 3.30–5.37; $p < 0.001$), whereas the mean VSS of the steroid injection segments decreased from 6.57 ± 2.11 at baseline to 2.52 ± 1.83 (95% CI, 2.49–5.61; $p < 0.001$). No significant differences in the mean VSS reduction between the TMFI + Steroid and steroid injection segments were present on each follow-up visit.

Patient self-assessment

At 6 months after the final treatment, 47.6% of the TMFI + Steroid group and 42.9% of the steroid injection group rated themselves as having more than 75% improvement from baseline. None of the patients reported 0% improvement. All patients preferred the overall treatment experience and outcome of the TMFI + Steroid segment compared to that of the steroid injection segment.

Recovery time, pain scores and adverse effects

Immediately after treatment, mild or moderate erythema and swelling lasting 3.12 ± 0.69 days were noted in all TMFI + Steroid segments. Bruise lasting 7.25 ± 0.69 was observed in 3 of 21 (14.2%) of the steroid injection segments. The mean VAS pain scores were 3.13 ± 1.84 and 4.79 ± 2.11 on the TMFI + Steroid with concomitant air cooling and steroid injection segments, respectively. The steroid injection segment was significantly more painful than the TMFI + Steroid segment with concomitant air cooling (95% CI, −2.16 to −1.29; $p < 0.001$). Adverse effects include skin atrophy (47.6%, 10/21 patients), telangiectasia (4.7%, 1/21), and post-inflammatory hyperpigmentation (9.5%, 2/21) which were noted in the steroid injection segments. No adverse effects were observed in the TMFI + Steroid segments on all follow-up visits.

DISCUSSION

The efficacy of a topical drug is correlated not only to its intrinsic potency but also to its ability to penetrate the layers of the skin, the principal barrier of which is the stratum corneum. Several modalities that alter or remove the stratum corneum have been used to facilitate the uptake of topical medications, including ablative fractional lasers, microdermabrasion, microneedling, sonophoresis, and radiofrequency, to name a few.[10,17,18]

As a means to enhance transdermal drug delivery, TMFI uses the transfer of thermal energy to create micropores on the skin. It combines a thermal effect of drying the skin and a motion effect of stretching the tissue in contact, leading to the formation of cracks that break through the stratum corneum. Due to the high temperature under the tip, it causes dehydration of tissue segments, creating a water concentration gradient allowing hydrophilic drugs to freely permeate through the gaps.[9–11] Pretreatment with TMFI has been demonstrated by previous studies to enhance transdermal drug delivery of several topical medications including verapamil, diclofenac, ascorbyl phosphate,[11] botulinum toxin type A,[14] and 5-amino-levulinic-acid hydrochloride (ALA).[10,15]

For this investigation, TMFI was followed by the topical application of TAC suspension. TAC suspensions contain triamcinolone acetonide, which is a lipophilic molecule in an aqueous solution. It is mainly intended for intralesional injection directly into the dermis for the treatment of HTS. Due to its lipophilicity, TAC suspension applied directly onto intact skin would be able to passively penetrate the stratum corneum as its molecular weight is <500 Daltons. This diffusion into the deeper layers of the skin is accelerated by the introduction of porous thermal injury sites from TMFI compared to the conventional intercellular route in between corneocytes.[10,19] Clinically, a blanching response was observed immediately after the TAC suspension was applied onto the HTS following TMFI, suggesting that the method facilitates cutaneous uptake of the suspension. The bioavailability of TAC in the skin following TMFI however, is beyond the scope of this investigation and should be explored further in future studies.

This study has shown that TMFI pretreatment before topical application of corticosteroids exhibits comparable therapeutic outcomes with intralesional corticosteroid injections for the treatment of HTS. Although the steroid injection arm exhibited a significant improvement in scar flattening over the TMFI + Steroid arm at 6-month follow-up (95% CI, 0.09–0.35; $p = 0.002$), the differences were not significant on any other follow-up visits. Furthermore, the scar volume and VSS scores did not demonstrate any significant differences between experimental groups on any follow-up assessment, showing comparable efficacies. Beyond its sufficient clinical effect, the other most notable benefit of TMFI pretreatment in combination with steroids is the significantly lower level of pain due to the procedure and the absence of any adverse events compared to intralesional corticosteroid injection. This makes this method of transdermal steroid delivery amenable for use in treating HTS in the pediatric population or in patients with large and/or multiple areas

of scarring. The additional cost of using TMFI, however, should be considered, as this method is more expensive than steroid injections alone.

A number of recent studies on the treatment of HTS have proven the adjunctive effect of TMFI with transcutaneous corticosteroid and/or 5-fluorouracil (5-FU) delivery. Artzi et al.[12] reported a significant reduction in the mean keloid VSS from 8.6 ± 1.2 to 5 ± 2.7 after eight TMFI-assisted TAC and 5-FU treatments in seven patients with recalcitrant keloid scars. The same investigator treated four children with hypertrophic burn scars and noted a statistically significant reduction in the mean scar VSS from 8.4 ± 0.8 to 5.2 ± 0.5 after eight treatments of TMFI combined with topical application of TAC 5-FU. Similarly, a lower pain score was reported with TMFI with a mean treatment pain VAS of 1.74 ± 0.9.[13] These findings are comparable to the treatment outcomes of our present study which shows a significant reduction in VSS from 6.61 ± 1.82 to 3.09 ± 1.57 during the 3rd month posttreatment follow-up, as well as a significantly lower pain score using TMFI. It should be noted, however, that the lower pain score of the TMFI + Steroid segment may be partly due to the concomitant air cooling during the treatment, whereas the steroid injection segment did not receive the same air cooling upon administration.

Ablative fractional lasers including Er:YAG and CO_2 lasers are means to provide deep transepidermal delivery of corticosteroids for the treatment of keloids and HTS. A study by Park et al.[20] conducted a prospective, split scar study on 10 Koreans with keloids on their left shoulder using an ablative fractional Er:YAG laser. Following laser treatment of the entire lesion, half of the scar received topical desoxymethasone 0.25% ointment, while the other half received intralesional triamcinolone acetonide (10 mg/ml) injections. Analogous to the findings of this study, the mean keloid VSS scores were significantly decreased from 8.59 ± 1.23 to 4.56 ± 1.09 on the laser and steroid injection side, and from 8.31 ± 2.09 to 5.02 ± 0.87 on the laser and topical steroid side after four treatments. There were no significant differences in VSS scores between the two treatment arms. Similarly, a retrospective study by Cavalie et al.[21] on 23 patients with 70 keloids that were resistant to first-line treatment showed 50% improvement in scar appearance after nine sessions of ablative fractional erbium laser treatment combined with topical betamethasone cream applied under occlusion twice daily. Another study done by Waibel et al.[22] using fractional CO_2 laser treatment combined with immediate postprocedure topical application of a TAC suspension (10–20 mg/ml) in 15 patients with HTS demonstrated an average overall improvement of 2.73 of HTS on a 0-3 scale. It is worth mentioning that for these other studies using ablative fractional lasers, the topical anesthetic was applied to the treatment area before the procedure, whereas no other anesthetic pretreatment was done for TMFI in this study apart from air-cooling during the procedure.

There are several limitations of the present study. First, the mean scar thickness of HTS is only 1.2 mm, thus, the outcome of this study may not necessarily represent the therapeutic response of thicker HTS. Second, it is generally difficult to demonstrate the appearance and improvement of HTS through two-dimensional photographs. Lastly, the design of this study cannot adequately dissociate the therapeutic effects of TMFI from the therapeutic agent, in this case, a corticosteroid. The repeated treatments of TMFI alone may sufficiently provide clinical improvement for hypetrophic scars as seen in studies on both non-ablative[23,24] and ablative[25,26] monotherapy fractional laser techniques for the treatment of HTS. Thermal energy delivered by fractional laser devices produces a controlled microwounding within the HTS, inducing wound remodeling leading to clinical improvement.[27] The remodeling process is hypothesized to be mediated by an increase in TGFβ3/type III collagen as seen in early wound healing and scarless fetal healing. However, a complex cascade of collagenases and the modulation of fibrotic pathways have complicated this picture.[28] A controlled prospective randomized study comparing TMFI alone and in combination with topical corticosteroid application will better evaluate this treatment technique and establish its superiority or inferiority. Another mandatory future study is to compare the TMFI versus laser-assisted corticosteroid delivery in the treatment of HTS.

CONCLUSIONS

All objective and patient-based assessments of the present study show that thermomechanical fractional injury-assisted topical corticosteroid delivery is a safe and effective treatment for hypertrophic scars with a lower risk of adverse effects and pain when used with concomitant air cooling compared with corticosteroid injections.

ACKNOWLEDGMENTS

The authors gratefully thank Ms. Chutikan Kiatphansodsai and Ms. Phonsuk Yamlexnoi for their assistance in recruiting subjects.

CONFLICT OF INTERESTS

The authors declare that there are no conflicts of interest.

ORCID

Woraphong Manuskiatti http://orcid.org/0000-0001-8393-7963

Rungsima Wanitphakdeedecha http://orcid.org/0000-0002-3926-2193

REFERENCES

1. Berman B, Maderal A, Raphael B. Keloids and hypertrophic scars: pathophysiology, classification, and treatment. Dermatol Surg. 2017; 43(suppl 1):S3–S18. https://doi.org/10.1097/DSS.0000000000000819

2. Zhu Z, Ding J, Shankowsky HA, Tredget EE. The molecular mechanism of hypertrophic scar. J Cell Commun Signal. 2013; 7(4):239–52. https://doi.org/10.1007/s12079-013-0195-5
3. Wolfram D, Tzankov A, Pulzl P, Piza-Katzer H. Hypertrophic scars and keloids—a review of their pathophysiology, risk factors, and therapeutic management. Dermatol Surg. 2009;35(2):171–81. https://doi.org/10.1111/j.1524-4725.2008.34406.x
4. Hochman B, Locali RF, Matsuoka PK, Ferreira LM. Intralesional triamcinolone acetonide for keloid treatment: a systematic review. Aesthetic Plast Surg. 2008;32(4):705–9. https://doi.org/10.1007/s00266-008-9152-8
5. Morelli Coppola M, Salzillo R, Segreto F, Persichetti P. Triamcinolone acetonide intralesional injection for the treatment of keloid scars: patient selection and perspectives. Clin Cosmet Investig Dermatol. 2018;11:387–96. https://doi.org/10.2147/CCID.S133672
6. Sherris DA, Larrabee WF, Jr., Murakami CS. Management of scar contractures, hypertrophic scars, and keloids. Otolaryngol Clin North Am. 1995;28(5):1057–68.
7. Ogawa R. The most current algorithms for the treatment and prevention of hypertrophic scars and keloids. Plast Reconstr Surg. 2010; 125(2):557–68. https://doi.org/10.1097/PRS.0b013e3181c82dd5
8. Foged C, Haedersdal M, Bik L, Dierickx C, Phillipsen PA, Togsverd-Bo K. Thermo-mechanical fractional injury enhances skin surface- and epidermis-protoporphyrin IX fluorescence: comparison of 5-aminolevulinic acid in cream and gel vehicles. Lasers Surg Med. 2021; 53(5):622–9. https://doi.org/10.1002/lsm.23326
9. Kokolakis G, von Grawert L, Ulrich M, Lademann J, Zuberbier T, Hofmann MA. Wound healing process after thermomechanical skin ablation. Lasers Surg Med. 2020;52(8):730–4. https://doi.org/10.1002/lsm.23213
10. Shavit R, Dierickx C. A new method for percutaneous drug delivery by thermo-mechanical fractional injury. Lasers Surg Med. 2020;52(1):61–9. https://doi.org/10.1002/lsm.23125
11. Sintov AC, Hofmann MA. A novel thermo-mechanical system enhanced transdermal delivery of hydrophilic active agents by fractional ablation. Int J Pharm. 2016;511(2):821–30. https://doi.org/10.1016/j.ijpharm.2016.07.070
12. Artzi O, Koren A, Niv R, Mehrabi JN, Friedman O. The scar bane, without the pain: a new approach in the treatment of elevated scars: thermomechanical delivery of topical triamcinolone acetonide and 5-fluorouracil. Dermatol Ther (Heidelb). 2019;9(2): 321–6. https://doi.org/10.1007/s13555-019-0298-x
13. Artzi O, Koren A, Niv R, Mehrabi JN, Mashiah J, Friedman O. A new approach in the treatment of pediatric hypertrophic burn scars: Tixel-associated topical triamcinolone acetonide and 5-fluorouracil delivery. J Cosmet Dermatol. 2020;19(1):131–4. https://doi.org/10.1111/jocd.13192
14. Friedman O, Koren A, Niv R, Mehrabi JN, Artzi O. The toxic edge-A novel treatment for refractory erythema and flushing of rosacea. Lasers Surg Med. 2019;51(4):325–31. https://doi.org/10.1002/lsm.23023
15. Hilerowicz Y, Friedman O, Zur E, Ziv R, Koren A, Salameh F, et al. Thermomechanical ablation-assisted photodynamic therapy for the treatment of acne vulgaris. A retrospective chart review of 30 patients. Lasers Surg Med. 2020;52(10):966–70. https://doi.org/10.1002/lsm.23246
16. Thompson CM, Sood RF, Honari S, Carrougher GJ, Gibran NS. What score on the Vancouver Scar Scale constitutes a hypertrophic scar? Results from a survey of North American burn-care providers. Burns. 2015;41(7):1442–8. https://doi.org/10.1016/j.burns.2015.04.018
17. Haedersdal M, Erlendsson AM, Paasch U, Anderson RR. Translational medicine in the field of ablative fractional laser (AFXL)-assisted drug delivery: a critical review from basics to current clinical status. J Am Acad Dermatol. 2016;74(5): 981–1004. https://doi.org/10.1016/j.jaad.2015.12.008
18. Waibel JS, Rudnick A, Shagalov DR, Nicolazzo DM. Update of ablative fractionated lasers to enhance cutaneous topical drug delivery. Adv Ther. 2017;34(8):1840–9. https://doi.org/10.1007/s12325-017-0516-9
19. Jeong WY, Kwon M, Choi HE, Kim KS. Recent advances in transdermal drug delivery systems: a review. Biomater Res. 2021; 25(1):24. https://doi.org/10.1186/s40824-021-00226-6
20. Park JH, Chun JY, Lee JH. Laser-assisted topical corticosteroid delivery for the treatment of keloids. Lasers Med Sci. 2017;32(3): 601–8. https://doi.org/10.1007/s10103-017-2154-5
21. Cavalie M, Sillard L, Montaudie H, Bahadoran P, Lacour JP, Passeron T. Treatment of keloids with laser-assisted topical steroid delivery: a retrospective study of 23 cases. Dermatol Ther. 2015;28(2):74–8. https://doi.org/10.1111/dth.12187
22. Waibel JS, Wulkan AJ, Shumaker PR. Treatment of hypertrophic scars using laser and laser assisted corticosteroid delivery. Lasers Surg Med. 2013;45(3):135–40. https://doi.org/10.1002/lsm.22120
23. Lin JY, Warger WC, Izikson L, Anderson RR, Tannous Z. A prospective, randomized controlled trial on the efficacy of fractional photothermolysis on scar remodeling. Lasers Surg Med. 2011;43(4):265–72. https://doi.org/10.1002/lsm.21061
24. Niwa AB, Mello AP, Torezan LA, Osorio N. Fractional photothermolysis for the treatment of hypertrophic scars: clinical experience of eight cases. Dermatol Surg. 2009;35(5):773–7. https://doi.org/10.1111/j.1524-4725.2009.01127.x
25. Azzam OA, Bassiouny DA, El-Hawary MS, El Maadawi ZM, Sobhi RM, El-Mesidy MS. Treatment of hypertrophic scars and keloids by fractional carbon dioxide laser: a clinical, histological, and immunohistochemical study. Lasers Med Sci. 2016;31(1): 9–18. https://doi.org/10.1007/s10103-015-1824-4
26. Tawfic SO, El-Tawdy A, Shalaby S, Foad A, Shaker O, Sayed SS, et al. Evaluation of fractional CO2 versus long pulsed Nd:YAG lasers in treatment of hypertrophic scars and keloids: a randomized clinical trial. Lasers Surg Med. 2020;52(10):959–65. https://doi.org/10.1002/lsm.23249
27. Purschke M, Laubach HJ, Anderson RR, Manstein D. Thermal injury causes DNA damage and lethality in unheated surrounding cells: active thermal bystander effect. J Invest Dermatol. 2010; 130(1):86–92. https://doi.org/10.1038/jid.2009.205
28. Ozog DM, Liu A, Chaffins ML, Ormsby AH, Fincher EF, Chipps LK, et al. Evaluation of clinical results, histological architecture, and collagen expression following treatment of mature burn scars with a fractional carbon dioxide laser. JAMA Dermatol. 2013;149(1):50–7. https://doi.org/10.1001/2013.jamadermatol.668

How to cite this article: Manuskiatti W, Yan C, Artzi O, Gervasio MKR, Wanitphakdeedecha R. Efficacy and safety of thermomechanical fractional injury-assisted corticosteroid delivery versus intralesional corticosteroid injection for the treatment of hypertrophic scars: A randomized split-scar trial. Lasers Surg Med. 2021;1–7. https://doi.org/10.1002/lsm.23511

Lasers in Medical Science
https://doi.org/10.1007/s10103-022-03558-4

ORIGINAL ARTICLE

Efficacy and safety of a thermal fractional skin rejuvenation system (Tixel) for the treatment of facial and/or scalp actinic keratoses

Meital Oren-Shabtai[1,2] · Nadezhda Sloutsky[2,3] · Moshe Lapidoth[1,2] · Daniel Mimouni[1,2] · Ilia Chorny[2,3] · Igor Snast[1,2] · Yael Anne Leshem[1,2] · Rivka Friedland[2,4] · Emmilia Hodak[1,2] · Ifat Klein[5] · Yael Agmon[5] · Assi Levi[1,2]

Received: 18 October 2021 / Accepted: 1 April 2022

Abstract

Actinic keratoses are common cutaneous lesions with a potential to progress to invasive squamous cell carcinoma. Therefore, treatment is crucial. The Tixel® is a noninvasive thermomechanical device designed to transfer heat to the upper dermis in a controlled manner according to a predetermined setting. This study aimed to evaluate the safety and efficacy of a thermomechanical fractional skin resurfacing technology for the treatment of facial and scalp actinic keratoses. A prospective, open-label, before–after study was conducted in a tertiary medical centre from May 2020 to April 2021. Patients presenting with facial/scalp actinic keratoses of mild-to-moderate thickness underwent 2 or 3 Tixel treatments (depending on clinical improvement), 3–4 weeks apart. The reduction in lesion count and overall improvement in appearance were assessed by clinical examination and digital photography. Findings were compared between baseline and follow-up at 3 months after the last treatment session. Patient satisfaction was evaluated by questionnaire, and adverse effects were documented. A total of 20 patients participated in the study. All completed 2–3 treatments and follow-up visits. Assessment of digital photographs was performed by 2 assessors blinded to the timepoint at which each photo was taken (before or after treatment). The average number of lesions at baseline was 9.8 (±4.8) and the mean reduction in lesion count was 7.9 (±4.4) (80.6%). Complete clearance was observed in 31.6% of patients. No adverse effects were noted during treatment and follow-up. Most patients reported being "very satisfied" or "satisfied" with the treatment results (85%) and experience (95%). Treating facial and scalp actinic keratoses with the Tixel device was found to be effective and safe.

Keywords Tixel · Actinic keratosis · Solar keratosis

Introduction

Actinic keratoses (AKs) are common epidermal lesions formed by proliferation of keratinocytes. AKs accounted for an estimated 5.2 million annual healthcare visits from 2000 to 2003 in the USA alone; 62% of the patients were aged 65 years or more [1]. Major risk factors for the development of multiple lesions (10 or more) were male gender, older age, and lighter skin phototype with a high tendency for sunburn [2]. The reported rates of malignant transformation of a single actinic keratosis vary among studies from 0.1 to 16% [3, 4]. The estimated 10-year incidence rate of AK progression to squamous cell sarcoma without proper treatment is about 10%, emphasizing the importance of prevention, follow-up, and treatment [5].

Therapy can be aimed at a solitary lesion (lesion-targeted therapy) using mostly destructive regimens, or field-directed, to reduce clinical and subclinical lesions across an entire

Key message A thermomechanical fractional device (Tixel) is safe and effective in treating facial/scalp actinic keratoses.

✉ Meital Oren-Shabtai
meital.oren@gmail.com

1 Division of Dermatology, Rabin Medical Center, 39 Zeev Jabotinsky St, 4941492 Petah Tikva, Israel

2 Sackler Faculty of Medicine, Tel Aviv University, Tel Aviv, Israel

3 Department of Anesthesiology, Rabin Medical Center – Hasharon Hospital, Petah Tikva, Israel

4 Pediatric Dermatology Unit, Schneider Children's Medical Center of Israel, Petah Tikva, Israel

5 Novoxel LTD, Netanya, Israel

Published online: 12 April 2022

potentially cancerous area [5, 6]. Treatment is individually tailored with consideration of clinical parameters (site and number of lesions), patient characteristics (age, immune system status, and compliance), and treatment cost and tolerability [5, 7]. Lesion-targeted treatment modalities include cryotherapy [8], laser therapy [9], surgical removal (wide or shave excision), and curettage [10]. Field-directed treatment modalities include 5-fluorouracil [11], diclofenac 3% gel [12], chemical peels [13], imiquimod [14, 15], and photodynamic therapy [16, 17]. Oral nicotinamide was found to have various photoprotective effects, and its administration to high-risk individuals led to a reduction in AK and nonmelanoma skin cancer incidence [18].

In recent years, there have been reports on the application of energy-based devices such as lasers for the treatment of nonmelanoma skin cancers [19]. However, their use was limited by high cost, need for technical acumen, and substantial side effects [20, 21].

Tixel® is a thermomechanical system designed to fulfill the clinical need for safe and efficient fractional skin resurfacing. It has been shown to improve skin complexion and attenuate wrinkles. The device consists of a metal element, termed the tip, made up of an array of miniature pyramids that are heated to a temperature of 385–405 °C. When placed in contact with the skin, the tip creates a thermal effect in the tissue by generating a matrix of coagulation sites (micropores) 200–300 µm deep. The heat is briefly conducted towards the skin (1–2 pulses of 5–18-ms duration) in a controlled manner based on predefined parameters (depth, penetration). The results mimic pulsed energy–based devices such as non-ablative lasers, but the side effects are minor, consisting mainly of mild transient discomfort to the patient, and the downtime is minimal [22].

Considering that the heat transferred can abolish superficial skin lesions and cause dermal coagulation, we sought to determine if the Tixel device might be amenable for use in patients with AKs. The purpose of the current study is to prospectively determine the efficacy and safety of a thermomechanical fractional skin resurfacing technology (Tixel) for treating facial and/or scalp AKs.

Methods

Study design and population

A prospective, open-label, before-after study was performed in a single tertiary medical centre. The primary objective of the present study was to evaluate the efficacy of the Tixel device for the treatment of facial and scalp AKs. The secondary objectives were to evaluate procedure-related safety and subjects' downtime, discomfort, and satisfaction.

The study population consisted of male and female patients aged 18–80 years with skin phototype I–VI who presented with AKs of mild-to-moderate thickness on the scalp and/or face from May 21, 2020, to April 19, 2021. All patients provided written informed consent to participate in the study and were willing and able to comply with the study requirements. The exclusion criteria were conditions that might bias the outcomes or pose a potential risk to patients, as listed in Supplementary Table S1.

Procedure

Initially, demographic and medical history data were collected, and a skin examination was performed. Up to 3 treatments, 3–4 weeks apart, with the Tixel device were applied. Treatment settings included protrusion depth of 400–700 µm, pulse duration of 10–12 ms, and a single pass covering the entire lesions (not the entire face/scalp), to a clinical endpoint of slight erythema. The precise number of treatments was determined by the investigators based on the clinical improvement. Follow-up visits to evaluate the safety and efficacy of treatment were conducted at 4 weeks (±7 days) and 3 months (±7 days) after the last treatment session, for a total of up to 6 clinic visits. The assessment schedule is detailed in Table 1.

Efficacy endpoints

Blinded efficacy assessment Efficacy was measured by the overall mean reduction in AK lesion count, calculated as the difference from baseline, and by the number of patients with an overall improvement in facial/scalp appearance of 26–50% (score 2). Those two primary efficacy outcomes were each assessed by two independent dermatologists (a total of 4 assessors) from photographic images taken at the baseline visit (visit 1) and 3 months after the last visit (visit 5, Table 1). The clinical appearance of the lesions was scored on a quartile scale of improvement, as follows: 0 = exacerbation, 1 = 1–25% improvement, 2 = 26–50% improvement, 3 = 51–75% improvement, or 4 = 76–100% improvement.

Unblinded (comparative) efficacy assessment As opposed to the primary efficacy outcomes, the secondary ones were performed by the unblinded primary investigator based on physical examination (not photographs) throughout the study. At the 3-month follow-up (visit 5), efficacy was measured as follows: overall mean reduction in AK lesion count from baseline and percentage of patients whose lesions were scored 2, 3, or 4.

Safety assessment Adverse effects (AEs) were recorded at each treatment visit (visits 1–3, Table 1). Anticipated treatment-related AEs were irritation, edema, or erythema.

Table 1 Schedule of assessments in 20 patients treated for actinic keratoses with the Tixel

	1 (0)	2 (3–4 W)	3 (6–8 W)	4 (10–12 W)	5 (study end, 5 M)
Evaluation	Sc*/Tx 1	FU/Tx 2	FU/Tx 3	FU	FU
Time from last Tx/visit	0	3–4 W	3–4 W	1 M **(±7 D)**	**3 M (±7 D)**
Inclusion/exclusion criteria	X				
Informed consent	X				
Medical history/medication	X				
Demographic/skin information	X				
Photography	X	X	X	X	X
Treatment	X	X	X		
Subject pain evaluation (VAS)	X	X	X		
Subject satisfaction (questionnaire)					X
Safety evaluation	X	X	X	X	X
Subject downtime evaluation		X	X	X	
Post-treatment AE	X	X	X		
Evaluation of lesion count and improvement by investigator (unblinded)	X	X	X	X	X
Assessor blinded evaluation of lesion count and improvement[†]	X				X

Sc, screening; *Tx*, treatment; *FU*, follow-up; *D*, days; *W*, weeks; *M*, months; *VAS*, visual analogue scale; *AE*, adverse effect

[*]Treatment may be performed on the same day of screening

[†]Primary endpoint. The blinded independent dermatologists performed these assessments 3 months after the last treatment (visit 5)

Patients also self-reported the degree of pain and discomfort associated with the procedure (visits 1–3, Table 1) using a 10-point visual analogue scale (VAS) (0 = no pain to 10 = intolerable pain). Downtime was defined as the period following the procedure (measured in hours or days) during which the patient felt unable/unwilling to go out in public due to edema, erythema, or any other AEs.

Satisfaction assessment At the 3-month follow-up (visit 5, Table 1), patients were asked to complete a satisfaction questionnaire covering the treatment results, the treatment experience, and the fulfilment of expectations. Each parameter was scored on a 5-point Likert scale (0 = very dissatisfied, 1 = dissatisfied, 2 = somewhat satisfied, 3 = satisfied, 4 = very satisfied).

Statistical analysis

Demographic and baseline clinical characteristics were summarized using descriptive statistics. All tests were two-tailed, and a *p*-value of 5% or less was considered statistically significant.

The Clopper–Pearson interval for proportions was calculated for the improvement score by visit and for the satisfaction score at visit 5. The Wilcoxon signed-rank test was applied to test the statistical significance of the change from baseline in number of lesions and VAS pain score and to determine if the difference between the mean clinical improvement achieved at each visit and score 2 was statistically significant.

The intention to treat (ITT) population included all patients who were enrolled and underwent at least one treatment with the study device. Safety analysis was performed on the ITT population. The per-protocol (PP) analysis set consisted of patients who received the full treatment and had qualified photos taken at the 3-month follow-up visit. Primary efficacy analysis was performed on the PP population. Missing values were not imputed.

The data were analyzed using SAS® version 9.4 (SAS Institute, Cary, NC, USA).

Ethical approval

The study was conducted according to ISO 14155:2011 Clinical Investigation of Medical Devices for Human Subjects and was approved by the Ethics Committee of Rabin Medical Center (approval no. RMC-0714–19).

Results

Study cohort

A total of 20 patients were enrolled in the study, 12 males and 8 females, of mean age 62.9 ± 11.5 years (median 67.5, range 36–74). Five patients had Fitzpatrick skin type I and 15 had Fitzpatrick skin type II. None of the patients had a clinically significant medical history that was relevant to the study. All concomitant medications taken by the patients were initiated to manage comorbidities and were unrelated to the study treatments or AEs. The medical history of the patients is detailed in Table S2.

All 20 patients completed the study, forming the ITT cohort: 19 (95%) completed 3 treatments and 1 completed 2 treatments (as per the primary investigators' decision, due to 100% lesion clearance after the second treatment). One subject had scalp hair growth at the 3-month follow-up which prevented photographic evaluation, limiting the PP population to 19 patients.

Efficacy analysis

The mean number of AKs at baseline evaluated by the two assessors who were blinded to the timing of the photos (before or after treatment) was 9.8 ± 4.9, and the overall mean reduction in the number of lesions was 7.9 (± 4.4), for a rate of 80.6% ($p < 0.0001$). At the 3-month follow-up (visit 5), 18 patients (94.7%) had at least 50% clearance, and 13 patients (68.4%) had at least 75% clearance. Six patients (31.6%) had complete clearance after treatment. Changes over time in the number of lesions and the clearance rates according to each assessor are detailed in Table 2 and Table S3, respectively.

Improvement scores were evaluated by another 2 blinded assessors. The rate of correct identification of the timing of the photographs (i.e., which were taken before treatment and which after) was 94.7% (18 patients) for one and 89.5% (17 patients) for the other. Table 3 depicts the distribution of the improvement scores. The mean improvement score was 2.0 (± 0.8). On the Wilcoxon signed-rank test, there was no significant difference between the average score assigned by the assessors, independently or together, and score 2 (26–50% improvement).

The mean number of AKs at baseline, assessed by physical examination of the unblinded assessor (primary investigator), was 10.1 ± 5.2 and the mean overall reduction in the number of lesions was 8.2 (± 4.7), for a rate of 81.2% ($p < 0.0001$, Table S4). Of the 20 patients analyzed, 18 (90.0%) had at least 50% clearance and 14 (70.0%) had at least 75% clearance at the 3-month follow-up visit. Six patients (30.0%) had complete clearance (Table S5).

The overall improvement in AKs evaluated by the unblinded assessor is shown in Table S6. The mean score at visit 2 (Tx 2) was 2.6 ± 0.9, and it gradually increased

Table 2 Number of AK lesions assessed by blinded assessors and changes in lesion count from baseline

Assessor	*N*	No. of lesions before Tx		No. of lesions at 3-M FU		Change in no. of lesions from baseline		
		Mean	± SD	Mean	± SD	Mean	± SD	*p* value*
Assessor 1	19	9.9	4.9	1.9	2.3	− 8.0	4.4	< 0.0001
Assessor 2	19	9.7	4.8	1.8	2.3	− 7.8	4.3	< 0.0001
Average of the two assessors	19	9.8	4.9	1.9	2.3	− 7.9	4.4	< 0.0001

Tx treatment, *FU* follow-up, *SD* standard deviation

*Wilcoxon signed-rank test

Table 3 Clinical improvement in actinic keratosis assessed by blinded assessors

Assessor	*N*	Improvement score distribution, *n* (%)					Mean improvement score	
		0	Score 1 1–25%	Score 2 26–50%	Score 3 51–75%	Score 4 76–100%	Mean	± SD
Assessor 1	19	1 (5.3)	3 (15.8)	10 (52.6)	4 (21.1)	1 (5.3)	2.1†	0.9
Assessor 2	19	2 (10.5)	2 (10.5)	10 (52.6)	5 (26.3)	—	1.9†	0.9
Average of the two assessors	19						2.0†	0.8

SD, standard deviation

†Confidence intervals: assessor 1 (1.6, 2.5), assessor 2 (1.5, 2.4), both assessors (1.6, 2.4)

over time to 3.6 ± 0.9 at the 3-month follow-up. By the follow-up visits, most of the patients had achieved the highest available improvement score (76–100%, grade 4): 14/20 patients at 4 weeks after the last treatment (visit 4) and 15/20 at 3 months after the last treatment (visit 5). None of the patients demonstrated worsening of the AKs following treatment. Figures 1 and 2 show the before-and-after photos of 2 representative patients.

Safety analysis

No unexpected AEs were observed in any of the patients throughout the study. Most patients had redness, edema, and scabs for 0–2 days after treatments and heat sensation for 0–2 h after treatment. The mean procedure-associated VAS scores (on a scale of 0–10) were as follows: 2.2 ± 1.2 at treatment visit 1 ($N = 20$), 2.2 ± 1.8 at treatment visit 2 ($N = 20$), and 2.5 ± 1.7 at treatment visit 3 ($N = 19$). There was little downtime; all participants reported feeling able and willing to return to work and social activities at ≤ 2 days following each treatment session (Table S7).

Patient satisfaction

On the satisfaction questionnaire completed at the 3-month follow-up visit, most of the patients reported being "very satisfied" overall. Specifically, 11 (55.0%) were very satisfied with the results of the treatment, 15 (75.0%) were very satisfied with the treatment experience, and 12 (60.0%) were very satisfied with the degree to which their expectations were met. The mean scores for each of these parameters on a scale of 1 to 5 were 4.3 ± 1.0, 4.6 ± 0.9, and 4.4 ± 1.0, respectively (Table 4).

Discussion

This study sought to evaluate the efficacy and safety of the Tixel technology for treating AKs of the face and scalp, which are in fact considered, by some, squamous cell carcinoma in situ [5]. All 20 patients enrolled completed the study with minimal anticipated AEs and downtime. Treatment was beneficial by all predefined parameters. The mean overall reduction in the number of lesions as evaluated by the blinded assessors correlated with the findings of the unblinded investigator. Most patients were either very satisfied or satisfied with the treatment results and experience.

It is noteworthy that the Tixel device is mainly used for aesthetic purposes. It was shown to improve skin complexion and attenuate wrinkles [22, 23] by thermomechanical fractional coagulation of the papillary dermis. Dermal coagulation and healing through fibroblast proliferation in

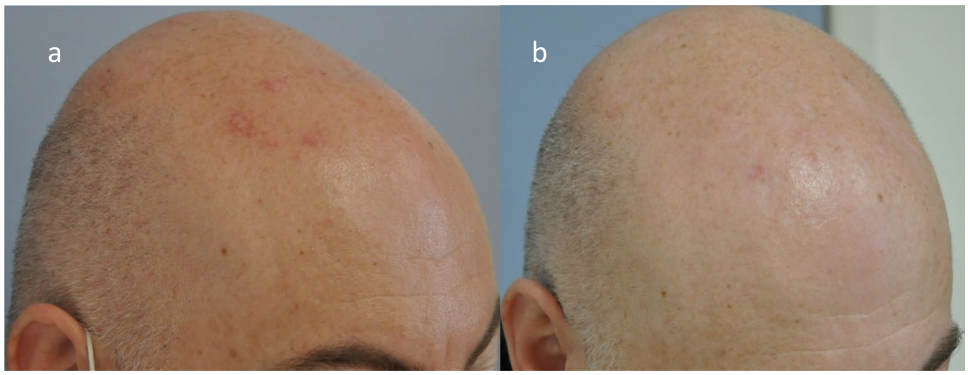

Fig. 1 Representative patient before treatment (**a**) and at the 3-month follow-up (visit 5) (**b**)

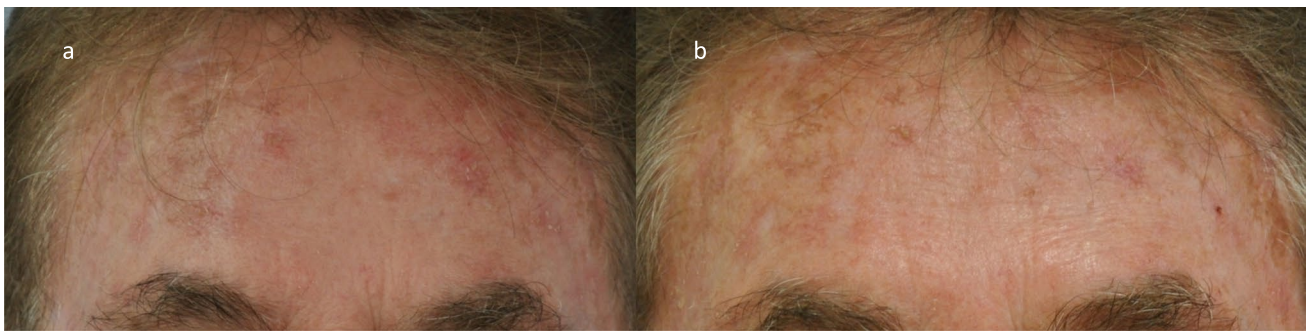

Fig. 2 Representative patient before treatment (**a**) and at the 3-month follow-up (visit 5) (**b**)

Table 4 Responses to satisfaction questionnaire at visit 5, 3 months after the last treatment

Parameters	*N*	%
Results of the treatment		
(1) Very dissatisfied	1	5.0
(3) Somewhat satisfied	2	10.0
(4) Satisfied	6	30.0
(5) Very satisfied	11	55.0
The treatment experience		
(1) Very dissatisfied	1	5.0
(4) Satisfied	4	20.0
(5) Very satisfied	15	75.0
Expectations (the treatment fulfilled the subject's expectations)		
(1) Very dissatisfied	1	5.0
(3) Somewhat satisfied	2	10.0
(4) Satisfied	5	25.0
(5) Very satisfied	12	60.0

the dermoepidermal cleft became apparent 7 days after treatment with the production of new collagen, and skin texture and appearance continued to improve with successive sessions [22].

AKs are epidermal lesions [1], and most of the heat transferred to the dermis by the Tixel device is absorbed by the epidermis [23], leading to the creation of epidermal microcraters. Tixel-induced epidermal microcraters have been found to fully restore as soon as 2 weeks after treatment [24], which explains the minimal skin symptoms, successful rapid wound healing, and minimal downtime observed in this study, in contrast to ablative lasers.

Indeed, it is possible that Tixel-induced improvement in skin aesthetics may have contributed to the patients' satisfaction and to the evaluation of the overall improvement.

Previous studies have shown that Tixel application can also improve drug delivery via the same thermomechanical mechanism. The Tixel has been used for percutaneous drug delivery of aminolevulinic acid for photosensitization [25] or acne vulgaris [26], triamcinolone acetonide and 5-fluorouracil for hypertrophic scars [27], and botulinum toxin type A for rosacea [28]. Thus, besides direct thermal treatment of AKs, the Tixel could potentially aid in increasing the permeability of topicals (such as diclofenac 3% gel or imiquimod), designated to treat AKs. This concept warrants further investigation.

The limitations of the present study include a relatively small sample size, lack of control group, and short follow-up period. Nevertheless, given that this is the first prospective study to evaluate application of the Tixel device for the treatment of AKs, the results obtained are quite compelling. An additional possible limitation is the lack of palpation in the blinded assessment which may have led to an increase in the AK count. However, this shortcoming was compensated by the correlation between the blinded photographic evaluation with the unblinded clinical evaluation. In addition, only fair-skinned individuals were included in the study, but this is the population at highest risk of nonmelanoma skin cancer.

In conclusion, the Tixel device was found to be a relatively efficient and safe modality for the treatment of mild-to-moderate AKs on the scalp and face.

Supplementary Information The online version contains supplementary material available at https://doi.org/10.1007/s10103-022-03558-4.

Author contribution Assi Levi designed the study and wrote the study protocol.

Meital Oren-Shabtai, Nadezhda Sloutsky, and Assi Levi collected and interpreted data and wrote the first draft of the study.

Moshe Lapidoth, Daniel Mimouni, Igor Snast, Yael Anne Leshem, Rivka Friedland, Ilia Chorny, and Emmilia Hodak collected and interpreted data.

All authors participated in writing the final draft of the paper and had critical input to its final form.

Funding The study was funded by Novoxel Ltd.

Data availability All data generated or analyzed during this study are included in this article and its supplementary material files. Further enquiries can be directed to the corresponding author.

Declarations

Ethics approval The study was conducted according to ISO 14155:2011 Clinical Investigation of Medical Devices for Human Subjects and was approved by the ethical committee of Rabin Medical Center (RMC-0714–19).

Conflict of interest The authors declare no competing interests.

References

1. Warino L, Tusa M, Camacho F, Teuschler H, Fleischer AB Jr, Feldman SR (2006) Frequency and cost of actinic keratosis treatment. Dermatol Surg 32(8):1045–1049
2. Flohil SC, van der Leest RJ, Dowlatshahi EA, Hofman A, de Vries E, Nijsten T (2013) Prevalence of actinic keratosis and its risk factors in the general population: the Rotterdam Study. J Investig Dermatol 133(8):1971–1978
3. Marks R, Rennie G, Selwood TS (1988) Malignant transformation of solar keratoses to squamous cell carcinoma. Lancet Lond Engl 1(8589):795–797
4. Glogau RG (2000) The risk of progression to invasive disease. J Am Acad Dermatol 42(1 Pt 2):23–24
5. Dianzani C, Conforti C, Giuffrida R, Corneli P, di Meo N, Farinazzo E et al (2020) Current therapies for actinic keratosis. Int J Dermatol 59(6):677–684
6. Cramer P, Stockfleth E (2020) Actinic keratosis: where do we stand and where is the future going to take us? Expert Opin Emerg Drugs 25(1):49–58
7. Werner RN, Stockfleth E, Connolly SM, Correia O, Erdmann R, Foley P, International League of Dermatological Societies, European Dermatology Forum et al (2015) Evidence- and

consensus-based (S3) Guidelines for the Treatment of Actinic Keratosis - International League of Dermatological Societies in cooperation with the European Dermatology Forum - Short version. J Eur Acad Dermatol Venereol 29(11):2069–79
8. Ianhez M, Miot HA, Bagatin E (2014) Liquid nitrogen for the treatment of actinic keratosis: a longitudinal assessment. Cryobiology 69(1):140–143
9. Marmur ES, Schmults CD, Goldberg DJ (2004) A review of laser and photodynamic therapy for the treatment of nonmelanoma skin cancer. Dermatologic Surg 30(2 Pt 2):264–271
10. Chetty P, Choi F, Mitchell T (2015) Primary care review of actinic keratosis and its therapeutic options: a global perspective. Dermatol Ther (Heidelb) 5(1):19–35
11. Krawtchenko N, Roewert-Huber J, Ulrich M, Mann I, Sterry W, Stockfleth E (2007) A randomised study of topical 5% imiquimod vs. topical 5-fluorouracil vs. cryosurgery in immunocompetent patients with actinic keratoses:a comparison of clinical and histological outcomes including 1-year follow-up. Br J Dermatol 157(Suppl 2):34–40
12. Rivers JK, Arlette J, Shear N, Guenther L, Carey W, Poulin Y (2002) Topical treatment of actinic keratoses with 3.0% diclofenac in 2.5% hyaluronan gel. Br J Dermatol 146(1):94–100
13. Berman B, Amini S (2012) Pharmacotherapy of actinic keratosis: an update. Expert Opin Pharmacother 13(13):1847–1871
14. Dirschka T, Peris K, Gupta G, Alomar A, Aractingi S, Dakovic R et al (2016) Imiquimod 3.75% in actinic keratosis: efficacy in patients with and without rest periods during treatment. J Eur Acad Dermatol Venereol. 30(8):1416–7
15. Stockfleth E, Gupta G, Peris K, Aractingi S, Dakovic R, Alomar A (2014) Reduction in lesions from Lmax: a new concept for assessing efficacy of field-directed therapy for actinic keratosis. Results with imiquimod 3.75%. Eur J Dermatol. 24(1):23–7
16. Lacour JP, Ulrich C, Gilaberte Y, Von Felbert V, Basset-Seguin N, Dreno B et al (2015) Daylight photodynamic therapy with methyl aminolevulinate cream is effective and nearly painless in treating actinic keratoses: a randomised, investigator-blinded, controlled, phase III study throughout Europe. J Eur Acad Dermatol Venereol 29:2342–2348
17. Enk CD, Levi A (2012) Low-irradiance red LED traffic lamps as light source in PDT for actinic keratoses. Photodermatol Photoimmunol Photomed 28(6):332–334
18. Damian DL (2017) Nicotinamide for skin cancer chemoprevention. Australas J Dermatol 58(3):174–180
19. Sharon E, Snast I, Lapidoth M, Kaftory R, Mimouni D, Hodak E et al (2021) Laser Treatment for non-melanoma skin cancer: a systematic review and meta-analysis. Am J Clin Dermatol 22(1):25–38
20. Trimas SJ, Ellis DA, Metz RD (1997) The carbon dioxide laser. An alternative for the treatment of actinically damaged skin. Dermatol Surg 23(10):885–9
21. Fulton JE, Rahimi AD, Helton P, Dahlberg K, Kelly AG (1999) Disappointing results following resurfacing of facial skin with CO2 lasers for prophylaxis of keratoses and cancers. Dermatol Surg 25(9):729–732
22. Elman M, Fournier N, Barnéon G, Bernstein EF, Lask G (2016) Fractional treatment of aging skin with Tixel, a clinical and histological evaluation. J Cosmet Laser Ther 18(1):31–37
23. Daniely D, Judodihardjo H, Rajpar SF, Mehrabi JN, Artzi O (2021) Thermo-mechanical fractional injury therapy for facial skin rejuvenation in skin types II to V: a retrospective double-center chart review. Lasers Surg Med. https://doi.org/10.1002/lsm.23400
24. Kokolakis G, Von Grawert L, Ulrich M, Lademann J, Zuberbier T, Hofmann MA (2020) Wound healing process after thermomechanical skin ablation. Lasers Surg Med 52(8):730–734
25. Shavit R, Dierickx C (2020) A new method for percutaneous drug delivery by thermo-mechanical fractional injury. Lasers Surg Med 52(1):61–69
26. Hilerowicz Y, Friedman O, Zur E, Ziv R, Koren A, Salameh F et al (2020) Thermomechanical ablation-assisted photodynamic therapy for the treatment of acne vulgaris. A retrospective chart review of 30 patients. Lasers Surg Med. 52:966–70
27. Artzi O, Koren A, Niv R, Mehrabi JN, Mashiah J, Friedman O (2020) A new approach in the treatment of pediatric hypertrophic burn scars: Tixel-associated topical triamcinolone acetonide and 5-fluorouracil delivery. J Cosmet Dermatol 19(1):131–134
28. Friedman O, Koren A, Niv R, Mehrabi JN, Artzi O (2019) The toxic edge - a novel treatment for refractory erythema and flushing of rosacea. Lasers Surg Med 51(4):325–331

Lasers in Surgery and Medicine 00:1–5 (2020)

Wound Healing Process After Thermomechanical Skin Ablation

Georgios Kokolakis,[1] Leonie von Grawert,[1] Martina Ulrich,[2] Juergen Lademann,[1] Torsten Zuberbier,[1] and Maja A. Hofmann[1,3]*

[1]*Department of Dermatology, Venereology and Allergology, Charité Universitätsmedizin-Berlin, Berlin, Germany*
[2]*Dermatologie am Regierungsviertel / Collegium Medicum Berlin GmbH, Berlin, Germany*
[3]*Department of Dermatology, University of Southern Denmark, Odense, Denmark*

Background and Objectives: Energy-based devices have been widely applied for skin ablation. A novel ablation technique based on thermomechanical principles (Tixel©) has been recently developed. The aim of this study was to examine the wound-healing process and clinical aspects after thermomechanical skin ablation.

Study Design/Materials and Methods: Six female participants were treated with Tixel© on healthy skin of the dorsal side of the right forearm in a single session with a 600 μm protrusion and 12 milliseconds pulse. The treated area was examined with confocal laser scanning microscopy on day 1, 2, 7, and 14 after treatment. Clinical symptoms were evaluated at the same time-points.

Results: All patients developed erythema and mild edema on the treated areas, which completely disappeared within 14 days. No post-inflammatory hyperpigmentation or scarring was observed. Thermomechanical skin ablation resulted in the formation of homogeneous micro-ablation zones. Two weeks after ablation, the honeycomb patterns of the epidermis in all examined layers was thoroughly restored. Thus, wound-healing was completed.

Conclusions: Wound healing after thermomechanical skin ablation is much faster compared with other fractionated ablation methods. Treatment intervals of 2–4 weeks could be recommended. Lasers Surg. Med. © 2020 The Authors. *Lasers in Surgery and Medicine* published by Wiley Periodicals, Inc.

Key words: thermomechanical skin ablation; Tixel©; wound-healing

INTRODUCTION

Skin ablation employing energy-based devices has increasingly attracted interest in the last few years. Not only for cosmetic purposes like antiaging, resurfacing, or treating scars but also for therapeutic applications, skin ablation is a well-established efficacious procedure. Side effects including thermal injury, crusting, long-lasting erythema, or hyperpigmentation may prolong the healing process [1]. Dividing the energy into fractions ensures deep dermal penetration of the energy with minimal affection of the epidermis. Thus, rapid recovery times are achieved compared with traditional ablative lasers [2].

Several ablative and non-ablative laser devices have been developed to improve skin laxity in the last decade, providing physicians with a wide palette of treatment options.

Currently, ablative fractionated CO_2 or Erbium:Yag lasers and bipolar radiofrequency are the most commonly applied techniques [2,3]. Novel technologies have also emerged that use sources of energy other than light, such as high-intensity focused ultrasound [4].

In the last few years, the development of a new technology based on thermomechanical principles offers a new treatment modality. A precise thermal energy is fractionally transferred to the skin creating an array of microchannels, minimizing downtime, and side effects compared with other fractional skin ablation techniques [5,6].

Confocal laser scanning microscopy (CLSM) is a non-invasive device, which visualizes the superficial layers of the skin *in vivo* in real-time. CLSM allows very detailed imaging with almost histopathological resolution of the epidermis and papillary dermis. The penetration depth is about 250 nm. CLSM was chosen to analyze the wound-healing process, as it is a non-invasive device able to regularly evaluate deeper skin layers. Therefore, the wound-healing process can be monitored over time without the need of surgical intervention [7].

The aim of this proof-of-concept trial was the investigation of the underlying wound-healing processes after skin ablation with thermomechanical ablation (TMA) and their correlation with clinical aspects.

Conflict of Interest Disclosures: All authors have completed and submitted the ICMJE Form for Disclosure of Potential Conflicts of Interest and none were reported.

*Correspondence to: Ass. Prof. Maja Hofmann, Department of Dermatology, Venereology and Allergology, Charité, Universitätsmedizin-Berlin, Charitéplatz 1, 10117 Berlin, Germany. E-mail: maja.hofmann@charite.de

Accepted 25 December 2019
Published online 00 Month 2020 in Wiley Online Library (wileyonlinelibrary.com).
DOI 10.1002/lsm.23213

MATERIALS AND METHODS

Patients

In total, six healthy female participants aged 32 ± 3.8 years (mean $\pm$ standard deviation [SD]) and of a Fitzpatrick skin type I-III were included in the trial. Skin conditions affecting the evaluation of the Tixel effects, skin malignancy, previous laser, radiofrequency (RF) or peeling treatments of the treated area were criteria for exclusion. One single TMA treatment of a 10×10 mm area of healthy skin on the dorsal side of the right forearm was applied. Use of topical products prior and after the procedure was not allowed. Clinical assessment of the treated areas with special interest on erythema, edema, crusting, pigmentation changes and scars was performed at day 1 (directly after the treatment), 2, 7, and 14 after treatment. Additionally, the level of pain was estimated using the pain visual analogue scale (0-10) at the same time-points.

The Ethics Committee of the Charité Universitätsmedizin-Berlin approved the protocol. Written informed consent was obtained from all patients. Study procedures were conducted according to the Principles of the Declaration of Helsinki.

Thermomechanical Ablation

Fractionated ablation of the skin was performed by means of an 81-pin thermomechanical system, which applies a Titanium tip (Tixel; Novoxel, Germany). The tip of the 1 cm^2 total surface with 9×9 pins is highly heated to 400°C and ablation occurs through the quick contact of the preheated tip directly onto the skin surface. The penetration depth (protrusion time), as well as the pulse duration, can be individually adjusted. Either a single or double-shot is also possible. For standardization reasons in this study, the protrusion time was adjusted to 600 µm and the pulse duration was set to 12 milliseconds as a single shot. These settings represent the typical ones commonly used for skin ablation in daily practice.

Confocal Laser Scanning Microscopy

For the estimation of the distribution and the size of the pores caused by the TMA as well as for the microscopic investigation of the wound-healing processes of the treated areas, CLSM was employed.

In brief, CLSM uses laser as a source of monochromatic coherent light and through reflection facilitates the non-interventional histological detection of cellular and subcellular structures of the skin. The laser beam passes through a splitter, a scanning and focusing optical lens and a skin contact device [8].

In this trial, CLSM was applied at day 1 (directly after the treatment), 2, 7, and 14 after treatment using VivaScope 1500 (Mavig, Munich, Germany).

The diameter of the microscopic ablation zone (MAZ) was measured at three depth levels: epidermis, dermoepidermal junction (DEJ) and papillary dermis. As previously published, for standardization purposes, the measurements were performed in 10–30, 50–70, and 90–100 µm for epidermis, DEJ, and papillary dermis, respectively, using VivaStack (Mavig) [9].

Statistical Analysis

The non-parametric Wilcoxon test was applied for the pairwise comparisons of the MAZ diameter measurements between and within the time-points; $P < 0.05$ was considered statistically significant. Outliers were excluded from the analysis. All values were entered in Microsoft Excel 2013 (Microsoft Corporation, Redmond WA), USA and analyzed with IBM SPSS Statistics Version 25 (IBM Corp., Armonk, NY).

RESULTS

Clinical Evaluation

Participants were clinically examined at day 1, 2, 7, and 14 for therapy-related complications of the treated area. All patients developed erythema and mild edema on the treated areas directly after the ablation. After 1 day, five of six patients developed crusts, whereas erythema and edema persisted. One week after skin ablation, the crusts almost disappeared. Erythema was still notably present but no edema was recognized. At the last time-point, treated skin was completely healed. In 2/6 patients, residual erythema was still detected. In none of the patients, crusts could be seen anymore (Fig. 1).

Evaluation of Pain

Skin ablation using TMA was well tolerated by all patients. Neither local anesthetics nor skin surface cooling were applied before or after the treatment. During the application on the skin, patients described a

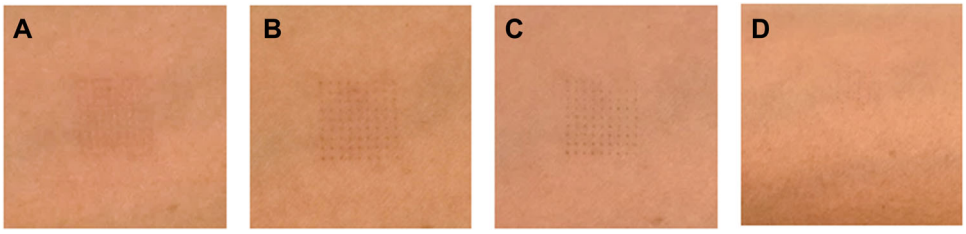

Fig. 1. Clinical manifestations of ablation area at day 1, 2, 7, and 14. (**A**) Edema and mild erythema directly after ablation. (**B**) Persistent erythema, edema, and crusts after 2 days. (**C**) Discrete erythema 1 week after ablation. (**D**) Complete remission of clinical signs 2 weeks after ablation.

mild-to-moderate pain of average 4 ± 1.9 in VAS pain. No further pain has been reported after the procedure.

Homogeneous Distribution of MAZ

First, we observed the distribution pattern of the MAZ. Like other fractionated skin ablation techniques, for example, bipolar radiofrequency or fractionated laser [3,9], TMA resulted in a homogenous distribution of 81 MAZ in a 10×10 mm area. MAZ were formed in a quadratic pattern with a regular distance. Between the MAZ skin appeared intact (Fig. 2M).

Microscopic Morphology Changes

Directly after skin ablation (day 1), MAZ are sharply defined as well-demarcated round epidermal and subepidermal defects without detection of any cell structures. Reflectance of deeper structures of DEJ and the papillary dermis could also be observed (Fig. 2A–C).

After 1 day, the beginning of the granulation process can be detected in all three examined levels. Islands of fibrinous tissue plunging in from the sites of the MAZ could be most prominently recognized in the papillary dermis, where regenerated tissue covers almost completely the defect area. Small round bright cells and

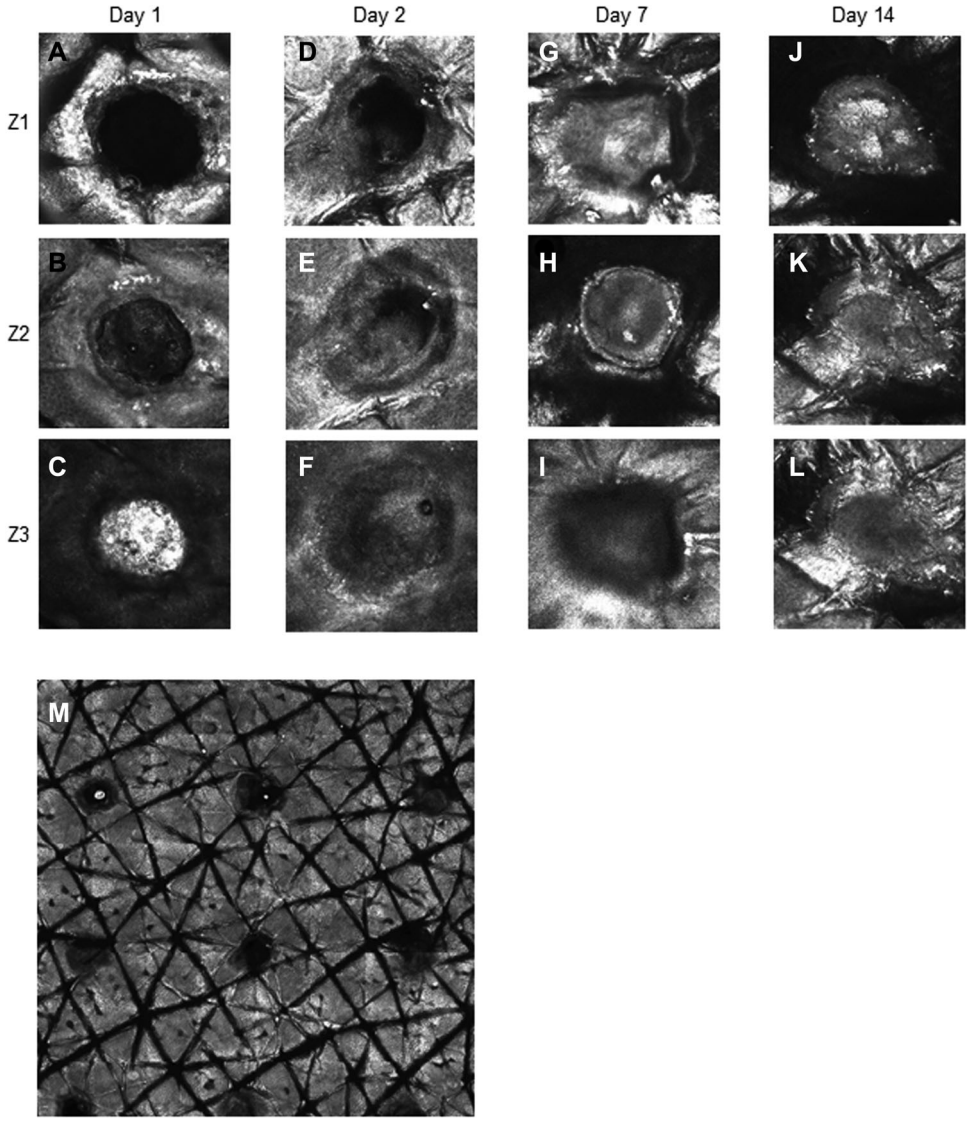

Fig. 2. (**A**–**L**) Confocal laser scanning microscopy (CLSM) scans of epidermis (Z1), dermoepidermal junction (Z2) and upper dermis (Z3) in horizontal sections at day 1, 2, 7, and 14 of treatment. Sharply defined round epidermal and subepidermal defects directly after ablation and complete restoration of honeycomb pattern after 14 days. (**M**) CLSM ViVaStack image of the treated area showing a homogeneous pattern of well-demarcated microscopic ablation zone (MAZ) directly after ablation.

diffuse edema surrounding MAZ indicate the inflammatory phase (Fig. 2D–F).

On the upper epidermal layer, as re-epithelization begins, the typical honeycomb pattern is almost completely reformed at day 7, whereas, in the deeper layers, low refractile amorphous tissue covers the total area of the defect (Fig. 2G–I).

On day 14, MAZ is completely re-epithelized in all three examined levels. The typical honeycomb pattern is thoroughly restored not only in the epidermis but also in the DEJ und papillary dermis level. Epidermal refractility is obviously higher all over the MAZ surface in all three levels (Fig. 2J–L).

Size of MAZ

As a consequence of the dynamic of wound-healing as observed in CLSM, a reduction of the diameter of MAZ should be expected. To clarify this assumption, we measured the diameter of the pores at the three levels as described above (Z1, Z2, and Z3) at all time-points. Interestingly, the diameter of MAZ did not significantly decrease over the observation time, with the exception of the Z3 level at day 7, where it reached a significant decrease compared with baseline ($P = 0.043$) (Fig. 3). Even if MAZ are filled with extracellular material during the healing process, they remain recognizable and stable in size.

DISCUSSION

Micro-invasive skin treatments have become more popular in the last few years. However, the development of new technologies with shortened downtime and reduced post-inflammatory hyperpigmentation (PIH) is needed. In particular, in the case of fractionated CO_2 lasers, a recovery time of up to 1 week and post-treatment erythema for longer than 4 weeks have been described [10]. Moreover, PIH has been reported to be more frequent in ablative fractionated CO_2 lasers depending on the dosages applied, and can occur in 20–92.3% of the patients [11].

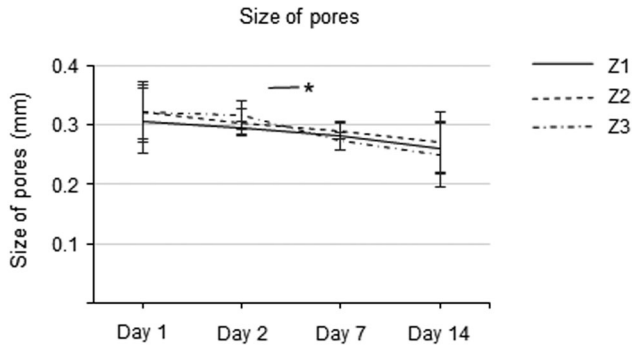

Fig. 3. Diameter of microscopic ablation zone (MAZ) at epidermis (Z1), dermoepidermal junction (Z2), and dermis (Z3) level at day 1 and after 2, 7, and 14 days of treatment. No statistically significant change of the size of pores observed between the time-points and within the same time-point, except in the Z1 level between day 2 and 7.

New devices providing the same efficacy of fractionated laser devices but with less side effects are required. As the process of wound healing is a crucial step to achieve optimal skin remodeling, in this proof-of-concept study, we aimed to examine the microscopic changes occurring during wound-healing after healthy skin ablation with TMA, an innovative skin ablation technology. Additionally, we monitored the clinical manifestations, tolerance and side effects on healthy skin.

The TMA occurs through high heated pins of a metal plate coming into short contact with the skin surface resulting in a fractionated pattern of ablation as known from other light or energy-based devices. TMA revolutionized the field of fractionated devices especially in dark skin types as no chromophores are targeted. The wound-healing procedures occurring after TMA skin ablation resembles models already known from fractional CO_2 laser or bipolar ablative radio frequencies [3,9].

Besides skin ablation, TMA causing a low-energy thermal decomposition of the stratum corneum can enhance the transepidermal penetration of substances [6]; recently proved for botulinum toxin and 5-amino-levulinic-acid [12,13]. These findings, showing an increased permeability of the epidermis after TMA, could maybe be extrapolated for aesthetic applications, like platelet-rich-plasma treatments.

Similarly, to RF, the production of fibrinous tissue begins from the sides of MAZ and presents an upward dynamic beginning from the DEJ heading up to the epidermis. However, the honeycomb pattern of the epidermis is restored much faster. In TMA, we observed a completed honeycomb pattern already after 14 days. In the case of CO_2 laser, 100% and 89.5% of skin damage was still visible on day 21 after ablation when treated with high or low dosage respectively [9]. In RF, 14 days after treatment the subepidermal damage could also be seen in all treated patients [3].

A limitation when using CLSM is incapability for measuring the collagen content in the skin. Collagen is the most abundant protein in human skin and it has been described to be possibly used as biomarker for skin regeneration [14]. Moreover, this proof-of-concept study lacks information about cytokine levels and expression of heat shock proteins and other factors that affect wound-healing and have already been examined following CO_2 fractional laser ablation [15]. Further studies are required to deeply understand the molecular mechanisms following this unique thermoablative technique.

In a recent publication, it could be shown that collagen plays a crucial role in the wound-healing process in acne scars after fractionated CO_2 laser treatment analysed by Raman spectroscopy [16]. A histological study in patients after bipolar RF revealed new collagen and elastin deposition in the treated areas [17]. Regarding TMA, also a histopathological study similarly revealed new collagen formation in the dermis after 7 days of treatment [5]. As TMA also initiated the wound-healing process like the fractionated CO_2 laser, it would be of interest to investigate if there is a difference in the collagen content after the different ablative fractionated systems.

TMA was well tolerated by the patients and only minor skin symptoms were observed. Compared with other skin ablation techniques, like fractionated CO_2 laser, symptoms were minor in intensity and lasted shorter. Similar to already published data with bipolar ablative radio frequencies, TMA caused no pigmentation abnormalities on the treated areas. Pain during treatment was also milder in comparison with CO_2 laser, where local or forced cold air anesthesia was required to achieve similar VAS scores during treatment [18]. Even when comparing with intralesional treatment of keloids with the combination of triamcinolone and 5-fluorouracil (5FU), a lower pain score was reported using TMA [19]. Thus, TMA could be suitable for sensible populations. In a retrospective study, pediatric hypertrophic burn scars were treated with Tixel for transdermal delivery of a topical solution containing triamcinolone and 5FU [20].

As expected, there are limitations in our study. The number of treated patients was restricted. However, the design was considered as a proof-of-concept study with a new technology, compared to already existing data for other fractionated devices. Although the number of the participants of this study is fairly limited, a similar wound-healing model in all patients could be observed, providing evidence for the underlying processes after TMA. Furthermore, only one setting was applied, which, however, represents the common clinical application.

CONCLUSION

In conclusion, as the wound-healing process after TMA is much faster, the recovery time is significantly minimized compared to other ablative techniques. Sessions shorter than 4 weeks could be clinically recommended, but they should not be further reduced than 2 weeks.

REFERENCES

1. Riggs K, Keller M, Humphreys TR. Ablative laser resurfacing: High-energy pulsed carbon dioxide and erbium:yttrium-aluminum-garnet. Clin Dermatol 2007;25(5):462–473.
2. Tierney EP, Eisen RF, Hanke CW. Fractionated CO_2 laser skin rejuvenation. Dermatol Ther 2011;24(1):41–53.
3. Kokolakis G, von Eichel L, Ulrich M, Lademann J, Zuberbier T, Hofmann MA. Kinetics and tissue repair process following fractional bipolar radiofrequency treatment. J Cosmet Laser Ther 2019;21(2):71–75.
4. Vachiramon V, Jurairattanaporn N, Harnchoowong S, Chayavichitsilp P. Non-invasive high-intensity focused ultrasound for UV-induced hyperpigmentation in Fitzpatrick skin types III and IV: A prospective, randomized, controlled, evaluator-blinded trial. Lasers Med Sci 2018;33(2):361–367.
5. Elman M, Fournier N, Barneon G, Bernstein EF, Lask G. Fractional treatment of aging skin with Tixel, a clinical and histological evaluation. J Cosmet Laser Ther 2016;18(1):31–37.
6. Sintov AC, Hofmann MA. A novel thermo-mechanical system enhanced transdermal delivery of hydrophilic active agents by fractional ablation. Int J Pharm 2016;511(2):821–830.
7. Srivastava R, Reilly C, Francisco G, Bhatti H, Rao BK. Life of a wound: Serial documentation of wound healing after shave removal using reflectance confocal microscopy. J Drugs Dermatol 2019;18(5):472–474.
8. Calzavara-Pinton P, Longo C, Venturini M, Sala R, Pellacani G. Reflectance confocal microscopy for in vivo skin imaging. Photochem Photobiol 2008;84(6):1421–1430.
9. Sattler EC, Poloczek K, Kastle R, Welzel J. Confocal laser scanning microscopy and optical coherence tomography for the evaluation of the kinetics and quantification of wound healing after fractional laser therapy. J Am Acad Dermatol 2013;69(4):e165–e173.
10. Chan NP, Ho SG, Yeung CK, Shek SY, Chan HH. Fractional ablative carbon dioxide laser resurfacing for skin rejuvenation and acne scars in Asians. Lasers Surg Med 2010;42(9):615–623.
11. Lee HS, Lee DH, Won CH, et al. Fractional rejuvenation using a novel bipolar radiofrequency system in Asian skin. Dermatol Surg 2011;37(11):1611–1619.
12. Friedman O, Koren A, Niv R, Mehrabi JN, Artzi O. The toxic edge-A novel treatment for refractory erythema and flushing of rosacea. Lasers Surg Med 2019;51(4):325–331.
13. Shavit R, Dierickx C. A new method for percutaneous drug delivery by thermo-mechanical fractional injury. Lasers Surg Med 2019. https://doi.org/10.1002/lsm.23125. [Epub ahead of print].
14. Yan W, Liu H, Deng X, et al. Raman spectroscopy enables noninvasive biochemical identification of the collagen regeneration in cutaneous wound healing of diabetic mice treated with MSCs. Lasers Med Sci 2017;32(5):1131–1141.
15. DeBruler DM, Blackstone BN, Baumann ME, et al. Inflammatory responses, matrix remodeling, and re-epithelialization after fractional CO_2 laser treatment of scars. Lasers Surg Med 2017;49(7):675–685.
16. Chiwo FS, Guevara E, Ramírez-Elías MG, et al. Use of Raman spectroscopy in the assessment of skin after CO_2 ablative fractional laser surgery on acne scars. Skin Res Technol 2019;25(6):805–809.
17. Hantash BM, Ubeid AA, Chang H, Kafi R, Renton B. Bipolar fractional radiofrequency treatment induces neoelastogenesis and neocollagenesis. Lasers Surg Med 2009;41(1):1–9.
18. Sari E, Bakar B. Which is more effective for pain relief during fractionated carbon dioxide laser treatment: EMLA cream or forced cold air anesthesia? J Cosmet Laser Ther 2018;20(1):34–40.
19. Artzi O, Koren A, Niv R, Mehrabi JN, Friedman O. The scar bane, without the pain: A new approach in the treatment of elevated scars: Thermomechanical delivery of topical triamcinolone acetonide and 5-fluorouracil. Dermatol Ther (Heidelb) 2019;9(2):321–326.
20. Artzi O, Koren A, Niv R, Mehrabi JN, Mashiah J, Friedman O. A new approach in the treatment of pediatric hypertrophic burn scars: Tixel-associated topical triamcinolone acetonide and 5-fluorouracil delivery. J Cosmet Dermatol 2019. https://doi.org/10.1111/jocd.13192. [Epub ahead of print].

Lasers in Surgery and Medicine 53:1152–1157 (2021)

Thermo-Mechanical Fractional Injury Therapy for Facial Skin Rejuvenation in Skin Types II to V: A Retrospective Double-Center Chart Review

Danny Daniely, MD[1,2*] **Harryono Judodihardjo, MB, BCh, BAO, MSC, PhD**[3] **Sajjad F. Rajpar, MB, ChB, FRCP**[3] **Joseph N. Mehrabi, MS**[2] **and Ofir Artzi, MD**[1,2,4]

[1]*Division of Dermatology, Tel Aviv Sourasky Medical Center, Tel Aviv, 642906, Israel*
[2]*Sackler Faculty of Medicine, Tel Aviv University, Tel Aviv, 6997801, Israel*
[3]*Belgravia Dermatology Limited, London, SW1X 9AE, UK*
[4]*Dr. Artzi and Associates - Treatment and Research Center, Tel Aviv, 6997712, Israel*

Background and Objectives: Thermo-mechanical fractional injury (TMFI) therapy (Tixel®; Novoxel®, Netanya, Israel) is an innovative technology. Along with its drug delivery enhancement features, it is widely used for facial skin rejuvenation. Our study explores the beneficial effect of the Tixel® on the different features of facial skin rejuvenation along with patients′ satisfaction rate, aiming to suggest practical recommendations for an optimal aesthetic result.

Study Design/Materials and Methods: A retrospective chart review of 24 patients (20 women, 4 men, average age 56 years old) with skin types II–V who received 2 or 3 Tixel® treatments, 3–5 weeks apart in two medical centers (12 from Israel, 12 from the United Kingdom). Four experienced dermatologists compared standardized clinical photographs taken before each treatment and 3 months after the final treatment based on seven parameters that were set by 10 physicians and rated the difference on a scale of −1 to 4. Furthermore, epidemiology, treatment data, satisfaction, and safety were reviewed.

Results: Out of the seven parameters that were compared (blood vessels and erythema, skin complexion, periorbital wrinkles, pigmentation and toning, pore size, vitality, wrinkles, and laxity), all features demonstrated an overall improvement, with the greatest improvement demonstrated in skin complexion (2.1 ± 0.49) and periorbital wrinkling (2.09 ± 0.65) followed by vitality (1.7 ± 0.49). Side effects were transient, including erythema and hyperpigmentation, and the average downtime was 1.7 days.

Conclusion: TMFI is a safe and effective method for improving facial skin quality. Addressing patient′s expectations while maximizing the benefits of this novel technology will provide superior aesthetical results.

Key words: Tixel; TMFI; Skin Rejuvenation

INTRODUCTION

Skin rejuvenation is an evolving field, focusing on a great interest for patients and physicians alike [1]. Nonetheless, the term *skin rejuvenation* is amorphous and may contain an improvement of several components [2]: skin pigmentation, wrinkling, laxity, skin glow, redness, prominent blood vessels, scarring, texture, pore size, and other skin imperfections. While many topical treatments, either minimally invasive or invasive, improve skin quality [3–5], each modality might provide a different change. Our study evaluates the clinical skin changes observed following treatment with thermo-mechanical fractional injury (TMFI) technology using the Tixel® device to establish the utility of this modality in skin rejuvenation.

METHODS

A retrospective chart review of all consecutive patients seeking treatment for facial skin rejuvenation treated in two centers (Tel Aviv, Israel and London, UK) using the Tixel® between March 2018 to January 2020 was conducted. The study was approved by an ethics committee and followed the tenets of the declaration of Helsinki.

The analysis included adults with skin type ranging from Fitzpatrick II–V. The subjects were treated according to the Tixel® TMFI technology systems′ instructions for use. Inclusion criteria were as follows: healthy males or females aged 20–80 years, seeking skin rejuvenation, and were willing and able to provide informed consent. Exclusion criteria were as follows: women who are pregnant or lactating, having severe sun damage, excessive skin laxity on the lower face and neck, keloid scarring or open wounds in the treatment areas, severe or cystic facial

Conflict of Interest Disclosures: All authors have completed and submitted the ICMJE Form for Disclosure of Potential Conflicts of Interest and none were reported.
Contract grant sponsor: Novoxel®, Israel.
*Correspondence to: Danny Daniely, MD, Division of Dermatology, Tel Aviv Sourasky Medical Center, 6 Weizman Street, Tel Aviv 642906 Israel.
E-mail: danielydanmd@gmail.com
Received 27 October 2020; revised 4 March 2021; Accepted 14 March 2021
Published online 30 March 2021 in Wiley Online Library (wileyonlinelibrary.com).
DOI 10.1002/lsm.23400

acne, a history of cosmetic treatments in the area to be treated (skin tightening procedure within the past year; injectable filler or botox within the past month; ablative or nonablative resurfacing/rejuvenating laser treatment or light treatment within the past 6 months; dermabrasion or deep facial peels within the past 6 months), isotretinoin treatment within the past 6 months, and inability to understand the treatment protocol or to give informed consent.

The Tixel® (Novoxel®, Israel) is a nonlaser, fractional, nonablative, thermomechanical skin rejuvenation system, which combines thermal energy with motion. The thermal energy is delivered to the tissue via a tip. The system consists of two types of tips, (i) a standard tip consisting of 81 (9×9) tiny titanium pyramids, and (ii) a small tip (also known as the periorbital tip) consisting of 24 (6×4) tiny pyramids. The tip base is heated to 400°C within a handpiece, which quickly moves toward the skin surface to achieve contact and coagulate tissue, creating microcraters by evaporation and desiccation. The amount of thermal energy delivered to the skin is determined by the pulse duration (PD; range: 5–18 milliseconds) and protrusion distance or depth (100–1000 μm). The protrusion is the distance the heated tip projects from the edge of the handpiece gauge per actuation. Hence a greater protrusion distance leading to a greater degree of skin contact between the titanium pyramids, fewer air gaps, and greater thermal transfer. Importantly, thermal transfer in TMFI technology does not involve any mechanical penetration of the epidermis.

Animal studies have shown that thermal lesions obtained at pulse duration ranging from 6 to 16 milliseconds and protrusion ranging from 400 to 800 μm exhibit nonablative results. For example, Tixel treatment settings (12 milliseconds and 600 μm) on a young porcine abdomen have shown a visualized and a localized dermoepidermal coagulation zone with an average depth of 237 ± 40 μm and width of 354 ± 67 μm. Tissue interactions presented with intra-epidermal vacuolization, subepidermal clefting, and intense eosin staining corresponding to the thermal treatment zone. The nonablative nature of the system's titanium tip and geometry of the thermal effect corresponds with mathematical analysis of skin temperature upon contact of the tip with the tissue. The analysis shows that a hemispherical heatwave is formed where the tip contacts the tissue. The tip is made of a gold-plated copper base rigidly connected to a thin-walled titanium shell. Analyzing the thermal behavior of the tip structure reveals that although the tip base is heated to 400°C, the titanium shell cools to below 150°C when making contact with the tissue for an extremely short duration (measured in milliseconds). For longer pulse durations (18 milliseconds and above), the titanium shell regains its high temperature and provides an ablative dermal treatment. The unique titanium tip and tissue thermal behavior are based on the dedicated tip's geometrical design combined with the thermal properties of the different material.

Treatment with Tixel® was delivered following the application of topical anesthetic cream. Patients received

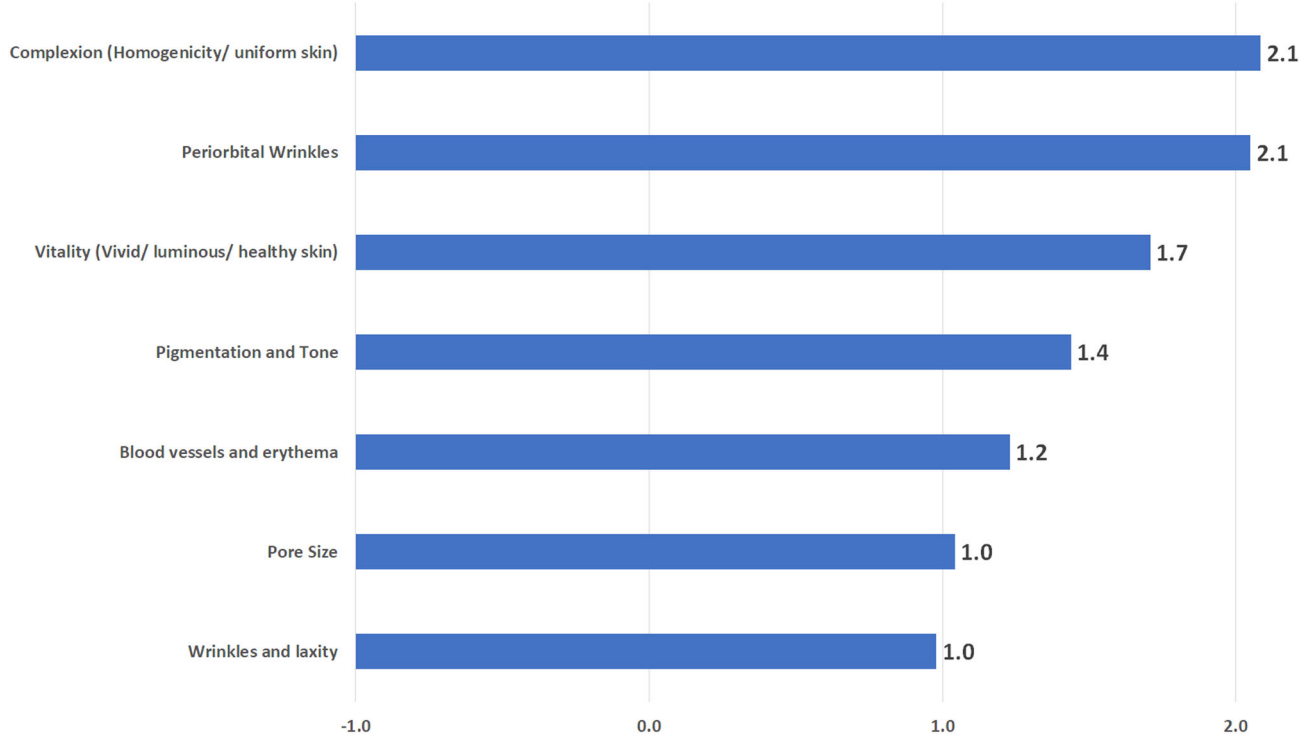

Fig. 1. The average weighted scores of the four dermatologists.

two or three treatments, and each treatment was 3–5 weeks apart. During each session, subjects received treatment with different PDs and different protrusion depths. The periorbital area (excluding the upper eyelids) was treated with a smaller (periorbital) tip while the rest of the face was treated with the standard tip in one to two passes with up to 0%–30% overlap. Adverse events and downtime (return to social activities) were assessed after each visit. As a standard of care, all patients were photographed preprocedure (before), at each visit, and 3 months postfinal treatment (after) by the "Visia" skin analysis imaging system (Canfield®, Parsippany, NJ, USA).

To define the changes observed following several Tixel® treatments, ten representatives before and after photographs were chosen and presented to 10 different non-involved physicians who were asked to offer 3 parameters, which were most improved. Changes that were mentioned more than twice by two different evaluators for at least two different sets of pictures were determined and included the following: blood vessels and erythema, skin complexion, periorbital wrinkles, pigmentation and toning, pore size, vitality, wrinkles, and laxity.

Then all left and right before and after photographs were randomly presented for evaluation. The above mentioned seven parameters as well as an extra general change parameter were scored by four experienced dermatologists on a 6-point scale according to the degree of improvement: -1 = worse result; 0 = no change; 1 = 1%–25% improvement; 2 = 26%–50% improvement; 3 = 51%–75% improvement; 4 = 76%–100% overall improvement. Finally, patient satisfaction with the results, treatment experience, and fulfillment of expectations were obtained on a 5-point scale (1–5).

Analyses were mainly descriptive in nature, summarized by count and percentage for categorical variables and mean, median, minimum, and maximum percentiles with standard error for continuous variables. Baseline and posttreatment outcomes were analyzed using Fisher′s test for categorical variables. All statistical analyses were performed by SPSS version 25.0 (IBM Corporation, Armonk, NY).

RESULTS

Twenty-four patients (12 from Israel, 12 from the United Kingdom; 20 women, 4 men) were included in this chart review. The age of the participants ranged from 39 to 69 years (average 56 years). Seven of them had Fitzpatrick skin type II, 11 had type III, 3 had type IV, and 3 type V. Patient demographics, medical history, and treatment characteristics are elaborated in Table 1. 87.5% ($n = 21$) and 12.5% ($n = 3$) of patients completed three and two treatments, respectively, every 3–5 weeks.

During each session, subjects received treatment with PD between 8 and 14 milliseconds and protrusion depths between 500 and 1000 μm. The face was treated with the standard tip and an average of 503 + 174 pulses were delivered per treatment. At each treatment, the periorbital skin was also treated with the periorbital tip and an average of 115 + 82 pulses were given per treatment. Treatment was delivered in one to two passes with 0%–30% overlap.

TABLE 1. Demographics and Treatment Characteristics

Age	Mean (SD)	56.2 (8.7)
	Median [IQR]	57.0 [48.5–64.5]
	Min–max	39.0-69.0
Sex	Female	20 (83.3%)
	Male	4 (16.7%)
Medical History	Anxiety	1 (4.2%)
	Cardiac arrhythmia	1 (4.2%)
	Cold sores	1 (4.2%)
	Depression	1 (4.2%)
	Herpes	1 (4.2%)
	Hip-joint pain	1 (4.2%)
	S/P Ca of breast	1 (4.2%)
	NA	17 (70.8%)
Fitzpatrick′s skin type	2	7 (29.2%)
	3	11 (45.8%)
	4	3 (12.5%)
	5	3 (12.5%)
Number of treatments	2	3 (12.5%)
	3	21 (87.5%)
Interval between treatments (weeks)	3	4 (16.7%)
	4	18 (75.0%)
	5	2 (8.3%)

IQR, interquartile range.

While processing four dermatologist′s assessments, all features demonstrated an overall improvement, and the greatest improvement was demonstrated in skin complexion (2.1 ± 0.49), and periorbital wrinkling (2.1 ± 0.65) followed by vitality (1.7 ± 0.49). The average weighted scores of the four dermatologists are shown in Figure 1. Figure 2 elaborates on the score distribution of every parameter. Skin complexion was improved in all patients, with a more than 50% improvement in 74% of cases. While addressing features with lower scores of improvement (wrinkles, laxity, and pore size), the κ coefficient of agreement between raters was 0.192 and 0.194, respectively, suggesting a disagreement between raters′ assessment, hence explaining the unfavorable result. The average patient′s satisfaction score (1–5) with skin improvement measured 3.6 (SD + 1.2), with treatment experience at 3.9 (SD + 1.3) and with the fulfillment of expectations at 3.4 (SD + 1.5). Patient satisfaction with improvement, treatment experience, and fulfillment of expectations correlated with treatment protrusion settings but not with pulse duration settings.

Posttreatment side effects included transient erythema lasting between 3 and 6 days in 3 out of 24 (12.5%) patients and hyperpigmentation in one patient with skin type III (healthy individual, F, 45, smoker). Notably, hyperpigmentation is not a common side effect of

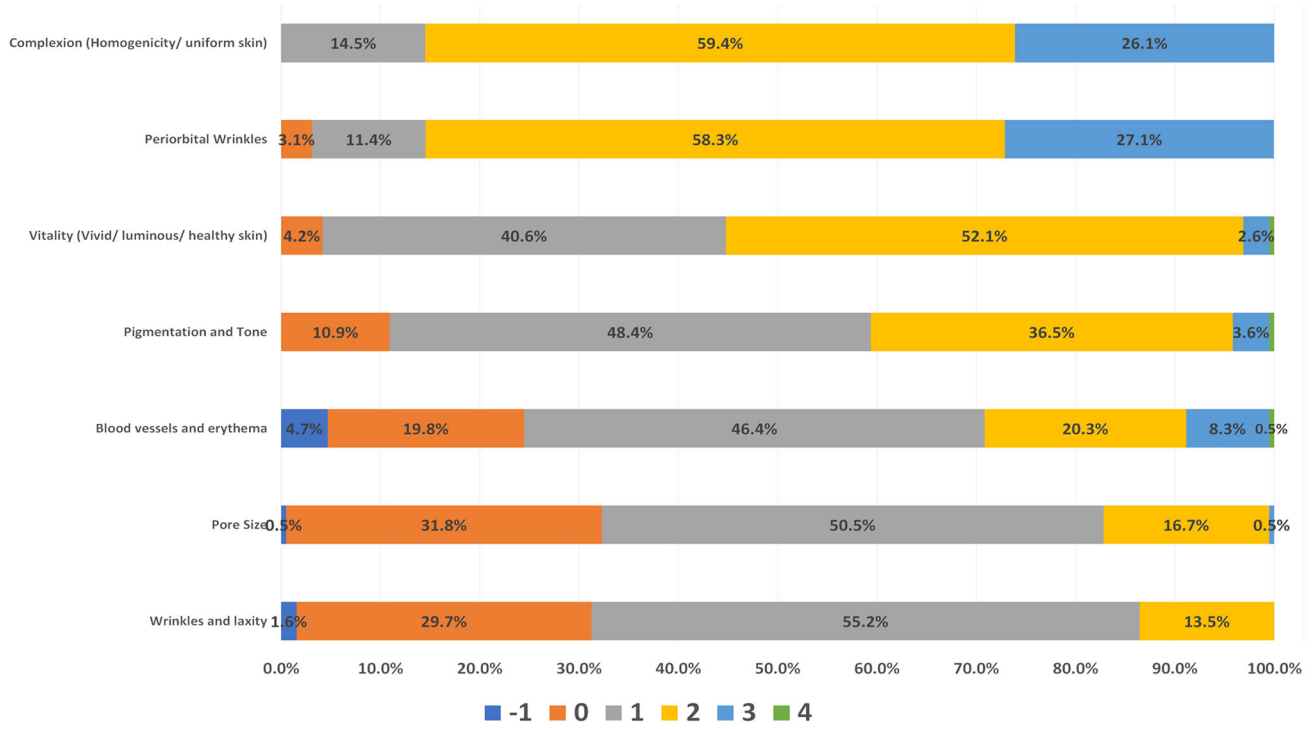

Fig. 2. The score distribution of every parameter.

TMFI; however, since this patient was treated with more aggressive settings (PD: 14 milliseconds; protrusion depth: 800 μm) for a higher-than-average number of pulses (669 and 162 pulses with the standard and small tip respectively), hyperpigmentation seems reasonable. The hyperpigmentation resolved after 9 months with bleaching agents. Average downtime (return to social activities) was 1.7 days (ranging 0–5 days) following medium settings.

DISCUSSION

The demand for skin rejuvenation modalities has greatly increased over the last few decades. *Skin rejuvenation* is a broad and amorphous term and includes many positive skin changes observed following various interventions. Different modalities are associated with different levels of improvement of the specific aspects of skin rejuvenation. The fractional CO_2 laser is considered to be the gold standard for skin resurfacing treatments [6]. However, its high cost, pain during treatment, and potential for complications are major disadvantages. Skin pigmentation is best treated with erbium laser [7], but IPL is considered to be an efficient alternative [8] with a shorter downtime [9]. Skin wrinkling [4] can be improved with the injection of hyaluronic acid-based fillers [10], peels [11], or ablative lasers [12], and skin laxity [13] can be improved by radiofrequency, ultrasound, or surgery. No well-defined guidelines exist for employing the correct modality to the suitable clinical scenario, thus turning facial skin rejuvenation, a fine art, into an exciting science.

The Tixel′s thermomechanical capabilities affect the dermal structure, implying a beneficial influence over skin appearance. Previous studies [14] demonstrated the unique characteristics of the epidermal microcraters and the beneficial effect of Tixel® on fibroblast proliferation and collagen production. Depending on the device settings, TMFI with the Tixel® creates a lesion 160-517μm in diameter and 170–350 μm in depth. The unique geometrical properties of the thermal lesion affect both the epidermis and superficial dermis with extensive coverage within a single treatment. In contrast to the effects of an ablative laser, the Tixel® craters are devoid of necrotic tissue without charring; thus, treatment is associated with accelerated recovery [15]. Posttreatment, the thermal effect spreads along the epidermis and superficial dermis. The temperature rapidly drops from 400°C at skin surface, to 50°C at 100 μm depth. Histological models [14] have demonstrated epidermal regeneration with a surface crust and a dermoepidermal cleft filled with new fibroblasts and macrophage cells 7 days posttreatment surrounded with new collagen formation. As shown in our study, the main improvements observed following several Tixel® treatments include changes in skin complexion (Fig. 3), periorbital wrinkling (Fig. 4), and vitality. These potential changes should be discussed with the patient prior to the initiation of the treatment course to meet expectations.

In comparison with ablative lasers, Tixel® treatment is associated with minimal procedural pain, short downtime, few side effects, and fast wound healing [15], allowing for a more frequent treatment regimen and a

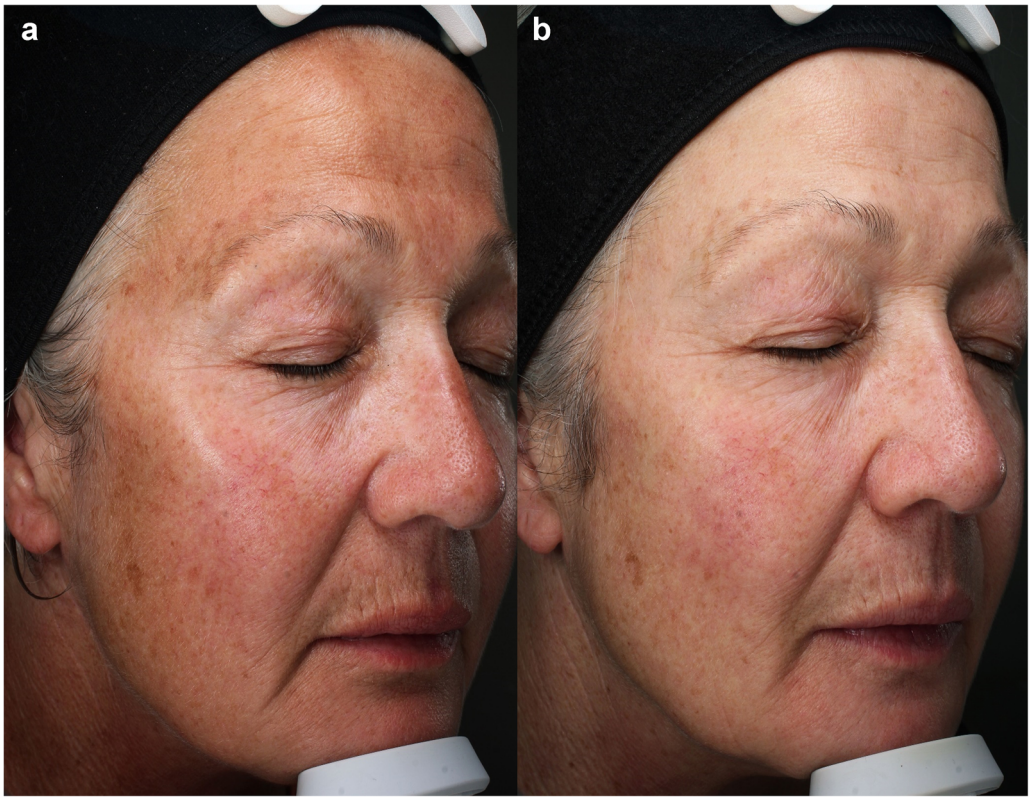

Fig. 3. A representative patient before (**a**) and after (**b**) several treatments. Please note the change in skin complexion.

shorter period to achieve the final result. In addition, Tixel® revolutionized the field of fractionated devices in dark skin types, as no chromophores are targeted. However, although less frequent than lasers, high settings and multiple passes of TMFI in dark skin patients might result in hyperpigmentation.

Several pearls can be elaborated to augment results:

(1) Higher protrusion depths reduce the air gaps between the tip and the skin, and better results are observed while applying the treatment over bony prominences (forehead, cheekbones) than over fatty tissue, empowering the importance of thermal matching. The physician should consider changing the protrusion while treating different areas. Bony areas deserve low protrusion, while fatty soft areas require higher protrusion. Hence, using a designated intraoral spatula might improve the therapeutical effect in the perioral areas.
(2) Multiple passes in a prior animal study conducted by Novoxel assessed the thermal damage created by the Tixel®. A single pass of mild (6 milliseconds/400 μm), moderate (12milliseconds/600 μm), and aggressive (16 milliseconds/800 μm) settings will provide treatment densities of 6.7%, 8%, and 15.5%, respectively. While it is difficult to calculate the exact coverage on multiple passes because some of the microthermal zones might overlap, the authors estimate the coverage to be around 15% if double passes of moderate settings are performed. More passes will increase the coverage, elongate downtime, and potentially be associated with more adverse effects.
(3) Surface debridement in between passes: The majority of heat transferred from Tixel® is absorbed by the epidermis. Much of the epidermis can be sloughed following three passes of Tixel® and wet gauze abrasion. This exposes the dermis, which can be treated directly. When Tixel® is used over the exposed dermis, augmented results can be achieved.
(4) TMFI-assisted drug delivery: Tixel, known to improve drug delivery [16], has already been utilized in the treatment of several medical conditions, including hypertrophic scars [17], acne [18], and rosacea [19]. Therefore, combining the esthetic thermomechanical effect with different cosmeceutical or drug delivery might augment the results. However, this fascinating combination still needs to be fully explored and validated.

The main limitation of this study is its retrospective nature. This is a noncontrolled retrospective study, not comparing Tixel® clinical performances and patients' satisfaction with other modalities and technologies. Therefore, more prospective research studies are required to reveal the full benefits of this novel technology.

In conclusion, Tixel® is a minimally invasive modality in facial skin rejuvenation, having a clear benefit in improving

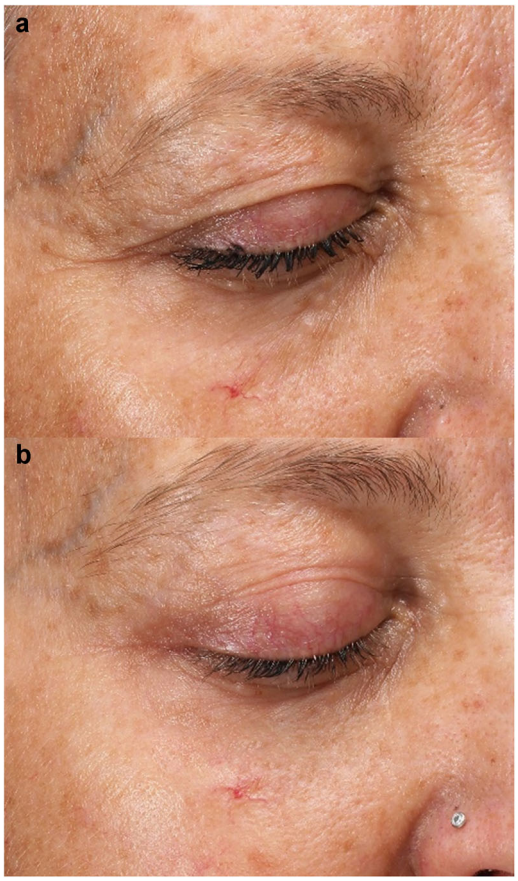

Fig. 4. A representative patient before (**a**) and after (**b**) several Tixel®treatments. Please note the change in periorbital wrinkles.

skin complexion, vitality, and periorbital wrinkling with a low incidence of side effects in a wide range of skin types. Although the objective physicians′ assessments indicate only mild-to-moderate improvements, patient′s satisfaction shows higher results. A baseline accurate clinical evaluation, an understanding of patients′ expectations, and full disclosure of the technology capabilities might allow the physician to optimize esthetic results.

ACKNOWLEDGMENT

This study was supported by Novoxel®, Israel.

REFERENCES

1. Gold MH. The future of non-invasive rejuvenation technology: Devices. J Drugs Dermatol 2017;16(6):s104–s107.
2. Fischer TC, Gauglitz GG. Nonsurgical facial rejuvenation. Facial Plast Surg 2016;32(3):243–244.
3. Nilforoushzadeh MA, Amirkhani MA, Zarrintaj P, et al. Skin care and rejuvenation by cosmeceutical facial mask. J Cosmet Dermatol 2018;17(5):693–702.
4. Bukhari SNA, Roswandi NL, Waqas M, et al. Hyaluronic acid, a promising skin rejuvenating biomedicine: a review of recent updates and pre-clinical and clinical investigations on cosmetic and nutricosmetic effects. Int J Biol Macromol 2018;120(Pt B):1682–1695.
5. Lipp M, Weiss E. Nonsurgical treatments for infraorbital rejuvenation: A review. Dermatol Surg 2019;45(5):700–710.
6. Filippini M, Del duca E, Negosanti F, et al. Fractional CO laser: From skin rejuvenation to vulvo-vaginal reshaping. Photomed Laser Surg 2017;35(3):171–175.
7. Britt CJ, Marcus B. Energy-based facial rejuvenation: Advances in diagnosis and treatment. JAMA Facial Plast Surg 2017;19(1):64–71.
8. Yi J, Hong T, Zeng H, et al. A Meta-analysis-based assessment of intense pulsed light for treatment of melasma. Aesthetic Plast Surg 2020;44(3):947–952.
9. Tao L, Wu J, Qian H, et al. Intense pulsed light, near infrared pulsed light, and fractional laser combination therapy for skin rejuvenation in Asian subjects: A prospective multicenter study in China. Lasers Med Sci 2015;30(7):1977–1983.
10. Kim JS. Fine Wrinkle Treatment and hydration on the facial dermis using hydrotoxin mixture of microbotox and microhyaluronic acid. Aesthet Surg J. 2020.
11. Pathak A, Mohan R, Rohrich RJ. Chemical peels: Role of chemical peels in facial rejuvenation today. Plast Reconstr Surg 2020;145(1):58e–66e.
12. Sanniec K, Afrooz PN, Burns AJ. Long-term assessment of perioral rhytide correction with erbium: YAG laser resurfacing. Plast Reconstr Surg 2019;143(1):64–74.
13. Gentile RD, Kinney BM, Sadick NS. Radiofrequency technology in face and neck rejuvenation. Facial Plast Surg Clin North Am 2018;26(2):123–134.
14. Elman M, Fournier N, Barnéon G, Bernstein EF, Lask G. Fractional treatment of aging skin with Tixel, a clinical and histological evaluation. J Cosmet Laser Ther 2016;18(1):31–37.
15. Kokolakis G, Von grawert L, Ulrich M, Lademann J, Zuberbier T, Hofmann MA. Wound healing process after thermomechanical skin ablation. Lasers Surg Med 2020;52(8):730–734.
16. Shavit R, Dierickx C. A new method for percutaneous drug delivery by thermo-mechanical fractional injury. Lasers Surg Med 2020;52(1):61–69.
17. Artzi O, Koren A, Niv R, Mehrabi JN, Mashiah J, Friedman O. A new approach in the treatment of pediatric hypertrophic burn scars: Tixel-associated topical triamcinolone acetonide and 5-fluorouracil delivery. J Cosmet Dermatol 2020;19(1):131–134.
18. Hilerowicz Y, Friedman O, Zur E, et al. Thermomechanical ablation-assisted photodynamic therapy for the treatment of acne vulgaris. A retrospective chart review of 30 patients. Lasers Surg Med 2020;52:966–970.
19. Friedman O, Koren A, Niv R, Mehrabi JN, Artzi O. The toxic edge—A novel treatment for refractory erythema and flushing of rosacea. Lasers Surg Med 2019;51(4):325–331.

DERMATOLOGIC SURGERY

Safety and Efficacy of a Thermomechanical Fractional Injury Device for Periorbital Rhytides

Jordan V. Wang, MD, MBE, MBA,* Shirin Bajaj, MD,* David Orbuch, MD,* Moshe Lapidoth, MD, MPH,†‡ Ifat Klein, PhD,§ Yael Agmon Gerstein, DVM,§ Roy G. Geronemus, MD,* and Assi Levi, MD†‡

BACKGROUND Periorbital rejuvenation is a common cosmetic concern. A fractional thermomechanical skin rejuvenation system was developed to offer clinical improvements from direct heat transfer.

OBJECTIVE A prospective study evaluated the efficacy and safety of the device for periorbital fine lines and wrinkles.

MATERIALS AND METHODS Subjects with moderate-to-severe periorbital rhytides were enrolled and underwent 4 monthly treatments with a novel device using thermomechanical fractional injury (Tixel 2; Novoxel, Netanya, Israel).

RESULTS Fifty-one subjects were enrolled. Mean age was 56.8 years, and 88.2% were women. Fitzpatrick skin Types I to IV were included. For Fitzpatrick Wrinkle Classification System (FWCS), mean baseline score was 5.7. Per investigator, there was a mean 2.0-grade improvement in FWCS at 3-month follow-up ($p < .0001$). Per 3 blinded physician raters, there was a mean improvement of 2.2 ($p < .0001$), 2.0 ($p < .0001$), and 1.2 ($p < .0001$) in FWCS at 3-month follow-up. Each of the raters correctly identified posttreatment images for 87.5%, 77.1%, and 75.0% of subjects. At least 2 raters agreed on grading 83.3% of subjects as responders. There were no severe adverse events. Subjects experienced minimal pain and downtime.

CONCLUSION A novel device using thermomechanical fractional injury was demonstrated to be safe and effective in the treatment of periorbital rhytides.

Periorbital rhytides are a common aesthetic concern of many patients. They are often an early manifestation of facial aging, especially since this area is prone to repetitive muscular movements and facial expressions. The dynamic nature of these rhytides can often make them difficult to effectively treat, in terms of skin texture, depth and length of lines, and laxity. Other factors contributing to their presence and severity include genetics, photoaging, skin type, hormonal status, ethnicity, nutrition, and environmental factors among others.[1,2] Since the eyes and adjacent area draw significant attention from others, especially during social interactions, treatment of the periorbital area is sought by many patients. These treatments have traditionally included injectable neurotoxins, soft-tissue fillers, and laser-, light-, and energy-based devices.

Recently, thermomechanical fractional injury has gained more attention in the dermatologic and aesthetic field, especially as a promising treatment modality for skin rejuvenation.[3–9] A recent chart review evaluated improvements in skin complexion, periorbital wrinkling, blood vessels and erythema, pigmentation and toning, pore size, vitality, and laxity with this device.[3] All measures were ultimately found to have overall clinical improvement. In a recent prospective study comparing the thermomechanical fractional injury device with a nonablative fractional 1,565 nm laser, moderate improvement in periorbital wrinkling was demonstrated in both groups.[4] This current study is meant to be a larger study that should support the early clinical outcomes and safety data currently available.

The authors hypothesize that the use of a novel fractional thermomechanical skin rejuvenation system can greatly improve the clinical appearance of periorbital rhytides in a safe and effective manner. The authors performed a prospective study to assess the utility of this treatment modality.

Materials and Methods

Fifty-one healthy subjects with moderate-to-severe periorbital rhytides at rest were enrolled. This study was conducted at 2 sites and approved by 2 independent Institutional Review Boards. Informed consent was obtained from all subjects. To be included, subjects had to be 35 to 70 years old and Fitzpatrick Skin Type (FST) I to V with a Fitzpatrick Wrinkle Classification System (FWCS) score of 3 to 7 in the periorbital area. Subjects were excluded if they had a cosmetic procedure to improve periorbital rhytides in the past 12 months; facial treatments with laser-, light-, and energy-based devices, chemical peels, or neurotoxins over the periorbital area in the past 12 months; injectable fillers in the mid and upper face in the past 12 months; recent significant exposure to ultraviolet light;

*From the *Laser & Skin Surgery Center of New York, New York, New York; †Photodermatosis Service Laser Unit, Division of Dermatology, Rabin Medical Center, Petah-Tikva, Israel; ‡Sackler Faculty of Medicine, Tel Aviv University, Tel Aviv, Israel; §Novoxel LTD, Netanya, Israel*

Supported by Novoxel. Roy Geronemus is on the advisory board for Novoxel. Ifat Klein and Yael Agmon Gerstein are employees of Novoxel.

The authors have indicated no significant interest with commercial supporters.

Address correspondence and reprint requests to: Jordan V. Wang, MD, MBE, MBA, Laser & Skin Surgery Center of New York, 317 E 34th Street, 6th Floor Research Department, New York, NY 10016, or e-mail: drjordanwang@gmail.com

http://dx.doi.org/10.1097/DSS.0000000000003728

visible scars over the area; active cut, infection, or inflammation in the area; history of skin malignancy or postinflammatory hyperpigmentation in the area; history of immunosuppression, autoimmune disease, collagen or vascular disease, bleeding disease, keloid formation, neuromuscular disorder, or condition affecting healing rate; use of oral retinoids in the past 6 months; use of oral steroids; and been planning to become pregnant, were currently pregnant, or have given birth less than 3 months prior.

Each subject received 4 treatments to the periorbital area with a novel device using thermomechanical fractional injury (Tixel 2; Novoxel, Netanya, Israel) at 28 (±7)-day intervals. Subjects were offered the option of air cooling during the treatment and cold packs after the treatment. There was no use of topical or local anesthesia. At investigator discretion, the device was allowed to be set to 8 to 12 milliseconds pulse duration and 400 to 600 μm protrusion depth, using a single or double pass, with the standard or small tip. Most of the treatments were performed at 12 milliseconds pulse duration and 600 μm protrusion depth using a double-pass method. The small tip was generally used in tighter areas around the eye. The treatment area encompassed above and below the eyebrow, lower eyelid, and beyond (1–2 cm at 45° above and below) the most lateral aspect of the periorbital rhytid.

Periorbital rhytides were graded using the FWCS scale at baseline and final follow-up visit at 3 months after the final visit. The Global Aesthetics Improvement Scale (GAIS) (5-point scale) was used by investigators to grade clinical improvement at the final follow-up visit at 3 months. Three blinded physicians were given photographs at baseline and 3-month follow-up to grade using FWCS scale. Subject pain and posttreatment downtime were assessed after every treatment, and subject satisfaction was assessed at 3-month follow-up. Adverse events were also assessed.

Results

Subject Demographics

Fifty-one subjects were enrolled into the study, and 48 subjects completed the study. Mean age was 56.8 years (range: 38–70 years). Of all subjects, 88.2% ($n = 45$) were women. In terms of FST, 25.5% ($n = 13$) were Type I, 37.2% ($n = 19$) were Type II, 25.5% ($n = 13$) were Type III, and 11.8% ($n = 6$) were Type IV.

Investigator Ratings

At baseline, subjects had a mean FWCS score of 5.67 (range: 3–7). At 3-month follow-up, the mean FWCS score decreased to 3.63 (range: 2–5), for a mean improvement of 2.04 (±0.58) units ($p < .0001$). All subjects (100%) were considered to be responders to the treatment regimen.

For investigator GAIS, all subjects (100%) had improvement at 3-month follow-up, with 56.3% ($n = 27$) having 76% to 100% improvement, 39.6% ($n = 19$) having 51% to 75% improvement, and 4.2% ($n = 2$) having 26% to 50% improvement. The mean score was 3.52 (±0.58) on a scale of 0 to 4.

Blinded Photographic Review

Three blinded physicians were provided with photographs of subjects at baseline and 3-month follow-up. Each of the raters correctly identified posttreatment images for 87.5% ($n = 42$), 77.1% ($n = 37$), and 75.0% ($n = 36$) of subjects. They rated a mean improvement of 2.17 (±0.74) ($p < .0001$), 2.00 (±0.86) ($p < .0001$), and 1.19 (±0.57) ($p < .0001$) in FWCS score from baseline to 3-month follow-up. At least 2 of the 3 raters were in agreement for grading 83.3% of subjects as responders.

Subject Pain and Downtime

For patient-reported pain during the treatment, the mean scores on a scale of 0 to 10 were 2.98 (±1.52), 2.94 (±1.14), 2.82 (±1.22), and 2.81 (±1.2) for each of the 4 treatments, respectively. All subjects felt ready to return to their work and social activities after a mean of 0.58 to 1.05 days after each treatment. Erythema lasted a mean of 2.43 to 3.01 days, and edema lasted a mean of 1.47 to 1.92 days after each treatment.

Subject Satisfaction

At 3-month follow-up, 93.8% ($n = 45$) of subjects were satisfied to some degree with their results, including half (50.0%; $n = 24$) who were "very satisfied." Additionally, 95.8% ($n = 46$) were satisfied to some degree with their

Figure 1. Photographs of a female subject at baseline and follow-up at 3 months (from left to right).

Figure 2. Photographs of a female subject at baseline and follow-up at 3 months (from left to right).

treatment experience, including nearly two-thirds (62.5%; $n = 30$) who were "very satisfied."

Safety

During the study, expected treatment effects were observed, which included transient erythema, transient roughness, and transient dryness. There were 2 adverse events reported: one being erythema and the other that was deemed to be unrelated to the study, which was back pain. They were mild in severity and nonserious in nature.

Discussion

Recently, thermomechanical fractional injury has gained traction as a novel treatment modality that can enhance aesthetic outcomes with minimal associated pain and downtime for patients, and no anesthesia is required. More traditional modalities have included laser-, light-, and energy-based devices, such as radiofrequency and ultrasound. This particular novel device uses heated metallic pyramidal tips that work by transferring heat through conduction upon brief tissue contact. A ceramic heater is attached to the base of the tips, which is heated to 400°C. The treatment is noninvasive in nature because the blunt pyramidal tips do not physically pierce or penetrate the skin surface. The thermal effects have been demonstrated to offer relatively wide and large volumes of dermal coagulation. Locally, this stimulates and supports neocollagenesis and neoelastogenesis, which can clinically translate to improvements in rhytides.

This study demonstrates that a thermomechanical fractional injury device can improve the clinical outcomes of periorbital rhytides in a safe and effective manner (Figures 1 and 2). At 3-month follow-up, investigators scored a greater than 2-unit mean improvement in FWCS, with all subjects having clinical improvement and more than half (56.3%) having 76% to 100% rated improvement. This was supported by the FWCS scores of 3 blinded physician raters, who ultimately assigned an 83.3% responder rate.

This treatment modality is unique in that it can offer clinical improvements in rhytides that are considered to be dynamic in nature. Traditionally, it has been more difficult to achieve improvement in dynamic rhytides with devices compared with their static counterparts. This is due to the nature of how dynamic lines have developed and how they are constantly being stressed due to repeated motions and muscle movements, which is certainly true for the periorbital area. Because the orbicularis oculi muscle undergoes constant and repetitive movement with expression, achieving improvement in this area has important clinical implications for patients. Notably, in this study, even at 3 months after the final treatment, patients continued to demonstrate meaningful improvement in their rhytides.

During treatments, there were relatively low levels of subject discomfort as well as short periods of posttreatment downtime. Due to the nature of how this device works, there is only brief contact of the heated pyramidal tips with the skin surface. For the settings in this particular study, the contact was for only a few milliseconds. This likely contributed to the low level of reported pain, which was commonly 2 to 3 out of 10. Treatments only included the optional use of air cooling, which is in stark contrast to many laser- and energy-based devices that can require topical anesthesia, local anesthesia, and/or sedation to offer a comfortable treatment experience. Topical anesthesia may even take up 10 to 60 minutes of patient's and physician's time, which can now be avoided with this device. Downtime from social engagements and work was typically 1 day or less for subjects, whereas local swelling and erythema generally lasted 1 to 2 days and 2 to 3 days, respectively. This is considerably less downtime compared to many other devices, which likely contributed to the high rates of patient satisfaction with the treatment experience.

Another important aspect of this novel thermomechanical fractional injury device is its high level of safety for use in the delicate periorbital area. No subject had any serious adverse events related to the treatment. In contrast to many laser and light devices, no eye protection (e.g., metal goggles or intraocular eye shields) is required for patients being treated because this device operates based on brief physical heat transfer and is not chromophore dependent. This adds an extra layer of protection when using this device to treat around the eye. Such complications that can occur when using laser- and light-based devices in this anatomic site include posterior synechiae, iris atrophy, macular holes, iris pigment dispersion, anterior uveitis, and blindness.[10–14] Most of the events occur in the absence of sufficient eye protection.

This prospective study demonstrates the efficacy of thermomechanical fractional injury for treating periorbital rhytides in subjects who were FST I through IV. Future large-scale trials can recruit additional subjects who are FST

V and VI. However, this particular device has already demonstrated real-world safety in darker skin types. Although investigator ratings demonstrated a 100% responder rate, blinded photographic reviewers were only able to correctly select images in 75.0% to 87.5% of cases. This demonstrates a detection bias, and future studies may benefit from a control or sham group. Computerized imaging can also be incorporated, which can improve the objective measurement of rhytides.

Conclusion

In this prospective study, a novel thermomechanical fractional injury device significantly improved periorbital rhytides. This treatment modality was demonstrated to be safe, well-tolerated, and well-liked by subjects.

References

1. Nkengne A, Bertin C. Aging and facial changes–Documenting clinical signs, part 1: clinical changes of the aging face. *Skinmed* 2013;11:281–6.
2. Mokos ZB, Ćurković D, Kostović K, Čeović R. Facial changes in the mature patient. *Clin Dermatol* 2018;36:152–8.
3. Daniely D, Judodihardjo H, Rajpar SF, Mehrabi JN, Artzi O. Thermomechanical fractional injury therapy for facial skin rejuvenation in skin types II to V: a retrospective double-center chart review. *Lasers Surg Med* 2021;53:1152–7.
4. Salameh F, Daniely D, Kauvar A, Carasso RL, et al. Treatment of periorbital wrinkles using thermo-mechanical fractional injury therapy versus fractional non-ablative 1565 nm laser: a comparative prospective, randomized, double-arm, controlled study. *Lasers Surg Med* 2022;54:46–53.
5. Manuskiatti W, Yan C, Artzi O, Gervasio MKR, Wanitphakdeedecha R. Efficacy and safety of thermomechanical fractional injury-assisted corticosteroid delivery versus intralesional corticosteroid injection for the treatment of hypertrophic scars: a randomized split-scar trial. *Lasers Surg Med* 2022;54:483–9.
6. Foged C, Haedersdal M, Bik L, Dierickx C, et al. Thermo-Mechanical fractional injury enhances skin surface- and epidermis- protoporphyrin IX fluorescence: comparison of 5-aminolevulinic acid in cream and gel vehicles. *Lasers Surg Med* 2021;53:622–9.
7. Hilerowicz Y, Friedman O, Zur E, Ziv R, et al. Thermomechanical ablation-assisted photodynamic therapy for the treatment of acne vulgaris. A retrospective chart review of 30 patients. *Lasers Surg Med* 2020;52:966–70.
8. Artzi O, Koren A, Niv R, Mehrabi JN, et al. A new approach in the treatment of pediatric hypertrophic burn scars: tixel-associated topical triamcinolone acetonide and 5-fluorouracil delivery. *J Cosmet Dermatol* 2020;19:131–4.
9. Shavit R, Dierickx C. A new method for percutaneous drug delivery by thermo-mechanical fractional injury. *Lasers Surg Med* 2020;52:61–9.
10. Huang A, Phillips A, Adar T, Hui A. Ocular injury in cosmetic laser treatments of the face. *J Clin Aesthet Dermatol* 2018;11:15–8.
11. Lin CC, Tseng PC, Chen CC, Woung LC, Liou SW. Iritis and pupillary distortion after periorbital cosmetic alexandrite laser. *Graefes Arch Clin Exp Ophthalmol* 2011;249:783–5.
12. Chuang LH, Lai CC, Yang KJ, Chen TL, Ku WC. A traumatic macular hole secondary to a high-energy Nd:YAG laser. *Ophthalmic Surg Lasers Imaging Retina* 2001;32:73–6.
13. Hammes S, Augustin A, Raulin C, Ockenfels HM, Fischer E. Pupil damage after periorbital laser treatment of a port-wine stain. *Arch Dermatol* 2007;143:392–4.
14. Hagemann LF, Costa RA, Ferreira HM, Farah ME. Optical coherence tomography of a traumatic Neodymium:YAG laser-induced macular hole. *Ophthalmic Surg Lasers Imaging* 2003;34:57–9.

Prospective Evaluation of the Safety and Efficacy of Thermomechanical Fractional Injury for Perioral Rhytides

Jordan V. Wang, MD, MBE, MBA,* Shirin Bajaj, MD,* Alexa Steuer, MD,† David Orbuch, MD, MBA,* and Roy G. Geronemus, MD*†

BACKGROUND: Perioral rhytides can be treated with laser and energy-based devices. More recently, a novel fractional thermomechanical skin rejuvenation system was developed to cause controlled thermal injury through direct heat transfer.

OBJECTIVE: A prospective clinical trial evaluated the safety and efficacy of a thermomechanical fractional injury device (Tixel 2, Novoxel, Netanya, Israel) for perioral rhytides.

MATERIALS AND METHODS: Subjects with moderate-to-severe perioral rhytides were enrolled and underwent 4 monthly treatments.

RESULTS: Twenty-three subjects were enrolled and completed all study visits. Mean age was 62.5 years, and 100.0% were women. Fitzpatrick Skin Types I-IV were included. For Fitzpatrick Wrinkle Classification System (FWCS), mean baseline score was 6.9. Per investigator, there was a mean 1.9-grade improvement in FWCS at 3-month follow-up ($p < .0001$). At 3-month follow-up, 8.7% (n = 2) of subjects had a 3-grade improvement, 69.6% (n = 16) had a 2-grade improvement, and 21.7% (n = 5) had a 1-grade improvement. For physician Global Aesthetics Improvement Scale at 3-month follow-up, 69.6% (n = 16) had 76% to 100% improvement, 13.0% (n = 3) had 51% to 75% improvement, and 17.4% (n = 4) had 26% to 50% improvement. There were no severe adverse events, and subjects experienced minimal pain.

CONCLUSION: A novel device using thermomechanical fractional injury was demonstrated to be safe and effective in the treatment of perioral rhytides.

Introduction

Age-related changes of the lower face, including the perioral region, may occur as early as the third decade of life.[1,2] Gradual structural changes to the dermis begin, and perioral rhytides can develop as a result of the natural loss of collagen and elastin that occurs with age, which is often accentuated by intrinsic hormonal and genetic factors and lifestyle habits, such as smoking and chronic photodamage.[2] Dynamic (present with muscle contraction of the orbicularis oris) and static (present at rest) rhytides may become more prominent in the perioral area, which can progress to a cobblestoned textural change over time.[1] Epidermal and superficial dermal resurfacing and thermal coagulation can improve the appearance of perioral rhytides through the upregulation of collagen and elastin formation, which can improve fine lines and surface texture.[1–3]

Traditional options for perioral rejuvenation include neurotoxins, soft-tissue fillers, chemical peels, dermabrasion, radiofrequency microneedling, ultrasound, and lasers, and a combination of treatments.[1,4,5] Fully ablative, fractional ablative, and fractional nonablative lasers have been used successfully, with fractional lasers typically offering clinical improvement with less postprocedural downtime and overall risk for adverse events.[6,7] Still, these procedures can be painful and often require topical or local analgesia beforehand, and they can be associated with prolonged downtime.[7]

More recently, a thermomechanical fractional injury device has become available and can offer a novel treatment modality for skin rejuvenation. Through conductive heat transfer by brief tissue contact with the noninvasive tip of the handpiece, thermal effects, such as dermal coagulation, can be achieved, while offering minimal post-treatment downtime without the need for anesthesia.[7,8] The thermomechanical fractional injury device has been shown to improve complexion, wrinkling, pore size, and laxity in a recent retrospective chart review.[6] Its effects on periorbital wrinkling were shown to be similar to that of a nonablative 1565-nm laser with minimal adverse events and recovery time.[6,9] In this prospective clinical trial, we evaluate the safety and efficacy of this novel fractional thermomechanical skin rejuvenation system for the improvement of perioral rhytides.

*From the *Laser & Skin Surgery Center of New York, New York, New York; † The Ronald O Perelman Department of Dermatology, New York University Langone Health, New York, New York*

Supported by Novoxel. R. G. Geronemus is on the advisory board for Novoxel. The authors have indicated no significant interest with commercial supporters.

Address correspondence and reprint requests to: Jordan V Wang, MD, MBE, MBA, Laser & Skin Surgery Center of New York, 317 E 34th Street, 6th Floor Research Department, New York, NY 10016, or e-mail: drjordanwang@gmail.com

Dermatol Surg 2023;00:1–4
http://dx.doi.org/10.1097/DSS.0000000000003762

Materials and Methods

Thirty healthy subjects with moderate-to-severe static perioral rhytides were enrolled. This study was approved by an independent IRB. Informed consent was obtained from all subjects. To be included, subjects had to be 35 to 70 years old and Fitzpatrick Skin Type (FST) I-V with a Fitzpatrick Wrinkle Classification System (FWCS) score of 3 to 7 in the perioral area. Subjects were excluded if they had a cosmetic procedure to improve perioral rhytides in the past 12 months; facial treatments with laser, light, and energy-based devices, chemical peels, or neurotoxins over the perioral area in the past 12 months; injectable fillers in the perioral area in the past 12 months; recent significant exposure to ultraviolet light; visible scars over the area; active cut, infection, or inflammation in the area; history of skin malignancy or postinflammatory hyperpigmentation in the area; history of immunosuppression, autoimmune disease, collagen or vascular disease, bleeding disease, keloid formation, neuromuscular disorder, or condition affecting healing rate; use of oral retinoids in the past 6 months; use of oral steroids; and been planning to become pregnant, were currently pregnant, or have given birth less than 3 months ago.

Each subject received 4 treatments to the perioral area with a novel device using thermomechanical fractional injury (Tixel 2, Novoxel, Netanya, Israel) at 28 ($\pm$ 7)-day intervals. Subjects were offered the option of air cooling during the treatment. There was no use of topical or local anesthesia. At physician investigator discretion, the device was allowed to be set to 6- to 12-ms pulse duration and 500- to 800-μm protrusion depth using two passes. This was based on various factors, including patient comfort, clinical severity, skin type, visual inspection, and previous experience.

Perioral rhytides were graded using the FWCS at baseline and follow-up visits at 1 month and 3 months. The Global Aesthetics Improvement Scale (GAIS) (5-point scale) was also used by physician investigators to grade clinical improvement at both follow-up visits. Subject pain was assessed after every treatment, and subject satisfaction was assessed at both follow-up visits. Adverse events were also assessed throughout the study period.

Results

Subject Demographics

Overall, 23 subjects were enrolled and completed all visits in the study. The mean age was 62.5 years (R: 53–70 years). Of all subjects, 100% (n = 23) were women. For FST, 21.7% (n = 5) were Type I, 69.6% (n = 16) were Type II, 4.3% (n = 1) were Type III, and 4.3% (n = 1) were Type IV.

Clinical Ratings

At baseline, subjects had a mean FWCS score of 6.9 (R: 6–7). At 1-month follow-up, the mean FWCS score decreased to 5.3 (R: 4–6), for a mean improvement of 1.7 units ($p < .0001$). At 3-month follow-up, the mean FWCS score decreased to 5.0 (R: 3–6), for a mean improvement of 1.9 ($p < .0001$). At 3-month follow-up, 8.7% (n = 2) of subjects had a 3-grade improvement, 69.6% (n = 16) had a 2-grade improvement, and 21.7% (n = 5) had a 1-grade improvement. All subjects (100%) had clinical improvement in FWCS score at both follow-up visits, and no subject worsened.

For physician GAIS, all subjects (100%) had improvement at 1-month and 3-month follow-up visits. At 1-month follow-up, 52.2% (n = 12) had 76% to 100% improvement, 39.1% (n = 9) had 51% to 75% improvement, and 8.7% (n = 2) had 26% to 50% improvement, for a mean score of 3.4 out of 4. At 3-month follow-up, 69.6% (n = 16) had 76% to 100% improvement, 13.0% (n = 3) had 51% to 75% improvement, and 17.4% (n = 4) had 26% to 50% improvement, for a mean score of 3.4 of 4.

Subject Experience

For patient-reported pain during the treatment, the mean scores on a scale of 0 (no pain) to 10 (worst pain) were 3.0, 3.4, 3.0, and 3.0 for each of the 4 treatments, respectively, for a mean score of 3.1 for all treatments combined. This included the use of only optional air cooling and no topical anesthesia.

At 1-month follow-up, 73.9% (n = 17) of subjects were satisfied with their clinical results, and 95.7% (n = 22) were satisfied with their treatment experience. At 3-month follow-up, 73.9% (n = 17) of subjects were satisfied with their clinical results, and 91.3% (n = 21) were satisfied with their treatment experience.

Safety

During the study, only expected treatment effects were observed, which included transient erythema, transient roughness, and transient dryness. No unexpected treatment effects were observed throughout the study period, and there were no serious adverse events.

Discussion

The perioral area is a unique anatomic region where dynamic and repetitive muscular forces and low subcutaneous fat contribute to the appearance of rhytides over time.[1,5] For perioral rhytides, neurotoxins and dermal fillers can typically offer modest short-term improvement; however, combination treatments, including with resurfacing, can often provide effective outcomes.[1–3] Although traditional resurfacing methods, including ablative and nonablative lasers, can be highly effective, they typically require the application of anesthesia to minimize treatment discomfort and are often associated with significant recovery time, especially with ablative modalities.[6,10,11]

Thermomechanical fractional injury can offer clinical improvement of fine lines and wrinkles with minimal downtime and discomfort during treatment, without the need for any anesthesia.[9] A chart review of 150 patients treated with a thermomechanical fractional injury device for photoaging (n = 145) and acne (n = 5) demonstrated improvements in both conditions. Notably, patients were able to use cosmetic makeup immediately after the

Figure 1. Photographs of female subject at baseline and follow-up at 3 months (from left to right).

treatment at lower settings, with no significant post-treatment downtime.[10] This device has also been shown to enhance percutaneous drug delivery,[8,12] improve periorbital rhytides,[9] and improve overall skin vitality and dyschromia.[6]

This novel device is fractional and nonablative in nature and transfers thermal energy directly to the skin through conduction during brief skin contact, on the order of 5 to 18 ms.[9,10] Heat is delivered to the tissue via a grid of blunt, pyramidal, titanium tips that make contact with the skin without piercing it.[6,9] The ceramic base of this grid is heated to 400°C, which provides heat to the pyramidal tips. A distance guide is attached to the handpiece, and upon placing the handpiece on the patient and pulsing, the tips are moved toward the skin, between 100 to 1,000 μm, to achieve brief tissue contact before being quickly retracted.[10] The amount of thermal energy delivered is determined by the contact duration of the tip (range of 5–18 ms) and protrusion distance of the tip (range of 100–1,000 μm), which can be individually adjusted.[6,9]

This study demonstrates that a thermomechanical fractional injury device can safely and effectively improve the clinical appearance of perioral rhytides after a series of treatments (Figures 1 and 2). By 1-month follow-up, there was a significant mean improvement in FWCS score by 1.7, which increased to 1.9 units by 3-month follow-up. All subjects had improvement in physician GAIS at both time points, with over two-thirds (69.6%) having 76% to 100% improvement at 3-month follow-up. Although the rhytides in this area can be static and dynamic in nature, significant clinical improvement can still be attained.

These clinical effects can be attributable in part to underlying wound healing responses elicited by the thermal coagulation from this device. Fractional thermomechanical injury via preheated tips can generate a matrix of controlled dermal injury, which can be slightly narrower when compared with fractional CO2 laser, but of a similar depth.[7] Their patterns of thermal injury are different.[13] Greater contact duration and protrusion distance with this particular device can create larger effects. This has benefits for fibroblast proliferation and collagen production, and unlike fractional CO2 laser, the craters associated with fractional thermomechanical injury are clean of necrotic tissue or charring.[7,11] Clinically, this translates into improvement in rhytides with a potentially shorter recovery time.[11] This modality of energy delivery does not target chromophores, thereby offering increased safety in darker skin types.[6,9,11] Moreover, the treatment tips are blunt, causing no mechanical perforation of the epidermis.[9]

There were neither unexpected treatment effects nor severe adverse events throughout the entire study period. This is notable, as prior studies, albeit with other and deeper treatments, have shown the perioral area to be particularly prone to adverse events, such as persistent dyschromia.[14] And unlike many laser and energy-based devices that may require topical anesthesia, local anesthesia, and/or sedation for a comfortable treatment experience, anesthetics were not required for the use of this device. Optional air cooling alone was offered, and still participants reported a low level of pain (on average about 3 out of 10). The necessity for anesthesia, even topically, adds to the physician and patient time burden for treatments and can be avoided with this device. Altogether, the efficiency, ease, and comfort of treatment in conjunction with positive cosmetic outcomes likely contributed to the high patient satisfaction observed in this study.

This prospective clinical trial demonstrates the efficacy and safety of thermomechanical fractional injury for

Figure 2. Photographs of female subject at baseline and follow-up at 3 months (from left to right).

treating perioral rhytides in subjects who were FST I through IV. Future studies may also consider combination treatment with cosmetic injectables, such as soft-tissue fillers, which are commonly used in the perioral region. Although this device has already demonstrated real-world safety in darker skin types, larger trials can recruit additional subjects who are FST V and VI.

Conclusion

This prospective study demonstrated that a novel thermo-mechanical fractional injury device can effectively and safely improve perioral rhytides. This treatment was well-tolerated and well-liked.

References

1. Grewal SK, Ortiz A. Perioral rejuvenation in aesthetics: review and debate. *Clin Dermatol* 2022;40:265–73.
2. Winslow C. Surgical and nonsurgical perioral/lip rejuvenation: beyond volume restoration. *Clin Plast Surg* 2018;45:601–9.
3. Morera Serna E, Serna Benbassat M, Terré Falcón R, Murillo Martín J. Anatomy and aging of the perioral region. *Facial Plast Surg* 2021;37:176–93.
4. Suryadevara AC. Update on perioral cosmetic enhancement. *Curr Opin Otolaryngol Head Neck Surg* 2008;16:347–51.
5. Chang CS, Chang BL, Lanni M, Wilson AJ, et al. Perioral rejuvenation: a prospective, quantitative dynamic three-dimensional analysis of a dual modality treatment. *Aesthet Surg* 2018;38:1225–36.
6. Daniely D, Judodihardjo H, Rajpar SF, Mehrabi JN, et al. Thermo-mechanical fractional injury therapy for facial skin rejuvenation in skin types II to V: a retrospective double-center chart review. *Lasers Surg Med* 2021;53:1152–7.
7. Elman M, Fournier N, Barnéon G, Bernstein EF, et al. Fractional treatment of aging skin with Tixel, a clinical and histological evaluation. *J Cosmet Laser Ther* 2016;18:31–7.
8. Shavit R, Dierickx C. A new method for percutaneous drug delivery by thermo-mechanical fractional injury. *Lasers Surg Med* 2020;52:61–9.
9. Salameh F, Daniely D, Kauvar A, Carasso RL, et al. Treatment of periorbital wrinkles using thermo-mechanical fractional injury therapy versus fractional non-ablative 1565 nm laser: a comparative prospective, randomized, double-arm, controlled study. *Lasers Surg Med* 2022;54:46–53.
10. Judodihardjo H, Rajpar S. Retrospective study on the safety and tolerability of clinical treatments with a novel thermomechanical ablation device on 150 patients. *J Cosme Dermatol* 2022;21:1477–81.
11. Kokolakis G, Grawert L, Ulrich M, Lademann J, et al. Wound healing process after thermomechanical skin ablation. *Lasers Surg Med* 2020;52:730–4.
12. Artzi O, Koren A, Niv R, Mehrabi JN, et al. A new approach in the treatment of pediatric hypertrophic burn scars: tixel-associated topical triamcinolone acetonide and 5-fluorouracil delivery. *J Cosmet Dermatol* 2020;19:131–4.
13. Wang JV, Mehrabi JN, Zachary CB, Geronemus RG. Evaluation of device-based cutaneous channels using optical coherence tomography: impact for topical drug delivery. *Dermatol Surg* 2022;48:120–5.
14. Weniger FG, Weidman AA, Barrero Castedo CE. Full-field erbium:yag laser resurfacing: complications and suggested safety parameters. *Aesthet Surg J* 2020;40:NP374–85.

Evaluation of Device-Based Cutaneous Channels Using Optical Coherence Tomography: Impact for Topical Drug Delivery

Jordan V. Wang, MD, MBE, MBA,* Joseph N. Mehrabi, MS,† Christopher B. Zachary, MBBS, FRCP,† and Roy G. Geronemus, MD*

BACKGROUND Topical medications play a large role in the management of cutaneous diseases, but penetration is limited. Device-assisted drug delivery using mechanical destruction, lasers, and other energy-based modalities can increase penetration and absorption through creation of transcutaneous channels.

OBJECTIVE To examine real-time, in vivo cutaneous changes in response to various devices used to improve topical drug delivery through optical coherence tomography (OCT) imaging.

METHODS AND MATERIALS Treatment was performed with 8 medical devices, including mechanical destruction, lasers, and other energy-based modalities. Optical coherence tomography was used for real-time, noninvasive, in vivo imaging.

RESULTS Using OCT, microneedling and radiofrequency microneedling demonstrated no cutaneous channels. Both low-energy, low-density, fractional nonablative lasers produced transient channels, which closed within hours. The fractional nonablative 1,927-nm thulium fiber and 1,550-nm erbium fiber lasers created channels with epidermal debris within, which were still closing at 24 hours. The fractional thermomechanical ablative device and the fractional ablative CO2 laser produced channels that were still open at 24 hours. CO2 laser channels had thick rims of coagulated tissue and remained open for longer.

CONCLUSION Demonstrable differences among the devices were seen, and only some can produce observable channels, the characteristics of which vary with each technology.

Topical medications play a large role in the treatment and management of cutaneous diseases. However, their absorption is greatly limited because of issues with epidermal penetration. Only 1% to 5% of most topically applied medications are typically absorbed by the skin, and the amount that reaches the target depth is frequently insufficient to be effective.[1–4] Topical molecules must cross through the rate-limiting barrier of the stratum corneum to be sufficiently absorbed.[5] Local injection and systemic administration are common methods used for molecules that are poorly absorbed through the topical route. However, these methods can be associated with undesirable local or systemic effects.

Device-assisted drug delivery using mechanical destruction, lasers, and other energy-based modalities is an evolving technique that can offer increased penetration and absorption of topical formulations. Ablative and nonablative fractional lasers improve drug delivery by creating microthermal treatment zones (MTZs), which act as cutaneous channels and reservoirs for topically applied medications.[1,6] Laser parameters will influence MTZ characteristics, such as depth, density, width, and coagulative features. Drug properties, such as molecular size, vehicle type, lipophilicity, and pH, can also affect drug delivery.[7] Other modalities currently used to disrupt the epidermal barrier and potentially improve drug delivery include microneedling, radiofrequency microneedling, and thermomechanical ablation.[8–11]

Optical coherence tomography (OCT) is a high-resolution, noninvasive, in vivo imaging technique that can capture the skin's reflective properties to reconstruct 2-dimensional and 3-dimensional images.[12] Widely introduced to skin imaging in 1997, OCT had demonstrated early promise in discerning skin structures, such as the dermoepidermal junction and sweat ducts.[12] Its use has since been refined for diagnosis of keratinocyte carcinomas and characterization of vascular skin conditions.[13–17]

In this study, the authors introduce the novel use of OCT to examine the real-time, in vivo cutaneous changes in response to various devices used to improve topical drug delivery. This study evaluated device-assisted drug delivery modalities while accounting for evolution related to real-time, in vivo inflammation and healing. The authors believe that OCT can provide accurate characterization of these cutaneous changes over time, allowing head-to-head comparison of their physical characteristics.

*From the *Laser & Skin Surgery Center of New York, New York, New York; †Department of Dermatology, University of California, Irvine, California*

R.G. Geronemus is on the advisory board for Solta, Lutronic, and Novoxel. C.B. Zachary is on the advisory board for Solta. The remaining authors have indicated no significant interest with commercial supporters.

Address correspondence and reprint requests to: Jordan V. Wang, MD, MBE, MBA, Laser & Skin Surgery Center of New York, 317 E 34th Street, 6th Floor, Research Department, New York, NY 10016, or e-mail: drjordanwang@gmail.com

http://dx.doi.org/10.1097/DSS.0000000000003275

Materials and Methods

A willing author (J.V.W.) voluntarily underwent treatment with various medical devices, including mechanical destruction, lasers, and other energy-based modalities. The devices included (1) microneedling pen (Dermapen 4, DermapenWorld, Sydney, Australia); (2) radiofrequency microneedling (Genius, Lutronic, Seoul, South Korea); (3) low-energy, low-density, fractional nonablative 1,927-nm thulium fiber laser (LaseMD, Lutronic, Seoul, South Korea); (4) low-energy, low-density, fractional nonablative 1,927-nm diode laser (Clear + Brilliant Perméa, Solta, Pleasanton, CA); (5) fractional nonablative 1,927-nm thulium fiber laser (Fraxel Dual, Solta, Pleasanton, CA); (6) fractional nonablative 1,550-nm erbium fiber laser (Fraxel Dual, Solta, Pleasanton, CA); (7) fractional thermomechanical ablative device (Tixel, Novoxel, Netanya, Israel); and (8) fractional ablative 10,600-nm carbon dioxide laser (Fraxel Repair, Solta, Pleasanton, CA).

The intended area of treatment was the left upper extremity. All treatments were performed in nonoverlapping areas of the same location to prevent inconsistencies in tissue characteristics, such as epidermal and dermal thickness and tissue response to treatments. Before each treatment, the intended area of the skin was cleansed with 70% isopropyl alcohol and allowed to dry. No topical or injectable anesthesia was used to prevent any potential undesired effects to the tissue for imaging evaluation.

An OCT scanner (VivoSight, Michelson Diagnostics, Kent, United Kingdom) was used for real-time, noninvasive, in vivo imaging of cutaneous changes after treatment by each of the medical devices. The OCT scanner uses a low-power 1,300 nm laser and is equipped with multibeam swept-source frequency-domain processing. This imaging device provides a 6 × 6 mm field of view, <5 μm resolution in axial, and 1 to 2 mm depth of penetration. The en face OCT images were captured with multislice scans consisting of up to 500 frames per scan. The software allows for surface curve fitting of the OCT images to capture en face views at the depth of interest.

The OCT images were taken before each treatment at baseline, immediately after each treatment, and at various time points thereafter to evaluate the real-time, in vivo temporal evolution of skin changes. In the treatment areas, the dermoepidermal junction was located at about 100 μm. Channels observed in the skin were interpreted as vertical columns of ablation and coagulation that appeared empty within. When channels were present immediately after each treatment, their widths were calculated and determined as the mean measurement of 5 representative channels within the field of view.

Results

Microneedling was performed with the first pass at 0.5 mm depth and second pass at 1 mm depth. Radiofrequency microneedling was performed with the first pass at 0.5 mm depth and second pass at 1 mm depth, at 5 W and 100 ms. Using OCT, no channels were observed post-treatment (Figure 1).

The low-energy, low-density, fractional nonablative 1,927-nm thulium fiber laser was performed at 5 W and 2.4 mJ. The low-energy, low-density, fractional nonablative 1,927-nm diode laser was performed at 5 mJ and 5% density. Using OCT, channels were observed post-treatment for each device (Figure 2). For the former device, the mean channel width was 78 μm and the channels were nearly closed by 30 minutes. For the latter device, the mean channel width was 178 μm and the channels were nearly closed by 5 hours.

The fractional nonablative 1,927-nm thulium fiber laser was performed at 10 mJ and 65% density. The fractional nonablative 1,550-nm erbium fiber laser was performed at 70 mJ and 35% density. Using OCT, channels were observed post-treatment for each device (Figure 3). For the former device, the mean channel width was 216 μm and the channels were still in the process of closing at 24 hours. For the latter device, the mean channel width was 274 μm and the channels were also still in the process of closing at 24 hours. Epidermal debris can be seen within the channels of both modalities, including up until the 7-hour time point for the former device and the 3-hour time point for the latter device.

Fractional thermomechanical ablation was performed at 400 μm protrusion and 6 ms. The fractional ablative 10,600-nm carbon dioxide laser was performed at 70 mJ and 15% density. Using OCT, channels were observed post-treatment for each device (Figure 4). For the former device, the mean channel width was 236 μm and the channels were still open at 24 hours. For the latter device, the mean channel width was 198 μm and the channels were also still open at 24 hours. Well-demarcated empty channels with a thick rim of surrounding coagulated tissue can be seen with

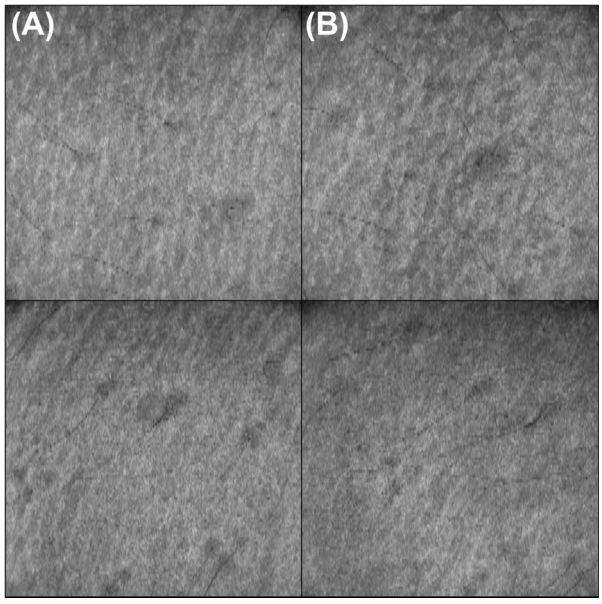

Figure 1. En face OCT images at 100 μm depth for microneedling (top) and radiofrequency microneedling (bottom) at (A) baseline and (B) immediately post-treatment.

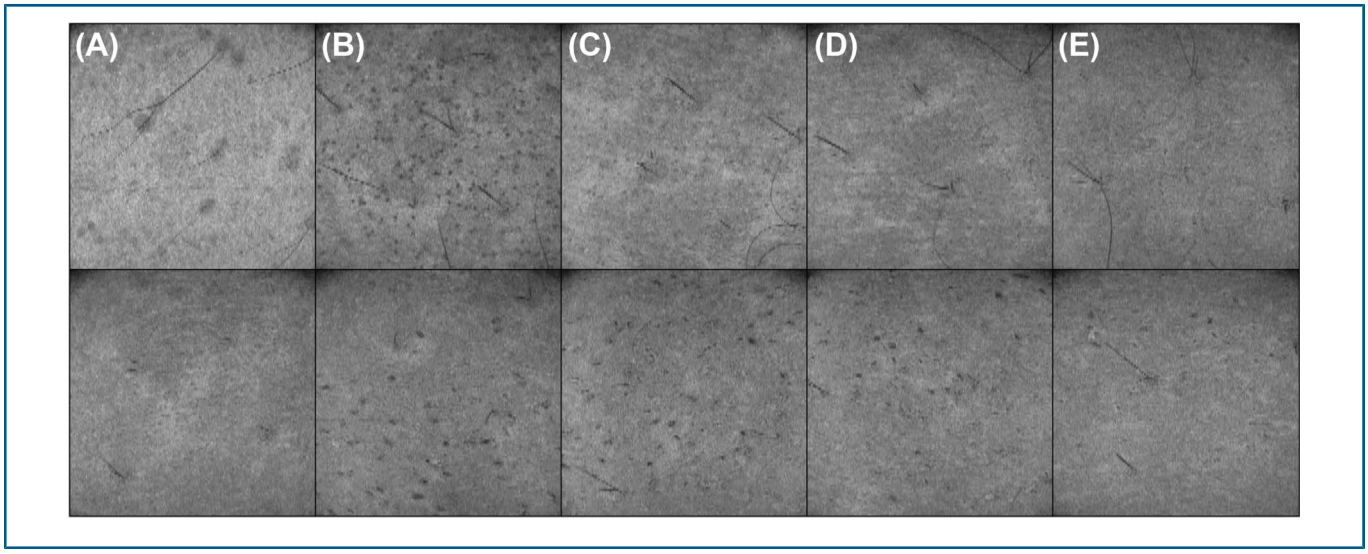

Figure 2. En face OCT images at 100 μm depth for the low-energy, low-density fractional nonablative 1,927-nm thulium fiber laser (top) and the low-energy, low-density fractional nonablative 1,927 nm diode laser (bottom) at (A) baseline, (B) immediately post-treatment, (C) 30 minutes post-treatment, (D) 1 hour post-treatment, and (E) 5 hours post-treatment.

the latter device, which is the most prominent immediately post-treatment and at the 3-hour time point.

Discussion

Device-assisted drug delivery relies on the creation of channels to enable epidermal transport of topically applied molecules and to serve as reservoirs for absorption in the epidermis and superficial dermis. In this study, 8 distinct devices were used to treat the upper arm, and the treated skin was imaged using OCT over a 24-hour period. The channels produced by each device were followed for real-time, in vivo evolution related to inflammation and healing. This study used OCT imaging to assess the channels created by these devices and to observe how they progress over time. The authors believe that this allows for a more accurate examination of what is truly occurring in the skin, which may affect the selection of devices and protocols for device-assisted drug delivery procedures.

Four devices were able to produce transepidermal channels that remained open for at least 24 hours. The fractional nonablative 1,550-nm erbium fiber laser produced the widest channels of this group, whereas the fractional ablative 10,600-nm carbon dioxide laser produced the narrowest. The former laser has already been associated with increased 5-aminolaevulinic acid absorption when paired with subsequent photodynamic therapy.[6] Marked improvement was also observed in patients with alopecia who were treated with this laser in combination

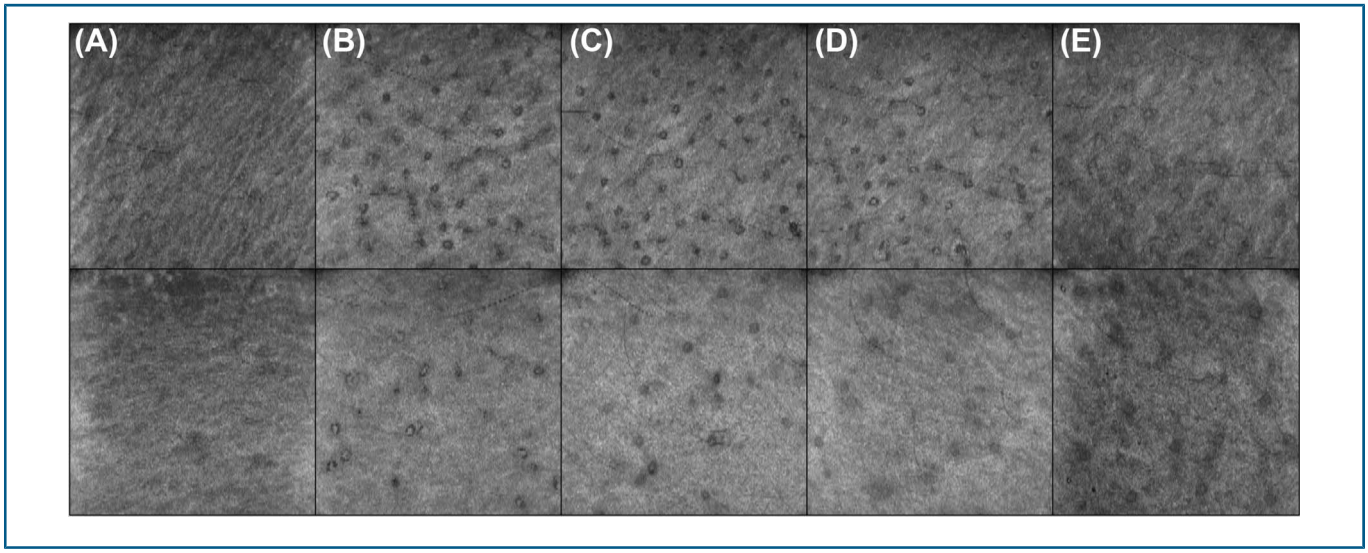

Figure 3. En face OCT images at 100 μm depth for the fractional nonablative 1,927-nm thulium fiber laser (top) and the fractional nonablative 1,550-nm erbium fiber laser (bottom) at (A) baseline, (B) immediately post-treatment, (C) 3 hours post-treatment, (D) 7 hours post-treatment, and (E) 24 hours post-treatment.

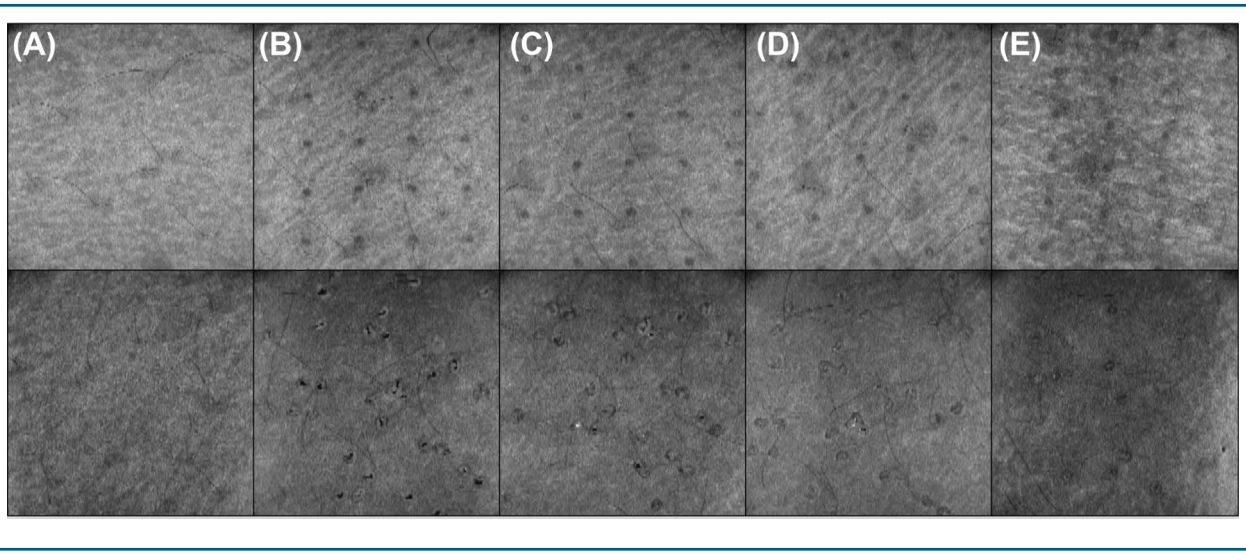

Figure 4. En face OCT images at 100 μm depth for the fractional thermomechanical ablative device (top) and the fractional ablative 10,600-nm carbon dioxide laser (bottom) at (A) baseline, (B) immediately post-treatment, (C) 3 hours post-treatment, (D) 7 hours post-treatment, and (E) 24 hours post-treatment.

with topical finasteride and various growth factors.[18] Although nonablative technologies still produce a partial epidermal layer that is intact to separate the outside environment from the inner channels, the porous nature of this barrier can be associated with more efficient penetration of topical molecules than the normal skin. The topical formulations only need diffuse across the remaining partial epidermis to reach the channels, which is a process dependent on time and properties of the topical preparation.

Fractional ablative lasers may remain the most common type of laser used for laser-assisted drug delivery.[1] In 2014, a review of 19 recent studies demonstrated significant improvement in the targeted condition and 18 studies showed significantly increased influx of molecules with fractional ablative lasers, such as the 10,600-nm CO2 and 2,940-nm Er:YAG lasers.[1] The utility of fractional ablative lasers depends on their ability to remove the entire epidermis that would be overlying the channels with fractional nonablative lasers, which may eliminate a barrier to topical penetration. However, other factors may still play a role, including channel depth and density, surrounding coagulation zone, time frame of topical application, and physicochemical properties of the topical medications.[19–25]

Fractional thermomechanical ablation was the only non-laser modality to produce channels, which also remained open for more than 24 hours. By contrast, both traditional microneedling and radiofrequency microneedling produced no observable channels. Recently, there has been a growing sentiment that microneedling may be inferior to lasers and other energy-based modalities for device-assisted drug delivery. Thermomechanical injury has already been used to deliver botulinum toxin to mediate rosacea and Hailey–Hailey disease,[26,27] triamcinolone and 5-fluorouracil to reduce scar size,[28,29] rapamycin for enhanced pulsed dye laser treatment of port-wine stains,[30] and beta blockers for infantile hemangiomas.[31] Depending on the selected treatment parameters, the fractional thermomechanical device can allow for ablative or nonablative histologic effects because of heat transfer from short contact of the 400°C-heated pyramidal tip,[11] which can attain similar ablative temperatures to the CO2 laser.[32]

Both low-energy, low-density, fractional nonablative lasers initially produced channels. However, they were only transient in nature. Of these 2 devices, the fiber-type laser produced thinner channels than the diode-type laser, which also closed earlier at 30 minutes compared to 5 hours with the latter device. The transient nature of the channels may allow for topical drug absorption with limited postprocedural downtime. This phenomenon has led to their use in laser-assisted drug delivery, including tranexamic acid for melasma.[33–35]

The presence of channels and their duration seem to be dependent on the amount of tissue coagulation surrounding the channels that are created by the devices. The stiffer coagulated tissue may act as a rigid scaffold to structurally support the channels and hold them open. For example, traditional microneedling and radiofrequency microneedling demonstrated no channels. Microneedling delivers no energy, so any channels that may be created would quickly close, and there would be no potential cutaneous reservoirs for the topically applied molecules to fill. The radiofrequency microneedling device used was insulated in the upper portion of the needles so that thermal energy was only delivered at the tips, which was located much deeper than the epidermis or superficial papillary dermis. This may explain the lack of visualized channels. Both low-energy, low-density, fractional nonablative 1,927-nm lasers deliver less energy than their stronger 1,927-nm thulium fiber laser counterpart. This may translate to the transient channels that close much sooner than those from the more powerful lasers. By contrast, the CO2 laser demonstrated a thick and

sharply demarcated rim of surrounding coagulated tissue, which may allow for the channels to remain more open for much longer.

The presence and nature of the channels may affect the penetration and absorption of topically applied formulations. This study used OCT to evaluate the effects of medical devices used to improve topical drug delivery. We believe that OCT can more accurately capture real-time, in vivo evolution related to inflammation and healing as opposed to histologic analysis from biopsies, which requires processing that can manipulate the tissue and only captures a representation of a single point in time. Our evaluation of the channels from these devices may change how physicians approach device-assisted drug delivery. Not every device is created equal nor offers the same tissue response when creating channels. Each device is associated with unique channel characteristics, including presence, width, depth, duration, surrounding coagulation, and internal debris. Even lasers with the same wavelength can differ from each other.

Although we used OCT to examine transepidermal channels produced by various devices, further studies should evaluate how certain channel characteristics can influence topical drug penetration and absorption and to what extent. It is important that future studies use in vivo models to capture the real-time effects of inflammation and healing. Because these treatments were only conducted in one area of a single volunteer, observations could vary between locations or individuals. Each location on the body has been associated with various epidermal thicknesses, which could affect the nature of the channels. There may also be variations in skin composition, such as the number of sebaceous glands and hair follicles. Future studies should look into a variety of locations.

Conclusion

Device-assisted drug delivery relies on the creation of transepidermal channels, which can improve the penetration and absorption of topically applied formulations. Data of this study demonstrate that OCT can examine real-time, in vivo cutaneous changes in response to various devices used to improve topical drug delivery. This study compared multiple different technologies used to facilitate drug delivery. Differences among the devices were seen, and only some can produce observable channels, the characteristics of which vary with each technology.

References

1. Sklar LR, Burnett CT, Waibel JS, Moy RL, et al. Laser assisted drug delivery: a review of an evolving technology. *Lasers Surg Med* 2014; 46:249–62.
2. Nino M, Calabrò G, Santoianni P. Topical delivery of active principles: the field of dermatological research. *Dermatol Online J* 2010;16: 4.
3. Sandberg C, Halldin CB, Ericson MB, Larkö O, et al. Bioavailability of aminolaevulinic acid and methylaminolaevulinate in basal cell carcinomas: a perfusion study using microdialysis in vivo. *Br J Dermatol* 2008;159:1170–6.
4. Soler AM, Warloe T, Berner A, Giercksky KE. A follow-up study of recurrence and cosmesis in completely responding superficial and nodular basal cell carcinomas treated with methyl 5-aminolaevulinate-based photodynamic therapy alone and with prior curettage. *Br J Dermatol* 2001;145:467–71.
5. Gorzelanny C, Mess C, Schneider SW, Huck V, et al. Skin barriers in dermal drug delivery: which barriers have to be overcome and how can we measure them? *Pharmaceutics* 2020;12:684.
6. Lim HK, Jeong KH, Kim NI, Shin MK. Nonablative fractional laser as a tool to facilitate skin penetration of 5-aminolaevulinic acid with minimal skin disruption: a preliminary study. *Br J Dermatol* 2014; 170:1336–40.
7. Wang JV, Griffin TD. Fractional ablative laser-assisted photodynamic therapy as field treatment for actinic keratoses: our anecdotal experience. *Skinmed* 2020;18:214–6.
8. Dharadhar S, Majumdar A, Dhoble S, Patravale V. Microneedles for transdermal drug delivery: a systematic review. *Drug Dev Ind Pharm* 2019;45:188–201.
9. Prasad AJR. Tixel Facethetics. A new paradigm in skin rejuvenation and scar treatment. Available from: http://www.facethetics.in/articles/dermatology/122-tixel-a-new-paradigm-in-skin-rejuvenation-and-scar-treatment. Accessed November 21, 2020.
10. Shavit R, Dierickx C. A new method for percutaneous drug delivery by thermo-mechanical fractional injury. *Lasers Surg Med* 2020;52:61–9.
11. Sintov AC, Hofmann MA. A novel thermo-mechanical system enhanced transdermal delivery of hydrophilic active agents by fractional ablation. *Int J Pharm* 2016;511:821–30.
12. Welzel J, Lankenau E, Birngruber R, Engelhardt R. Optical coherence tomography of the human skin. *J Am Acad Dermatol* 1997;37: 958–63.
13. Olmedo JM, Warschaw KE, Schmitt JM, Swanson DL. Optical coherence tomography for the characterization of basal cell carcinoma in vivo: a pilot study. *J Am Acad Dermatol* 2006;55:408–12.
14. Coleman AJ, Richardson TJ, Orchard G, Uddin A, et al. Histological correlates of optical coherence tomography in non-melanoma skin cancer. *Skin Res Technol* 2013;19:10–9.
15. Maier T, Braun-Falco M, Hinz T, Schmid-Wendtner MH, et al. Morphology of basal cell carcinoma in high definition optical coherence tomography: en-face and slice imaging mode, and comparison with histology. *J Eur Acad Dermatol Venereol* 2013;27:e97–e104.
16. Hussain AA, Themstrup L, Jemec GB. Optical coherence tomography in the diagnosis of basal cell carcinoma. *Arch Dermatol Res* 2015;307: 1–10.
17. Ulrich M, Themstrup L, de Carvalho N, Manfredi M, et al. Dynamic optical coherence tomography in dermatology. *Dermatology* 2016; 232:298–311.
18. Bertin ACJ, Vilarinho A, Junqueira ALA. Fractional non-ablative laser-assisted drug delivery leads to improvement in male and female pattern hair loss. *J Cosmet Laser Ther* 2018;20:391–4.
19. Wenande E, Anderson RR, Haedersdal M. Fundamentals of fractional laser-assisted drug delivery: an in-depth guide to experimental methodology and data interpretation. *Adv Drug Deliv Rev* 2020;153: 169–84.
20. Haedersdal M, Erlendsson AM, Paasch U, Anderson RR. Translational medicine in the field of ablative fractional laser (AFXL)-assisted drug delivery: a critical review from basics to current clinical status. *J Am Acad Dermatol* 2016;74:981–1004.
21. Haak CS, Bhayana B, Farinelli WA, Anderson RR, et al. The impact of treatment density and molecular weight for fractional laser-assisted drug delivery. *J Control Release* 2012;163:335–41.
22. Banzhaf CA, Thaysen-Petersen D, Bay C, Philipsen PA, et al. Fractional laser-assisted drug uptake: impact of time-related topical application to achieve enhanced delivery. *Lasers Surg Med* 2017;49: 348–54.
23. Taudorf EH, Lerche CM, Erlendsson AM, Philipsen PA, et al. Fractional laser-assisted drug delivery: laser channel depth influences biodistribution and skin deposition of methotrexate. *Lasers Surg Med* 2016;48:519–29.
24. Haak CS, Hannibal J, Paasch U, Anderson RR, et al. Laser-induced thermal coagulation enhances skin uptake of topically applied compounds. *Lasers Surg Med* 2017;49:582–91.

25. Kositratna G, Evers M, Sajjadi A, Manstein D. Rapid fibrin plug formation within cutaneous ablative fractional CO2 laser lesions. *Lasers Surg Med* 2016;48:125–32.
26. Friedman O, Koren A, Niv R, Mehrabi JN, et al. The toxic edge-A novel treatment for refractory erythema and flushing of rosacea. *Lasers Surg Med* 2019;51:325–31.
27. Bar-Ilan E, Koren A, Shehadeh W, Mashiah J, et al. An enhanced transcutaneous delivery of botulinum toxin for the treatment of Hailey-Hailey disease. *Dermatol Ther* 2020;33:e13184.
28. Artzi O, Koren A, Niv R, Mehrabi JN, et al. The scar bane, without the pain: a new approach in the treatment of elevated scars: thermomechanical delivery of topical triamcinolone acetonide and 5-fluorouracil. *Dermatol Ther* 2019;9:321–6.
29. Artzi O, Koren A, Niv R, Mehrabi JN, et al. A new approach in the treatment of pediatric hypertrophic burn scars: tixel-associated topical triamcinolone acetonide and 5-fluorouracil delivery. *J Cosmet Dermatol* 2020;19:131–4.
30. Artzi O, Mehrabi JN, Heyman L, Friedman O, et al. Treatment of port wine stain with Tixel-induced rapamycin delivery following pulsed dye laser application. *Dermatol Ther* 2020;33:e13172.
31. Mashiah J, Bar-Ilan E, Koren A, Friedman O, et al. Enhanced percutaneous delivery of beta-blockers using thermal resurfacing drug delivery system for topical treatment of infantile hemangiomas. *Dermatology* 2020;236:565–70.
32. Choi B, Chan EK, Barton JK, Thomsen SL, et al. Thermographic and histological evaluation of laser skin resurfacing scans. *IEEE J Selected Top Quan Electronics* 1999;5:1116–26.
33. Wanitphakdeedecha R, Sy-Alvarado F, Patthamalai P, Techapichetvanich T, et al. The efficacy in treatment of facial melasma with thulium 1927-nm fractional laser-assisted topical tranexamic acid delivery: a split-face, double-blind, randomized controlled pilot study. *Lasers Med Sci* 2020;35:2015–21.
34. Wang JV, Christman MP, Feng H, Ferzli G, et al. Laser-assisted delivery of tranexamic acid for melasma: pilot study using a novel 1927 nm fractional thulium fiber laser. *J Cosmet Dermatol*. EPub 2020 Nov 12.
35. Friedman PM, Polder KD, Sodha P, Geronemus RG. The 1440 nm and 1927 nm nonablative fractional diode laser: current trends and future directions. *J Drugs Dermatol* 2020;19:s3–e11.

Accepted: 29 March 2024

DOI: 10.1002/lsm.23786

CLINICAL REPORT

Percutaneous delivery of liquid tetracycline using a thermal resurfacing drug delivery system for the treatment of festoons

Margarita Safir MD[1] | **Inbar Waizer MD**[2] | **Ari Safir MD**[3] | **Morris E. Hartstein MD**[1] | **Ofir Artzi MD**[3]

[1]Ophthalmology Department, Shamir Medical Center, The Faculty of Medicine, Tel Aviv University, Tel Aviv, Israel

[2]Department of Military Medicine, Faculty of Medicine, The Hebrew University of Jerusalem, Jerusalem, Israel

[3]Division of Dermatology, Tel Aviv Sourasky Medical Center, The Faculty of Medicine, Tel Aviv University, Tel Aviv, Israel

Correspondence

Margarita Safir, MD, Ophthalmology Department, Shamir Medical Center, The Faculty of Medicine, Tel Aviv University, Tel Aviv, Israel.
Email: sapir.margarita@gmail.com

Abstract

Objectives: To examine the effects of percutaneous tetracycline delivery to the malar area using a thermomechanical device (Tixel) in patients suffering from festoons.

Methods: This retrospective study included patients who underwent combination treatment with a thermomechanical device (Tixel) followed by application of topical tetracycline 1% at two private clinics between 2019 and 2023. Demographic and medical data, treatment parameters along with before and after treatment photographs were retrieved retrospectively. All patients were asked to answer a questionnaire, assessing self-reported pre and posttreatment disturbance, patient global impression of change (PGIC) score, overall satisfaction with treatment, and the onset and duration of treatment effect. Finally, three masked reviewers evaluated and graded the severity of before and after treatment photographs.

Results: Twenty healthy patients received the combination treatment. The mean age was 59.4 ± 8.2 years (range: 45–72 years), and 90.0% ($n = 18$) were female. The number of treatment sessions per patient ranged from 2 to 8, mean of 5.0 ± 1.9, performed at 5.4 ± 1.2-week intervals. The masked reviewers' grading scores demonstrated a significant improvement (2.81 ± 1.3 before vs. 1.6 ± 1.1 after, $p < 0.001$). The self-reported disturbance caused by the festoons improved significantly as well (4.7 ± 0.98 vs. 1.7 ± 1.1, $p < 0.001$). On the PGIC score, 85% (17/20) reported moderate (grade 5) to significant (grade 7) improvement of symptoms and life quality after treatment. Improvement onset was reported to occur 11.2 ± 6.6 days after the first treatment (range 2−30 days), and 90% (18/20) of the patients reported improvement lasting at least 4 months after completion of the second treatment.

Conclusions: Topical tetracycline application following Tixel treatment induced significant improvement in patient with festoons.

KEYWORDS

festoon, tetracycline, Tixel

INTRODUCTION

The word festoon derives from Latin (festo), describing a wreath or garland hanging down from two points. The medical adaptation of this term refers to inferiorly displaced lax skin, orbicularis tissue and edema hanging below the medial and lateral canthi.[1] More recently, this term has been used to encompass a larger group of findings, including tissue edema or fullness over the prezygomatic or malar region.[1,2]

Currently, there is no treatment modality for festoons that is considered consistently reliable as a gold standard.[2] The therapeutic approach consists of identifying and addressing treatable causes of local edema, followed by various medical or surgical interventions, all with varying and often unpredictable success rates.[1,2] Local injection of tetracycline antibiotics has been described as effective treatment in numerous cases.[3–5] These easily available medications are presumed to assist in festoon reduction by inhibiting matrix metalloproteinases (MMPs) and growth

factor activity, indirectly inducing sclerosis of the potential space within the festoon.[2] While this method has been reported to be quite effective (59.0%), it is often accompanied by patient discomfort due to the pain and bruising associated with the injection.[5]

Tixel (Novoxel®) is a thermomechanical device, transferring heat to the skin by means of brief contact with the handpiece's titanium tip, heated to a uniform temperature of 397−400°C. During its brief contact with the skin, the Tixel tip dehydrates the stratum corneum and superficial epidermis, creating micropore channels[6] which can be successfully and safely used for enhanced intradermal delivery of various topical medications.[7–10]

We report our experience of applying tetracycline HCL 1% topical solution immediately following treatment with the thermomechanical drug delivery system (Tixel-Novoxel) in 20 patients with festoons.

METHODS

Ethics

This retrospective study was approved by the Institutional Review Board of Shamir Medical Center and adhered to the tenets of the Declaration of Helsinki.

Tixel treatment technique

Tixel (Novoxel@) technology combines thermal energy with motion (protrusion). The system consists of a handpiece with titanium tip heated to 400°C (Figure 1A,B). The tip's active surface consists of an array of 81 (9 × 9) pyramidal pins evenly spaced within a boundary area of 1 × 1 cm. During treatment, the tip is advanced until it makes contact with the skin, and the duration of this contact (the pulse duration) determines the amount of thermal energy delivered to the tissue. The system provides the user with predefined pulse duration parameters that range from 5 to 18 ms. A second system parameter is protrusion, defined as the distance that the heated tip is advanced into the skin from the edge of the handpiece. Larger protrusion acquires better thermal coupling and higher heat transfer between the tip and the treated tissue without skin perforation. Most of the thermal effect is concentrated in the stratum corneum, leading to rapid heat transfer and dehydration of the layer.[11]

All treatments in our study were performed by one of two doctors (O. A., M. H.) who had been trained in operating the device. The patients with festoons were placed in supine position, and the titanium tip of the Tixel device was applied on the skin overlying the festoons in overlapping rows. Skin contact duration and tip protrusion distance were set according to patient sensitivity (more protrusion and longer duration when feasible). No topical nor systemic analgetic treatment was required. Treatment lasted up to 5 min per patient. Immediately following treatment, a homogeneous layer of topical tetracycline 1% cream was applied over the festoon area.

Patient evaluation and data gathering

The combination treatment for festoons was performed at two private practices in central Israel (Medical Center 1 and Medical Center 2 for the purpose of the study) between 2019 and 2023. This treatment method was offered all patients presenting with festoons to either clinic starting from 2019. Patients with festoons who attended the clinics underwent routine intake and evaluation including medical background, previously

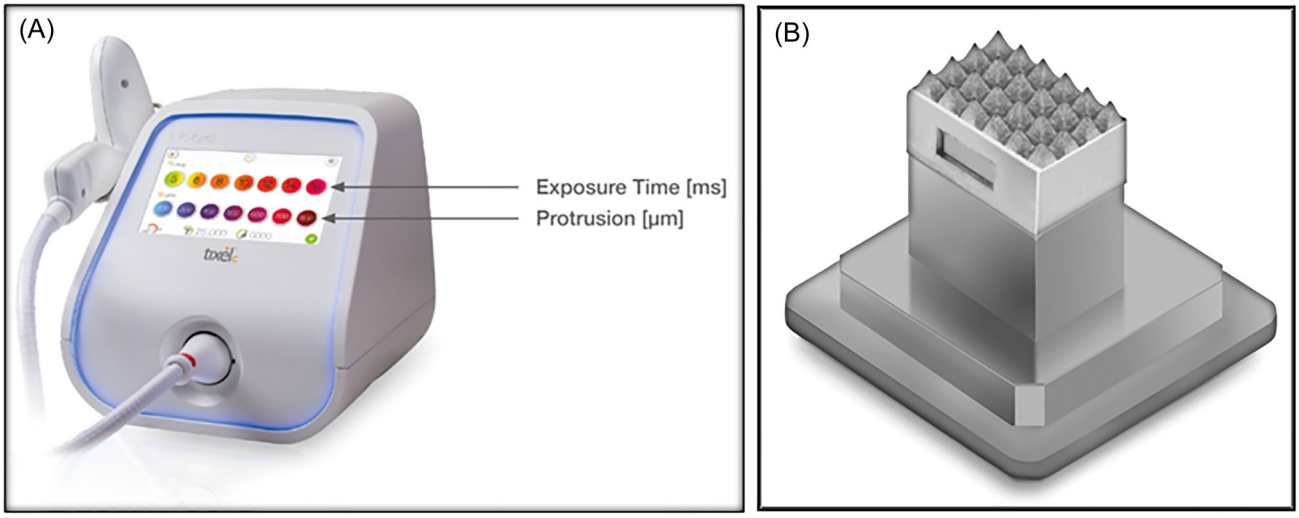

FIGURE 1 Treatment with the Tixel device. (A) Tixel console with attached handpiece, and treatment parameters. (B) The Tixel tip is a 1 × 1 cm titanium made structure, consisting of 9 × 9 evenly spaced small pyramids.

attempted interventions and festoon existence duration. High-quality color photographs were taken in-clinic before and after treatment cessation. Tixel tip protrusion and contact duration with the skin were recorded. This data was collected retrospectively from the patients' medical files at the two clinics upon initiation of the current study.

A comprehensive questionnaire was built based on several previously validated questionnaires (see Supporting Information Material), and included self-reported patient global impression of change (PGIC) score,[12] overall pre and posttreatment disturbance, treatment-related pain and inconvenience as well as improvement timing and duration. Patients were requested to fill the questionnaire 3−5 months after treatment completion.

The authors invited three masked reviewers, all certified plastic surgeons, to evaluate the before and after treatment photographs. The photographs were sent to them via email, with no identifying information, and in a random order, without disclosing which picture was captured first. In the absence of a consensus regarding a severity grading score for festoons, the authors composed a grading score for the purpose of this study. The reviewers were required to grade the photographs on a 6-point scale ranging from no festoon (0) to significant fullness of the zygomatic area with skin folds[5] (Figure 2). The final score of each patient was calculated as the mean reviewer score.

Statistical analysis

Statistical analysis was performed using SPSS for windows version 23.0 by IBM. For categorical variables, χ^2 tests were used. Clinical parameters distributions were tested for normality by the Shapiro−Wilk test. Independent and paired *t*-tests were conducted for continuous variables with a normal distribution and the Mann–Whitney *U* and Wilcoxon tests for variables with a non-normal distribution. *p* Values less than 0.05 on a two-sided test were considered statistically significant.

RESULTS

Of all patients who were offered to undergo combination therapy by topical tetracycline and Tixel, 23 patients agreed, and 20 of them, when approached after treatment termination, gave their consent to participate in the current study. Twenty patients were included, 8 from Medical Center 1, and 12 from Medical Center 2 (Table 1). The mean age was 59.4 ± 8.2 years (range: 45–72 years) and 90.0% ($n = 18$) were female. All patients were otherwise healthy, except for one patient who had medically controlled hypothyroidism and one with hypertension. Half of the patients (10/20) had previously undergone another treatment modality for their festoons (performed at other medical centers), and 70% of them (7/10) reported suboptimal results of the previous treatment. Baseline pretreatment festoon severity grading, calculated as the average grading of all three masked reviewers, was 2.8 ± 1.3 (range: 0.7−4.7).

All patients underwent combination treatment of Tixel followed by topical tetracycline application to the festoon area. Total number of treatment sessions per patient ranged from 2 to 8, mean 5.0 ± 1.9, median 5. The pulse duration and protrusion of the Tixel tip during treatment ranged between 6 and 12 ms (median 10 ms) and 400 and 600 microns (median 500), respectively. These treatments were performed at 5.4 ± 1.2-week intervals, median 4 weeks, range 2−12 weeks. The inter-treatment intervals were smaller at the beginning of treatment (mean 1st to 6th intervals 4.0−5.7 weeks, mean 7th interval when applicable- 8.5 weeks, $p < 0.001$). All treatment parameters were comparable between the groups, except for tip protrusion which was slightly smaller in Medical Center 2 compared to Medical Center 1 (450.1 ± 36.5 vs. 491.7 ± 23.6 microns, respectively) (Table 1).

The three masked reviewers' grading scores were compiled for all included patients (Table 2). Paired *t*-test analysis demonstrated a significant grading improvement from 2.81 ± 1.3 before treatment to 1.6 ± 1.1 after treatment, $p < 0.001$. All patients exhibited improvement

FIGURE 2 Festoon severity grading score. All patients were evaluated by three masked reviewers. Festoon severity grading was performed based on severity of zygomatic fullness and the presence of overlying skin folds.

TABLE 1 Baseline characteristics of patients receiving combination treatment of topical tetracycline with Tixel application for festoons.

Patient characteristics	Medical center 1 ($n = 8$)	Medical center 2 ($n = 12$)	p Value
Age, years (mean ± SD)	59.9 ± 7.8	59.0 ± 8.8	0.82
Female sex (%)	8/8 (100)	2/12 (83.3)	0.50
Festoon existence years (mean ± SD)	15.3 ± 4.4	6.7 ± 8.2	0.007
Previous festoon treatment (%)	3/8 (37.5)	7/12 (58.3)	0.65
Previous festoon treatment type			
Radio-ablation	1/3 (33.3)	1/7 (14.3)	0.70
Laser	0	1/7 (14.3)	
Cream application	1/3 (33.3)	1/7 (14.3)	
Surgery	1/3 (33.3%)	4/7 (57.1)	
Previous treatment effect			
None	1/3 (33.3)	3/7 (42.9)	0.96
Partial resolution	1/3 (33.3)	2/7 (28.6)	
Full resolution	1/3 (33.3)	2/7 (28.6)	
Masked reviewer pretreatment festoon grading (mean ± SD)	3.2 ± 1.3	2.6 ± 1.3	0.34
Number of treatments (mean ± SD)	4.25 ± 1.5	5.5 ± 2.1	0.16
Tip protrusion microns (mean ± SD)	491.7 ± 23.6	450.1 ± 36.5	0.01
Contact duration milliseconds (mean ± SD)	9.7 ± 0.5	8.5 ± 1.9	0.10
Interval between treatments, weeks (mean ± SD)	5.5 ± 0.5	5.3 ± 1.3	0.69

Abbreviation: SD, standard deviation.

TABLE 2 Pre and postmarkers for treatment effectiveness in study population.

Patient characteristics	Before treatment	After treatment completion	p Value
Masked reviewer grading	2.81 ± 1.3	1.6 ± 1.1	<0.001
Self-reported disturbance	4.7 ± 0.98	1.7 ± 1.1	<0.001
Self-reported improvement (PGIC, grade 1−7, 7 best)	-	5.8 ± 1.2	-
Self-reported improvement grading (PGIC, grade 0−10, 0 best)	-	2.4 ± 2.4	-

Note: All values presented as mean ± standard deviation.
Abbreviation: PGIC, patient global impression of change score.

of the calculated grading score after treatment, with mean delta between the before and after treatment photos of 1.3 ± 0.8, range 0.3−3.0 (Figure 3).

All participants responded to the study questionnaire after completion of treatment. The self-reported disturbance caused by the festoons improved significantly from before to after treatment completion (4.7 ± 0.98 vs. 1.7 ± 1.1, respectively, $p < 0.001$) (Table 2). Patients reported a significant improvement according to the PGIC score as well, with 85% (17/20) reporting moderate (grade 5) to significant (grade 7) improvement in symptoms and in quality-of-life quality after treatment (Figure 4). Onset of improvement was reported to occur 11.2 ± 6.6 days after first treatment (range 2−30 days). After the first session, the improvement lasted 21.2 ± 18.9 days (range 0−60 days), and after the second treatment, session 139.0 ± 92.1 days (range 0−365 days). Ninety percent (18/20) of the patients reported improvement lasting at least 4 months after second treatment.

When asked about returning to everyday life activities following treatment, the mean reported time was 2.0 ± 1.7 days after. On a scale of 1−10, patient-reported pain level during treatment was 3.9 ± 1.7 (range 1−8), while discomfort level was 3.6 ± 1.8 (range 1−8).

FIGURE 3 Before and after photographs of study patients. Photographs were acquired at treatment initiation and after completion (A−H). Three masked reviewers' grading scores were compiled for all included patients. A significant improvement in festoon grading was observed (2.81 ± 1.3−1.6 ± 1.1, $p < 0.001$). All patients exhibited improvement of the calculated grading score after treatment, with mean improvement of 1.3 ± 0.8, range 0.3−3.0.

Overall patient satisfaction with the treatment was 8.2 ± 2.4 out of 10 (range 2−10). When asked regarding their willingness to repeat treatment if needed on a scale of 1−10, mean patient response was 9.5 ± 2.0, and a mean score of 9.3 ± 2.3 regarding the desire to recommend this treatment to others. No major adverse events occurred or were reported during treatment or follow-up.

DISCUSSION

Malar festoons are characterized by the presence of tissue fullness located at the transition zone between the lower eyelids and the cheek. The anatomy of malar festoons involves a combination of skin laxity, loss of collagen and elastin, and underlying fat redistribution

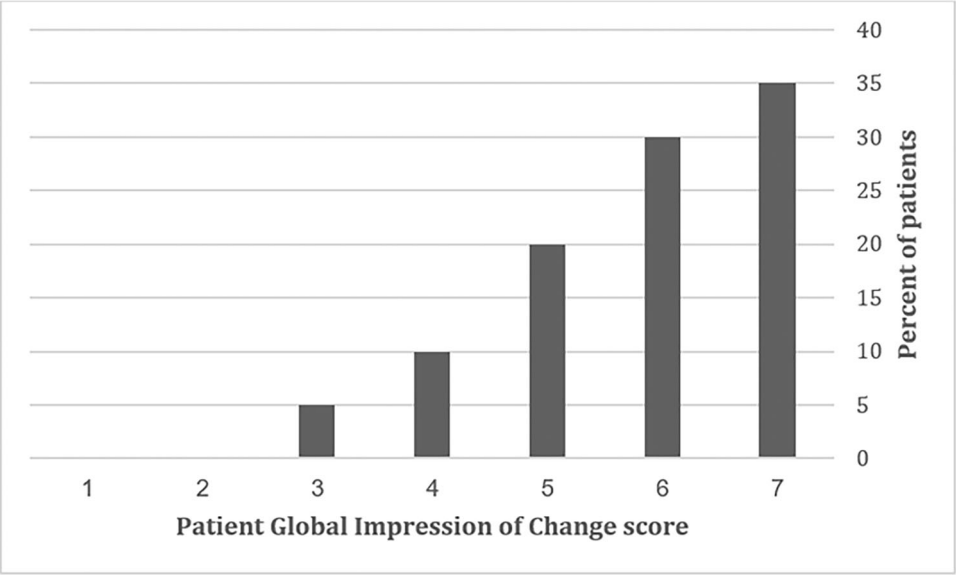

FIGURE 4 Patient global impression of change (PGIC) score of the study patients. Patients were questioned according to the PGIC grading score. Eighty percent of the patients reported moderate to significant improvement in symptoms and quality of life following festoon treatment with topical tetracycline and Tixel.

along with local tissue edema.[1,2] Despite being a natural part of the aging process, they can be a concern for those seeking facial rejuvenation, prompting various cosmetic and surgical interventions to address these distinctive facial contours.

Aging appears to have a major contribution to festoon development, as soft tissue laxity in the malar area increases progressively.[1,2] Nevertheless, malar festoons may appear at a younger age, or even be congenital. Additional conditions associated with festoon formation include rosacea, systemic autoimmune or fluid accumulation disorders, and hypothyroidism.[1,2] Regardless of their etiology, festoons are prone to accumulate fluid, further aggravating patients' appearance. Thus, local inflammation, allergy, edema, or disturbance in lymphatic drainage will all exacerbate preexisting festoons.[2] Pessa and Garza suggested that chronic malar edema is the cause, rather than the exacerbating factor of malar festoons, inducing chronic distention and attenuation of the orbicularis oculi and overlying skin.[13]

Successful esthetic interventions have been shown to have a significant impact on patient's quality of life.[14] Currently, no gold standard for successful and long-lasting festoon management exists.[2] Understanding the mechanisms underlying festoon formation may aid in finding more effective, longstanding treatment modalities for this condition.

Local tetracycline injection has been previously described to be effective in sclerosing fluid-filled structures throughout the body. In the facial region tetracyclines have been used in the treatment of low flow venous malformations, lymphangiomas and lymphatic malformations.[15] Safe and effective tetracycline intralesional injection has also been reported for periocular lesions, including blepharochalasis and chronic bulbar chemosis following blepharoplasty.[16,17] The positive sclerosing effect is achieved via induction of collagen and fibrin deposition, creating dense adhesions and fibrosis in the affected space.[18] Tetracyclines have also been shown to downregulate multiple aspects of the inflammatory response including: MMPs, proinflammatory cytokines (TNF-α, IL-1β, IL-8, IL-10),[19,20] leukocyte movement and proliferation, granuloma formation, and angiogenesis.[20] Thus, since local inflammation and fluid accumulations are major contributing factors to festoon formation, tetracyclines should indeed be beneficial in festoon management.

Previous studies have reported the outcomes of local tetracycline injection into the festoon area.[3–5] Godfrey et al. examined the outcome of 11 patients injected with intralesional doxycycline hyclate 10 mg/mL with significant festoon regression.[3] Perry et al. examined 11 patients injected with tetracycline 2% and found similar results.[4] The largest case series thus far examined 61 patients, with most patients reporting improvement following treatment.[5] Side effects of this treatment method included pain and bruising.[4,5]

The aforementioned patient discomfort led us to seek an alternative, less invasive method of intradermal tetracycline delivery. Topical therapeutic agents demonstrate poor total absorption into the skin, ranging between 1% and 5%.[21] The major rate-limiting step of drug permeation is passage through stratum corneum, which has the highest water content among the epidermal layers.[21] The stratum corneum's ability to act as a barrier is greatly compromised when its relative humidity is diminished.[22] Tixel is a thermomechanical system, which

has been shown to cause dehydration of the stratum corneum,[23] thus facilitating better topical drug penetration. Moreover, drug penetrance is further enhanced by the microchannels created by the pyramidal pins of the Tixel tip, remaining open for at least 6 h after treatment.[6,11] Taking advantage of this dual mechanism of penetrance enhancement has been demonstrated to enhance topical drug delivery in previous studies on various topical hydrophilic drugs.[7–10]

Tetracycline antibiotics are hydrophilic as well.[24] When utilized for festoon management in the current study, the pretreatment with Tixel followed by topical tetracycline 1% application induced significant objective and subjective improvement of signs and symptoms, with all patients experiencing some degree of improvement. This is in contrast to previous reports of tetracycline injection for festoon management, where only 59% reported improvement and 6.6% reported worsening after treatment.[5] The onset of tetracycline's positive effect in our study was earlier than in a previous report of injected tetracycline: 11.2 ± 6.6 days, and 100% of patients in up to 30 days for the topical treatment, whereas only 55% of the 59% who experienced improvement reported it to happen within 1 month in the injection study.[5]

While no direct comparison to the effects of tetracycline injection has been performed, this treatment method is clearly advantageous in terms of patient convenience. No significant side effects were reported, and no systemic or topical analgesics were required. In performing this noninvasive topical treatment patients avoided the side effects of tetracycline injection, including pain, bruising, non-smooth facial appearance, and local sensitivity.[4,5] Indeed, patient-reported satisfaction was high (8.2 ± 2.4 out of 10), and the willingness to repeat treatment if required was almost maximal (9.5 ± 2.0 out of 10). This is in contrast to a study examining festoon management with tetracycline injection where only 67% were willing to repeat treatment.[5] In addition, Tixel treatment in our study was safe, with no reported side effect or complications. This is in concordance with previous reports, which described a low rate of side effects, which were all mild (transient stinging sensation, erythema, mild edema, or pigmentation), and even milder with low treatment parameters as were used in the current study.[6,9,10,23,25]

Currently available technological methods for enhancing transcutaneous drug delivery include ultrasound, electrically-assisted methods, fractional ablative lasers, and microneedling.[26] To our knowledge, there are no studies comparing the efficacy and safety of Tixel to the aforementioned technological methods. Possible advantage of Tixel may include the 6 h window of micropore persistence following treatment,[6,11] compared to the shorter effect of microneedling.[27] As compared to laser, low setting Tixel treatment is considered less painful. Further prospective comparative randomized trials are needed. This study has several limitations. First, no comparison was made to either placebo or other treatment modalities for festoons. In addition, due to the novelty of this treatment protocol, a limited amount of cases was available for analysis at the current timepoint. Finally, a recall bias may be present due to the retrospective filling of the questionnaire. Nevertheless, this is the first study to report on a promising, noninvasive, patient-friendly and apparently effective treatment protocol for festoons, in the reality where a gold standard treatment for this disorder is lacking. Further large-scale, prospective randomized trials are needed.

CONCLUSIONS

Our study explored a novel combination therapy for festoons involving Tixel, a thermomechanical system, followed by application of tetracycline HCL 1% topical solution. This therapy resulted in a significant improvement of festoon severity grading, as assessed by three masked reviewers. Patient-reported outcomes, including self-reported disturbance, PGIC scores, and duration of improvement, indicated a high level of satisfaction with the treatment. The longevity of improvement, lasting at least 4 months in 90% of patients after the second treatment, suggests a sustained effect.

CONFLICT OF INTEREST STATEMENT

The authors declare no conflict of interest.

ORCID

Margarita Safir http://orcid.org/0000-0002-1814-8316
Ofir Artzi http://orcid.org/0000-0003-1391-5843

REFERENCES

1. Kpodzo DS, Nahai F, McCord CD. Malar mounds and festoons. Aesthet Surg J. 2014;34(2):235–48.
2. Chon BH, Hwang CJ, Perry JD. Treatment options for lower eyelid festoons. Facial Plast Surg Clin North Am. 2021;29(2):301–9.
3. Godfrey KJ, Kally P, Dunbar KE, Campbell AA, Callahan AB, Lo C, et al. Doxycycline injection for sclerotherapy of lower eyelid festoons and malar edema: preliminary results. Ophthalmic Plastic Reconstructive Surg. 2019;35(5):474–7.
4. Perry JD, Mehta VJ, Costin BR. Intralesional tetracycline injection for treatment of lower eyelid festoons: a preliminary report. Ophthalmic Plastic Reconstructive Surg. 2015;31(1):50–2.
5. Chon BH, Hwang CJ, Perry JD. Long-term patient experience with tetracycline injections for festoons. Plastic Reconstructive Surg. 2020;146(6):737e–43e.
6. Elman M, Fournier N, Barnéon G, Bernstein EF, Lask G. Fractional treatment of aging skin with Tixel, a clinical and histological evaluation. J Cosmetic Laser Ther. 2016;18(1):31–7.
7. Friedman O, Koren A, Niv R, Mehrabi JN, Artzi O. The toxic edge: a novel treatment for refractory erythema and flushing of rosacea. Lasers Surg Med. 2019;51(4):325–31.
8. Bar-Ilan E, Koren A, Shehadeh W, Mashiah J, Sprecher E, Artzi O. An enhanced transcutaneous delivery of botulinum toxin for the treatment of Hailey-Hailey disease. Dermatol Ther. 2020;33(1):e13184.
9. Artzi O, Koren A, Niv R, Mehrabi JN, Mashiah J, Friedman O. A new approach in the treatment of pediatric hypertrophic burn scars: Tixel-associated topical triamcinolone acetonide and 5-fluorouracil delivery. J Cosmet Dermatol. 2020;19(1):131–4.

10. Artzi O, Mehrabi JN, Heyman L, Friedman O, Mashiah J. Treatment of port wine stain with Tixel-induced rapamycin delivery following pulsed dye laser application. Dermatol Ther. 2020;33(1):e13172.
11. Sintov AC, Hofmann MA. A novel thermo-mechanical system enhanced transdermal delivery of hydrophilic active agents by fractional ablation. Int J Pharm. 2016;511(2):821–30.
12. Rampakakis E, Ste-Marie PA, Sampalis JS, Karellis A, Shir Y, Fitzcharles MA. Real-life assessment of the validity of patient global impression of change in fibromyalgia. RMD Open. 2015;1(1):e000146.
13. Pessa J, Garza J. The malar septum: the anatomic basis of malar mounds and malar edema. Aesthet Surg J. 1997;17(1):11–7.
14. Papadopulos NA, Archimandritis T, Henrich G, Kovacs L, Machens HG, Klöppel M. Quality of life improvement following blepharoplasty: a prospective study. J Craniofacial Surg. 2023;34(3):888–92.
15. Burrows PE, Mitri RK, Alomari A, Padua HM, Lord DJ, Sylvia MB, et al. Percutaneous sclerotherapy of lymphatic malformations with doxycycline. Lymphat Res Biol. 2008;6(3–4):209–16.
16. Moesen I, Mombaerts I. Subconjunctival injection of tetracycline 2% for chronic bulbar chemosis after transcutaneous four-eyelid blepharoplasty. Ophthal Plastic Reconstructive Surg. 2008;24(3):219–20.
17. Karaconji T, Skippen B, Di Girolamo N, Taylor SF, Francis IC, Coroneo MT. Doxycycline for treatment of blepharochalasis via inhibition of matrix metalloproteinases. Ophthal Plastic Reconstructive Surg. 2012;28(3):e76–8.
18. Hurewitz AN, Lidonicci K, Wu CL, Reim D, Zucker S. Histologic changes of doxycycline pleurodesis in rabbits. Chest. 1994;106(4):1241–5.
19. Lee H, Min K, Kim EK, Kim TI. Minocycline controls clinical outcomes and inflammatory cytokines in moderate and severe meibomian gland dysfunction. Am J Ophthalmol. 2012;154(6):949–57.
20. Korting HC, Schöllmann C. Tetracycline actions relevant to rosacea treatment. Skin Pharmacol Physiol. 2009;22(6):287–94.
21. Erlendsson A, Wenande E, Haedersdal M. Transepidermal drug delivery: overview, concept, and applications 2018;1:447–61.
22. Wildnauer RH, Bothwell JW, Douglass AB. Stratum corneum biomechanical properties. I. Influence of relative humidity on normal and extracted human stratum corneum. J Invest Dermatol. 1971;56(1):72–8.
23. Kokolakis G, von Grawert L, Ulrich M, Lademann J, Zuberbier T, Hofmann MA. Wound healing process after thermomechanical skin ablation. Lasers Surg Med. 2020;52(8):730–4.
24. Kavallaris M, Madafiglio J, Norris MD, Haber M. Resistance to tetracycline, a hydrophilic antibiotic, is mediated by P-glycoprotein in human multidrug-resistant cells. Biochem Biophys Res Commun. 1993;190(1):79–85.
25. Safir M, Hecht I, Ahimor A, Zmujack-Yehiam S, Stein R, Bakshi E, et al. The effect of thermo-mechanical device (Tixel) treatment on evaporative dry eye disease: a pilot prospective clinical trial. Contact Lens Anterior Eye. 2022;45(6):101741.
26. Alkilani A, McCrudden MT, Donnelly R. Transdermal drug delivery: innovative pharmaceutical developments based on disruption of the barrier properties of the stratum corneum. Pharmaceutics. 2015;7(4):438–70.
27. Kalluri H, Kolli CS, Banga AK. Characterization of microchannels created by metal microneedles: formation and closure. AAPS J. 2011;13(3):473–81.

SUPPORTING INFORMATION

Additional supporting information can be found online in the Supporting Information section at the end of this article.

How to cite this article: Safir M, Waizer I, Safir A, Hartstein ME, Artzi O. Percutaneous delivery of liquid tetracycline using a thermal resurfacing drug delivery system for the treatment of festoons. Lasers Surg Med. 2024;1–8. https://doi.org/10.1002/lsm.23786